The endothelial compartment as a disease modifier in bleeding disorders

Laan, S.N.J.

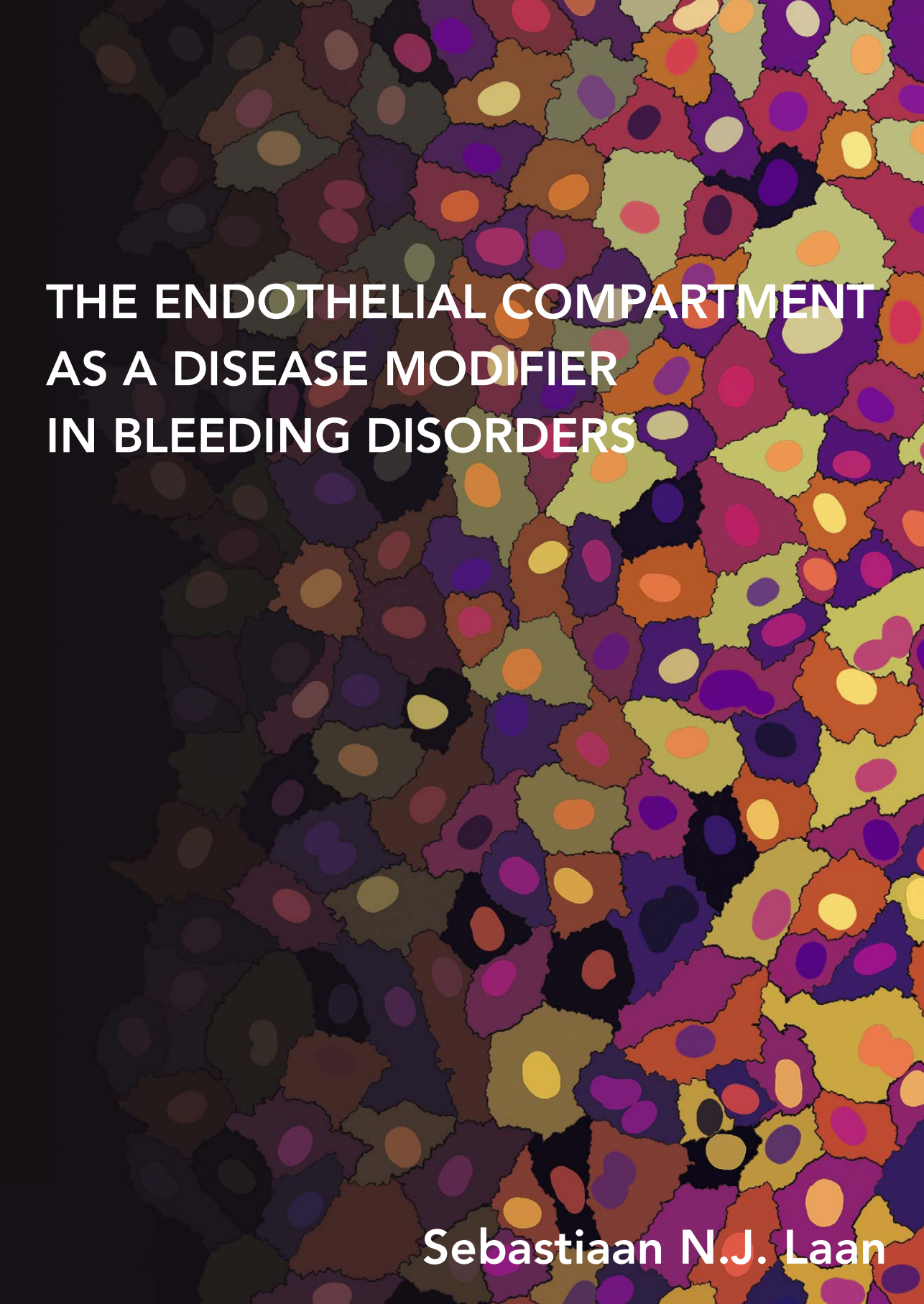

THE ENDOTHELIAL COMPARTMENT AS A DISEASE MODIFIER IN BLEEDING DISORDERS

Sebastiaan N.J. Laan

The endothelial compartment as a disease modifier in bleeding disorders

Sebastiaan Nicolaas Johannes Laan

The endothelial compartment as a disease modifier in bleeding disorders

The research described in this thesis was funded by a grant from the Netherlands Organization for Scientific Research (NWO) in the framework of the NWA-ORC Call grant agreement NWA.1160.18.038 (SYMPHONY: personalized treatment for patients with a bleeding disorder)

Financial support by CSL Behring, Swedish Orphan Biovitrum (The Netherlands) B.V., Stago BNL, Stichting Haemophilia and Chipsoft for the publication of this thesis is gratefully acknowledged.

ISBN: 978-94-6522-265-3
Provided by the thesis specialist Ridderprint, ridderprint.nl
Cover and chapter design: Bas Laan & Inge Laan (www.ingelaanillustraties.nl)
Layout and design: Jacolijn de Krom, persoonlijkproefschrift.nl
Printing: Ridderprint

The endothelial compartment as a disease modifier in bleeding disorders

Proefschrift

ter verkrijging van
de graad van doctor aan de Universiteit Leiden,
op gezag van rector magnificus prof.dr.ir. H. Bijl,
volgens besluit van het college voor promoties
te verdedigen op woensdag 24 september 2025
klokke 16:00 uur

door

Sebastiaan Nicolaas Johannes Laan
geboren te Wervershoof
in 1995

Promotoren

Prof. Dr. H.C.J. Eikenboom	
Prof. Dr. F.W.G. Leebeek	Erasmus University Medical Center
Dr. Ir. R. Bierings	Erasmus University Medical Center

Leden promotiecommissie

Prof. Dr. H.H. Versteeg	
Dr. B.J.M van Vlijmen	
Prof. Dr. M.H. Cnossen	Erasmus MC Sophia Children's Hospital
Prof. Dr. J. Voorberg	Amsterdam University Medical Center

Table of contents

General introduction and outline of the thesis

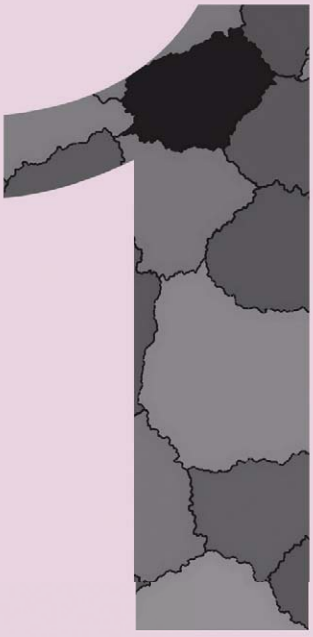

Hemostasis is the vital physiological process that prevents excessive bleeding by maintaining the integrity of vessels and controlling blood coagulation. This involves an intricate and highly regulated interplay between many factors. The balance within this interplay, between pro- and anticoagulant and pro- and antifibrinolytic mechanisms, is sensitive to fluctuations and can lead to disease if changes are not corrected accordingly. Tipping too far to one side might lead to defective or overly active coagulation which increases the chance of bleeding or thrombosis respectively.

The role of endothelial cells and von Willebrand factor in hemostasis

One of the major players in the anti- and procoagulant as well as fibrinolytic mechanisms are the endothelial cells, which both passively and actively contribute to hemostasis. Primarily, the endothelium forms a physical barrier between blood and tissues. The barrier blocks binding to the underlying subendothelial matrix thus preventing activation of platelets and circulating coagulation factors (1). One of the main procoagulant roles of endothelial cells is the production and secretion of von Willebrand factor (VWF). 85% of this large multimeric protein is produced by endothelial cells and in lower levels by megakaryocytes (2). VWF produced by endothelial cells is stored in cell specific secretory organelles called Weibel-Palade bodies (WPB) (3). VWF multimers are coiled and stored in WPBs as long tubules which is determinant of the characteristic rod like shape of WPBs (4, 5). Once stimulated, the endothelial cells secrete the WPB and release large quantities of VWF into the vessel lumen (6, 7). VWF is also continuously secreted by endothelial cells to maintain steady state levels in the plasma. At sites of vascular injury, VWF can bind to the exposed subendothelial matrix and become activated. Subsequent binding to circulating platelets causes aggregation and the start of platelet plug formation (8). Steady state levels of VWF in the blood also protect coagulation factor VIII (FVIII) from degradation and ensure sufficient levels of circulating FVIII (9). In this general introduction we only scratch the surface of the intricate processes involved. See **Chapter 2** for a more elaborate and detailed review of endothelial cell functions, VWF and their role in the hemostasis (10).

Von Willebrand disease

When defects in the hemostatic process occur, bleeding disorders can arise. These can lead to excessive bleeding or faulty clotting. In von Willebrand disease (VWD), VWF is either defect or absent in varying degrees causing mild to severe bleeding abnormalities (1, 11). When defects occur in VWF, as a carrier protein of FVIII, the levels of FVIII can also be reduced. Defects or low levels of FVIII lead to a bleeding disorder called hemophilia A. VWD is found in roughly 1 in 100 people with symptomatic disease that requires specific treatment occurring in 1 in 10.000 people, making it the most common bleeding disorder worldwide (12). VWD can be divided into three subtypes. Type 1 and type 3

VWD are caused by defects leading to a quantitative deficiency of VWF. Type 1 VWD patients have reduced but not absent levels of VWF, usually presenting with a mild or moderate bleeding phenotype. A subtype of type 1 VWD, Type 1C, has also recently been recognized and is associated with an increased clearance of VWF from the plasma (13). Type 3 VWD is characterized by a complete absence of VWF, making it the most severe type. Type 2 VWD is associated with qualitative defects in VWF (1, 11) which can be further divided into subtypes. Type 2A is characterized by lack of the highest molecular weight multimers, type 2B by enhanced or spontaneous binding to platelets, type 2M by decreased binding to platelets or collagen and finally type 2N, where VWF has decreased binding to FVIII.

Large variation in bleeding phenotype between but also within the subtypes of VWD exist. Over the past three decades more than 750 unique mutations in *VWF* have been found (14). Interestingly, approximately 30-50% of patients with type 1 VWD do not have pathogenic *VWF* gene variants (15-17). The reduced levels may be caused by increased clearance of VWF or due to impaired synthesis or secretion of VWF and it is hypothesized that other genetic modifiers may be the cause of the reduced VWF levels and bleeding phenotype in those patients (18). Previous genome-wide association studies have studied genetic determinants of VWF levels outside of the *VWF* gene. They have found genetic variability in genes which correlated with VWF levels either by affecting the WPB secretory processes, like *STXBP5* and *STX2* (19) or by affecting clearance (*CLEC4M*) (20). This suggests that exocytosis of WPB is important in the regulation of VWF levels. However, these findings only explain a limited part of the regulation of VWF levels and thus encourages further research into additional genetic modifiers. In this thesis, one of the research aims was to identify determinants of lower VWF levels in patients without pathogenic *VWF* variants (**Chapter 7**) and we hypothesized that defects in the components of the secretory machinery of VWF are causative for those lowered levels.

Treatment of von Willebrand disease

Most treatment options for VWD aim to prevent or treat the bleeding when it occurs. Logically, one of the treatment options aims to increase the levels of functional VWF and/or FVIII in the plasma by administering factor concentrates (21). Alternatively, VWD and other bleeding disorders can be treated by 1-deamino-8-D-arginine vasopressin (DDAVP) also known as desmopressin (22). This synthetic vasopressin analogue can activate the vasopressin V2 receptor (V2R) on endothelial cells (Figure 1). This is a G-protein coupled receptor (GPCR) on the membrane of endothelial cells in blood vessels. Upon binding of DDAVP to V2R, the receptor undergoes a conformational change that activates the cyclic adenosine monophosphate (cAMP) pathway (23). cAMP,

in turn, activates protein kinase A (PKA) which plays a central role in various cellular responses. One of which is the induction of exocytosis of WPBs in endothelial cells which increases the levels of VWF and FVIII in the plasma. Alternatively, cAMP can activate Epac1 which also induces WPB secretion (24). In endothelial cells, it has been shown that VWF and FVIII are co-trafficked to the WPBs (25-27) although the majority of FVIII is synthesized and stored in the liver sinusoid endothelial cells (LSECs) (28-30). It has also been shown that FVIII is produced in other endothelial beds, such as in kidney (30), and in lung (31). Interestingly, vascular endothelial cells, especially lung endothelial cells express V2R (23), but it is unclear whether LSECs express this receptor. Furthermore, it has been shown that DDAVP increases VWF levels, but not FVIII levels in hemophilia A patients after receiving a liver transplant (32). Collectively, this suggests that FVIII release after DDAVP administration is mainly caused by secretion of FVIII together with VWF by vascular endothelium and not liver endothelial cells.

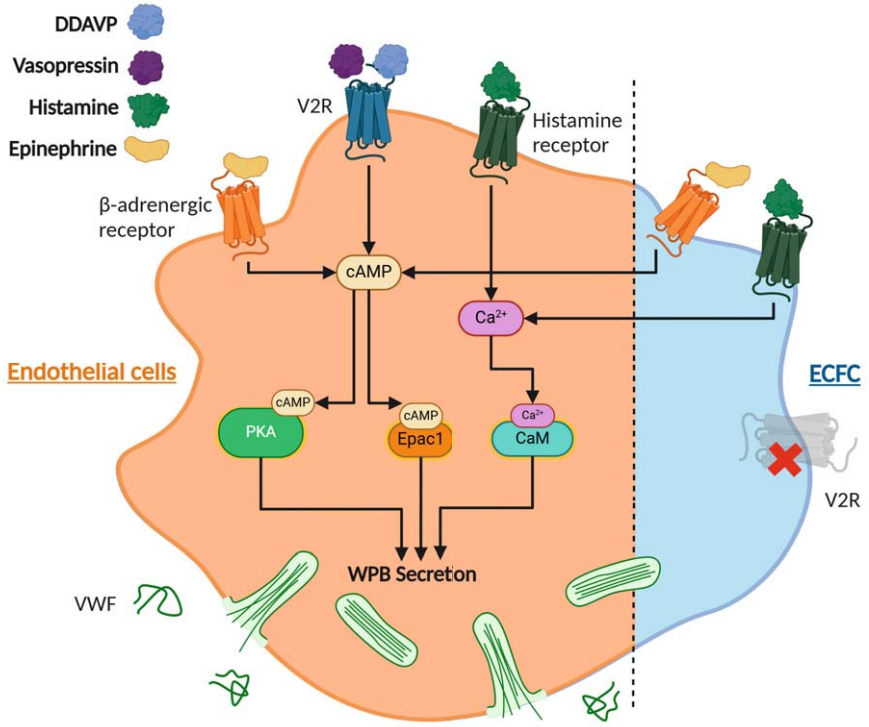

Figure 1. Simplified overview of the secretory pathways in endothelial cells. The schematic model depicts general endothelial cells (orange) and endothelial colony forming cells (ECFC) (blue). Abbreviations: VWF, von Willebrand factor; WPB, Weibel-Palade body; DDAVP, 1-deamino-8-D-arginine vasopressin; V2R, vasopressin 2 receptor; PKA, protein kinase A; cAMP, cyclic adenosine monophosphate; CaM, calmodulin; Epac1, exchange factor directly activated by cAMP 1. Created with BioRender.com

The stimulation of endothelial cells by DDAVP increases the levels of both FVIII and VWF in the plasma by 2-5 fold (33). This fold change is largely dependent on the amount of protein stored within the cells, the efficacy of secretion and the rate of clearance. Therefore, DDAVP is often administered in patients with low, but not deficient levels of VWF, like type 1 VWD or mild to moderate hemophilia A. DDAVP is one of the most readily available treatments for patients with bleeding disorders. Furthermore, because it can be administered intranasally by patients at home, it greatly improves quality of life. However, large inter-individual differences in response to DDAVP have been observed. Studies have been performed to elucidate the determinants of response like age, blood group, disease severity or mutation type (**Chapter 6**). Unfortunately, the cause of the variation is not yet fully understood. Comparatively to the unexplained low levels of VWF in VWD patients without a *VWF* variant, the variation and/or lack of response to DDAVP could be caused by undetermined genetic modifiers that affect the endothelial secretory pathway. A second research aim in this thesis was to identify determinants of DDAVP non-response in VWD patients (**Chapter 7**). The question then is, how can we study and understand this variation?

Endothelial cell models

Over the years, a number of approaches have been developed to investigate the pathophysiology and the underlying cause of bleeding in patients with bleeding disorders. For example, plasma coagulation factor levels can be measured in the plasma taken from the patients. These factors can also be functionally tested using aggregation or activity assays. However, these tests do not take into account how the factors are synthesized, stored and secreted by the endothelial cells. Model systems have been developed that can reflect the cellular context from which the pathogenic mechanisms could be investigated. VWF can be brought to expression through transfection into non-endothelial cells like Chinese hamster ovary and human embryonic kidney 293 cells (HEK293). The ectopic expression of VWF in HEK293 cells also induces the formation of pseudo-WPBs. These models can be used to study VWF *in vitro* and the pathogenic effect of mutations can be analyzed by transfecting a mutant version of VWF (34). However, these models are limited as they do not have a native environment wherein VWF is produced and the complete secretory machinery. Furthermore, only known mutations can be tested in these models.

Endothelial cells from the patient can be directly collected from various vascular beds. However, these invasive procedures are not ideal as they burden the patient. Fortunately, two methods exist where endothelial cells can be derived from whole blood via venipuncture. In the first model, peripheral blood mononuclear cells can be reprogrammed into induced pluripotent stem cells (iPSCs) (35). These can then be

differentiated into iPSC endothelial cells (iPSC-ECs) which have the great advantage of carrying the genetic background of the patient it was derived from. Unfortunately, maturation of WPB is impaired in iPSC-ECs, making it difficult to study this aspect of endothelial function (36) (**Chapter 5**). The second model cell is named endothelial colony forming cells (ECFCs), previously known as blood outgrowth endothelial cells. ECFCs also carry the genetic background of the donor from which the whole blood was collected. Additionally, in ECFCs, WPB mature fully allowing studies to be performed on their formation, maturation and secretion. ECFCs have already been used extensively as a model to study VWD patient specific defects (37-42) (reviewed in **Chapter 2**). Although ECFCs do not express the V2R receptor (42) and can thus not be stimulated by DDAVP, they can be stimulated by other agonists like epinephrine or histamine to activate the cAMP or Ca^{2+} pathways respectively (Figure 1). This means that ECFCs can also be used to study stimulated secretion defects like in VWD patients that do not respond to DDAVP. Despite these advantages, ECFCs can also be challenging to work with. Large heterogeneity exists not only between ECFC clones derived from healthy controls, but also between clones from the same donor. Variation has been observed in cell size, VWF production, WPB quantity and size, cell growth, migration and RNA expression (43-45). It is currently unclear what causes these differences warranting further research. Another research aim of this thesis was to elucidate the extent and the potential cause of this variation (**Chapter 4**).

The importance of hemostasis and the challenges of managing bleeding disorders underscore the need for ongoing research. Understanding both the clinical aspect and the fundamental pathophysiology of bleeding disorders on a cellular level is therefore essential in improving outcomes and developing innovative treatments for affected individuals. Therefore, in this thesis we studied various aspects of the endothelial compartment as a disease modifier in bleeding disorders. This is further elaborated on in the outline of the thesis.

Outline of the thesis

In this thesis, the endothelial compartment and its role in the pathophysiology of bleeding disorders is analyzed in multiple ways. First, in **Chapter 2,** the use of ECFCs in analyzing the pathophysiology in bleeding disorders is reviewed. There, we go into detail what contribution endothelial cells play in the primary and secondary hemostasis. Specifically, how the endothelial cell model, ECFCs, was used in previous research to explore pathogenic effects, but also mechanical aspects in patients with various disorders. Following this, **Chapter 3** introduces the concept of automated

quantification techniques which can be used to analyze and quantify the morphology of many parameters of the cell. In this chapter, we developed an extensive automated pipeline using CellProfiler for the quantitative analysis of cell and organelle morphology, localization, and content. We show that the pipeline can be used on various cell models and organelles, specifically endosomes and WPBs. Furthermore, we show the quantitative power of the pipeline by comparing different groups of ECFCs clones. It is known in literature that large heterogeneity between ECFC clones exists. We used this heterogeneity as an example in **Chapter 3** to display the quantification capabilities of the pipeline. In **Chapter 4**, however, we dive into this heterogeneity and the challenge it poses for all research groups using this model. There, we look beyond the basic morphologic characterization and explore the transcription signature of a large panel of control-derived ECFCs. Using this signature, we created a minimal qPCR panel which can be used to classify and cluster ECFC clones. Between the clusters we show that inflammation and endothelial to mesenchymal transition may act as potential drivers for the phenotypic heterogeneity.

ECFCs offer a great way to get an inside look at the potential endothelial defects of patients. However, they are not the only endothelial model that offers this advantage. iPSC-ECs are another model that can be used to investigate patient specific defects. Our group has shown that one major disadvantage of the model is that the iPSC-EC do not seem to mature fully, showing low levels of synthesized VWF and small, round WPBs. In **Chapter 5**, we strived to optimize the cell culture, isolation and differentiation protocol to create iPSC-ECs that fully mature and especially, synthesize sufficient amounts of VWF and WPB with typical cigar-shaped morphology.

Patients with bleeding disorders are usually treated with appropriate factor concentrates or, when effective, with DDAVP. This drug is widely used for patients with VWD and hemophilia A as it quickly increases the plasma levels of both VWF and FVIII. However, a substantial portion of patients do not or only partially respond to this medication. In **Chapter 6** we undertake a systematic review and meta-analysis to elucidate the rate of response and possible determinants of DDAVP response in patients with bleeding disorders, offering valuable insights into therapeutic approaches.

Chapter 7 can be seen as the culmination of all chapters in this thesis. Here, we analyze the ECFCs derived from two groups of patients with VWD. Patients with VWD without a pathogenic gene variant identified within *VWF* and patients with VWD that do not respond to DDAVP. ECFCs were characterized and clustered according to our minimal qPCR panel (**Chapter 4**). The ECFC panel was analyzed extensively with various assays including imaging and subsequent image quantification (**Chapter 3**). In this study we

found patient specific functional defects which explain the bleeding phenotype in some patients. Furthermore, we correlated the large panel of functional aspects of the endothelial cells with their proteome, revealing processes and proteins of interest.

In **Chapter 8** the findings from the preceding chapters are summarized and discussed, paving the way for future research directions and potential implications in clinical practice. Through this structured journey, the thesis contributes to the growing body of knowledge in endothelial biology and its relevance in the context of bleeding disorders, offering valuable insights and avenues for future investigation.

References

1. Leebeek FWG, Eikenboom JCJ. Von Willebrand's Disease. New England Journal of Medicine. 2016;375(21):2067-80.
2. Nichols WL, Hultin MB, James AH, Manco-Johnson MJ, Montgomery RR, Ortel TL, et al. von Willebrand disease (VWD): evidence-based diagnosis and management guidelines, the National Heart, Lung, and Blood Institute (NHLBI) Expert Panel report (USA). Haemophilia. 2008;14(2):171-232.
3. Weibel ER, Palade GE. NEW CYTOPLASMIC COMPONENTS IN ARTERIAL ENDOTHELIA. J Cell Biol. 1964;23(1):101-12.
4. Berriman JA, Li S, Hewlett LJ, Wasilewski S, Kiskin FN, Carter T, et al. Structural organization of Weibel-Palade bodies revealed by cryo-EM of vitrified endothelial cells. Proc Natl Acad Sci U S A. 2009;106(41):17407-12.
5. Kat M, Karampini E, Hoogendijk AJ, Bürgisser PE, Mulder AA, Van Alphen FPJ, et al. Syntaxin 5 determines Weibel-Palade body size and von Willebrand factor secretion by controlling Golgi architecture. Haematologica. 2022;107(8):1827-39.
6. Schillemans M, Karampini E, Kat M, Bierings R. Exocytosis of Weibel-Palade bodies: how to unpack a vascular emergency kit. J Thromb Haemost. 2019;17(1):6-18.
7. Hordijk S, Carter T, Bierings R. A new look at an old body: molecular determinants of Weibel-Palade body composition and VWF exocytosis. J Thromb Haemost. 2024.
8. Ruggeri ZM. Von Willebrand factor, platelets and endothelial cell interactions. J Thromb Haemost. 2003;1(7):1335-42.
9. Pipe SW, Montgomery RR, Pratt KP, Lenting PJ, Lillicrap D. Life in the shadow of a dominant partner: the FVIII-VWF association and its clinical implications for hemophilia A. Blood. 2016;128(16):2007-16.
10. Laan SNJ, Lenderink BG, Eikenboom JCJ, Bierings R. Endothelial colony-forming cells in the spotlight: insights into the pathophysiology of von Willebrand disease and rare bleeding disorders. Journal of Thrombosis and Haemostasis. 2024.
11. Seidizadeh O, Eikenboom JCJ, Denis CV, Flood VH, James P, Lenting PJ, et al. von Willebrand disease. Nature Reviews Disease Primers. 2024;10(1):51.
12. Murray EW, Lillicrap D. von Willebrand disease: pathogenesis, classification, and management. Transfus Med Rev. 1996;10(2):93-110.
13. James PD, Connell NT, Ameer B, Di Paola J, Eikenboom J, Giraud N, et al. ASH ISTH NHF WFH 2021 guidelines on the diagnosis of von Willebrand disease. Blood Adv. 2021;5(1):280-300.
14. de Jong A, Eikenboom J. Von Willebrand disease mutation spectrum and associated mutation mechanisms. Thromb Res. 2017;159:65-75.
15. Atiq F, Boender J, van Heerde WL, Tellez Garcia JM, Schoormans SC, Krouwel S, et al. Importance of Genotyping in von Willebrand Disease to Elucidate Pathogenic Mechanisms and Variability in Phenotype. Hemasphere. 2022;6(6):e718.
16. James PD, Notley C, Hegadorn C, Leggo J, Tuttle A, Tinlin S, et al. The mutational spectrum of type 1 von Willebrand disease: Results from a Canadian cohort study. Blood. 2007;109(1):145-54.
17. Lavin M, Aguila S, Schneppenheim S, Dalton N, Jones KL, O'Sullivan JM, et al. Novel insights into the clinical phenotype and pathophysiology underlying low VWF levels. Blood. 2017;130(21):2344-53.

18. Swystun LL, Lillicrap D. Genetic regulation of plasma von Willebrand factor levels in health and disease. J Thromb Haemost. 2018;16(12):2375-90.
19. van Loon JE, Leebeek FW, Deckers JW, Dippel DW, Poldermans D, Strachan DP, et al. Effect of genetic variations in syntaxin-binding protein-5 and syntaxin-2 on von Willebrand factor concentration and cardiovascular risk. Circ Cardiovasc Genet. 2010;3(6):507-12.
20. Sanders YV, van der Bom JG, Isaacs A, Cnossen MH, de Maat MP, Laros-van Gorkom BA, et al. CLEC4M and STXBP5 gene variations contribute to von Willebrand factor level variation in von Willebrand disease. J Thromb Haemost. 2015;13(6):956-66.
21. Castaman G. How I treat von Willebrand disease. Thromb Res. 2020;196:618-25.
22. Leissinger C, Carcao M, Gill JC, Journeycake J, Singleton T, Valentino L. Desmopressin (DDAVP) in the management of patients with congenital bleeding disorders. Haemophilia. 2014;20(2):158-67.
23. Kaufmann JE, Oksche A, Wollheim CB, Günther G, Rosenthal W, Vischer UM. Vasopressin-induced von Willebrand factor secretion from endothelial cells involves V2 receptors and cAMP. J Clin Invest. 2000;106(1):107-16.
24. van Hooren KW, van Agtmaal EL, Fernandez-Borja M, van Mourik JA, Voorberg J, Bierings R. The Epac-Rap1 signaling pathway controls cAMP-mediated exocytosis of Weibel-Palade bodies in endothelial cells. J Biol Chem. 2012;287(29):24713-20.
25. Van Den Biggelaar M, Bierings R, Storm G, Voorberg J, Mertens K. Requirements for cellular co-trafficking of factor VIII and von Willebrand factor to Weibel–Palade bodies. Journal of Thrombosis and Haemostasis. 2007;5(11):2235-42.
26. Turner NA, Moake JL. Factor VIII Is Synthesized in Human Endothelial Cells, Packaged in Weibel-Palade Bodies and Secreted Bound to ULVWF Strings. PLOS ONE. 2015;10(10):e0140740.
27. Jacquemin M, Neyrinck A, Hermanns MI, Lavend'homme R, Rega F, Saint-Remy J-M, et al. FVIII production by human lung microvascular endothelial cells. Blood. 2006;108(2):515-7.
28. Hollestelle MJ, Poyck PPC, Hollestelle JM, Marsman HA, Van Mourik JA, Van Gulik TM. Extra-hepatic factor VIII expression in porcine fulminant hepatic failure. Journal of Thrombosis and Haemostasis. 2005;3(10):2274-80.
29. Shahani T, Covens K, Lavend'homme R, Jazouli N, Sokal E, Peerlinck K, et al. Human liver sinusoidal endothelial cells but not hepatocytes contain factor VIII. Journal of Thrombosis and Haemostasis. 2014;12(1):36-42.
30. Everett LA, Cleuren ACA, Khoriaty RN, Ginsburg D. Murine coagulation factor VIII is synthesized in endothelial cells. Blood. 2014;123(24):3697-705.
31. Olsen EH, McCain AS, Merricks EP, Fischer TH, Dillon IM, Raymer RA, et al. Comparative response of plasma VWF in dogs to up-regulation of VWF mRNA by interleukin-11 versus Weibel-Palade body release by desmopressin (DDAVP). Blood. 2003;102(2):436-41.
32. Lamont PA, Ragni MV. Lack of desmopressin (DDAVP) response in men with hemophilia A following liver transplantation. J Thromb Haemost. 2005;3(10):2259-63.
33. Mannucci PM. Desmopressin (DDAVP) in the treatment of bleeding disorders: the first 20 years. Blood. 1997;90(7):2515-21.
34. Michaux G, Hewlett LJ, Messenger SL, Goodeve AC, Peake IR, Daly ME, et al. Analysis of intracellular storage and regulated secretion of 3 von Willebrand disease-causing variants of von Willebrand factor. Blood. 2003;102(7):2452-8.
35. Lin Y, Gil CH, Yoder MC. Differentiation, Evaluation, and Application of Human Induced Pluripotent Stem Cell-Derived Endothelial Cells. Arterioscler Thromb Vasc Biol. 2017;37(11):2014-25.

36. de Boer S, Laan S, Dirven R, Eikenboom J. Approaches to induce the maturation process of human induced pluripotent stem cell derived-endothelial cells to generate a robust model. PLoS One. 2024;19(2):e0297465.
37. Berber E, James PD, Hough C, Lillicrap D. An assessment of the pathogenic significance of the R924Q von Willebrand factor substitution. J Thromb Haemost. 2009;7(10):1672-9.
38. Groeneveld DJ, van Bekkum T, Dirven RJ, Wang JW, Voorberg J, Reitsma PH, et al. Angiogenic characteristics of blood outgrowth endothelial cells from patients with von Willebrand disease. J Thromb Haemost. 2015;13(10):1854-66.
39. Randi AM, Laffan MA. Von Willebrand factor and angiogenesis: basic and applied issues. J Thromb Haemost. 2017;15(1):13-20.
40. Starke RD, Ferraro F, Paschalaki KE, Dryden NH, McKinnon TA, Sutton RE, et al. Endothelial von Willebrand factor regulates angiogenesis. Blood. 2011;117(3):1071-80.
41. Starke RD, Paschalaki KE, Dyer CE, Harrison-Lavoie KJ, Cutler JA, McKinnon TA, et al. Cellular and molecular basis of von Willebrand disease: studies on blood outgrowth endothelial cells. Blood. 2013;121(14):2773-84.
42. Wang JW, Bouwens EA, Pintao MC, Voorberg J, Safdar H, Valentijn KM, et al. Analysis of the storage and secretion of von Willebrand factor in blood outgrowth endothelial cells derived from patients with von Willebrand disease. Blood. 2013;121(14):2762-72.
43. de Jong A, Weijers E, Dirven R, de Boer S, Streur J, Eikenboom J. Variability of von Willebrand factor-related parameters in endothelial colony forming cells. J Thromb Haemost. 2019;17(9):1544-54.
44. de Boer S, Bowman M, Notley C, Mo A, Lima P, de Jong A, et al. Endothelial characteristics in healthy endothelial colony forming cells; generating a robust and valid ex vivo model for vascular disease. J Thromb Haemost. 2020;18(10):2721-31.
45. Laan SNJ, de Boer S, Dirven RJ, van Moort I, Kuipers TB, Mei H, et al. Transcriptional and functional profiling identifies inflammation and endothelial-to-mesenchymal transition as potential drivers for phenotypic heterogeneity within a cohort of endothelial colony forming cells. J Thromb Haemost. 2024;22(7):2027-38.

Endothelial Colony Forming Cells in the spotlight, insights into the pathophysiology of von Willebrand disease and rare bleeding disorders

Laan SNJ, Lenderink BG, Eikenboom JC, Bierings R

Journal of Thrombosis and Haemostasis. 2024 Sep 5:S1538-7836(24)00497-5.
doi: 10.1016/j.jtha.2024.08.011

Abstract

Endothelial cells deliver a vital contribution to the maintenance of hemostasis by constituting an anatomical as well as functional barrier between the blood and the rest of the body. Apart from the physical barrier function, endothelial cells maintain the hemostatic equilibrium by their pro- and anticoagulant functions. An important part of their procoagulant contribution is the production of von Willebrand factor (VWF), which is a carrier protein for coagulation factor VIII (FVIII) and facilitates the formation of a platelet plug. Thus, VWF is indispensable for both the primary and secondary hemostasis, which is exemplified by the bleeding disorder von Willebrand disease (VWD) that results from qualitative or quantitative deficiencies in VWF.

A cellular model that was found to accurately reflect the endothelium and its secretory organelles are endothelial colony forming cells (ECFCs), which can be readily isolated from peripheral blood and constitute a robust *ex vivo* model to investigate the donor's endothelial cell function. This review summarizes some of the valuable insights on biology of VWF and pathogenic mechanisms of VWD that have been made possible using studies with ECFCs derived from patients with bleeding disorders.

Introduction

Hemostasis is the cessation of bleeding through coagulation in the event of vascular injury. The hemostatic balance is an interplay of pro-coagulant and anti-coagulant mechanisms and can be regarded as a balance. Tipping too far to one side without sufficient adjustments in response ultimately leads to defective or overactivated coagulation, which increases the risk of bleeding or thrombosis, respectively. Much of the research in this field has been, and still is, revolving around identifying and investigating (new) hemostatic players. With the aim of unraveling their underlying mechanisms, and how their interplay can give rise to a pathogenic state. In this review we will briefly outline how endothelial cells (ECs) actively participate in preserving the hemostatic balance, with particular focus on their role in regulating acute and steady state levels of the hemostatic protein Von Willebrand factor (VWF). Our molecular understanding of the biosynthesis and secretion of VWF primarily originates from *in vitro* studies in endothelial cells. Here, we will highlight endothelial colony forming cells (ECFCs) as a versatile, *ex vivo* endothelial cell model for studying basic principles of endothelial cell biology and hemostasis in their native environment. ECFCs are uniquely suited to study the links between genetic mutations in patients and their cellular phenotype. This will be illustrated by the insights obtained from patient-derived ECFCs, such as for the bleeding disorder von Willebrand disease (VWD), the process of angiogenesis and for regulated secretion of VWF via Weibel-Palade body (WPB) exocytosis.

The role of endothelial cells in hemostasis

Endothelial cells passively and actively contribute to anti- and procoagulant as well as fibrinolytic mechanisms (Figure 1). Their anticoagulant function is vital as it prevents blood from unintentional clotting, and in doing so averts the formation of clots that can cause thrombosis, infarcts or stroke. The endothelium acts first and foremost as a physical barrier between blood and tissue. As such, it also prevents contact of platelets and coagulation factors in the circulation with procoagulant components in the subendothelial matrix, such as collagen and tissue factor (TF), thereby restricting initiation of primary and secondary hemostasis pathways, respectively (1).

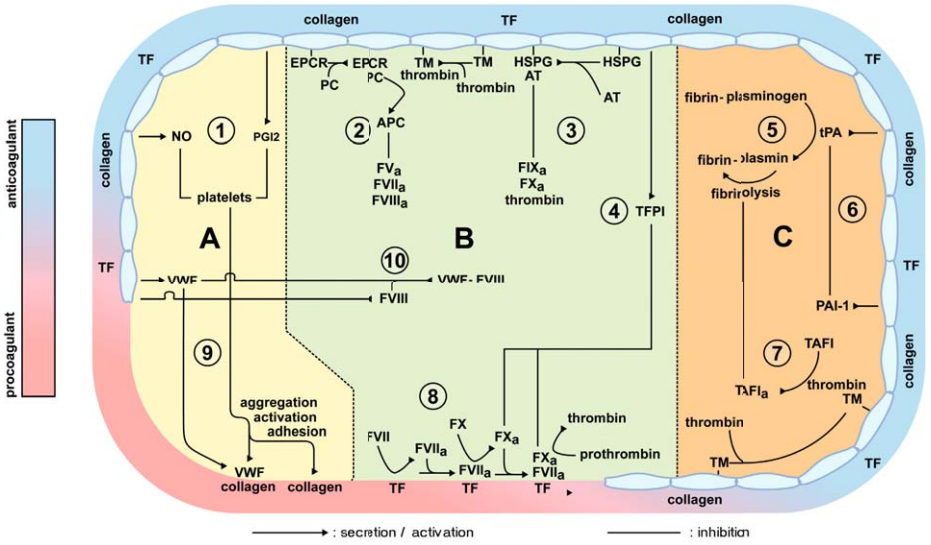

Figure 1. Anti- and procoagulant functions of endothelial cells. Endothelial cells (ECs) directly and indirectly contribute to anti- and procoagulant mechanisms in primary and secondary hemostasis (**A**, respectively **B**) and fibrinolysis (**C**). Anticoagulant mechanisms in primary and secondary hemostasis include synthesis of the platelet inhibitors Nitric Oxide (NO) and prostaglandin I2 (PGI2) (**1**), the protein C (PC) pathway supported by the endothelial protein C receptor (EPCR) – thrombomodulin (TM) tandem on ECs (**2**), the antithrombin (AT) pathway on Heparan Sulphate Proteoglycans (HPSGs) on ECs (**3**) and the synthesis of Tissue Factor Pathway Inhibitor (TFPI), which negatively regulates the Tissue factor (TF) pathway (**4**). Endothelial cell control over fibrinolysis includes secretion of tissue plasminogen activator (tPA), which activates plasminogen on fibrin into plasmin, thereby promoting degradation of fibrin (**5**). Activation of fibrinolysis is counteracted by Plasminogen Activator Inhibitor-1 (PAI-1) produced by endothelial cells (**6**) and by the conversion of Thrombin Activatable Fibrinolysis Inhibitor (TAFI) by the thrombin-TM complex on ECs (**7**). Damage to the vessel wall exposes TF within the subendothelial matrix and activates the TF pathway, resulting in the generation of thrombin (**8**). Binding of VWF to exposed collagen promotes adhesion and subsequent, activation and aggregation of platelets (**9**), while binding of VWF to FVIII prevents FVIII from premature clearance (**10**).

Endothelial cells also take more active roles in preserving the hemostatic balance. Nitric oxide (NO) and prostacyclin (PGI2), which are continuously synthesized by endothelial cells, are potent vasodilators and platelet inhibitors that are used for local control of hemodynamic forces in the blood and of adhesion and aggregation of platelets (2,3). ECs also produce Tissue Factor Pathway Inhibitor (TFPI), which blocks the TF-activated factor VII (TF-FVIIa) complex and prothrombinase of the extrinsic pathway (4). Additionally, ECs can act on the intrinsic pathway by producing and presenting anticoagulants like heparan sulphate proteoglycans (HSPG) on their membranes, which bind liver-produced antithrombin (AT) to the vessel wall. This induces conformational changes of AT and enhances its interaction with the blood clotting cascade proteinases

factor Xa and IXa to inhibit their activity (5). Additionally, ECs modulate the common pathway through their production of thrombomodulin, which is a thrombin-specific receptor on the endothelial cell membrane that decreases circulating thrombin levels. Moreover, ECs express endothelial cell protein C receptor (EPCR) on their membranes, which can bind to protein C (PC). This facilitates activation of PC into activated protein C (APC) by the thrombin-thrombomodulin complex, which leads to the subsequent inactivation of coagulation factors such as FV, FVII and FVIII (6).

Stimulated and constitutive secretion of tissue plasminogen activator (tPA) from endothelial cells (7,8) leads to the conversion of fibrin-bound plasminogen to plasmin, which is a serine protease that degrades fibrin during fibrinolysis and clot resolution (9). Endothelial cells also express inhibitors of fibrinolysis, such as the serpin plasminogen activator inhibitor-1 (PAI-1) (10), which inhibits tPA by binding its active site thereby preventing the interaction of tPA with plasminogen and the latter's subsequent conversion to fibrin (11). Furthermore, the thrombin-thrombomodulin complex, which is found on the surface of endothelial cells, activates the thrombin-activatable fibrinolysis inhibitor (TAFI). TAFI cleaves C-terminal lysine residues from fibrin, which decreases its affinity for plasminogen and tPA, reduces plasmin generation and thus attenuates fibrinolysis (12).

The procoagulant function of the endothelium is mainly mediated by Von Willebrand factor, which is secreted by endothelial cells and takes a central role in primary and secondary hemostasis. At steady state, VWF is critical for the maintenance of sufficient levels of circulating FVIII by physically preventing the latter's premature clearance from plasma (13). Following vascular injury and exposure of the subendothelial matrix, VWF circulating in plasma as well as VWF that is locally secreted by activated endothelial cells binds to collagen via its A3 domain. As a result of the hemodynamic forces of the blood flow, these tethered VWF strings unfold and expose a binding site for the platelet GP1bα receptor within the VWF A1 domain that supports the adhesion and subsequent activation and aggregation of platelets to sites of vascular injury, a critical step in the formation of a platelet plug (14). The importance of VWF is highlighted by the mild to severe bleeding abnormalities that occur in patients with (partial) quantitative reduction or a qualitative defect of VWF circulating in plasma, as seen in VWD and in what was formerly known as "Low VWF" (15,16). Partial deficiencies of functionally normal VWF are often the result of *VWF* missense mutations (17) that reduce its synthesis and/or secretion or lead to enhanced clearance from the circulation as evidenced by altered VWF propeptide (VWFpp)/VWF Antigen (VWF:Ag) and FVIII activity (FVIII:C)/VWF:Ag ratios in plasma (18). However, approximately 30-50% of patients with quantitative VWF reductions lack pathogenic *VWF* variants (18–21). In these cases other genetic modifiers,

including those acting on clearance, synthesis and secretion, may be responsible for the reduced VWF levels (22).

Cell biology of Von Willebrand factor

Endothelial cells are responsible for the production of nearly all VWF that is found in plasma (23). VWF is first synthesized as a pre-proVWF monomer, consisting of an N-terminal signal peptide, the VWFpp and the mature VWF subunit, which contains its ligand-binding domains and domains responsible for dimerization and multimerization (24). Following signal peptide cleavage and dimerization of proVWF monomers in the ER, the acidic conditions in the trans-Golgi network (TGN) promote concatemerization of VWF dimers along helical self-templates, leading to the formation of long tubules that consist of ultra-large VWF multimers (25–27). Expression of VWF drives the formation of WPBs, EC-specific secretory organelles that are formed at the TGN and store VWF for basal or stimulated release (28–30). WPBs are generally 1-5 µm long, 0.1 to 0.3 µm wide and owe their characteristic rod shape to the dimensions and parallel arrangement of the VWF tubules (26,30,31).

Newly synthesized WPBs are considered immature and lack the ability to undergo stimulus-induced secretion (32). WPBs go through a post-Golgi maturation process that involves the recruitment of proteins to the WPB membrane and a further acidification to ~pH 5.4 (30,33). A key step in this process is the acquisition of Rab GTPases Rab27A and isoforms of Rab3 (32,34,35), which depends on their activation by the guanine nucleotide exchange factor MAP kinase activating death domain (MADD) (36). In turn, active Rabs on the membrane of mature WPBs recruit effectors that interact with Soluble N-ethylmaleimide-sensitive factor attachment protein receptors (SNARE) proteins and other exocytotic components that perform essential functions in cytoskeletal interactions, organelle acidification and exocytosis of WPBs (32,37–46). As a result of recruitment of their secretory machinery WPBs become secretion competent and can undergo exocytosis upon activation of the endothelial cell, such as during vascular injury (30). Apart from VWF, WPBs are known to store a variety of other vasoactive agents, including chemokines, angiogenic mediators such as Insulin-like growth factor binding protein 7 (IGFBP7) and Angiopoietin-2 (Ang-2), as well as hemostatic proteins FVIII and tPA (reviewed in (30)). Co-release of these proteins together with VWF may help the endothelium to further fine-tune its hemostatic responses while simultaneously initiating inflammatory and blood vessel repair pathways.

The SNARE proteins syntaxin-2 (STX2) and syntaxin-binding protein 5 (STXBP5), which are part of this machinery, have previously been identified in quantitative trait locus mapping studies for genetic associations with VWF (47–50), suggesting that alterations

in the exocytotic process of WPBs contribute to the wide range of plasma VWF levels in the population. Together, this highlights the potential role of the endothelial secretory pathway as a major determinant of circulating VWF levels and bleeding phenotype.

Cellular model systems

With the growing insight from large-scale genomic screenings into the genetic mechanisms that underpin VWF abnormalities, investigators now face the challenge to find experimental evidence of the functional impact of variants in *VWF* or other genetic determinants that explains alterations in VWF found in patients. Over the years, a number of approaches have been developed to test these genotype-phenotype relationships in model systems that, to a varying extent, reflect the cellular context in which these pathogenic mechanisms play out. Expression of VWF in non-endothelial cell types such as Chinese hamster ovary (CHO) and human embryonic kidney 293 (HEK293) cell lines has long been the method of choice to study how pathogenic VWF variants affect its biosynthesis, post-translational modification and molecular composition. Because ectopic expression of VWF induces the formation of so-called pseudo-WPBs (51,52), elongated storage organelles that have a striking resemblance to WPBs in terms of morphology and composition, these studies can also reveal how mutations translate to altered storage and secretion of VWF and other WPB constituents (52–54). Such studies do require *a priori* knowledge of the mutations involved and can be difficult to interpret considering that the vast majority (up to 90%) of pathogenic *VWF* variants in VWD are heterozygous dominant-negative mutations (17) that express in conjunction with a normal functional allele in patients. Moreover, other caveats of studying VWF biology outside of its proper cellular context include lack of endothelial cell specific gene expression, non-physiological expression levels from expression constructs with constitutive promoters, as well as the absence of a regulated secretory pathway and many components of the associated exocytotic machinery. This makes ectopic systems such as HEK293 cells of very limited value for functional studies of stimulated VWF secretion or angiogenesis.

To study these processes in their native cellular context it is inevitable to turn to endothelial cells, ideally from the patients themselves. Primary endothelial cells from a multitude of vascular beds, such as from the dermis, brain, lungs, heart, aorta, retina, umbilical cords and foreskin, are nowadays commercially available. Nonetheless, the invasive procedures involved to isolate these endothelial subtypes from patients would make most of them impractical for study purposes. Differentiation of endothelial cells from patient-derived induced pluripotent stem cells (iPSC-ECs) could potentially overcome such hurdles, but varying levels of VWF synthesis between clonal lines and

impaired maturation of WPBs (55) are currently still precluding iPSC-ECs from becoming a viable model system for this purpose.

Endothelial cells can also be derived from a population of cells that circulates in blood, so-called endothelial progenitor cells (EPCs), which can be divided into two populations, early and late, based on their appearance in culture. Late appearing EPCs, first described by Lin *et al.* (56), are of *bona fide* endothelial lineage as judged by the expression of a set of canonical endothelial markers, including VWF, VEGFR2, PECAM and VE-cadherin, and several endothelial cell specific properties such as angiogenic capacity. These cells have been referred to by various other names including endothelial outgrowth cells (EOCs) and blood outgrowth endothelial cells (BOECs). To bring order to the nomenclature conundrum, a consensus was reached to rename them endothelial colony forming cells (ECFCs) (57), which is also the terminology we will use in this review.

ECFCs can be regarded as liquid biopsies of the endothelium (58) and are excellent model systems to investigate pathogenic cellular mechanisms that affect the vasculature, since they carry the genetic background of the patient (59). Despite the fact that their exact origin is still a matter of debate (60,61), ECFCs can be acquired quite reliably from various sources, including venous blood (56,62,63), cord blood (64,65) and even from cryopreserved peripheral blood mononuclear cells (PBMCs) (66). However, some concerns exist regarding their intra- and interindividual phenotypic heterogeneity (67,68), which can potentially influence outcomes of studies and may have its basis in a progression of some ECFC lines into an endothelial-to-mesenchymal transition (EndoMT) state (69).

Despite these challenges, ECFCs are a robust model to directly assess how disease genotype translates to endothelial phenotype *ex vivo,* which is invaluable for research on pathologies that are characterized by an affected endothelium, such as VWD.

ECFCs: von Willebrand disease

The first use of VWD patient-derived ECFCs was by Berber and colleagues who investigated the common R924Q polymorphism in ECFCs of a compound heterozygous VWD type 2N patient (R816W/R924Q), but failed to find conclusive evidence for the pathogenic nature of this variant (70). Back-to-back publications by Starke *et al.* and Wang *et al.* followed shortly after, which used ECFCs from type 1 and type 2 VWD patients to investigate the cellular phenotypes that are associated with a variety of exonic mutations within *VWF* (71,72). This marked a key advance in the field as the consequences of the pathogenic mechanisms involved in VWD could be revealed to their full extent for the first time. Depending on the mutations involved, these

mechanisms include retention of VWF inside the endoplasmic reticulum (ER), incorrect proteolytic processing, reduced high molecular weight VWF multimers, impaired stimulus-induced secretion and the loss of the characteristic elongated morphology of WPBs, and reduction or loss of these organelles entirely. Moreover, Wang *et al.* showed that in selected cases these defects can lead to reduced ability to generate long VWF strings upon release from the endothelium, which is expected to exacerbate bleeding complications in patients that already have reduced circulating VWF levels. Later studies focusing on ECFCs from VWD type 3 patients, as well as patients with mutations in the VWF propeptide region, the C-terminal cysteine knot domain or with large in-frame deletions, also reported retention of VWF in the ER in conjunction with reduced numbers of small, spherical WPBs (73–76), underlining that this is a common pathogenic mechanism in quantitative and qualitative VWD (Figure 2). Since unrestrained progression of VWF through the secretory pathway is important for the generation of sufficient numbers of elongated WPBs that are capable of secreting long VWF strings (77), any variant of VWF which causes (partial) retention in the ER can be expected to be accompanied by impaired secretory responses.

The VWD mutational spectrum also includes a large number of non-coding and splice site mutations for which the pathogenic mechanisms long remained elusive. An early study using VWD ECFCs detailed the mechanism by which a heterozygous 13 bp deletion in the *VWF* promoter in a VWD type 1 patient brought on reduced VWF transcript production from that allele, thereby showing for the first time how VWF promoter mutations can lead to quantitative VWF deficiencies (78). Additional studies using VWD patient ECFCs unraveled the pathogenic mechanisms of splice site mutations, a silent exonic mutation that led to intron retention and a deep intronic mutation (79–81). It is worth noting that some of these studies involving *VWF* mutations in non-coding regions or splice site mutations would have been impossible in ectopic expression systems.

VWD ECFCs have also been used to identify new genetic modifiers of *VWF* that could contribute to quantitative deficiencies of VWF. Two studies used transcriptomic analysis of ECFCs from patients with "Low VWF" and VWD type 1 (82,83), identifying the transcription factor friend leukaemia integration 1 (FLI1) and the microRNA miR-23b as potential modifiers of *VWF* transcription and stimulated VWF secretion, respectively. Such screenings are of a hypothesis-generating nature and will require further experimental validation of candidates to assess their biological and clinical relevance.

Finally, patient-derived ECFCs have significant potential as an ex vivo model for the development of new therapeutics for VWD, for instance as a platform to test strategies

for permanent or temporal correction of VWF defects. Proof of principle for phenotypic correction was shown in VWD type 3 dog ECFCs that were transduced with lentivirus carrying VWF cDNA (84). More recently, siRNAs targeting exonic single nucleotide polymorphisms (SNPs) in *VWF* were used to allele-selectively silence a heterozygous p.C1190Y mutation in ECFCs of a VWD type 2A patient, resulting in loss of mutant allele expression and phenotypic correction *ex vivo* (85). This could pave the way for more individualized approaches by using ECFCs as an *ex vivo* validation model for possible VWD treatments.

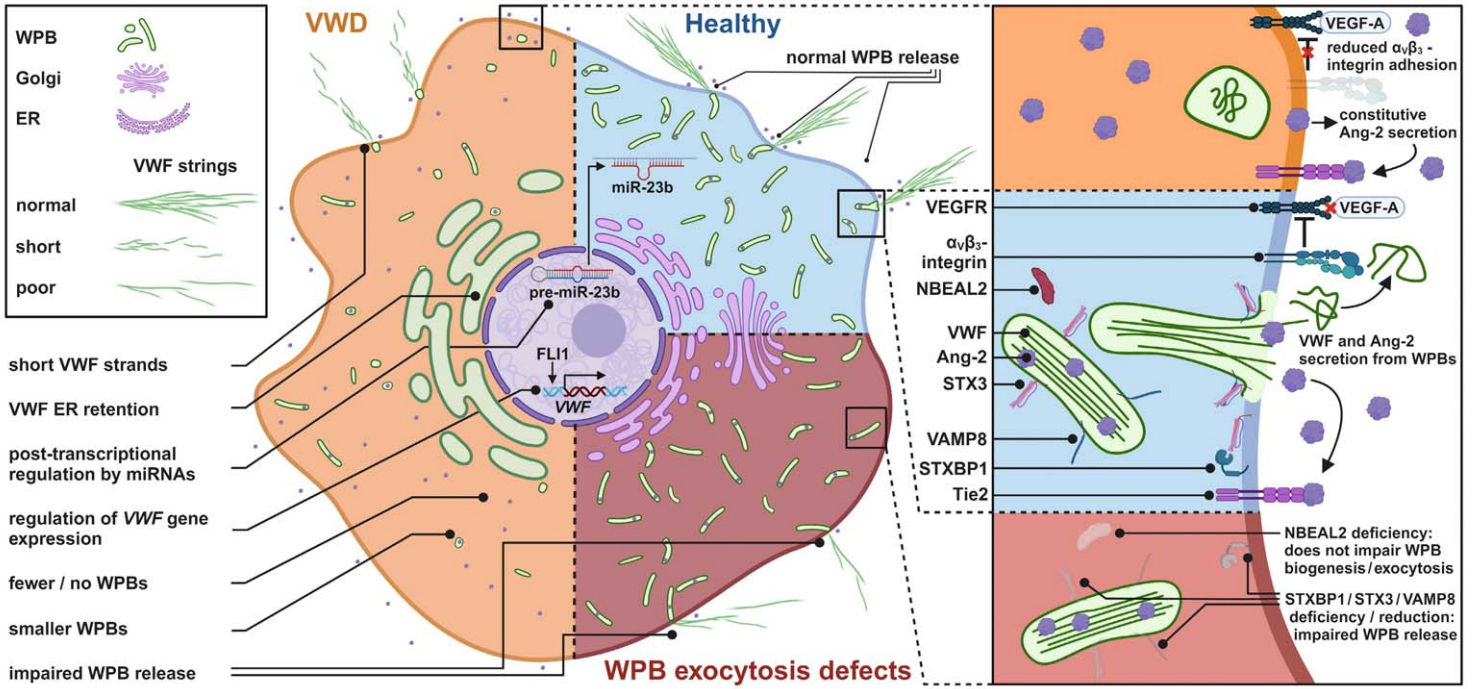

Figure 2. Insights into the pathophysiology of bleeding disorders from studying endothelial colony forming cells. The model depicts three states of an endothelial cell; in healthy condition (blue), when derived from a patient with VWD (orange) or in other disease where WPB secretion defects occur (red). On the right, a zoomed in panel displays components of the secretory pathway and how it may be affected in patients with bleeding disorders. αVβ3, alphaVbeta3-integrin; Ang-2, angiopoietin-2; ER, endoplasmic reticulum; FLI1, Friend leukemia integration 1; NBEAL2, Neurobeachin-Like 2; miR-23b, microRNA 23b; STX3, Syntaxin 3; STXBP1, Syntaxin-Binding Protein 1; VAMP8, Vesicle-Associated Membrane Protein 8; VEGF-A, Vascular Endothelial Growth Factor A; VEGFR, Vascular Endothelial Growth Factor Receptor; VWF, von Willebrand factor; VWD, von Willebrand disease WPB; Weibel-Palade body. Created with BioRender.com

ECFCs: von Willebrand disease and angiogenesis

Angiodysplastic lesions in the gastrointestinal (GI) tract are fragile vascular networks that are associated with recurrent GI bleeding, which can result in anemia and a decrease in quality of life (86). In up to 38% of VWD patients with GI bleeding, angiodysplastic lesions are present in the GI tract (87), which pose significant challenges in combination with the bleeding disorder (88). Angiodysplasia is the result of abnormal angiogenesis, the process that generates new blood vessels from existing vasculature. Directed migration and reorganization of endothelial cells during angiogenesis is highly dependent on growth factors such as vascular endothelial growth factor (VEGF) and Angiopoietin-1 and -2 (Ang-1 and Ang-2). VEGF is a potent stimulus of VWF secretion from WPBs (89), which also store the Tie2 receptor ligand Ang-2 and other pro-angiogenic components such as IGFBP7 (90,91). Targeted release of Ang-2 by exocytosis of WPBs activates autocrine and paracrine Tie2 signalling, which contributes to vessel lumen formation and shaping of new blood vessels (44,92,93). VWF is also a ligand for adhesion receptors such as $\alpha_V\beta$-3integrin, which is an important regulator of endothelial cell migration that can also quench VEGFR-2 signalling when in complex with ligands such as VWF (94). VWF binds a large array of pro-angiogenic growth factors via its heparin-binding domain (95), and also binds Ang-2 and IGFBP7 post-release (91,96,97), which may serve as a mechanism to focus these factors in areas of wound healing and active blood vessel formation.

The first evidence for a role in angiogenesis for VWF was presented by Starke and co-workers, who found increased migration, proliferation and angiogenesis in endothelial cells that were depleted of VWF using RNAi and in ECFCs from a cohort of VWD type 1, 2M and 2A patients (98). This was accompanied by reduced β3-integrin expression, reduced αVβ-3integrin-dependent adhesion and increased constitutive Ang2- secretion, possibly as a result of reduced intracellular retention of Ang2- due to loss of WPBs. A second study by Groeneveld et al. reported that compared to control ECFCs, most type 1 and type 2 VWD ECFCs had a slightly lower directionality of migration in a wound-healing assay, while VWD type 3 ECFCs, which are entirely devoid of VWF synthesis, had a higher migration velocity (99). However, no clear effects of *VWF* mutations on overall angiogenic potential were seen in this VWD cohort. Selvam *et al.* found wide variation in parameters such as migration, proliferation and tube formation in VWD patient-derived ECFCs, but also reported that type 1, 2 and some type 3 VWD ECFCs had significantly increased constitutive Ang-2 secretion compared to controls (100). A similar observation was made in cord blood ECFCs in which CRISPR/Cas9-mediated VWF gene knockout led to increased constitutive secretion of Ang-2 and association of Ang-2 with the Tie2 receptor (101). Since these cells are also devoid of WPBs and no longer capable of storing Ang-2, stimulus-induced Ang-2 release was severely reduced.

All together, these (patient-)ECFC based studies have provided some evidence for a role for VWF in angiogenesis (Figure 2). However, the exact function remains unclear perhaps due to the limitations of this model which are associated with the phenotypic heterogeneity and gradual loss of proliferative capacity of patient and control ECFCs.

ECFCs: Weibel-Palade body exocytosis defects and Storage Pool Disorders

The cellular machinery involved in biogenesis and secretion of WPBs is complex (30). Because regulated secretion is fundamental to the function of numerous different cell types, many components of the WPB machinery are also involved in similar secretory processes in non-endothelial cells. Defects in shared secretory components can therefore affect more than one cell type and may lead to complex, multi-system manifestations in patients. In several cases, endothelial cells isolated from rare patients with abnormalities in non-endothelial cell functions have contributed to identification and functional characterization of new regulators of WPB secretion (Figure 2). The SNARE proteins syntaxin-2 (STX2), STX3 and syntaxin-binding protein 1 (STXBP1) were identified as hits in an interactomic screen of downstream effectors of the Rab27A-Slp4-a complex in endothelial cells. *De novo* mutations in *STXBP1* are associated with early infantile epileptic encephalopathy type 4 (EIEE4), an epileptic disorder that is thought to result from impaired neurotransmitter release due to STXBP1 haploinsufficiency. In keeping with the defective secretory responses in neurons in these patients, STXBP1 haploinsufficient EIEE4 patient-derived ECFCs also showed severely impaired Ca^{2+}- and cAMP-mediated VWF secretion, confirming the role of STXBP1 in stimulus-induced WPB exocytosis (39). Homozygous nonsense mutations in *STX3* are causative for microvillus inclusion disease (MVID), a rare congenital disorder of the gut characterized by severe diarrhoea, which is the result of incorrect targeting of microvilli that normally migrate/move to the apical side of intestinal epithelial cells (102). MVID patient-derived ECFCs, which were entirely devoid of STX3, had reduced VWF and VWFpp secretion at submaximal stimulation and strikingly showed signs of loss of polarity of VWF and VWFpp release during basal secretion (42).

Storage Pool Disorders (SPDs) are a heterogeneous group of disorders that affect the formation of lysosome related organelles (LROs), which include platelet alpha- and dense granules, but also WPBs (103). Due to the universal mechanisms involved in the formation of LROs, SPDs often present as multi-system disorders and affect secretory function of both platelets and a variety of other cell types. Hermansky-Pudlak syndrome 2 (HPS2) is a rare genetic SPD characterized by interstitial lung disease, neutropenia and bleeding, which may find its origin in the lack of dense granules in platelets. HPS2 is caused by mutations in *AP3B1* which encodes for the beta subunit of the AP-3 complex, a cargo sorting complex that traffics secretory cargo and membrane

proteins from endosomes to LROs. Whole proteome analysis of ECFCs derived from HPS2 patients revealed that loss of the AP-3 complex due to compound heterozygous *AP3B1* mutations was accompanied by loss of VAMP8 (104). VAMP8 is an R-SNARE that cycles via an endosomal compartment to WPBs, where it supports exocytotic fusion of WPBs via interaction with plasma membrane based Q-SNAREs. Lacking VAMP8 on their WPBs, HPS2 ECFCs showed severely reduced stimulus-induced WPB exocytosis, suggesting that WPBs acquire secretion competence partly by recruitment of membrane proteins such as SNAREs from the endosomal compartment in an AP-3 dependent manner. It also indicates that the bleeding abnormalities that are seen in some SPDs and that were generally attributed to impaired platelet function, may in some cases be further compounded by decreased endothelial secretory responses. This can however not be extrapolated to all SPDs: Kat *et al.* found that NBEAL2–deficient ECFCs from patients with Gray Platelet Syndrome, a bleeding disorder characterized by loss of platelet alpha-granules as well as abnormalities in formation of secretory organelles in neutrophils, had normal biogenesis, maturation and exocytosis of WPBs (105). This also underscores the divergent mechanisms that control VWF storage in endothelial WPBs and in alpha-granules in megakaryocytes. In aforementioned studies, the ECFCs originate from individuals suffering from rare genetic disorders. While these results come from very small sample sizes, they can still be very useful to unravel complex cellular mechanisms of disease.

The road ahead for ECFCs

ECFCs are unique personalized endothelial model systems to study endothelial cell function in health and disease and have already led to major advances in our understanding of VWD and WPB biology (Figure 2). While they have generated great interest in the hemostasis community and various other focus areas of vascular biology, their use is still complicated by poor standardization of isolation and culturing methods and substantial intra- and inter-individual phenotypic variability. This can negatively impact the interpretability of experimental results, which for now may preclude their wider adaptation within the scientific community. Future efforts should be aimed at understanding the source of this variation and designing strategies that can prevent or minimize its impact on experimental outcome. Disease modeling using ECFCs, such as described here for VWD, has so far been limited to studying these cells in isolation using 2D cell culture platforms. To fully appreciate endothelial cell function within its authentic (patho-)physiological context, for instance within an injured blood vessel or during organotypic function, it is pertinent that the physical and chemical milieu that is induced by blood flow or neighbouring cells is present. Integration of ECFCs with vessel- or organ-on-a-chip technologies offers the exciting opportunity to develop miniature *ex vivo* personalized disease models that include the patient's own diseased endothelium.

Acknowledgements

The SYMPHONY consortium, which aims to orchestrate personalized treatment in patients with bleeding disorders, is a unique collaboration between patients, health care professionals, and translational and fundamental researchers specializing in inherited bleeding disorders, as well as experts from multiple disciplines (106). It aims to identify best treatment choice for each individual based on bleeding phenotype. To achieve this goal, work packages (WP) have been organized according to 3 themes (e.g. Diagnostics [WPs 3 and 4], Treatment [WPs 5–9], and Fundamental Research [WPs 10–12]). Principal investigator: M.H. Cnossen; project manager: S.H. Reitsma.

Beneficiaries of the SYMPHONY consortium: Erasmus University Medical Center-Sophia Children's Hospital, project leadership and coordination; Sanquin Diagnostics; Sanquin Research; Amsterdam University Medical Centers; University Medical Center Groningen; University Medical Center Utrecht; Leiden University Medical Center; Radboud University Medical Center; Netherlands Society of Hemophilia Patients (NVHP); Netherlands Society for Thrombosis and Hemostasis (NVTH); Bayer B.V., CSL Behring B.V., Swedish Orphan Biovitrum (Belgium) BVBA/SPRL.

Funding by SYMPHONY: NWO-NWA.1160.18.038 (received by SNJL, RB and JE) and Landsteiner Foundation for Blood Transfusion Research, LSBR-1707 and -2005 (received by RB).

References

1 Versteeg HH, Heemskerk JWM, Levi M, Reitsma PH. New fundamentals in hemostasis. Physiol Rev 2013; 93: 327–58.

2 Radomski M., Palmer RM., Moncada S. Endogenous Nitric Oxide Inhibits Human Platelet Adhesion To Vascular Endothelium. Lancet 1987; 330: 1057–8.

3 Moncada S, Higgs EA, Vane JR. Human arterial and venous tissues generate prostacyclin (prostaglandin x), a potent inhibitor of platelet aggregation. Lancet 1977; 1: 18–20.

4 Mast AE. Tissue Factor Pathway Inhibitor: Multiple Anticoagulant Activities for a Single Protein. Arterioscler Thromb Vasc Biol 2016; 36: 9–14.

5 Olson ST, Richard B, Izaguirre G, Schedin-Weiss S, Gettins PGW. Molecular mechanisms of antithrombin-heparin regulation of blood clotting proteinases. A paradigm for understanding proteinase regulation by serpin family protein proteinase inhibitors. Biochimie 2010; 92: 1587–96.

6 Esmon CT. The protein C pathway. Chest 2003; 124: 26S-32S.

7 Emeis JJ, Van Den Eijnden-Schrauwen Y, Van Den Hoogen CM, De Priester W, Westmuckett A, Lupu F. An endothelial storage granule for tissue-type plasminogen activator. J Cell Biol 1997; 139: 245–56.

8 Knipe L, Meli A, Hewlett L, Bierings R, Dempster J, Skehel P, Hannah MJ, Carter T. A revised model for the secretion of tPA and cytokines from cultured endothelial cells. Blood 2010; 116: 2183–91.

9 Longstaff C, Kolev K. Basic mechanisms and regulation of fibrinolysis. J Thromb Haemost 2015; 13: S98–105.

10 van Mourik JA, Lawrence DA, Loskutoff DJ. Purification of an inhibitor of plasminogen activator (antiactivator) synthesized by endothelial cells. J Biol Chem 1984; 259: 14914–21.

11 Morrow GB, Whyte CS, Mutch NJ. A Serpin With a Finger in Many PAIs: PAI-1's Central Function in Thromboinflammation and Cardiovascular Disease. Front Cardiovasc Med 2021; 8: 653655.

12 Plug T, Meijers JCM. Structure-function relationships in thrombin-activatable fibrinolysis inhibitor. J Thromb Haemost 2016; 14: 633–44.

13 Pipe SW, Montgomery RR, Pratt KP, Lenting PJ, Lillicrap D. Life in the shadow of a dominant partner: the FVIII-VWF association and its clinical implications for hemophilia A. Blood 2016; 128: 2007–16.

14 Ruggeri ZM. Von Willebrand factor, platelets and endothelial cell interactions. J Thromb Haemost 2003; 1: 1335–42.

15 Leebeek FWG, Eikenboom JCJ. Von Willebrand's Disease. N Engl J Med 2016; 375: 2067–80.

16 Atiq F, Blok R, van Kwawegen CB, Doherty D, Lavin M, van der Bom JG, O'Connell NM, de Meris J, Ryan K, Schols SEM, Byrne M, Heubel-Moenen FCJI, van Galen KPM, Preston RJS, Cnossen MH, Fijnvandraat K, Baker RI, Meijer K, James P, Di Paola J, et al. Type 1 VWD classification revisited: novel insights from combined analysis of the LoVIC and WiN studies. Blood 2024; 143: 1414–24.

17 de Jong A, Eikenboom J. Von Willebrand disease mutation spectrum and associated mutation mechanisms. Thromb Res 2017; 159: 65–75.

18 Atiq F, Boender J, van Heerde WL, Tellez Garcia JM, Schoormans SC, Krouwel S, Cnossen MH, Laros-van Gorkom BAP, de Meris J, Fijnvandraat K, van der Bom JG, Meijer K, van Galen KPM, Eikenboom J, Leebeek FWG. Importance of Genotyping in von Willebrand Disease to Elucidate Pathogenic Mechanisms and Variability in Phenotype. HemaSphere 2022; 6: e718.
19 James PD, Notley C, Hegadorn C, Leggo J, Tuttle A, Tinlin S, Brown C, Andrews C, Labelle A, Chirinian Y, O'Brien L, Othman M, Rivard G, Rapson D, Hough C, Lillicrap D. The mutational spectrum of type 1 von Willebrand disease: results from a Canadian cohort study. Blood 2007; 109: 145–54.
20 Goodeve A, Eikenboom J, Castaman G, Rodeghiero F, Federici AB, Batlle J, Meyer D, Mazurier C, Goudemand J, Schneppenheim R, Budde U, Ingerslev J, Habart D, Vorlova Z, Holmberg L, Lethagen S, Pasi J, Hill F, Soteh MH, Baronciani L, et al. Phenotype and genotype of a cohort of families historically diagnosed with type 1 von Willebrand disease in the European study, Molecular and Clinical Markers for the Diagnosis and Management of Type 1 von Willebrand Disease (MCMDM-1VWD). Blood 2007; 109: 112–21.
21 Lavin M, Aguila S, Schneppenheim S, Dalton N, Jones KL, O'Sullivan JM, O'Connell NM, Ryan K, White B, Byrne M, Rafferty M, Doyle MM, Nolan M, Preston RJS, Budde U, James P, Di Paola J, O'Donnell JS. Novel insights into the clinical phenotype and pathophysiology underlying low VWF levels. Blood 2017; 130: 2344–53.
22 Swystun LL, Lillicrap D. Genetic regulation of plasma von Willebrand factor levels in health and disease. J Thromb Haemost 2018; 16: 2375–90.
23 Kanaji S, Fahs SA, Shi Q, Haberichter SL, Montgomery RR. Contribution of platelet vs. endothelial VWF to platelet adhesion and hemostasis. J Thromb Haemost 2012; 10: 1646–52.
24 Zhou Y-F, Eng ET, Zhu J, Lu C, Walz T, Springer TA. Sequence and structure relationships within von Willebrand factor. Blood 2012; 120: 449–58.
25 Huang R-H, Wang Y, Roth R, Yu X, Purvis AR, Heuser JE, Egelman EH, Sadler JE. Assembly of Weibel Palade body-like tubules from N-terminal domains of von Willebrand factor. Proc Natl Acad Sci 2008; 105: 482–7.
26 Berriman JA, Li S, Hewlett LJ, Wasilewski S, Kiskin FN, Carter T, Hannah MJ, Rosenthal PB. Structural organization of Weibel-Palade bodies revealed by cryo-EM of vitrified endothelial cells. Proc Natl Acad Sci 2009; 106: 17407–12.
27 Zeng J, Shu Z, Liang Q, Zhang J, Wu W, Wang X, Zhou A. Structural basis of von Willebrand factor multimerization and tubular storage. Blood 2022; 139: 3314–24.
28 Weibel ER, Palade GE. NEW CYTOPLASMIC COMPONENTS IN ARTERIAL ENDOTHELIA. J Cell Biol 1964; 23: 101–12.
29 Schillemans M, Karampini E, Kat M, Bierings R. Exocytosis of Weibel–Palade bodies: how to unpack a vascular emergency kit. J Thromb Haemost 2019; 17: 6–18.
30 Hordijk S, Carter T, Bierings R. A new look at an old body: molecular determinants of Weibel-Palade body composition and von Willebrand factor exocytosis. J Thromb Haemost 2024; 22: 1290–303.
31 Kat M, Karampini E, Hoogendijk AJ, Bürgisser PE, Mulder AA, Van Alphen FPJ, Olins J, Geerts D, Van den Biggelaar M, Margadant C, Voorberg J, Bierings R. Syntaxin 5 determines Weibel-Palade body size and von Willebrand factor secretion by controlling Golgi architecture. Haematologica 2022; 107: 1827–39.
32 Bierings R, Hellen N, Kiskin N, Knipe L, Fonseca A-V, Patel B, Meli A, Rose M, Hannah MJ, Carter T. The interplay between the Rab27A effectors Slp4-a and MyRIP controls hormone-evoked Weibel-Palade body exocytosis. Blood 2012; 120: 2757–67.

33 Erent M, Meli A, Moisoi N, Babich V, Hannah MJ, Skehel P, Knipe L, Zupancic G, Ogden D, Carter TD. Rate, extent and concentration-dependence of histamine-evoked Weibel-Palade body exocytosis determined from individual fusion events in human endothelial cells. J Physiol 2007; 583: 195-212.
34 Hannah MJ, Hume AN, Arribas M, Williams R, Hewlett LJ, Seabra MC, Cutler DF. Weibel-Palade bodies recruit Rab27 by a content-driven, maturation-dependent mechanism that is independent of cell type. J Cell Sci 2003; 116: 3939–48.
35 Knop M, Aareskjold E, Bode G, Gerke V. Rab3D and annexin A2 play a role in regulated secretion of vWF, but not tPA, from endothelial cells. EMBO J 2004; 23: 2982–92.
36 Kat M, Bürgisser PE, Janssen H, De Cuyper IM, Conte IL, Hume AN, Carter T, Voorberg J, Margadant C, Bierings R. GDP/GTP exchange factor MADD drives activation and recruitment of secretory Rab GTPases to Weibel-Palade bodies. Blood Adv 2021; 5: 5116–27.
37 Nightingale TD, Pattni K, Hume AN, Seabra MC, Cutler DF. Rab27a and MyRIP regulate the amount and multimeric state of VWF released from endothelial cells. Blood 2009; 113: 5010–8.
38 Terglane J, Menche D, Gerke V. Acidification of endothelial Weibel-Palade bodies is mediated by the vacuolar-type H+-ATPase. PLoS One 2022; 17: e0270299.
39 Van Breevoort D, Snijders AP, Hellen N, Weckhuysen S, van Hooren KWEM, Eikenboom J, Valentijn K, Fernandez-Borja M, Ceulemans B, De Jonghe P, Voorberg J, Hannah M, Carter T, Bierings R. STXBP1 promotes Weibel-Palade body exocytosis through its interaction with the Rab27A effector Slp4-a. Blood 2014; 123: 3185–94.
40 Conte IL, Hellen N, Bierings R, Mashanov GI, Manneville J-B, Kiskin NI, Hannah MJ, Molloy JE, Carter T. Interaction between MyRIP and the actin cytoskeleton regulates Weibel–Palade body trafficking and exocytosis. J Cell Sci 2016; 129: 592–603.
41 Chehab T, Santos NC, Holthenrich A, Koerdt SN, Disse J, Schuberth C, Nazmi AR, Neeft M, Koch H, Man KNM, Wojcik SM, Martin TFJ, van der Sluijs P, Brose N, Gerke V. A novel Munc13-4/S100A10/annexin A2 complex promotes Weibel-Palade body exocytosis in endothelial cells. Mol Biol Cell 2017; 28: 1688–700.
42 Schillemans M, Karampini E, van den Eshof BL, Gangaev A, Hofman M, van Breevoort D, Meems H, Janssen H, Mulder AA, Jost CR, Escher JC, Adam R, Carter T, Koster AJ, van den Biggelaar M, Voorberg J, Bierings R. Weibel-Palade Body Localized Syntaxin-3 Modulates Von Willebrand Factor Secretion From Endothelial Cells. Arterioscler Thromb Vasc Biol 2018; 38: 1549–61.
43 Lenzi C, Stevens J, Osborn D, Hannah MJ, Bierings R, Carter T. Synaptotagmin 5 regulates Ca 2+ -dependent Weibel–Palade body exocytosis in human endothelial cells. J Cell Sci 2019; 132: jcs221952.
44 Francis CR, Claflin S, Kushner EJ. Synaptotagmin-Like Protein 2a Regulates Angiogenic Lumen Formation via Weibel-Palade Body Apical Secretion of Angiopoietin-2. Arterioscler Thromb Vasc Biol 2021; 41: 1972–86.
45 Holthenrich A, Terglane J, Naß J, Mietkowska M, Kerkhoff E, Gerke V. Spire1 and Myosin Vc promote Ca2+-evoked externalization of von Willebrand factor in endothelial cells. Cell Mol Life Sci 2022; 79: 96.
46 Naß J, Koerdt SN, Biesemann A, Chehab T, Yasuda T, Fukuda M, Martín-Belmonte F, Gerke V. Tip-end fusion of a rod-shaped secretory organelle. Cell Mol Life Sci 2022; 79: 344.

47 Smith NL, Chen M-H, Dehghan A, Strachan DP, Basu S, Soranzo N, Hayward C, Rudan I, Sabater-Lleal M, Bis JC, de Maat MPM, Rumley A, Kong X, Yang Q, Williams FMK, Vitart V, Campbell H, Mälarstig A, Wiggins KL, Van Duijn CM, et al. Novel Associations of Multiple Genetic Loci With Plasma Levels of Factor VII, Factor VIII, and von Willebrand Factor. Circulation 2010; 121: 1382–92.

48 Desch KC, Ozel AB, Siemieniak D, Kalish Y, Shavit J a, Thornburg CD, Sharathkumar A a, McHugh CP, Laurie CC, Crenshaw A, Mirel DB, Kim Y, Cropp CD, Molloy AM, Kirke PN, Bailey-Wilson JE, Wilson AF, Mills JL, Scott JM, Brody LC, et al. Linkage analysis identifies a locus for plasma von Willebrand factor undetected by genome-wide association. Proc Natl Acad Sci 2013; 110: 588–93.

49 Van Loon J, Dehghan A, Weihong T, Trompet S, McArdle WL, Asselbergs FW, Chen M-HH, Lopez LM, Huffman JE, Leebeek FWG, Basu S, Stott DJ, Rumley A, Gansevoort RT, Davies G, Wilson JJFF, Witteman JCMM, Cao X, de Craen AJMM, Bakker SJLL, et al. Genome-wide association studies identify genetic loci for low von Willebrand factor levels. Eur J Hum Genet 2016; 24: 1035–40.

50 Schillemans M, Karampini E, Hoogendijk AJ, Wahedi M, van Alphen FPJ, van den Biggelaar M, Voorberg J, Bierings R. Interaction networks of Weibel-Palade body regulators syntaxin-3 and syntaxin binding protein 5 in endothelial cells. J Proteomics 2019; 205: 103417.

51 Hannah MJ, Williams R, Kaur J, Hewlett LJ, Cutler DF. Biogenesis of Weibel–Palade bodies. Semin Cell Dev Biol 2002; 13: 313–24.

52 Michaux G, Hewlett LJ, Messenger SL, Goodeve AC, Peake IR, Daly ME, Cutler DF. Analysis of intracellular storage and regulated secretion of 3 von Willebrand disease–causing variants of von Willebrand factor. Blood 2003; 102: 2452–8.

53 van den Biggelaar M, Meijer AB, Voorberg J, Mertens K. Intracellular cotrafficking of factor VIII and von Willebrand factor type 2N variants to storage organelles. Blood 2009; 113: 3102–9.

54 Wang J-W, Valentijn KM, de Boer HC, Dirven RJ, van Zonneveld AJ, Koster AJ, Voorberg J, Reitsma PH, Eikenboom J. Intracellular Storage and Regulated Secretion of Von Willebrand Factor in Quantitative Von Willebrand Disease. J Biol Chem 2011; 286: 24180–8.

55 de Boer S, Laan S, Dirven R, Eikenboom J. Approaches to induce the maturation process of human induced pluripotent stem cell derived-endothelial cells to generate a robust model. Aly RM, editor. PLoS One 2024; 19: e0297465.

56 Lin Y, Weisdorf DJ, Solovey a, Hebbel RP. Origins of circulating endothelial cells and endothelial outgrowth from blood. J Clin Invest 2000; 105: 71–7.

57 Medina RJ, Barber CL, Sabatier F, Dignat-George F, Melero-Martin JM, Khosrotehrani K, Ohneda O, Randi AM, Chan JKY, Yamaguchi T, Van Hinsbergh VWM, Yoder MC, Stitt AW. Endothelial Progenitors: A Consensus Statement on Nomenclature. Stem Cells Transl Med 2017; 6: 1316–20.

58 Smadja DM. Vasculogenic Stem and Progenitor Cells in Human: Future Cell Therapy Product or Liquid Biopsy for Vascular Disease. Advances in experimental medicine and biology. 2019. p. 215–37.

59 Zhang Q, Cannavicci A, Kutryk MJB. Exploring Endothelial Colony-Forming Cells to Better Understand the Pathophysiology of Disease: An Updated Review. Stem Cells Int 2022; 2022: 1–14.

60 Tura O, Skinner EM, Barclay GR, Samuel K, Gallagher RCJ, Brittan M, Hadoke PWF, Newby DE, Turner ML, Mills NL. Late Outgrowth Endothelial Cells Resemble Mature Endothelial Cells and Are Not Derived from Bone Marrow. Stem Cells 2013; 31: 338–48.

61 Lin Y, Banno K, Gil C-H, Myslinski J, Hato T, Shelley WC, Gao H, Xuei X, Liu Y, Basile DP, Yoshimoto M, Prasain N, Tarnawsky SP, Adams RH, Naruse K, Yoshida J, Murphy MP, Horie K, Yoder MC. Origin, prospective identification, and function of circulating endothelial colony-forming cells in mice and humans. JCI Insight 2023; 8: e164781.
62 Martin-Ramirez J, Hofman M, van den Biggelaar M, Hebbel RP, Voorberg J. Establishment of outgrowth endothelial cells from peripheral blood. Nat Protoc 2012; 7: 1709–15.
63 Smadja DM, Melero-Martin JM, Eikenboom J, Bowman M, Sabatier F, Randi AM. Standardization of methods to quantify and culture endothelial colony-forming cells derived from peripheral blood. J Thromb Haemost 2019; 17: 1190–4.
64 Ingram DA, Mead LE, Tanaka H, Meade V, Fenoglio A, Mortell K, Pollok K, Ferkowicz MJ, Gilley D, Yoder MC. Identification of a novel hierarchy of endothelial progenitor cells using human peripheral and umbilical cord blood. Blood 2004; 104: 2752–60.
65 van Beem RT, Verloop RE, Kleijer M, Noort WA, Loof N, Koolwijk P, van der Schoot CE, van Hinsbergh VWMM, Zwaginga JJ. Blood outgrowth endothelial cells from cord blood and peripheral blood: angiogenesis-related characteristics in vitro. J Thromb Haemost 2009; 7: 217–26.
66 Béland S, Désy O, Bouchard-Boivin F, Gama A, De Serres SA. Endothelial colony forming cells generated from cryopreserved peripheral blood mononuclear cells. Hum Immunol 2021; 82: 309–14.
67 de Jong A, Weijers E, Dirven R, de Boer S, Streur J, Eikenboom J. Variability of von Willebrand factor-related parameters in endothelial colony forming cells. J Thromb Haemost 2019; 17: 1544–54.
68 de Boer S, Bowman M, Notley C, Mo A, Lima P, de Jong A, Dirven R, Weijers E, Lillicrap D, James P, Eikenboom J. Endothelial characteristics in healthy endothelial colony forming cells; generating a robust and valid ex vivo model for vascular disease. J Thromb Haemost 2020; 18: 2721–31.
69 Laan SNJ, de Boer S, Dirven RJ, van Moort I, Kuipers TB, Mei H, Bierings R, Eikenboom J, SYMPHONY consortium. Transcriptional and functional profiling identifies inflammation and endothelial-to-mesenchymal transition as potential drivers for phenotypic heterogeneity within a cohort of endothelial colony forming cells. J Thromb Haemost 2024; in press.
70 Berber E, James PD, Hough C, Lillicrap D. An assessment of the pathogenic significance of the R924Q von Willebrand factor substitution. J Thromb Haemost 2009; 7: 1672–9.
71 Starke RD, Paschalaki KE, Dyer CEF, Harrison-Lavoie KJ, Cutler JA, McKinnon TAJ, Millar CM, Cutler DF, Laffan MA, Randi AM. Cellular and molecular basis of von Willebrand disease: studies on blood outgrowth endothelial cells. Blood 2013; 121: 2773–84.
72 Wang JW, Bouwens EAM, Pintao MC, Voorberg J, Safdar H, Valentijn KM, De Boer HC, Mertens K, Reitsma PH, Eikenboom J. Analysis of the storage and secretion of von Willebrand factor in blood outgrowth endothelial cells derived from patients with von Willebrand disease. Blood 2013; 121: 2762–72.
73 Bowman ML, Pluthero FG, Tuttle A, Casey L, Li L, Christensen H, Robinson KS, Lillicrap D, Kahr WHA, James P. Discrepant platelet and plasma von Willebrand factor in von Willebrand disease patients with p.Pro2808Leufs*24. J Thromb Haemost 2017; 15: 1403–11.
74 Bowman M, Casey L, Selvam SN, Lima PDA, Rawley O, Hinds M, Tuttle A, Grabell J, Iorio A, Walker I, Lillicrap D, James P. von Willebrand factor propeptide variants lead to impaired storage and ER retention in patient-derived endothelial colony-forming cells. J Thromb Haemost 2022; 20: 1599–609.

75 Okamoto S, Tamura S, Sanda N, Odaira K, Hayakawa Y, Mukaide M, Suzuki A, Kanematsu T, Hayakawa F, Katsumi A, Kiyoi H, Kojima T, Matsushita T, Suzuki N. VWF-Gly2752Ser, a novel non-cysteine substitution variant in the CK domain, exhibits severe secretory impairment by hampering C-terminal dimer formation. J Thromb Haemost 2022; 20: 1784–96.
76 Yadegari H, Jamil MA, Muller J, Marquardt N, Rawley O, Budde U, El-Maarri O, Lillicrap D, Oldenburg J. Multifaceted pathomolecular mechanism of a VWF large deletion involved in the pathogenesis of severe VWD. Blood Adv 2022; 6: 1038–53.
77 Kat M, Margadant C, Voorberg J, Bierings R. Dispatch and delivery at the ER–Golgi interface: how endothelial cells tune their hemostatic response. FEBS J 2022; 289: 6863–70.
78 Othman M, Chirinian Y, Brown C, Notley C, Hickson N, Hampshire D, Buckley S, Waddington S, Parker AL, Baker A, James P, Lillicrap D. Functional characterization of a 13-bp deletion (c.-1522-–1510del13) in the promoter of the von Willebrand factor gene in type 1 von Willebrand disease. Blood 2010; 116: 3645–52.
79 Hawke L, Bowman ML, Poon M-C, Scully M-F, Rivard G-E, James PD. Characterization of aberrant splicing of von Willebrand factor in von Willebrand disease: an underrecognized mechanism. Blood 2016; 128: 584–93.
80 Yadegari H, Biswas A, Akhter MS, Driesen J, Ivaskevicius V, Marquardt N, Oldenburg J. Intron retention resulting from a silent mutation in the VWF gene that structurally influences the 5′ splice site. Blood 2016; 128: 2144–52.
81 Yadegari H, Jamil MA, Marquardt N, Oldenburg J. A Homozygous Deep Intronic Variant Causes Von Willebrand Factor Deficiency and Lack of Endothelial-Specific Secretory Organelles, Weibel–Palade Bodies. Int J Mol Sci 2022; 23: 3095.
82 Ng CJ, Liu A, Venkataraman S, Ashworth KJ, Baker CD, O'Rourke R, Vibhakar R, Jones KL, Di Paola J. Single-cell transcriptional analysis of human endothelial colony-forming cells from patients with low VWF levels. Blood 2022; 139: 2240–51.
83 Kloosterman R, Zago-Schmitt M, Grabell J, Thibeault L, De Lima PA, Bowman M, Tyryshkin K, Hindmarch CCT, Renwick N, James P. A transcriptome analysis of basal and stimulated VWF release from endothelial cells derived from patients with type 1 VWD. Blood Adv 2023; 7: 1477–87.
84 De Meyer SF, Vanhoorelbeke K, Chuah MK, Pareyn I, Gillijns V, Hebbel RP, Collen D, Deckmyn H, VandenDriessche T. Phenotypic correction of von Willebrand disease type 3 blood-derived endothelial cells with lentiviral vectors expressing von Willebrand factor. Blood 2006; 107: 4728–36.
85 de Jong A, Dirven RJ, Boender J, Atiq F, Anvar SY, Leebeek FWGG, Van Vlijmen BJMM, Eikenboom J. Ex vivo Improvement of a von Willebrand Disease Type 2A Phenotype Using an Allele-Specific Small-Interfering RNA. Thromb Haemost 2020; 120: 1569–79.
86 Randi AM, Smith KE, Castaman G. von Willebrand factor regulation of blood vessel formation. Blood 2018; 132: 132–40.
87 Makris M, Federici AB, Mannucci PM, Bolton-Maggs PHB, Yee TT, Abshire T, Berntorp E. The natural history of occult or angiodysplastic gastrointestinal bleeding in von Willebrand disease. Haemophilia 2015; 21: 338–42.
88 Ocran E, Chornenki NLJ, Bowman M, Sholzberg M, James P. Gastrointestinal bleeding in von Willebrand patients: special diagnostic and management considerations. Expert Rev Hematol 2023; 16: 575–84.

89 Lorenzi O, Frieden M, Villemin P, Fournier M, Foti M, Vischer UM. Protein kinase C-delta mediates von Willebrand factor secretion from endothelial cells in response to vascular endothelial growth factor (VEGF) but not histamine. J Thromb Haemost 2008; 6: 1962–9.
90 Fiedler U, Scharpfenecker M, Koidl S, Hegen A, Grunow V, Schmidt JM, Kriz W, Thurston G, Augustin HG. The Tie-2 ligand Angiopoietin-2 is stored in and rapidly released upon stimulation from endothelial cell Weibel-Palade bodies. Blood 2004; 103: 4150–6.
91 van Breevoort D, van Agtmaal EL, Dragt BS, Gebbinck JK, Dienava-Verdoold I, Kragt A, Bierings R, Horrevoets AJG, Valentijn KM, Eikenboom JC, Fernandez-Borja M, Meijer AB, Voorberg J. Proteomic Screen Identifies IGFBP7 as a Novel Component of Endothelial Cell-Specific Weibel-Palade Bodies. J Proteome Res 2012; 11: 2925–36.
92 Pergolizzi M, Bizzozero L, Riccitelli E, Pascal D, Samarelli AV, Bussolino F, Arese M. Modulation of Angiopoietin 2 release from endothelial cells and angiogenesis by the synaptic protein Neuroligin 2. Biochem Biophys Res Commun 2018; 501: 165–71.
93 Cossutta M, Darche M, Carpentier G, Houppe C, Ponzo M, Raineri F, Vallée B, Gilles M-E, Villain D, Picard E, Casari C, Denis C, Paques M, Courty J, Cascone I. Weibel-Palade Bodies Orchestrate Pericytes During Angiogenesis. Arterioscler Thromb Vasc Biol 2019; 39: 1843–58.
94 Somanath PR, Malinin NL, Byzova T V. Cooperation between integrin alphavbeta3 and VEGFR2 in angiogenesis. Angiogenesis 2009; 12: 177–85.
95 Ishihara J, Ishihara A, Starke RD, Peghaire CR, Smith KE, McKinnon TAJ, Tabata Y, Sasaki K, White MJ V., Fukunaga K, Laffan MA, Lutolf MP, Randi AM, Hubbell JA. The heparin binding domain of von Willebrand factor binds to growth factors and promotes angiogenesis in wound healing. Blood 2019; 133: 2559–69.
96 Mobayen G, Smith K, Ediriwickrema K, Starke RD, Solomonidis EG, Laffan MA, Randi AM, McKinnon TAJ. von Willebrand factor binds to angiopoietin-2 within endothelial cells and after release from Weibel–Palade bodies. J Thromb Haemost 2023; 21: 1802–12.
97 Texier A, Lenting PJ, Denis C V., Roullet S, Christophe OD. Angiopoietin-2 binds to multiple interactive sites within von Willebrand factor. Res Pract Thromb Haemost 2023; 7: 102204.
98 Starke RD, Ferraro F, Paschalaki KE, Dryden NH, McKinnon TA, Sutton RE, Payne EM, Haskard DO, Hughes AD, Cutler DF, Laffan M a, Randi AM. Endothelial von Willebrand factor regulates angiogenesis. Blood 2011; 117: 1071–80.
99 Groeneveld DJ, van Bekkum T, Dirven RJ, Wang J-W, Voorberg J, Reitsma PH, Eikenboom J. Angiogenic characteristics of blood outgrowth endothelial cells from patients with von Willebrand disease. J Thromb Haemost 2015; 13: 1854–66.
100 Selvam SN, Casey LJ, Bowman ML, Hawke LG, Longmore AJ, Mewburn J, Ormiston ML, Archer SL, Maurice DH, James P. Abnormal angiogenesis in blood outgrowth endothelial cells derived from von Willebrand disease patients. Blood Coagul Fibrinolysis 2017; 28: 521–33.
101 Schillemans M, Kat M, Westeneng J, Gangaev A, Hofman M, Nota B, van Alphen FPJJ, de Boer M, van den Biggelaar M, Margadant C, Voorberg J, Bierings R. Alternative trafficking of Weibel-Palade body proteins in CRISPR/Cas9-engineered von Willebrand factor-deficient blood outgrowth endothelial cells. Res Pract Thromb Haemost 2019; 3: 718–32.
102 Wiegerinck CL, Janecke AR, Schneeberger K, Vogel GF, van Haaften-Visser DY, Escher JC, Adam R, Thöni CE, Pfaller K, Jordan AJ, Weis C-A, Nijman IJ, Monroe GR, van Hasselt PM, Cutz E, Klumperman J, Clevers H, Nieuwenhuis EES, Houwen RHJ, van Haaften G, et al. Loss of syntaxin 3 causes variant microvillus inclusion disease. Gastroenterology 2014; 147: 65-68. e10.

103 Karampini E, Bierings R, Voorberg J. Orchestration of Primary Hemostasis by Platelet and Endothelial Lysosome-Related Organelles. Arterioscler Thromb Vasc Biol 2020; 40: 1441–53.
104 Karampini E, Schillemans M, Hofman M, van Alphen F, de Boer M, Kuijpers TW, van den Biggelaar M, Voorberg J, Bierings R. Defective AP-3-dependent VAMP8 trafficking impairs Weibel-Palade body exocytosis in Hermansky-Pudlak Syndrome type 2 blood outgrowth endothelial cells. Haematologica 2019; 104: 2091–9.
105 Kat M, van Moort I, Bürgisser PE, Kuijpers TW, Hofman M, Favier M, Favier R, Margadant C, Voorberg J, Bierings R. Mutations in Neurobeachin-like 2 do not impact Weibel-Palade body biogenesis and von Willebrand factor secretion in gray platelet syndrome Endothelial Colony Forming Cells. Res Pract Thromb Haemost 2023; 7: 100086.
106 Cnossen MH, van Moort I, Reitsma SH, de Maat MPM, Schutgens REG, Urbanus RT, Lingsma HF, Mathot RAA, Gouw SC, Meijer K, Bredenoord AL, van der Graaf R, Fijnvandraat K, Meijer AB, van den Akker E, Bierings R, Eikenboom JCJ, van den Biggelaar M, de Haas M, Voorberg J, et al. SYMPHONY consortium: Orchestrating personalized treatment for patients with bleeding disorders. J Thromb Haemost 2022; 20: 2001–11.

Automated segmentation and quantitative analysis of organelle morphology, localization and content using CellProfiler

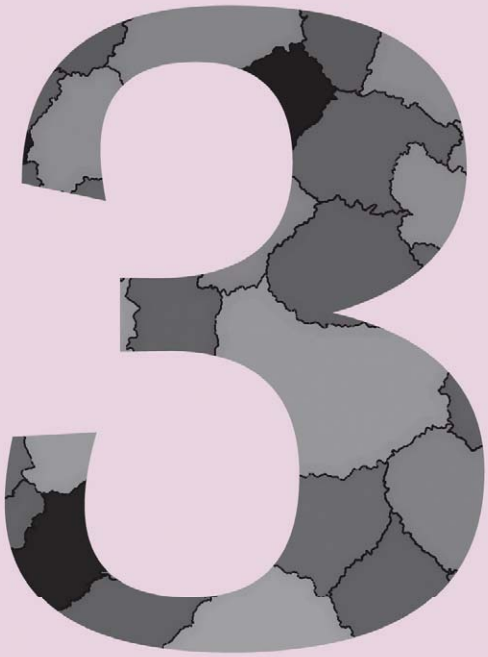

Laan SNJ, Dirven RJ, Bürgisser PE, Eikenboom J, Bierings R

PLoS One. 2023 Jun 14;18(6):e0278009.
doi: 10.1371/journal.pone.0278009

Abstract

One of the most used and versatile methods to study number, dimensions, content and localization of secretory organelles is confocal microscopy analysis. However, considerable heterogeneity exists in the number, size and shape of secretory organelles that can be present in the cell. One thus needs to analyze large numbers of organelles for valid quantification. Properly evaluating these parameters requires an automated, unbiased method to process and quantitatively analyze microscopy data. Here, we describe two pipelines, run by CellProfiler software, called OrganelleProfiler and OrganelleContentProfiler. These pipelines were used on confocal images of endothelial colony forming cells (ECFCs), which contain unique secretory organelles called Weibel-Palade bodies (WPBs), and on early endosomes in ECFCs and human embryonic kidney 293T (HEK293T) cells. Results show that the pipelines can quantify the cell count, size, organelle count, organelle size, shape, relation to cells and nuclei, and distance to these objects in both endothelial and HEK293T cells. Additionally, the pipelines were used to measure the reduction in WPB size after disruption of the Golgi and to quantify the perinuclear clustering of WPBs after triggering of cAMP-mediated signaling pathways in ECFCs. Furthermore, the pipeline is able to quantify secondary signals located in or on the organelle or in the cytoplasm, such as the small WPB GTPase Rab27A. Cell profiler measurements were checked for validity using Fiji. To conclude, these pipelines provide a powerful, high-processing quantitative tool for the characterization of multiple cell and organelle types. These pipelines are freely available and easily editable for use on different cell types or organelles.

Introduction

Eukaryotic cells are compartmentalized into organelles, subcellular entities separated from the cytoplasm by a limiting membrane that enable them to more efficiently carry out specialized functions in the cell, such as energy production and protein synthesis, transport and degradation. A specific class of organelles consists of secretory vesicles, which serve to temporarily store and then rapidly secrete molecules into the extracellular space on demand. Secretory organelles are vital to maintaining homeostasis, as they allow a cell to communicate with other, distant cells or to respond to immediate changes in its environment, such as in the case of injury or when encountering pathogens. Their function is often defined by the content that is secreted, which is cell type and context specific, and depends on a sufficient magnitude of release, which directly relates to the number and dimensions of the secretory organelles that can undergo exocytosis. Moreover, the intracellular location of secretory organelles in relation to their site of biogenesis (i.e. the Golgi apparatus), filaments of the cytoskeleton and the plasma membrane also indirectly determines their exocytotic behavior.

Weibel-Palade bodies (WPBs) are cigar-shaped endothelial cell specific secretory organelles that contain a cocktail of vasoactive molecules that are released into the circulation in response to vascular injury or stress (1). WPBs owe their typical elongated morphology to the condensation of its main cargo protein, the hemostatic protein Von Willebrand factor (VWF), into organized parallel tubules that unfurl into long platelet-adhesive strings upon release (2). The size and shape of WPBs are of interest from a biological and medical perspective as they correlate with the hemostatic activity of the VWF strings that are released (3) and can be reflective of disease states, such as in the bleeding disorder von Willebrand disease (VWD) (4). A model frequently used to study the pathophysiology of vascular diseases like VWD is the endothelial colony forming cell (ECFC). A major advantage of this model is that ECFCs can be derived from whole blood of patients, which allows analysis of patient endothelial cell function, WPB morphology and secretion *ex vivo*. However, substantial phenotypic heterogeneity can exist between ECFCs (5, 6), which stresses the need for robust quantitative analytical methods to evaluate their phenotype.

One of the most used and versatile methods to study number, dimensions, content and localization of secretory organelles is confocal microscopy analysis. However, as with all biological samples, considerable variability exists in the number, size and shapes of secretory organelles that can be present in the cell. One thus needs to analyze large numbers of organelles while ideally collecting this information in such a manner that it can be analyzed in a cell-by-cell manner. The crowded intracellular environment

in combination with optical and immunostaining limitations presents an additional, technical challenge to separate individual organelles, which often precludes analysis on single organelle detail. Proper evaluation of these parameters requires an automated, unbiased method to process and quantitatively analyze microscopy data.

Here we describe 2 pipelines developed in CellProfiler (7), a free, easy to use image analysis software that uses separate module-based programming, for the identification, quantification and morphological analysis of secretory organelles within endothelial cells. The automated analysis pipeline OrganelleProfiler (OP) segments cells, organelles, nuclei and cell membranes from microscopy images, quantifies number, location, size and shape of organelles and extracts these data per cell and relative to the location of nucleus and perimeter of the cell. The function of the OrganelleProfiler pipeline is demonstrated by automated analysis of WPBs in 2 previously established phenotypic classes of healthy donor ECFCs (6), which identifies clear differences in number, length, eccentricity and intracellular localization of WPBs, and by morphometric analysis of early endosomes in ECFCs and HEK293T cells. Furthermore, the OrganelleProfiler was able to measure reduction in WPB size after Golgi ribbon disruption and to quantify perinuclear clustering of WPBs after stimulation with cAMP-mediated agonists. A second pipeline, called OrganelleContentProfiler (OCP), expands on the capabilities of the OrganelleProfiler by offering additional modules to measure the intensity of proteins of the secretory pathway both inside and outside the WPB, which we illustrate by analyzing the presence of the WPB GTPase Rab27A (8-10) and the endoplasmic reticulum marker protein disulfide isomerase (PDI).

Our CellProfiler pipelines provide robust and unbiased quantitative analysis tools for WPB morphometrics and can, with minimal adaptation, also be used to obtain quantitative data for other organelles and/or other cellular systems.

Materials & Methods

Endothelial Colony Forming Cells and Ethical Approval

The study protocols for acquisition of ECFCs were approved by the Leiden University Medical Center and Erasmus MC ethics review boards. Informed consent was obtained from 4 subjects in accordance with the Declaration of Helsinki. Healthy participants were 18 years or older and had not been diagnosed with or known to have VWD or any other bleeding disorder. ECFCs used in this study have previously been classified as group 1 or group 3 (6).

Cell Culture, Immunofluorescence and Image Acquisition

General cell culture of endothelial colony forming cells (ECFCs) and HEK293T cells was performed as described (5) and (11). ECFCs and HEK293T cells were grown on gelatin- or collagen-coated glass coverslips (9mm) and left confluent for 5 days before fixing with 70% methanol on ice for 10 minutes or with 4% paraformaldehyde for 15 minutes as described previously (10). Disruption of Golgi ribbons was done by exposure of ECFCs to 2 µg/ml of nocodazole (Sigma, M1404) for 46 hours. For triggering of cAMP-mediated signaling to induce perinuclear clustering of WPBs, post-confluent monolayers of ECFCs were treated with 10 µM Forskolin (Merck, F3917) and 100 µM 3-isobutyl-1-methylxanthine (IBMX) (Merck, I5879) for 30 minutes as described previously (12). Samples for OrganelleProfiler were stained with antibodies against VWF, EEA1, VE-cadherin, β-catenin, TGN46 and nuclei were stained with Hoechst or DAPI (Supplemental Table 1 for supporting information on antibodies). Samples for OrganelleContentProfiler were stained with Hoechst and antibodies against VWF, VE-cadherin and either Rab27A or PDI. After staining with appropriate fluorescently labeled secondary antibodies, coverslips were mounted using ProLong® Diamond Antifade Mountant (Thermo Fisher Scientific). Visualization of the cells for the OrganelleProfiler example was done using the Imagexpress Micro Confocal System using the 63x objective without magnification or with the Leica Stellaris 5 Low Incidence Angle using the 63x oil immersion objective. The OrganelleContentProfiler samples were imaged using the Zeiss LSM900 Airyscan2 upright confocal microscope using the 63x oil immersion objective. For both the OrganelleProfiler and OrganelleContentProfiler images a Z-stack was made which was transformed to a maximum Z-projection.

CellProfiler-Based pipelines for cell organelle analysis and manual scoring with Fiji

CellProfiler (version 4.2.1 at time of publication) was used, which can be downloaded from the CellProfiler website (www.cellprofiler.org). For the initial development of the pipelines, confocal images from 33 ECFC clones from several healthy donors were used. These ECFCs have previously been classified into separate phenotypic groups based on cellular morphology (6). The final pipeline was tested on 5 tile scans from one group 1 and one clone belonging to group 3. Images have to be of high enough resolution that individual organelles can be identified and do not blur together. Magnification, laser intensity, detector sensitivity and other acquisition parameters should be the same for each image set. Image format has to be similar as well. We recommend uncompressed TIFF files. Pipelines developed are available in the Supplementary Files (file 1 and 2) and have been deposited in our laboratory GitHUB repository (https://github.com/Clotterdam). Adjusted pipelines optimized for the use on endosome quantification (in HEK293T cells – Supplemental File 3 and in ECFCs – Supplemental File 4), WPB

quantification after Golgi ribbon disruption (Supplemental File 5) and after forskolin stimulation (Supplemental File 6) are also made available. To compare the CellProfiler measurements and validate these, manual scoring of cell count, cell surface area, WPB count, WPB length, and VWF and Rab27A intensity inside and outside the WPBs was performed using Fiji version 2.3.0 (13). Scoring was performed by using the built in scale and drawing regions of interest per cell and per WPB.

Statistical Analysis

Output data of the OrganelleProfiler pipeline was compared by Mann-Whitney U test if data was not normally distributed and unpaired T test with Welch's correction was performed on normally distributed data. Data of the OrganelleContentProfiler pipeline was compared with RM one way ANOVA with Geisser-Greenhouse correction. Data are presented as median with min/max boxplot. Results with p value < 0.05 were considered statistically significant. P values are indicated on the graphs in the figures. Data analyses were performed using GraphPad Prism 9.3.1 (GraphPad Software, San Diego, CA, USA).

Results

Development of OrganelleProfiler (OP) – Automated identification and quantification of nuclei, cells and secretory organelles

Described here are the modules used in the OrganelleProfiler pipeline for the identification and measurement of endothelial cells, their nuclei and WPBs. The most important parameters and how these can be adjusted for use on other tissues for each module are mentioned in Supplemental File 7. Full explanations of other variables are available from the help function within the CellProfiler software or from the user manual on the CellProfiler website. For the development of OrganelleProfiler we used confocal images from 33 ECFC clones from several healthy donors. These ECFCs have previously been classified into separate phenotypic groups based on cellular morphology and showed clear differences in expression of cell surface markers, proliferation and storage and secretion of VWF (6). Representative images of 1 clone of group 1 (top) and 1 clone of group 3 (bottom) ECFCs used for this study are shown in Figure 1. The CellProfiler modules that together form the OrganelleProfiler pipeline can be divided into 6 steps (Figure 2), which are described below.

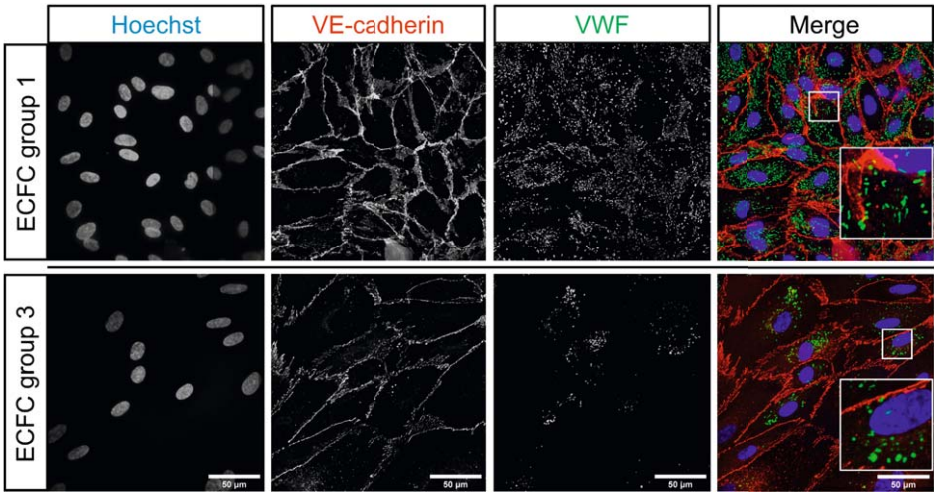

Figure 1. Representative images of healthy ECFC controls belonging to previously classified groups based on morphology (6). Group 1 ECFCs (top) and group 3 ECFCs (bottom) were stained with Hoechst (blue) and antibodies against VE-cadherin (red) and VWF (green). Scale bar represents 50 µm. Images were taken with a 63x objective.

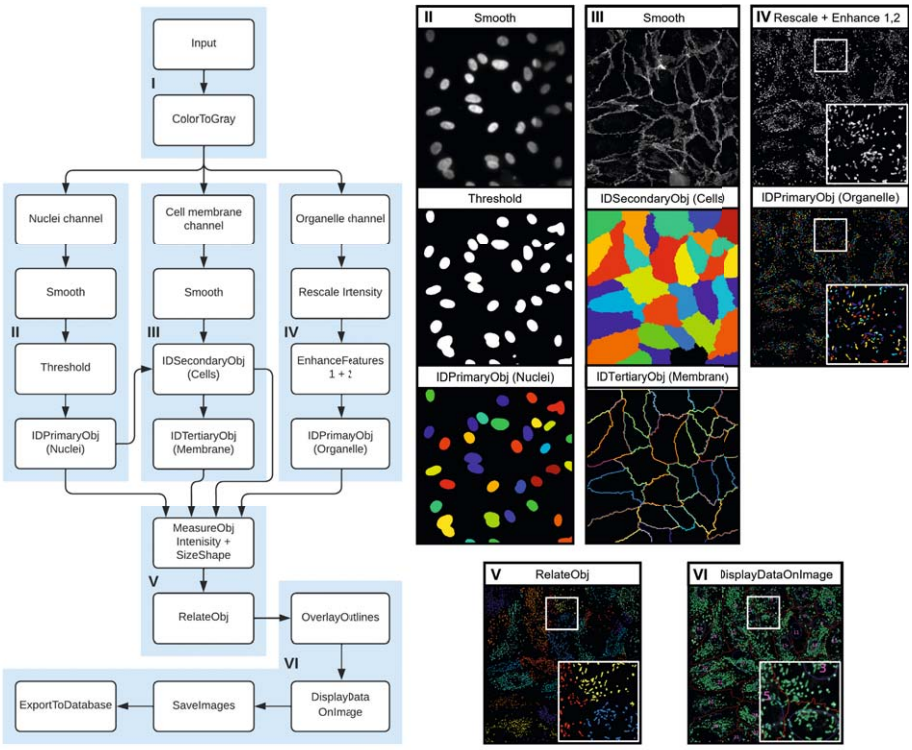

Figure 2. OrganelleProfiler: Quantitative and qualitative analysis of cells and cell secretory organelles. Left, flowchart of the modules within the OrganelleProfiler pipeline. I) Input of images and splitting of channels. II) Smoothing (top), thresholding (middle) and identification of the nuclei (bottom). Every different color indicates a different object. III) Smoothing of the cell membrane (top), identification of the cells (middle) and identification of cell membranes (bottom) as objects. IV) VWF signal rescaling and enhancement (top) and identification of WPB objects (bottom). V) Relating WPBs and Cells as child and parent respectively. Same colored objects indicate a relationship to the same cell. VI) Generated output image overlaying the outline of the nuclei (blue), cells (red), and WPBs (green) objects on the VWF channel. With the addition of the cell number (purple).

Step I – Input of images

Firstly, images of interest are imported into the software. In this example, 5 images from two groups of ECFCs were compared. Each image has 3 channels, 1 for the nuclei staining (Hoechst), one for cell membrane staining (VE-cadherin) and a third channel for organelle specific staining (VWF) (Figure 1). Channels are separated at this point so that each channel is processed separately in the following steps.

Step II, III and IV – Identification of nuclei, cell membranes, cells and organelles
Second, the nuclei staining signal is smoothed and a threshold is applied for the identification of the nuclei as objects. This object, together with the smoothed cell membrane staining signal is used in step III for the identification of the whole cell as secondary object. The nuclei are used as a starting point from which the object propagates outward in all directions until it encounters a secondary signal, in this case the smoothed cell membrane. A third object is generated using the cell object. This third object consists of only the cell membrane which is needed in the OrgannelleContentPipeline. In parallel to steps II and III, step IV uses the organelle staining signal for identification of the organelles. The signal is first rescaled and the speckle and neurite features are enhanced, which yields a better separation of organelles if they are located close to, or on top of, each other. After modification, the organelles are identified as the fourth object class.

Step V – Measurement and relating of objects
All objects that are generated in step II, III and IV are measured here. Size, shape and intensity, where relevant, is measured. Organelle objects are related to the nuclei and to the cell membrane in this step as well. This yields counts of secondary objects (organelles) per primary objects (cells) and distance of the secondary object to either the nuclei or the cell membrane. Measurements that we performed on the objects are eccentricity (as indicator for round or elongated WPB morphology), length of WPBs (maximum ferret diameter) and absolute as well as relative distance of WPBs to the nuclei and the cell membrane (Figure 3A).

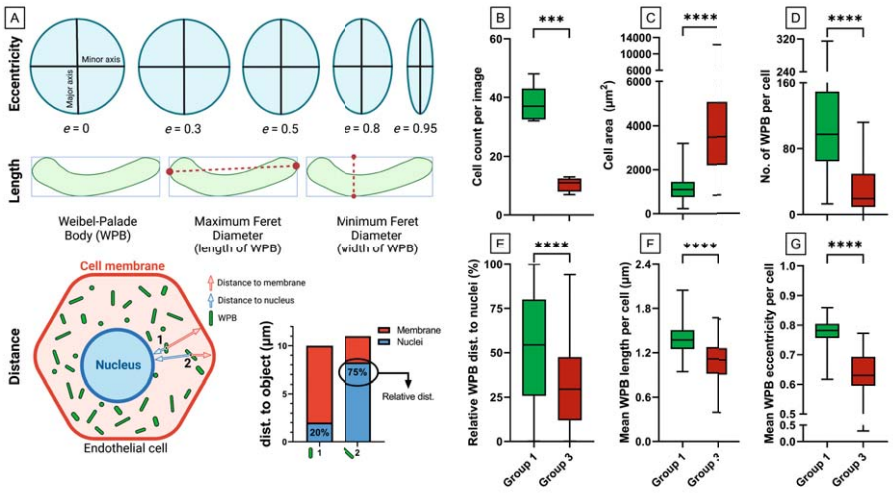

Figure 3. Quantitative and morphological differences between ECFC control groups. Two previously classified ECFCs based on morphology (6), group 1 (green) and group 3 (red), were stained for Hoechst, VE-cadherin and VWF. Per control, 5 images were analyzed with the OrganelleProfiler pipeline (each 44100 µm^2 in size). A) Graphical representation of the measurements that were performed on the objects. Eccentricity (top), length of Weibel-Palade bodies (WPBs) measured as maximum ferret diameter (middle) and distance of WPBs to the nuclei and the cell membrane was measured (bottom). Relative distance of the WPB to the nucleus in the cell was calculated as 100% x (distance to nucleus) / (distance to nucleus + distance to cell membrane). B) Cell count per image. C) The cell area (µm^2) per cell of all 5 images pooled (n = 188 in group 1 and n = 52 in group 3). D) Number of WPBs per cell. E) Distance of the WPB to the nucleus relative to their position in the cell in percentage. F) Mean WPB length per cell in µm. G) Mean eccentricity of WPBs per cell. Data is shown as median with min/max boxplot. Mann-Whitney U test was performed on not normally distributed data (D and G). Unpaired T test with Welch's correction was performed on normally distributed data (B, C, E and F); *p<0.05 **p<0.01, ***p<0.001.

Step VI – Quality control and analysis of output

For quality control, all objects' outlines are overlaid on the VWF signal. This overlay allows the user to check whether the pipeline was accurate in the identification of objects. Cells are numbered so potential outliers can be easily identified and the pipeline can be adjusted if needed. The exported output can be used to quantify and perform qualitative analysis on images of interest.

Automated quantification using OrganelleProfiler revealed significant differences in cell count, cell area and number, size, shape and localization of WPBs between group 1 and group 3 ECFCs (Figure 3B-G). Figure 3B shows a significantly lower number of cells per image in group 3 (mean ± SD, 10.40 ± 2.40) compared to group 1 (37.60 ± 2.80)

(p=0.0003). Logically, as all ECFCs were confluent, we observed a larger mean cell area in group 3 (4016 ± 2445 μm^2) than in group 1 (1143 ± 516.60 μm^2) (Figure 3C) (p<0.0001). The total number of WPBs per image was lower in group 1 compared to group 3 (not shown). Additionally, the number of WPBs per cell was significantly lower in group 3 (30.92 ± 29.54) than in group 1 (107.30 ± 58.51) (p<0.0001) (Figure 3D). The distance of WPBs to the nuclei relative to their position in the cell was determined and shown in Figure 3E. The relative distance was significantly lower in group 3 ECFCs (32.31 ± 23.62%) when compared to group 1 (53 ± 30.10%) (p<0.0001) indicating that within the cell, WPBs were located closer to the nucleus in group 3 ECFCs. Finally, the mean WPB length was lower in group 3 (1.10 ± 0.27 μm) versus (1.38 ± 0.21 μm) in group 1 ECFCs (p<0.0001) and the WPBs were significantly more round in group 3 (0.63 ± 0.08)) versus (0.78 ± 0.04) (p<0.0001) (Figure 3F/G). The lower number of WPBs and the observation that they are smaller and rounder in group 3 when compared to group 1 could explain the decreased production and secretion of VWF observed previously (de Boer, JTH, 2020).

To further validate the quantitative data obtained from our automated OrganelleProfiler pipeline we also performed a manual quantification of several of these parameters using Fiji image analysis software, specifically the region of interest manager (13). One image of the group 1 ECFCs was used for the scoring. The manual scoring of the cells using the freehand selection resulted in 34 cells with a mean surface area of 1264 ± 497.93 μm^2. For three cells all WPBs were scored by measuring the longest distance in the WPB using a straight line. In these cells the manual scoring showed a mean WPB count of 117 ± 38.63 and a length of 1.57 ± 0.09 μm. All measurements were compared with the CellProfiler measurements on the same image and none of the results differed significantly. Taken together, we can conclude that both measurements with CellProfiler and Fiji are comparable and thus CellProfiler can be used to accurately measure cells and organelles.

Validation and application of OrganelleProfiler

Identification of HEK293T cells and early endosomes

To demonstrate the versatility of the OrganelleProfiler pipeline, we extended our analyses to a different type of organelle (early endosome, visualized by staining for early endosome antigen 1, EEA1) and a different cell type (HEK293T). Representative images of ECFCs and HEK293T cells and the analyzed output of the OrganelleProfiler are shown in Figure 4A. The OrganelleProfiler was used to analyze three tile scans of each condition. Figure 4B shows significantly more HEK293T cells per image (1539 ± 82.71) than ECFCs (359.30 ± 4.16) (p=0.0016) which were also smaller (397.8 ± 150 μm^2) than ECFCs (1793 ± 866.3 μm^2) (Figure 4C) (p<0.0001). The number of early endosomes per cell was slightly lower in HEK293T cells (39.27 ± 16.22) compared to ECFCs (63.30 ± 41.02) (p<0.0001) (Figure 4D). The relative distance of the early endosomes to the nuclei (Figure 4E) was higher in the

HEK293T cells (45.34 ± 8.29%) when compared to ECFCs (40.05 ± 12.70%) ($p<0.0001$). Finally, the mean early endosome eccentricity is slightly higher in HEK293T cells (0.59 ± 0.05) versus (0.58 ± 0.04) in ECFCs ($p<0.0001$) (Figure 4F). Comparatively, the early endosomes are clearly rounder when compared to WPBs (0.78 ± 0.04, indicated by the red dotted line, data from Figure 3G) which are more elongated organelles.

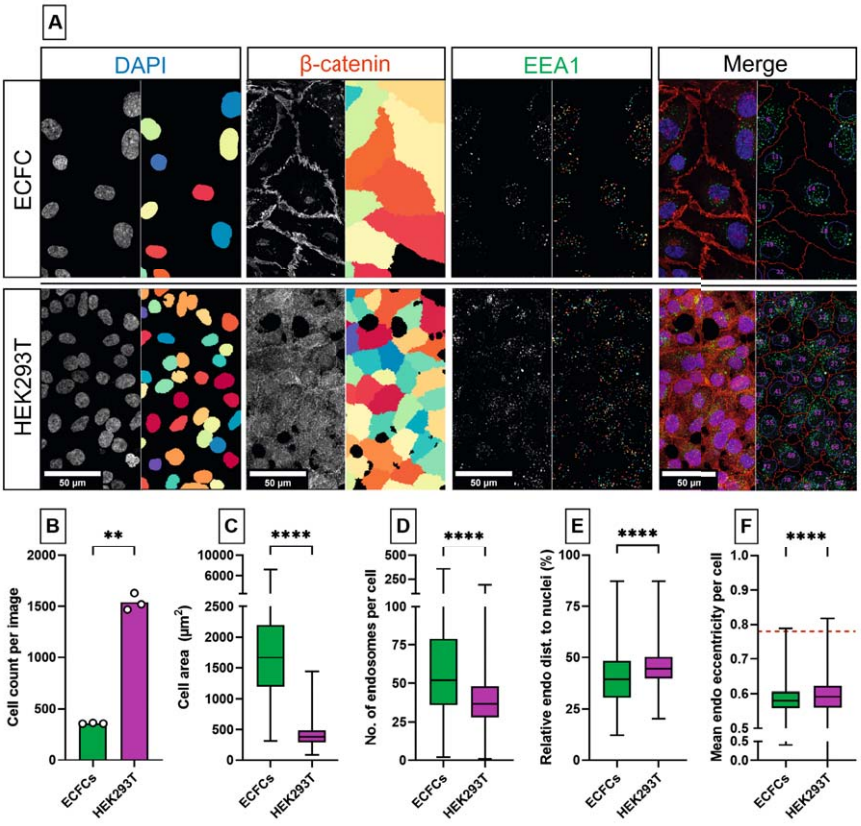

Figure 4. Quantitative and morphological differences between early endosomes in ECFCs and HEK293T cells. A) Representative images of ECFC (top) and HEK293T (bottom) cells where each panel shows the raw confocal image (left) and the identified object in Cellprofiler (right). Every different color indicates a different object. Cells were stained with DAPI (blue) and antibodies against β-catenin (red) and EEA1 (green). Scale bar represents 50 µm. Images were taken with a Leica Stellaris 5 LIA fitted with a 63x objective. Per cell type, 3 tile scans (each 754630 μm^2 in size) were analyzed with the OrganelleProfiler pipeline. B) Cell count per image. C) The cell area (μm^2) per cell of all 3 tile scans pooled (n = 1078 ECFCs and n = 4618 HEK293T cells). D) Number of endosomes per cell. E) Mean relative distance of the endosome to the nucleus per cell. F) Mean eccentricity of endosomes per cell. Data is shown as median with min/max boxplot. Dashed red line represents mean eccentricity of WPBs as determined in Figure 3G. Mann-Whitney U test was performed on not normally distributed data (C,D,E,F). Unpaired T test with Welch's correction was performed on normally distributed data (B); **p<0.01, ***p<0.001, ****p<0.0001.

WPB shortening after Golgi ribbon disruption and perinuclear clustering after stimulation

WPB length directly relates to the integrity of the Golgi ribbon: fragmented Golgi ribbons generate small WPBs while the longest WPBs require an extended, intact Golgi ribbon (3, 14-16). Pharmacological inhibition of microtubules using nocodazole can be used to unlink Golgi ribbons (17) and this has been shown to reduce the size of newly generated WPBs (14, 18). We used OrganelleProfiler to quantify the reduction of WPB length in ECFCs that were treated for 46 hours with vehicle (DMSO, control) or 2 µg/ml nocodazole. Staining for VWF and the trans-Golgi network marker TGN46 revealed a clear disruption of the Golgi in nocodazole-treated cells (Figure 5A). The OrganelleProfiler was used to analyze three tile scans of each condition. Nocodazole exposure caused a lower cell count per image (Figure 5B) (n=184.7 ± 5.51 versus n=553 ± 36.43, p=0.0027) with larger surface area (2859 ± 1314 μm^2) than control ECFCs (1673 ± 641.6 μm^2) (Figure 5C) (p<0.0001). In the nocodazole treated cells we observed significantly rounder (nocodazole: 0.76 ± 0.06 vs control: 0.87 ± 0.02; p<0.0001) and shorter WPBs (nocodazole: 1.17 µm ± 0.18 vs. control: 1.54 ± 0.17 µm; p<0.0001) compared to the control cells (Figure 5D and E). The relative distance of the WPBs to the nuclei (Figure 5E) was slightly higher after nocodazole exposure (62.25 ± 13.77%) when compared to control (60.18 ± 8.17%) (p<0.0018).

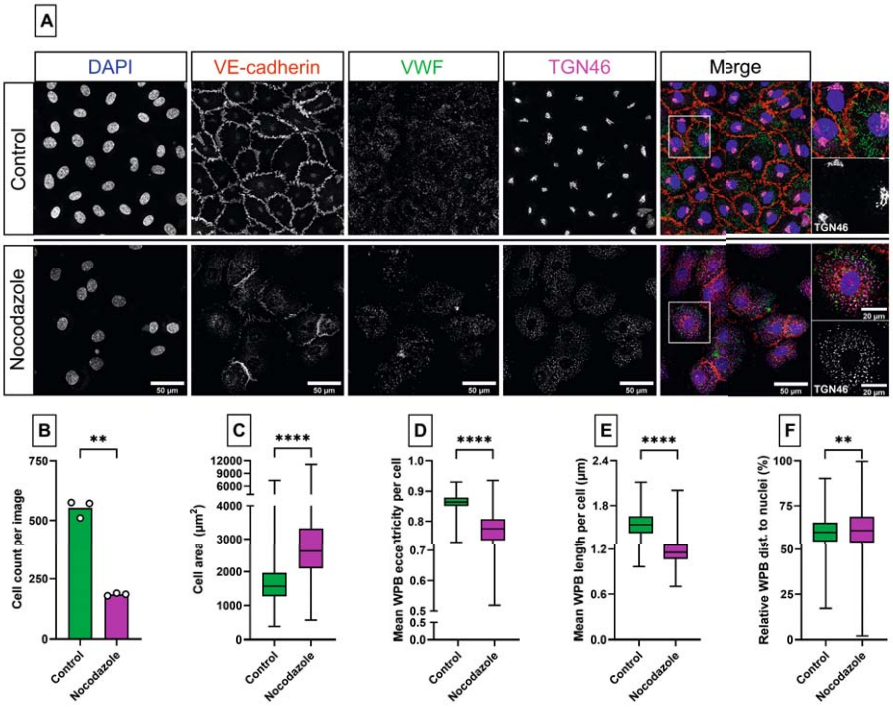

Figure 5. Microtubule disruption leads to Golgi fragmentation and smaller and rounder WPBs. A) Representative images of ECFCs treated for 46 hours with vehicle (control, top) or 2 µg/ml nocodazole (bottom). Cells were stained with DAPI (blue) and antibodies against VE-cadherin (red), VWF (green) and TGN46 (magenta). Scale bar represents 50 µm and 20 µm in the zoom in. Images were taken with a 63x objective. Per cell type, 3 tile scans (each 936054 µm^2 in size) were analyzed with the OrganelleProfiler pipeline. B) Cell count per image. C) The cell area (µm^2) per cell of all 3 tile scans pooled (n = 1659 in the control and n = 554 in the nocodazole treated cells). D) Mean eccentricity of WPBs per cell. E) Mean length (µm) of WPBs per cell F) Mean relative distance of the WPBs to the nucleus per cell. Data is shown as median with min/max boxplot. Mann-Whitney U test was performed on not normally distributed data (C,D,E,F). Unpaired T test with Welch's correction was performed on normally distributed data (B); **p<0.01, ***p<0.001, ****p<0.0001.

It has previously been shown that, upon activation with cAMP-mediated agonists such as epinephrine or forskolin, endothelial cells cluster a subset of their WPBs at the microtubule organizing center (MTOC) via retrograde microtubular transport that depends on the minus-end motor protein dynein (19, 20). We used OrganelleProfiler to quantify the reorganization of WPBs in forskolin-stimulated ECFCs (Figure 6A). Quantitative data gathered from one tile scan per condition shows that the per cell mean relative distance to the nucleus, which is directly adjacent to the MTOC and can therefore be used as a surrogate reference point for clustered WPBs, is lower in

forskolin-treated cells (50.67 ± 14.76%, n=352 cells) than in untreated cells (58.15 ± 10.22%, n=537 cells) (Figure 6B, top). This indicates that in forskolin-treated cells, WPBs have on average moved towards the nucleus and thus into the direction of the MTOC. Also, when quantified on a single organelle basis, we see a shift towards lower relative distance to the nucleus in forskolin-treated cells (45.32 ± 31.39%, n=17241 WPBs) compared with untreated cells (54.03 ± 30.77%, n=21866 WPBs) (Figure 6B, bottom).

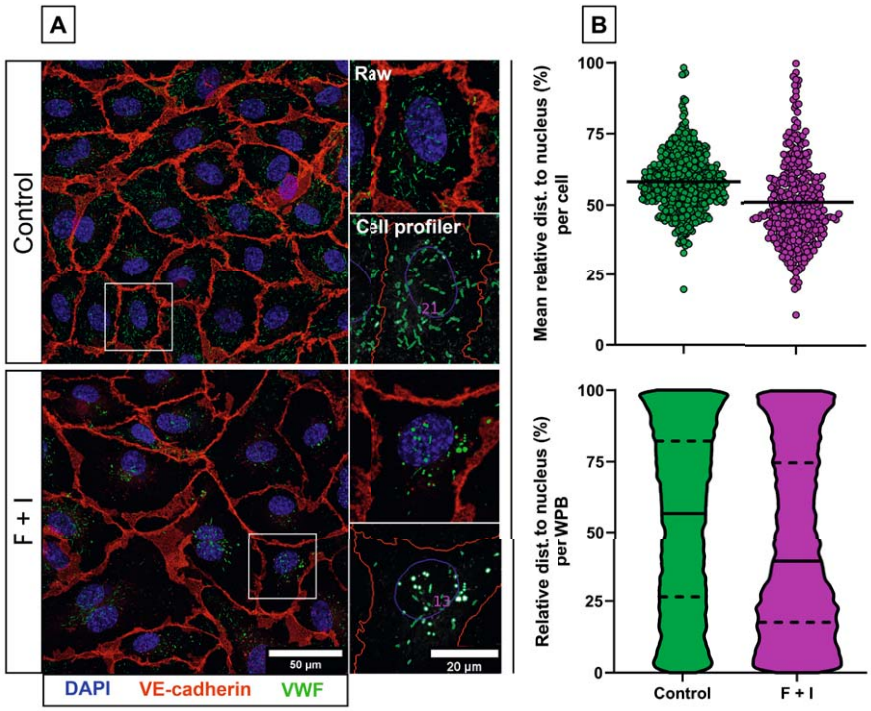

Figure 6. Perinuclear clustering of WPBs after cAMP-mediated signaling in ECFCs. A) Representative images of ECFCs treated for 30 minutes with vehicle (control, top) or 10 uM Forskolin and 100 uM IBMX (F+I, bottom). Cells were stained with DAPI (blue) and antibodies against VE-cadherin (red) and VWF (green). Scale bar represents 50 µm and 20 µm in the zoom in. Images were taken with a 63x objective. Per condition, 1 tile scan (970221 μm^2 in size) was analyzed with the OrganelleProfiler pipeline. B) Mean relative distance of the WPBs to the nucleus per cell (top) (n = 537 in the control and n = 352 in the stimulated ECFCs) and per WPB (bottom) shown as violin plot (n= 21866 for the control and n=17241 for the stimulated ECFCs). The black bar indicates the median with quartiles.

OrganelleContentProfiler (OCP) – Automated measurement of proteins in secretory organelles

The OrganelleContentProfiler pipeline is an addition to the OrganelleProfiler pipeline. By adding 4 extra steps, secondary proteins of interest in, on or outside the organelle can be measured. For this purpose we analyzed the presence of Rab27A, a small GTPase that promotes WPB exocytosis and that is recruited to the WPB membrane during the maturation of these organelles after their separation from the Golgi complex (9, 10, 21). We also determined, as a control, the presence of protein disulfide isomerase (PDI), a marker for the endoplasmic reticulum which should not show specific localization in or on the WPBs (5, 15). Figure 7 shows example images of Rab27A as well as PDI co-staining in group 1 healthy donor ECFCs that were used in this pipeline. The CellProfiler modules that together form the OrganelleContentProfiler pipeline can be divided into 4 steps (Figure 8), which are described below. Further details on every module are described in Supplemental File 7.

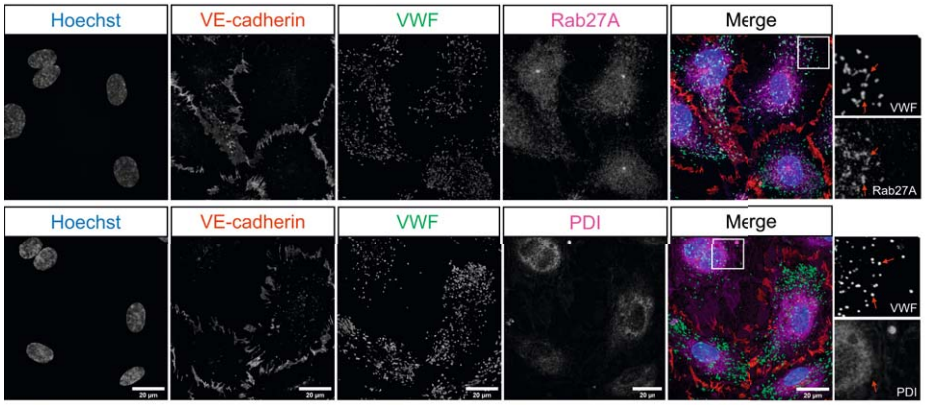

Figure 7. Representative images of one healthy group 1 ECFC control belonging to previously classified groups based on morphology (6). Cells were stained for Hoechst (blue), VE-cadherin (red), VWF (green) and Rab27A (top) or PDI (bottom). Scale bar represents 20 µm. Images were taken with a 63x objective. Red arrows indicate WPBs as identified in the VWF channel and the same location in the Rab27A or PDI channel.

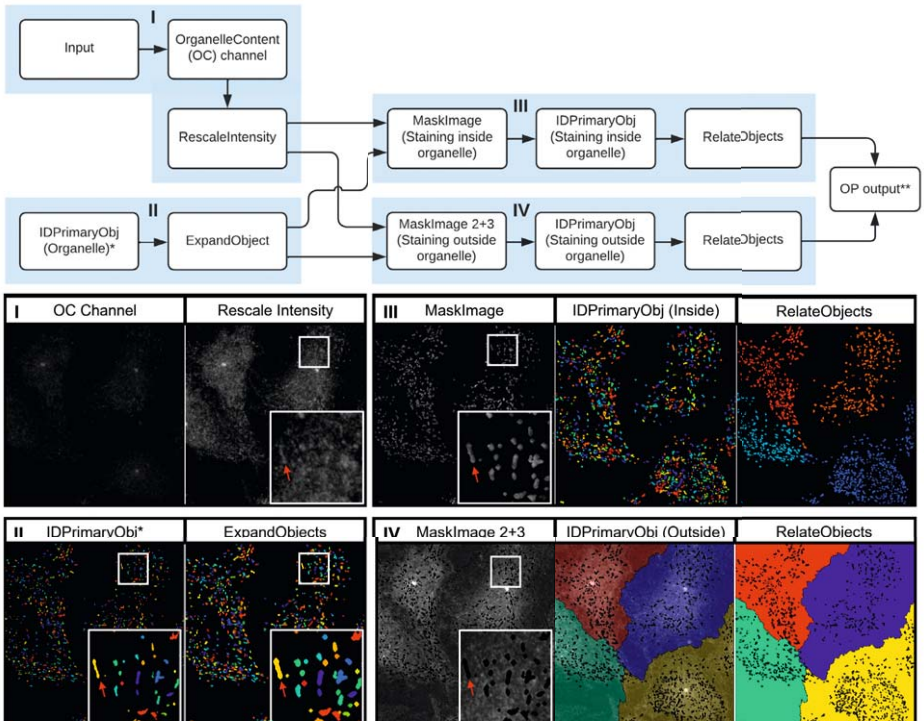

Figure 8. OrganelleContentProfiler: Quantitative and qualitative analysis of other organelle proteins. Top, flowchart of the modules within the OrganelleContentProfiler pipeline. I) Input of Rab27A (Organelle content) channel and rescaling of this channel. II) Input of primary object (Organelle) (left) and expansion of this object (right). III) Masking of the Rab27A channel using the Expanded organelle objects to leave only Rab27A signal inside the organelle (left). Identification of the Rab27A signal per WPB as object (middle) and relating these objects to the cells as child and parent respectively (right). IV) Masking of the Rab27A channel using the Expanded organelle objects to leave only Rab27A signal outside the organelle (left). Identification of the Rab27A signal in the cell as object without the WPBs (middle) and relating these objects to the cells as child and parent respectively (right). * Identified in step IV of the OrganelleProfiler pipeline (Figure 2). ** Pipeline continues with step V and VI from the OrganelleProfiler pipeline.

Step I – Input of an additional channel

Similarly to the OrganelleProfiler, images are imported into the software. In this example, images have one additional channel containing the staining for either Rab27A or PDI. Again, channels are separated and the fourth channel is rescaled in order to view the channel in the final quality control.

Step II – Import of organelle object identified in the OrganelleProfiler pipeline

In this step, the organelle object as identified in the OrganelleProfiler pipeline is modified. The objects are initially identified using the staining for VWF, which is a

cargo protein that is contained within the organelle. The secondary protein of interest, Rab27A, is a membrane protein that is located on the cytoplasmic face of the WPB membrane. To ensure full encapsulation of the Rab27A signal the object is therefore expanded by 2 pixels in all directions.

Step III and IV – Identification of the secondary protein of interest "inside" and outside the organelle

In these parallel steps, the expanded organelle objects and the rescaled secondary staining channel are used. The expanded objects are used as a mask to remove all signal of the Rab27A or PDI staining outside the organelle (step III) and inside the organelle (step IV). The remaining signal is then identified as object, resulting in two new objects containing the signal inside the organelles and outside the organelles respectively. These new objects are processed according to step V from the OrganelleProfiler including the measurements, relating, quality control and export.

Step V and VI – Measurements, quality control and analysis of results

In the OrganelleContentProfiler pipeline, different stainings on the same ECFC control are compared. In addition to the output from the OrganelleProfiler, the OrganelleContentProfiler provides measurements of the intensity of a secondary signal inside the organelle. Furthermore, it can quantify the cytoplasmic intensity values outside of the organelle which can be used for correction of the "inside" organelle signal. Signal intensity is noted as arbitrary intensity units (A.U.) as microscopes are not calibrated to an absolute scale.

We first confirmed that the number of WPBs quantified using OrganelleContentProfiler does not depend on the co-staining used (Rab27A: 204.8 ± 70.48; PDI: 146, ± 56.38; p=0.24) (Figure 9A). ECFCs were stained with Hoechst and with antibodies against VE-cadherin, VWF and Rab27A or PDI. Figure 9B shows the A.U. inside and outside organelles and the A.U. inside the organelle corrected for the outside value. First, the VWF A.U. was analyzed as a measurement of a protein that is located predominantly in the WPB. The results show that the VWF A.U. values outside the WPBs was nearly zero (0.00076 ± 0.00033) and differed significantly from the inside A.U. (0.028 ± 0.0040) (p=0.0016) indicating that VWF is almost exclusively present in WPBs. Secondly, it was determined that the Rab27A staining shows a significantly higher A.U. inside (0.081 ± 0.0085) the WPBs when compared to the outside measurement (0.052 ± 0.0041) (p=0.0062). From this it can be concluded that part of the Rab27A protein is present in or on the WPB. Finally, the A.U. of the PDI staining was analyzed. PDI is only present inside the endoplasmic reticulum and should not yield increased A.U. inside the WPB. Indeed, the A.U. inside (0.074 ± 0.016) and outside (0.062 ± 0.0082) the organelle were

similar (p=0.20), indicating that PDI is not located specifically in or on WPBs. Once more, to validate the quantitative data obtained by CellProfiler, we also performed a manual scoring using Fiji for the A.U. of the Rab27A and VWF staining inside and outside of all WPBs (n=199) in one cell. We observed that the results determined manually using Fiji (A.U. VWF inside = 0.039, VWF outside = 0.000029; Rab27A inside = 0.094, Rab27A outside = 0.053) lie within the same range as those determined by CellProfiler. This shows that the OrganelleContentProfiler can determine organelle specific stainings and measure the intensity of the staining corrected for the cytoplasmic value.

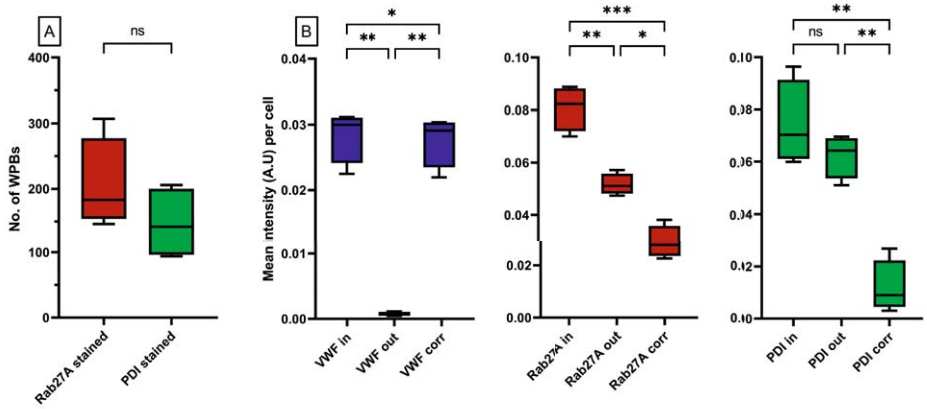

Figure 9. Quantification of signal intensity inside cell organells. A group 1 ECFC control as defined previously (6) was stained with Hoechst and with antibodies against VE-cadherin, VWF and PDI or Rab27A. One image (12769 μm^2) per staining was analyzed using the OrganelleContentProfiler pipeline. A) Both images had the same number of cells (n=4) and roughly the same number of WPBs. B) the mean intensity in arbitrary intensity units (A.U.) per cell for the PDI (left), Rab27A (middle) and VWF (right) staining. Each graph shows the measured mean intensity inside (in) the WPBs, outside (out) the WPBs and the intensity inside the WPB after correcting for the out signal (corr). Data is shown as median with min/max boxplot. RM one way ANOVA was performed with Geisser-Greenhouse correction; *p<0.05 **p<0.01, ***p<0.001.

Discussion

Quantifying large numbers of organelles is challenging due to the density and morphological heterogeneity of the organelles. The pipelines described here can be used to overcome these challenges and can provide organelle analysis in great detail on a larger scale. The OrganelleProfiler allows for measurement of cell and nucleus quantity and shape, and organelle quantity, shape, size and location within the cell. The organelles are also related to the cells which allows for cell-by-cell analysis. This information can be used to determine differences between a heterogeneous cell

population or between patient and control cells. The OrganelleProfiler pipeline has shown significant differences between group 1 and group 3 ECFC controls based on only 5 images. Moreover, we were able to quantitatively determine differences in WPB length upon treatment with cytoskeletal drugs and differences in intracellular localization after induction of retrograde transport of WPBs. Once optimized for a set of images, the pipeline can analyze thousands of cells and hundreds of thousands of organelles within hours without potential bias associated with manual image processing and quantification. As shown with the early endosome staining, it is possible to adjust the pipeline to quantify other cell types and organelles. The pipeline was able to quantify differences between ECFCs and HEK293T cells and showed clear differences in eccentricity of the elongated WPBs compared to the round early endosomes.

With the OrganelleContentProfiler, secondary organelle markers can be measured and quantified. We showed 3 stainings of proteins with different localizations; PDI, which is only present on the endoplasmic reticulum, Rab27A which is present in the cytoplasm, but is also trafficked to the WPBs, and VWF which is mostly present in WPBs. Using the OrganelleContentProfiler pipeline we were able to quantify these stainings and determine the localization of these proteins. It is also possible to measure other organelle stainings at the same time by duplicating modules 3 to 8 of this pipeline and adjusting these for the additional channels.

Finetuning of the smoothing, thresholds and enhancement of the signal is necessary to ensure correct identification of objects. For every image set, a balance must be found to prevent over and under segmentation of organelles. Despite optimization, perfect segmentation of organelles is not always possible, especially in areas where organelles are crowded together. These imperfections may lead to incorrect identification of organelles, which could play out as underestimations of WPB numbers or overestimation of WPB dimensions. However, as all images are analyzed by the same pipeline, this error is expected to occur to a similar extent in all samples. One point of improvement on the OrganelleContentProfiler pipeline could be the correction of the organelle secondary staining with the intensity levels directly surrounding the organelle instead of the mean intensity in the entire cytoplasm. This was not possible within the CellProfiler software but could be done in data processing afterwards using the MeasureObjectIntensityDistribution module and relating this to the distance of WPBs to the nucleus (7).

A comparison with manual scoring using Fiji was performed to check the validity of the results generated by our automated pipelines. We generally found that the results obtained with OrganelleProfiler and OrganelleContentProfiler correspond very

well with manual quantifications using Fiji, although subtle differences were found for two parameters. First, the maximum ferret diameter is calculated based on the smallest convex hull that is created around the WPB. The manual scoring measured the length of the WPB in a line and not as the inside of a convex hull. This could cause the slight difference in length as measured between CellProfiler and Fiji. Second, VWF and Rab27A intensities inside WPBs as determined by manual scoring was slightly higher than from the OrganelleContentProfiler measurements. Possibly, the outlines that were drawn around WPBs manually were more strict than those generated by OrganelleContentProfiler, because the human eye is less capable at detecting the very small changes in signal intensity near the edges of the organelles. As such, the signal intensities in these edges may have not been included in the manual analysis, resulting in a higher mean value per WPB.

To conclude, the OrganelleProfiler and OrganelleContentProfiler pipelines provide powerful, high-processing quantitative tools for analysis of cell and organelle count, size, shape, location and content. These pipelines were created with the purpose of analyzing morphometric parameters of WPBs in endothelial cells, but as shown for the HEK293T cells and early endosomes, they can be easily adjusted for use on different cell types or organelles. This can be especially useful for analysis of large datasets where manual quantification of organelle parameters would be unfeasible.

Acknowledgements

The SYMPHONY consortium, which aims to orchestrate personalized treatment in patients with bleeding disorders, is a unique collaboration between patients, health care professionals, and translational and fundamental researchers specializing in inherited bleeding disorders, as well as experts from multiple disciplines (22). It aims to identify best treatment choice for each individual based on bleeding phenotype. To achieve this goal, work packages (WP) have been organized according to 3 themes (e.g. Diagnostics [WPs 3 and 4], Treatment [WPs 5-9], and Fundamental Research [WPs 10-12]). Principal investigator: M.H. Cnossen; project manager: S.H. Reitsma.

References

1. Schillemans M, Karampini E, Kat M, Bierings R. Exocytosis of Weibel-Palade bodies: how to unpack a vascular emergency kit. J Thromb Haemost. 2019;17(1):6-18.
2. Valentijn KM, Sadler JE, Valentijn JA, Voorberg J, Eikenboom J. Functional architecture of Weibel-Palade bodies. Blood. 2011;117(19):5033-43.
3. Kat M, Margadant C, Voorberg J, Bierings R. Dispatch and delivery at the ER-Golgi interface: how endothelial cells tune their hemostatic response. FEBS J. 2022;289(22):6863-70.
4. Valentijn KM, Eikenboom J. Weibel-Palade bodies: a window to von Willebrand disease. J Thromb Haemost. 2013;11(4):581-92.
5. de Jong A, Weijers E, Dirven R, de Boer S, Streur J, Eikenboom J. Variability of von Willebrand factor-related parameters in endothelial colony forming cells. J Thromb Haemost. 2019;17(9):1544-54.
6. de Boer S, Bowman M, Notley C, Mo A, Lima P, de Jong A, et al. Endothelial characteristics in healthy endothelial colony forming cells; generating a robust and valid ex vivo model for vascular disease. J Thromb Haemost. 2020;18(10):2721-31.
7. Stirling DR, Swain-Bowden MJ, Lucas AM, Carpenter AE, Cimini BA, Goodman A. CellProfiler 4: improvements in speed, utility and usability. BMC Bioinformatics. 2021;22(1):433.
8. Hannah MJ, Hume AN, Arribas M, Williams R, Hewlett LJ, Seabra MC, et al. Weibel-Palade bodies recruit Rab27 by a content-driven, maturation-dependent mechanism that is independent of cell type. J Cell Sci. 2003;116(Pt 19):3939-48.
9. Bierings R, Hellen N, Kiskin N, Knipe L, Fonseca AV, Patel B, et al. The interplay between the Rab27A effectors Slp4-a and MyRIP controls hormone-evoked Weibel-Palade body exocytosis. Blood. 2012;120(13):2757-67.
10. Kat M, Bürgisser PE, Janssen H, De Cuyper IM, Conte IL, Hume AN, et al. GDP/GTP exchange factor MADD drives activation and recruitment of secretory Rab GTPases to Weibel-Palade bodies. Blood Adv. 2021;5(23):5116-27.
11. Schillemans M, Kat M, Westeneng J, Gangaev A, Hofman M, Nota B, et al. Alternative trafficking of Weibel-Palade body proteins in CRISPR/Cas9-engineered von Willebrand factor-deficient blood outgrowth endothelial cells. Res Pract Thromb Haemost. 2019;3(4):718-32.
12. van Hooren KW, van Breevoort D, Fernandez-Borja M, Meijer AB, Eikenboom J, Bierings R, et al. Phosphatidylinositol-3,4,5-triphosphate-dependent Rac exchange factor 1 regulates epinephrine-induced exocytosis of Weibel-Palade bodies. J Thromb Haemost. 2014;12(2):273-81.
13. Schindelin J, Arganda-Carreras I, Frise E, Kaynig V, Longair M, Pietzsch T, et al. Fiji: an open-source platform for biological-image analysis. Nature Methods. 2012;9(7):676-82.
14. Ferraro F, Kriston-Vizi J, Metcalf DJ, Martin-Martin B, Freeman J, Burden JJ, et al. A two-tier Golgi-based control of organelle size underpins the functional plasticity of endothelial cells. Dev Cell. 2014;29(3):292-304.
15. Kat M, Karampini E, Hoogendijk AJ, Bürgisser PE, Mulder AA, Van Alphen FPJ, et al. Syntaxin 5 determines Weibel-Palade body size and von Willebrand factor secretion by controlling Golgi architecture. Haematologica. 2022;107(8):1827-39.
16. Karampini E, Bürgisser PE, Olins J, Mulder AA, Jost CR, Geerts D, et al. Sec22b determines Weibel-Palade body length by controlling anterograde ER-Golgi transport. Haematologica. 2021;106(4):1138-47.

17. Thyberg J, Moskalewski S. Microtubules and the organization of the Golgi complex. Exp Cell Res. 1985;159(1):1-16.
18. Ferraro F, Patella F, Costa JR, Ketteler R, Kriston-Vizi J, Cutler DF. Modulation of endothelial organelle size as an antithrombotic strategy. Journal of Thrombosis and Haemostasis. 2020;18(12):3296-308.
19. Rondaij MG, Bierings R, Kragt A, Gijzen KA, Sellink E, van Mourik JA, et al. Dynein-dynactin complex mediates protein kinase A-dependent clustering of Weibel-Palade bodies in endothelial cells. Arterioscler Thromb Vasc Biol. 2006;26(1):49-55.
20. van Agtmaal EL, Bierings R, Dragt BS, Leyen TA, Fernandez-Borja M, Horrevoets AJG, et al. The Shear Stress-Induced Transcription Factor KLF2 Affects Dynamics and Angiopoietin-2 Content of Weibel-Palade Bodies. PLOS ONE. 2012;7(6):e38399.
21. Zografou S, Basagiannis D, Papafotika A, Shirakawa R, Horiuchi H, Auerbach D, et al. A complete Rab screening reveals novel insights in Weibel-Palade body exocytosis. J Cell Sci. 2012;125(Pt 20):4780-90.
22. Cnossen MH, van Moort I, Reitsma SH, de Maat MPM, Schutgens REG, Urbanus RT, et al. SYMPHONY consortium: Orchestrating personalized treatment for patients with bleeding disorders. J Thromb Haemost. 2022;20(9):2001-11.
23. Hordijk S, Carter T, Bierings R. A new look at an old body: molecular determinants of Weibel-Palade body composition and VWF exocytosis. J Thromb Haemost. 2024.
24. Murray EW, Lillicrap D. von Willebrand disease: pathogenesis, classification, and management. Transfus Med Rev. 1996;10(2):93-110.
25. Leebeek FWG, Eikenboom JCJ. Von Willebrand's Disease. New England Journal of Medicine. 2016;375(21):2067-80.
26. Lin Y, Weisdorf DJ, Solovey A, Hebbel RP. Origins of circulating endothelial cells and endothelial outgrowth from blood. J Clin Invest. 2000;105(1):71-7.
27. van den Biggelaar M, Bouwens EA, Kootstra NA, Hebbel RP, Voorberg J, Mertens K. Storage and regulated secretion of factor VIII in blood outgrowth endothelial cells. Haematologica. 2009;94(5):670-8.
28. Berber E, James PD, Hough C, Lillicrap D. An assessment of the pathogenic significance of the R924Q von Willebrand factor substitution. J Thromb Haemost. 2009;7(10):1672-9.
29. Groeneveld DJ, van Bekkum T, Dirven RJ, Wang JW, Voorberg J, Reitsma PH, et al. Angiogenic characteristics of blood outgrowth endothelial cells from patients with von Willebrand disease. J Thromb Haemost. 2015;13(10):1854-66.
30. Randi AM, Laffan MA. Von Willebrand factor and angiogenesis: basic and applied issues. J Thromb Haemost. 2017;15(1):13-20.
31. Starke RD, Ferraro F, Paschalaki KE, Dryden NH, McKinnon TA, Sutton RE, et al. Endothelial von Willebrand factor regulates angiogenesis. Blood. 2011;117(3):1071-80.
32. Starke RD, Paschalaki KE, Dyer CE, Harrison-Lavoie KJ, Cutler JA, McKinnon TA, et al. Cellular and molecular basis of von Willebrand disease: studies on blood outgrowth endothelial cells. Blood. 2013;121(14):2773-84.
33. Wang JW, Bouwens EA, Pintao MC, Voorberg J, Safdar H, Valentijn KM, et al. Analysis of the storage and secretion of von Willebrand factor in blood outgrowth endothelial cells derived from patients with von Willebrand disease. Blood. 2013;121(14):2762-72.
34. Galili T, O'Callaghan A, Sidi J, Sievert C. heatmaply: an R package for creating interactive cluster heatmaps for online publishing. Bioinformatics. 2017;34(9):1600-2.

35. Ashburner M, Ball CA, Blake JA, Botstein D, Butler H, Cherry JM, et al. Gene Ontology: tool for the unification of biology. Nature Genetics. 2000;25(1):25-9.
36. Consortium TGO, Aleksander SA, Balhoff J, Carbon S, Cherry JM, Drabkin HJ, et al. The Gene Ontology knowledgebase in 2023. Genetics. 2023;224(1).
37. Laan SNJ, Dirven RJ, Bürgisser PE, Eikenboom J, Bierings R. Automated segmentation and quantitative analysis of organelle morphology, localization and content using CellProfiler. PLoS One. 2023;18(6):e0278009.
38. Goncharov NV, Popova PI, Avdonin PP, Kudryavtsev IV, Serebryakova MK, Korf EA, et al. Markers of Endothelial Cells in Normal and Pathological Conditions. Biochem (Mosc) Suppl Ser A Membr Cell Biol. 2020;14(3):167-83.
39. Dejana E, Hirschi KK, Simons M. The molecular basis of endothelial cell plasticity. Nature Communications. 2017;8(1):14361.
40. Yang J, Antin P, Berx G, Blanpain C, Brabletz T, Bronner M, et al. Guidelines and definitions for research on epithelial–mesenchymal transition. Nature Reviews Molecular Cell Biology. 2020;21(6):341-52.
41. Reimand J, Isserlin R, Voisin V, Kucera M, Tannus-Lopes C, Rostamianfar A, et al. Pathway enrichment analysis and visualization of omics data using g:Profiler, GSEA, Cytoscape and EnrichmentMap. Nature Protocols. 2019;14(2):482-517.
42. Medina RJ, O'Neill CL, O'Doherty TM, Wilson SE, Stitt AW. Endothelial progenitors as tools to study vascular disease. Stem Cells Int. 2012;2012:346735.
43. Bowman M, Casey L, Selvam SN, Lima PDA, Rawley O, Hinds M, et al. von Willebrand factor propeptide variants lead to impaired storage and ER retention in patient-derived endothelial colony-forming cells. J Thromb Haemost. 2022;20(7):1599-609.
44. Selvam SN, Casey LJ, Bowman ML, Hawke LG, Longmore AJ, Mewburn J, et al. Abnormal angiogenesis in blood outgrowth endothelial cells derived from von Willebrand disease patients. Blood Coagul Fibrinolysis. 2017;28(7):521-33.
45. Tien TY, Wu YJ, Su CH, Hsieh CL, Wang BJ, Lee YN, et al. Pannexin 1 Modulates Angiogenic Activities of Human Endothelial Colony-Forming Cells Through IGF-1 Mechanism and Is a Marker of Senescence. Arterioscler Thromb Vasc Biol. 2023;43(10):1935-51.
46. Sanchez-Duffhues G, Orlova V, ten Dijke P. In Brief: Endothelial-to-mesenchymal transition. The Journal of Pathology. 2016;238(3):378-80.
47. Kalluri R, Weinberg RA. The basics of epithelial-mesenchymal transition. J Clin Invest. 2009;119(6):1420-8.
48. Maleszewska M, Moonen JR, Huijkman N, van de Sluis B, Krenning G, Harmsen MC. IL-1β and TGFβ2 synergistically induce endothelial to mesenchymal transition in an NFκB-dependent manner. Immunobiology. 2013;218(4):443-54.
49. Romero LI, Zhang DN, Herron GS, Karasek MA. Interleukin-1 induces major phenotypic changes in human skin microvascular endothelial cells. J Cell Physiol. 1997;173(1):84-92.
50. Kutikhin AG, Tupikin AE, Matveeva VG, Shishkova DK, Antonova LV, Kabilov MR, et al. Human Peripheral Blood-Derived Endothelial Colony-Forming Cells Are Highly Similar to Mature Vascular Endothelial Cells yet Demonstrate a Transitional Transcriptomic Signature. Cells. 2020;9(4).
51. Yoshimatsu Y, Kimuro S, Pauty J, Takagaki K, Nomiyama S, Inagawa A, et al. TGF-beta and TNF-alpha cooperatively induce mesenchymal transition of lymphatic endothelial cells via activation of Activin signals. PLOS ONE. 2020;15(5):e0232356.

52. Hulshoff MS, Xu X, Krenning G, Zeisberg EM. Epigenetic Regulation of Endothelial-to-Mesenchymal Transition in Chronic Heart Disease. Arteriosclerosis, Thrombosis, and Vascular Biology. 2018;38(9):1986-96.
53. Tura O, Skinner EM, Barclay GR, Samuel K, Gallagher RC, Brittan M, et al. Late outgrowth endothelial cells resemble mature endothelial cells and are not derived from bone marrow. Stem Cells. 2013;31(2):338-48.
54. Toshner M, Dunmore BJ, McKinney EF, Southwood M, Caruso P, Upton PD, et al. Transcript analysis reveals a specific HOX signature associated with positional identity of human endothelial cells. PLoS One. 2014;9(3):e91334.
55. Potente M, Mäkinen T. Vascular heterogeneity and specialization in development and disease. Nature Reviews Molecular Cell Biology. 2017;18(8):477-94.
56. Lin Y, Banno K, Gil CH, Myslinski J, Hato T, Shelley WC, et al. Origin, prospective identification, and function of circulating endothelial colony-forming cells in mice and humans. JCI Insight. 2023;8(5).
57. Sánchez-Duffhues G, García de Vinuesa A, van de Pol V, Geerts ME, de Vries MR, Janson SG, et al. Inflammation induces endothelial-to-mesenchymal transition and promotes vascular calcification through downregulation of BMPR2. J Pathol. 2019;247(3):333-46.
58. Rieder F, Kessler SP, West GA, Bhilocha S, de la Motte C, Sadler TM, et al. Inflammation-induced endothelial-to-mesenchymal transition: a novel mechanism of intestinal fibrosis. Am J Pathol. 2011;179(5):2660-73.
59. Derada Troletti C, Fontijn RD, Gowing E, Charabati M, van Het Hof B, Didouh I, et al. Inflammation-induced endothelial to mesenchymal transition promotes brain endothelial cell dysfunction and occurs during multiple sclerosis pathophysiology. Cell Death & Disease. 2019;10(2):45.
60. Medina RJ, O'Neill CL, O'Doherty TM, Chambers SE, Guduric-Fuchs J, Neisen J, et al. Ex vivo expansion of human outgrowth endothelial cells leads to IL-8-mediated replicative senescence and impaired vasoreparative function. Stem Cells. 2013;31(8):1657-68.
61. Smadja DM, Bièche I, Uzan G, Bompais H, Muller L, Boisson-Vidal C, et al. PAR-1 activation on human late endothelial progenitor cells enhances angiogenesis in vitro with upregulation of the SDF-1/CXCR4 system. Arterioscler Thromb Vasc Biol. 2005;25(11):2321-7.
62. Bompais H, Chagraoui J, Canron X, Crisan M, Liu XH, Anjo A, et al. Human endothelial cells derived from circulating progenitors display specific functional properties compared with mature vessel wall endothelial cells. Blood. 2004;103(7):2577-84.
63. Smadja DM, Melero-Martin JM, Eikenboom J, Bowman M, Sabatier F, Randi AM. Standardization of methods to quantify and culture endothelial colony-forming cells derived from peripheral blood. Journal of Thrombosis and Haemostasis. 2019;17(7):1190-4.
64. Blandinières A, Randi AM, Paschalaki KE, Guerin CL, Melero-Martin JM, Smadja DM. Results of an international survey about methods used to isolate human endothelial colony-forming cells: guidance from the SSC on Vascular Biology of the ISTH. J Thromb Haemost. 2023;21(9):2611-9.
65. Smadja DM, Melero-Martin JM, Eikenboom J, Bowman M, Sabatier F, Randi AM. Standardization of methods to quantify and culture endothelial colony-forming cells derived from peripheral blood: Position paper from the International Society on Thrombosis and Haemostasis SSC. J Thromb Haemost. 2019;17(7):1190-4.

Supplemental Table 1. Antibodies used in immunofluorescence (IF)

Antibody	Manufacturer	Cat. Number	Dilution
IF Primary (OP)			
VWF (rabbit)	DAKO	A0082	1:1000/ 1:50000
VE-cadherin (mouse)	BD Pharming	55561	1:250
β-catenin (rabbit)	Santa Cruz	Sc-7199	1:500
EEA1 (mouse)	BD Biosciences	610457	1:500
Hoechst	Sigma-Aldrich	H3569	1:10000
DAPI	Thermo Fisher	D3571	1:33000
VE-cadherin (goat)	R&D systems	AF938	1:250
VE-cadherin (mouse)	Santa Cruz	sc-9989	1:250
TGN46 (sheep)	Serotec	AHP500	1:1000
IF Primary (OCP)			
VWF (sheep)	Abcam	ab11713	1:1000
VE-cadherin (mouse)	BD Pharming	55561	1:250
Hoechst	Sigma-Aldrich	H3569	1:10000
Rab27A (rabbit)	Protein Tech	17817	1:100
PDI (rabbit)	Enzo Life Sciences	SPA-890	1:250
IF Secondary			
Donkey-anti-Rabbit AF647	Invitrogen Molecular Probes	A31573	1:750
Donkey-anti-Mouse AF568	Invitrogen Molecular Probes	A10037	1:750
Donkey-anti-Sheep AF488	Invitrogen Molecular Probes	A11015	1:750
Donkey-anti Rabbit AF568	Invitrogen Molecular Probes	A10042	1:400
Donkey-anti Goat AF647	Invitrogen Molecular Probes	A32849	1:400
Donkey-anti Mouse CF568	Biotium	20105	1:1000
Donkey-anti Mouse CF488A	Biotium	20014	1:1000

Transcriptional and functional profiling identifies inflammation and endothelial-to-mesenchymal transition as potential drivers for phenotypic heterogeneity within a cohort of endothelial colony forming cells

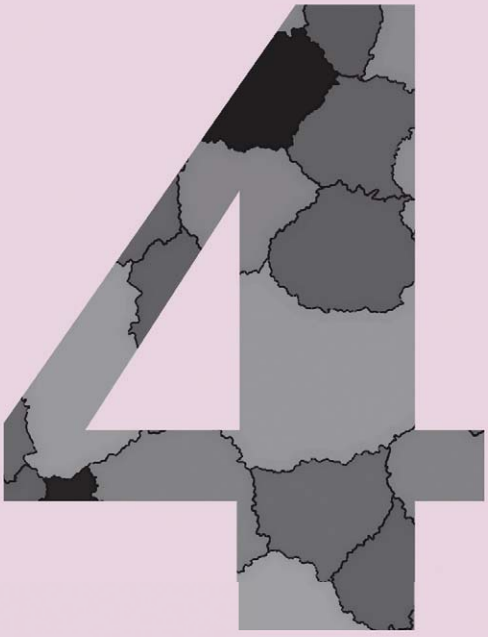

Laan SNJ, de Boer S, Dirven RJ, van Moort I, Kuipers TB, Mei H, Bierings R, Eikenboom J

Journal of Thrombosis and Haemostasis. 2024 Jul;22(7):2027-2038.
doi: 10.1016/j.jtha.2024.03.018.

Abstract

Background

Endothelial colony forming cells (ECFCs) derived from patients can be used to investigate pathogenic mechanisms of vascular diseases like Von Willebrand disease. Considerable phenotypic heterogeneity has been observed between ECFC clones derived from healthy donors. This heterogeneity needs to be well understood in order to use ECFCs as endothelial models for disease. Therefore, we aim to determine phenotypic and gene expression differences between control ECFCs.

Methods

A total of 34 ECFC clones derived from 16 healthy controls were analyzed. The transcriptome of a selection of ECFC clones (n=15) was analyzed by bulk RNA sequencing and gene set enrichment analysis. Gene expression was measured in all ECFC clones by qPCR. Phenotypic profiling and migration speed of the ECFCs was done using confocal microscopy, followed by automated quantification of cell morphometrics and migration speed.

Results

Through hierarchical clustering of RNA expression profiles, we could distinguish two major clusters within the ECFC cohort. Major differences were associated with proliferation and migration in cluster 1, and inflammation and endothelial to mesenchymal transition in cluster 2. Phenotypic profiling showed significantly more and smaller ECFCs in cluster 1 which contained more and longer Weibel-Palade bodies (WPBs). Migration speed in cluster 1 was also significantly higher.

Conclusion

We observed a range of different RNA expression patterns between ECFC clones mostly associated with inflammation and clear differences in WPB count and structure. We developed a qPCR panel which can be used for the characterization of ECFC clones which is essential for the correct analysis of pathogenic mechanisms in vascular disorders.

Introduction

Due to their role in hemostasis, endothelial cells play a major part in many bleeding disorders, which are caused by the disruption of normal functioning hemostasis. Von Willebrand factor (VWF) is a main component of hemostasis and is produced by endothelial cells and megakaryocytes and can bind to collagen at sites of injury and mediate the formation of a platelet plug. VWF is stored in endothelial specific cigar-shaped organelles called Weibel-Palade bodies (WPB) (2, 23). These organelles can secrete their contents without stimulation to provide a steady level of VWF in the blood, thus maintaining homeostasis. WPBs secretion can also be stimulated by vascular damage to quickly increase local concentration of VWF. Von Willebrand disease (VWD) is the most common inherited bleeding disorder worldwide, occurring in roughly 1 in 100 people (24), caused by defects in concentration or structure-function of VWF (25).

One model that can be used to study pathogenic mechanisms involving the endothelium are endothelial colony forming cells (ECFCs), first described by Lin *et al.* (26). A major advantage of this model is that ECFCs can be derived from whole blood and when cultured, display endothelial characteristics such as the production of VWF, storage of VWF in WPBs, a typical cobblestone like morphology, and response to endothelial specific stimuli (27). When these cells are derived from patients, they can be used to study the pathogenic mechanisms of vascular diseases like VWD in their native environment (28-33). These studies performed patient-specific *ex vivo* analysis of endothelial cell function, endogenous production and secretion of VWF and WPB morphology.

Unfortunately, despite the advantages, there is also a challenge with using ECFCs. Substantial phenotypic heterogeneity can exist between ECFC controls from different donors, but also between clones from the same donor (5, 6). Our group has previously shown that, when comparing ECFCs categorized by their morphology, clear differences can be observed in expression of cell surface markers, proliferation, and storage and secretion of VWF (6). In the study by de Boer *et al.* (6), ECFCs were categorized into three groups. Group 1 consisted of ECFC clones with classic endothelial morphology, and group 2 and 3 consisted of larger, more elongated ECFCs. ECFCs in all groups expressed endothelial cell surface markers. However, group 1 ECFCs produced and secreted more VWF in steady state and after stimulation than groups 2 and 3. Furthermore, cell proliferation was lower in group 3. It is currently unclear what causes the heterogeneity observed among healthy control ECFCs.

In order to use ECFCs as a robust model to study pathogenic mechanisms in patients with bleeding disorders or other diseases involving endothelium and to compare with healthy donor ECFCs, it is essential to match proper control ECFCs which are characterized similarly to patient ECFCs. Use of non-characterized control ECFCs could lead to invalid conclusions when analyzing patient ECFCs. Therefore, in the current study, we analyzed differences in ECFC RNA expression, WPB count, morphology and cellular location, and migration speed of ECFCs. We found significant differences in RNA expression between ECFCs clones and these results were used to categorize the EFCFs in two distinct clusters. Between these clusters, large differences were found in WPB count, morphology and in ECFC migration speed.

Methods

ECFC isolation and culture

The study protocol for the acquisition and culturing of the ECFCs was approved by the Leiden University Medical Center ethics review board. From 16 healthy participants informed consent was obtained in accordance with the declaration of Helsinki. Participants were 18 years or older and were not diagnosed with a bleeding disorder nor known to have a bleeding phenotype. Isolation and cell culture of ECFCs was performed as described (6). In short, whole blood was obtained via venipuncture and peripheral blood mononuclear cells (PBMCs) were isolated and cultured in EGM-10 (EBM-2 Basal Medium with EGM-2 supplements & growth factors (Lonza, Basel, Switzerland or PromoCell, Heidelberg, Germany)). In general, clones appeared between days 10 and 21 and were frozen once they confluently filled 3 T75 flasks at passage 3. Multiple clones were isolated per donor, totaling 34 clones for this study. The experiments were performed on the clones at passage 5. See Supplemental Table 1 for a detailed description per clone.

RNA isolation and sequencing

All ECFC clones were cultured in 6-well plates, after they reached confluency they were kept in culture for 5-7 days. ECFC lysates were collected in 400 µl RNA lysis buffer + 4 µl β-Mercaptoethanol. RNA was isolated using RNeasy Mini Kit, according to the manufacturers' protocol (Qiagen, Hilden, Germany). 20 ng/µl of isolated RNA from 15 samples (Supplemental Table 1) was further processed by the GenomeScan facility (Leiden, The Netherlands) using the NEBNext Ultra Direction RNA library Prep Kit from Illumina (San Diego, United States). All 15 samples met the quality criteria and were selected for Bulk mRNA sequencing (polyA enriched) using Illumina NovaSeq6000. RNA sequencing (FASTQ) files were processed using the opensource BIOWDL RNA

sequencing pipeline v5.0.0 (https://zenodo.org/record/3975552) developed at the Leiden University Medical Center (Leiden, The Netherlands). This pipeline performs FASTQ preprocessing (including quality control (QC), quality trimming, and adapter clipping), RNA sequencing read alignment, read quantification, and optionally transcript assembly. FastQC (v0.11.9) was used for checking raw read QC. Adapter clipping was performed using Cutadapt (v2.10) with default settings. RNA sequencing reads' alignment was performed using STAR (v2.7.5a) on the GRCh38 human reference genome. The gene read quantification was performed using HTSeq-count (v0.12.4) with the setting "–stranded=yes". The gene annotation used for quantification was Ensembl version 105.

RNA quantification with quantitative PCR (qPCR)

RNA isolate was acquired as mentioned above. Complementary DNA (cDNA) was synthesized using SuperScript II Reverse Transcriptase (Thermo Fisher Scientific, Waltham, United States) with poly(T) primers (Sigma-Aldrich, Saint Louis, United states). Sybr Select Master Mix (Thermo Fisher Scientific) was used for qPCR which was measured on the ViiA 7 Real-Time PCR system (Thermo Fisher Scientific). GAPDH was used as housekeeping gene. Results were analyzed using the comparative Ct method. One gene panel was used on all 34 samples. The primer sequence is available as Supplemental Table 2. For analysis and creation of the heatmaps, the heatmaply package was used in R (version 4.2.1) (34). See Supplemental File 1 for an R script template that can be used to generate the heatmaps (also made available on GitHub https://github.com/Clotterdam/Laan-et-al-2023-ECFC).

Expression analysis

For the gene expression based clustering analysis, R was used. First, the edgeR package (v3.36) was used to calculate CPM (Count Per Million) of all genes in our samples. Then we selected expressed genes with a CPM higher than 1 in at least 25% of all samples (4 out of 15 samples). 12663 genes passed this filtering step. Using the dgeAnalysis package (v1.5.2), Principal Component Analysis (PCA) was performed using these 12663 genes. Plotting principal component (PC) variance showed that PC 1-4 explained most of the variance (Supplemental Figure 1A). Samples were then hierarchically clustered based on these four PCs with package cluster (v2.1.6) (Supplemental Figure 1B). The read count data of the 15 samples was labelled either as cluster 1 or cluster 2 based on the hierarchical clustering mentioned previously. Next, EdgeR (v3.36) was used to detect the differentially expressed genes between cluster 1 and cluster 2 with the trimmed mean of M values (TMM) normalization. All genes with a False Discovery Rate (FDR) adjusted p-value < 0.05 were declared significant. Gene set enrichment analysis (GSEA) was performed using the enrichplot package (version 1.18.4) and ClusterProfiler (version

4.8.2) in R on the GO:BP, GO:CC, GO:MF, KEGG and Reactome databases (35, 36). GSEA results were also visualized as a GSEA map using the enrichplot package. In the map, each node represents a significantly enriched gene-set and edge thickness represents the similarity between nodes. Node clusters were identified by the package and given a generated label. This label was later manually revised to fit the contents of the cluster.

Immunofluorescence of ECFCs and Image Acquisition

When ECFCs were plated for RNA isolation, 48-well plates (Nunclon) filled with collagen (50 µg/mL Collagen type I rat tail (BD Biosciences, Franklin lakes, United states) coated 9 mm glass coverslip (VWR, Radnor, United States) were also plated. Cells were left confluent for 5 days before fixation with 70% ethanol on ice for 10 minutes. After fixation, samples were blocked using blocking buffer (PBS; 1% bovine serum albumin (Sigma-Aldrich); 1% fetal calf serum (Gibco)). Then, samples were stained with antibodies against VWF and VE-cadherin (Supplemental Table 3 for supporting information on antibodies) diluted in blocking buffer. After, samples were stained with secondary antibodies diluted in blocking buffer and then with Hoechst in PBS, coverslips were placed on a glass slide and mounted with ProLong® Diamond Antifade Mountant (Thermo Fisher Scientific). Imaging was performed with the Imagexpress Micro Confocal System which made a tile scan (4x4) using the 63x objective without extra magnification. A z-stack was made which spanned the entire thickness of the confluent cell layer. This was transformed into a maximum Z-projection using ImageJ (version 2.3.0) (13).

Migration assay and image acquisition

Six ECFC clones were selected for the migration assay (Supplemental Table 1). We chose clones from each identified cluster 1 and cluster 2 (for both clusters n=3). These clones also belonged to each of the previously identified morphological groups 1, 2 and 3 (6) (for all groups, n=2). These clones were cultured in 48-well plates. Each clone was plated in six randomly chosen per plate. Three days post-confluency, cells were washed once with PBS and then labeled with CellTracker Green (Life Technologies) diluted 1:10,000 in 200 µL EGM-10 for 45 minutes. Three of the wells per clone were then treated with 12.5 µg/mL Mitomycin C (Sigma-Aldrich) diluted in 200 µL EGM-10 for 2 hours. The remaining wells just received EGM-10. After 2 hours, the confluent cell layer was scratched using a p100 pipet tip. Cells were washed once to remove debris. Live cell imaging was performed using the confocal AF6000 (Leica, Wetzlar, Germany) microscope with a 10x lens at 37^0C and 5% CO_2. A grid was prepared so that the same spot in the center of each well was imaged for 20 hours at 30 minutes intervals, with auto-focus correction.

Automated quantification of morphology and migration speed using CellProfiler

For the quantification of cell and organelle morphology and migration speed, CellProfiler (version 4.2.1) was used (7). We used the OrganelleProfiler (37) which is a pipeline specifically designed for the identification and quantification of cell shape, size and organelle count, shape, size and relative location in the cell. The pipeline was optimized for the antibodies and intensity in this set of tile scans. For the migration assay, a new pipeline was developed. Using the CellTracker Green signal, each cell is identified as an object. Then, cells in close vicinity to each other (confluent cells) are combined as one object. The surface area of that object was then measured. Closing speed was calculated as the increase in number of covered pixels per hour over the first 10 hours. The pipeline developed for the migration assay is available in the supplement (Supplemental File 2) and made available on GitHub (https://github.com/Clotterdam/Laan-et-al-2023-ECFC).

Statistical Analysis

Data analyses was performed using GraphPad Prism 9.3.1 (GraphPad Software, San Diego, CA, USA) if not otherwise indicated. Results with p-value < 0.05 were considered statistically significant. P-values are indicated in the figures where applicable. Unpaired T-test was performed on normally distributed data and Mann-Whitney U test was performed on not normally distributed data to compare ECFCs. A two-way ANOVA was used for the migration assay.

Results

RNA expression profile-based characterization identifies two clusters of ECFCs

A total of 34 ECFC clones derived from 16 healthy controls were analyzed, covering the previously defined phenotypic groups 1, 2 and 3 (6). Since these groups have been shown to differ in terms of surface levels of endothelial markers and storage and secretion of VWF, we also wanted to analyze differences in the RNA expression profile. Bulk RNA sequencing was performed as an unbiased method to examine transcriptional heterogeneity between healthy ECFC clones. The transcriptomes of a selection of ECFC clones (n=15) (Supplemental Table 1) were analyzed. Principal Component analysis (PCA) (Figure 1A) revealed considerable variety between the ECFC clones. Hierarchical clustering of the samples (Supplemental Figure 1) based on the PCA resulted in 2 main clusters, from here on named cluster 1 (n=11, green) and cluster 2 (n=4, blue). There is an unbalanced number of replicates between the clusters, which may cause a slight bias towards the detected differentially expressed genes to be more robust towards

cluster 1 and less robust towards cluster 2. The clusters somewhat correspond to the previously defined phenotypic groups 1 and 3 (Figure 1A). However, group 2 ECFCs do not fall specifically in either of the two clusters and showed high variation in RNA expression, likely due to this group of cells being difficult to categorize based on their morphological characteristics. Morphological group 2 ECFCs possibly represent an intermediate between cluster 1 and 2.

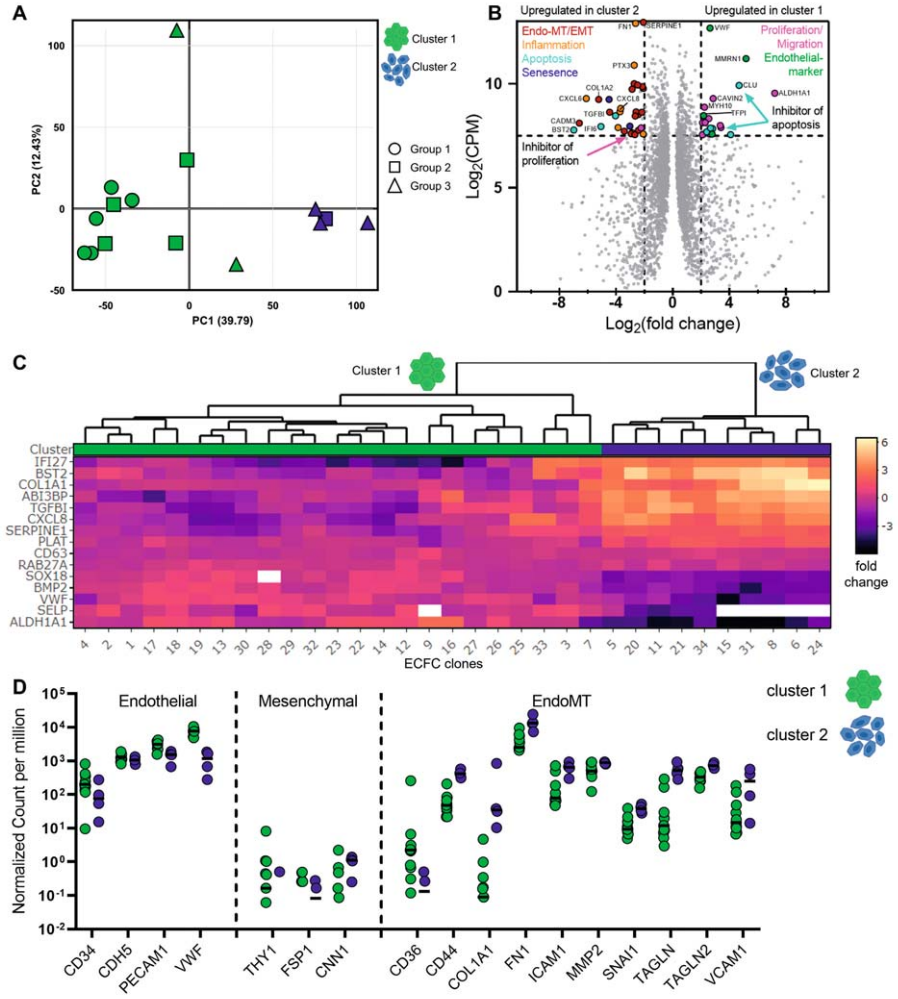

Figure 1. RNA expression analysis showing differential gene expression between ECFC clones. A) PCA plot of 15 ECFC clones, color-coded by their associated cluster as measured by hierarchical clustering. Circles, squares and triangles indicate the original categorization of ECFCs based on cell morphology in group 1, group 2 and group 3 respectively (13). B) Bulk RNA sequencing transcriptome analysis shows differential gene expression between ECFC clusters. The volcano plot shows significantly upregulated genes (grey, adjusted P-value < 0.05) between

cluster 1 and cluster 2 (3758 genes). Dashed lines represent the threshold where fold change was > 2 and counts per million (CPM) were > 7.5. Genes involved with proliferation and migration are shown in pink and endothelial markers are indicated in green. Genes involved in endothelial to mesenchymal transition (EndoMT) and epithelial to mesenchymal transition (EMT), inflammation, apoptosis, and senescence are shown in red, orange, cyan and blue respectively. Gene names of genes with the highest fold change and count per million are displayed. C) Heatmap showing the log nFOLD difference of the RNA expression with the median of 33 ECFC clones as measured by qPCR. Hierarchical clustering of the ECFCs is shown by the dendrogram (top). All ECFCs were tested on a panel of genes (Supplemental Table 2). White squares marks data points that could not be measured. D) Normalized RNA count per million (CPM) for endothelial, mesenchymal and EndoMT markers. The y-axis is shown as a log(10) scale. Based on differential gene expression analysis between clusters, PECAM1, VWF and all EndoMT markers were significant (adjusted p-value). CD34, CDH5 and all mesenchymal were not significant. Each dot represents the CPM per clone.

Gene expression differences between cluster 1 and cluster 2 ECFCs were analyzed. From all samples, 11,817 genes were measured and 3,758 genes showed significant differential expression (Figure 1B). Genes with a fold change higher than 2 and a count per million (CPM) higher than 7.5 were further investigated. This cut-off resulted in 54 genes of interest (Supplemental Table 4). Fold change is reported as the difference in expression in cluster 1 compared to cluster 2. Genes with a positive fold change are thus upregulated in cluster 1. Genes of interest involved in processes like endothelial to mesenchymal transition (EndoMT), inflammation, apoptosis, and senescence were upregulated in cluster 2 ECFCs. In contrast, upregulated genes in cluster 1 ECFCs are associated with proliferation and migration. Cluster 2 ECFCs also showed significant upregulation of Collagen Type I Alpha 1 Chain and C-X-C Motif Chemokine Ligand 8, and cluster 1 ECFCs showed upregulation of SRY-Box 18, Ephrin B2 and Thrombomodulin which corresponds with previous findings of de Jong *et al.* (5).

We designed a minimal qPCR panel with the aim to easily characterize the clones based on their gene expression. The panel was created based on the results of the bulk RNA sequencing and consists of genes which showed the strongest fold change, highest CPM and biological relevance to characterize ECFC clones (Supplemental Table 2). The qPCR panel was used to analyze the RNA expression of all clones. Per clone, gene fold change was compared to the median of all ECFC clones, as shown in a heat map (Figure 1C). Considerable variation between the clones can be observed, especially for the genes Interleukin-8 (*CXCL8*), Interferon alpha-inducible protein 27 (*IFI27*), Bone Marrow Stromal Cell Antigen 2 (*BST2*) and Collagen type I alpha (*1COL1A1*) which where downregulated in cluster 1 ECFCs. Whereas VWF, P-selectin (*SELP*) and aldehyde dehydrogenase 1 family member A1 (*ALDH1A1*) were upregulated in cluster 1. The hierarchical clustering of the clones based on this selection of genes results in the

same clusters as those observed in the PCA plot. This indicates that the qPCR panel can accurately categorize ECFC clones using a minimal list of targets.

Differential expression indicates a role for EndoMT. To further substantiate this claim, we have highlighted endothelial markers (*VWF, CD34, CD144* and *PECAM1*) (38), mesenchymal markers (*CNN1, THY1* and *FSP1*) (39), and early and late EndoMT markers (*TAGLN, CD44, FN1, 1COL1A1, MMP2, VCAM, ICAM1* and *SNAI1*) (39, 40) from the RNA sequencing results (Figure 1D). All the ECFCs show strong expression of endothelial markers although cluster 2 cells show significantly decreased expression of endothelial markers *PECAM1* and *VWF*. It was also observed that the mesenchymal markers *CNN1, THY1* and *FSP1* had very low expression in almost all samples which were not significantly different between clusters, indicating that the cells are not fully mesenchymal. Interestingly, the EndoMT markers where expressed by all ECFCs and were all significantly upregulated in cluster 2 compared to cluster 1. This further emphasizes that ECFCs are still endothelial and not fully mesenchymal cells and that the EndoMT pathway plays a significant role in the heterogeneity between clones. These findings give an indication of the differences between clones on an expression level, but additional experimental evidence is needed to confirm this.

Inflammation and endothelial to mesenchymal transition pathways are differentially regulated in cluster 1 and cluster 2 ECFCs

To formally identify and prioritize relevant gene sets associated with the observed differences between the cluster 1 and cluster 2 ECFCs (Figure 2), we employed Gene Set Enrichment Analysis (GSEA). GSEA is a powerful computational approach that offers several advantages in the analysis of bulk RNA sequencing data like reducing the impact of random noise in large-scale transcriptomic datasets (41). We applied GSEA to the Gene Ontology (GO) Biological Process (BP), Cellular Component (CC) and Molecular Function (MF) databases. GSEA from the GO:BP (Figure 2A) demonstrated significant differences (q-value < 0.05) with a positive normalized enrichment score (NES) (meaning an upregulation in cluster 1 ECFCs) in the gene set "regulation of endothelial cell migration" (NES = 1.56), and a negative NES (meaning a downregulation in cluster 1 ECFCs) in "inflammatory response" (-1.60), "extracellular matrix organization" (-1.69), and "endodermal cell differentiation" (-2.20). Furthermore the "epithelial to mesenchymal transition" (-1.57) gene set showed borderline significant differences (q-value of 0.06). This highlights the potential variation in cytokine regulation, migration and differentiation.

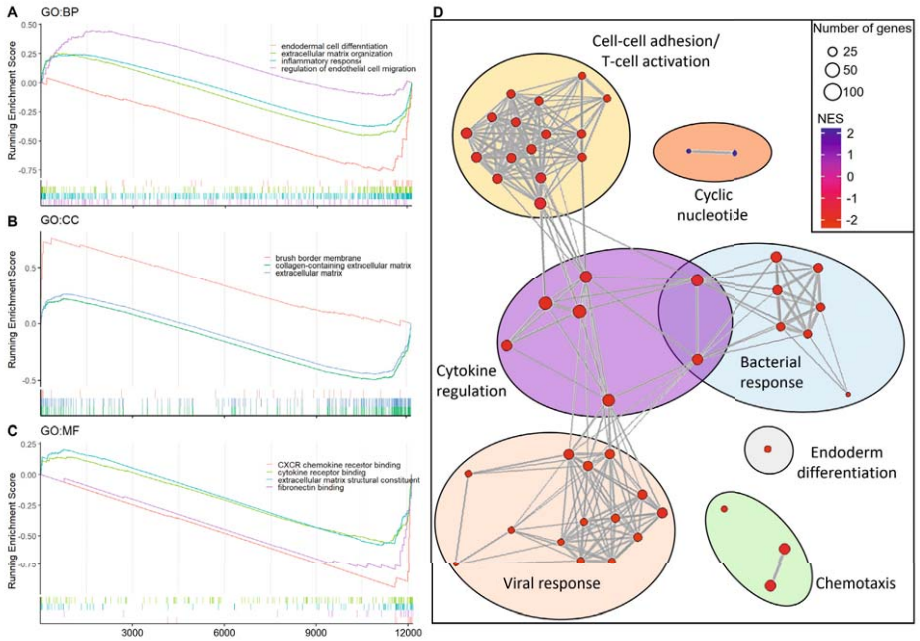

Figure 2. Gene Set Enrichment Analysis of cluster 1 versus cluster 2 ECFC RNA expression. (A-C) GSEA showed the significantly enriched gene sets (FDR < 0.05) between cluster 1 and cluster 2 ECFCs for various databases; GO:BP (A), GO:CC (B) and GO:MF (C). D) GSEA map of the top 50 gene sets from the GO:BP database constructed with the enrichplot package. Red nodes indicate gene sets with a negative NES while blue indicates a positive NES score. Thickness of lines between nodes correspond with the similarity between gene sets. Abbreviations: Normalized enrichment score (NES); Genome Ontology (GO); Biological Processes (BP); Cellular Component (CC); Molecular Function (MF).

Additionally, GSEA from the GO:CC (Figure 2B) and GO:MF (Figure 2C) databases resulted in gene sets scoring negatively for "collagen-containing extracellular matrix" (-1.90), "extracellular matrix" (-1.78), "CXCR chemokine receptor binding" (-2.12), "cytokine receptor binding" (-2.16), "extracellular matrix structural constituent" (-1.96) and "fibronectin binding" (-2.01). The Gene set "Brush border membrane" had a positive NES (1.94). Genes often participate in multiple pathways and GSEA can thus yield large numbers of broadly overlapping gene sets. Therefore we collapsed redundant pathways into single functional or biological themes and created a GSEA map for the top 50 enriched GO:BP gene sets (Figure 2D), thereby further aiding in interpretation. Clusters of gene sets indicate that most negatively enriched gene sets are associated with inflammation and immune responses, either to viruses or bacteria. These findings collectively provide a view of the transcriptional distinctions between the clusters,

offering novel insights into the underlying molecular mechanisms regulating their distinct characteristics.

Quantitative differences in cell and WPB morphology between ECFC clusters

RNA expression showed a significant difference in genes associated with cell proliferation and VWF production. It has been shown that VWF production is directly linked to the length of WPBs (14). Previous research has also shown significant differences in VWF protein production, cell size and proliferation between ECFC clones (5, 6). Therefore, we imaged cluster 1 and cluster 2 ECFC clones (Figure 3A) to quantify the cell count, cell size and shape number (Figure 3B-D). To analyze WPB count and morphology we also quantified their eccentricity and maximum ferret diameter as an approximation of roundness and length respectively (Figure 3E-H), using a specialized CellProfiler pipeline for automated WPB identification and quantification (37). Data is shown as mean ± SD. Cell count was significantly lower in cluster 2 ECFCs (n = 152.90 ± 109.60) than in cluster 1 (n = 409.90 ± 164.80, p=0.0003). As endothelial cells form a confluent layer, it follows that we observed a larger cell size in cluster 2 ECFCs (4490 μm^2 ± 2799) compared to cluster 1 ECFCs (1529 μm^2 ± 684.90, p=0.0006). We also observed that cluster 2 ECFCs were significantly rounder (0.77 ± 0.02) than cluster 1 ECFCs (0.83 ± 0.04, p=0.0006) as measured by their eccentricity. Furthermore, WPB count per cell was significantly lower in cluster 2 ECFCs (n = 25.40 ± 30.40 vs. 118.00 ± 44.40, p=0.0001). WPB eccentricity and length of the WPBs were measured and WPBs were both rounder and shorter in cluster 2 ECFCs (0.66 ± 0.03 vs. 0.72 ± 0.05, p=0.0024 and 0.76 µm ± 0.12 vs. 0.97 µm ± 0.26, p=0.017 respectively). Finally, the relative distance of the WPBs to the nucleus in percentage was measured. We found that WBPs of cluster 1 ECFCs (56.48% ± 7.20) tend to locate more to the periphery of the cell than cluster 2 ECFCs which seem to locate relatively closer the nucleus (46.09% ± 13.79, p=0.06). This is likely explained by the larger size of the cluster 2 ECFCs. Collectively, these findings could explain the reduced VWF production and secretion observed in previous research (6).

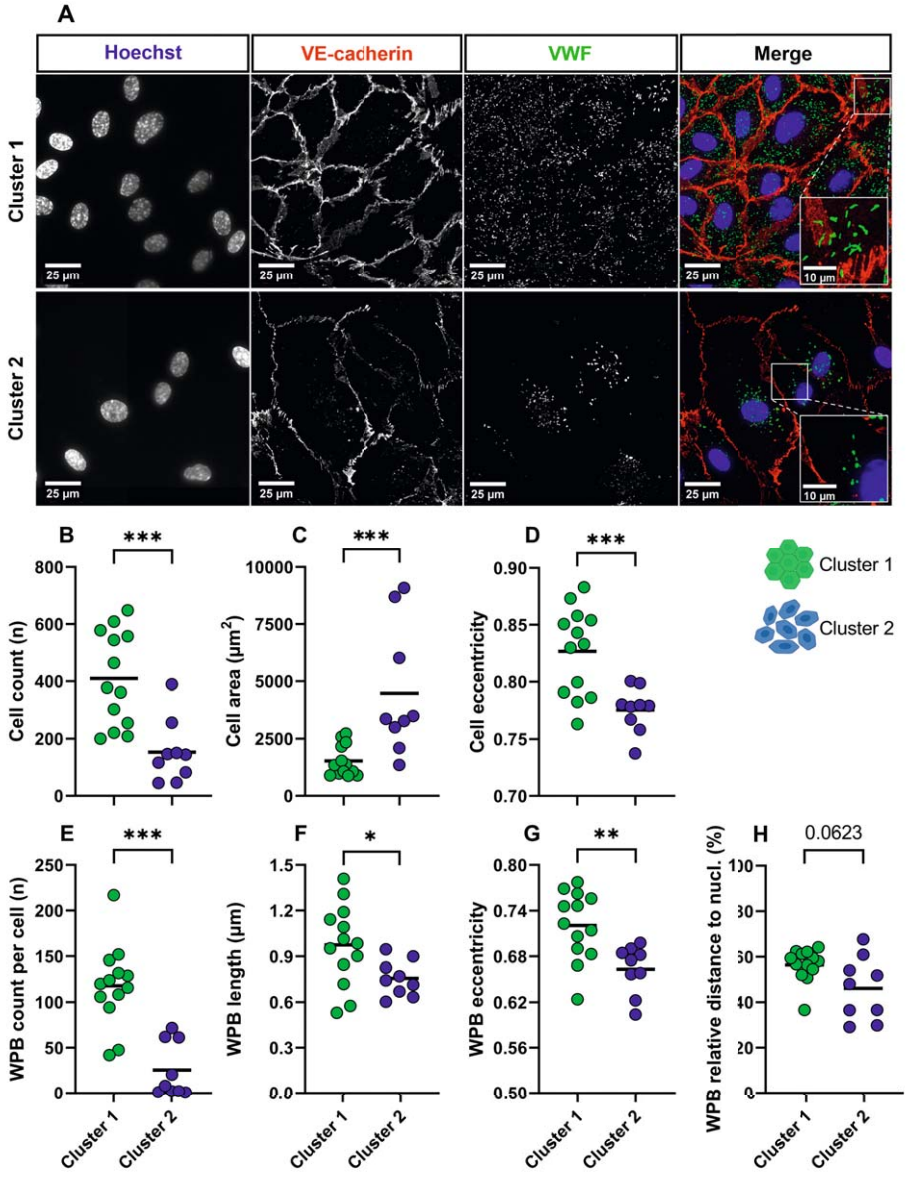

Figure 3. Morphological differences of cell and organelle count and shape. Phenotypic profiling of the ECFCs was done using tile scans (707381 µm2). ECFC clones were divided by hierarchical clustering based on RNA expression in cluster 1 (n=13) and 2 (n=9). A) Representative confocal images of ECFCs stained with Hoechst (blue) and antibodies against VE-cadherin (red) and VWF (green) from cluster 1 (top) and cluster 2 (bottom, scale bar represents 25 µm). The white box shows a 2.5x zoom in of the merge (scale bar represents 10 µm). Images were taken with a 63x times objective. B) Cell count per surface area of the tile scan. C) Median surface area of cells per clone. D) Median cell eccentricity. E) WPB count per cell per ECFC clone. F) Median WPB length per ECFC clone. G) Median eccentricity of WPBs per ECFC clone. H) Distance of the

WPB to the nucleus relative to their position in the cell in percentage. Values are median per clone. Line shows median. Unpaired T-test was performed on normally distributed data (B, D, F, G and H). Mann-Whitney U test was performed on not normally distributed data (C and E); * p <0.05, ** p < 0.01, *** p <0.001.

Decreased cell migration in cluster 2 ECFCs

According to the GSEA, genes associated with regulation of endothelial cell migration were differentially expressed between cluster 1 and cluster 2. To determine the rate of migration of the ECFCs, a scratch assay was performed three times on a selection of cluster 1 and cluster 2 ECFCs (n=3 per cluster) and closing speed was quantified (Figure 4A). The mean cell count per cluster at T0 was 418.01 ± 52.25 in cluster 1 and 252.06 ± 82.43 in cluster 2. We observed that the closing speed in the first 20 hours after the scratch was significantly higher in cluster 1 ECFCs (29143.67 ± 6713.37) than in cluster 2 ECFCs (13889.50 ± 1278.76, p=0.0097) (Figure 4B). Furthermore, the same effect was seen when the potential contribution of proliferation to the closing speed was excluded by inhibition of proliferation using Mitomycin C (26901.67 ± 6882.52 vs 12610.83 ± 399.18, p=0.0138). This indicates that the difference in closing speed is caused mostly by the migration capabilities of the cells within this time frame. This is in line with previous research where proliferation between clones of different morphological groups was analyzed (6). There, the phenotypic groups of ECFCs showed no significant difference in proliferation in the first 24 and 48 hour period, but group 1 did show increased proliferation after 48 hours in culture.

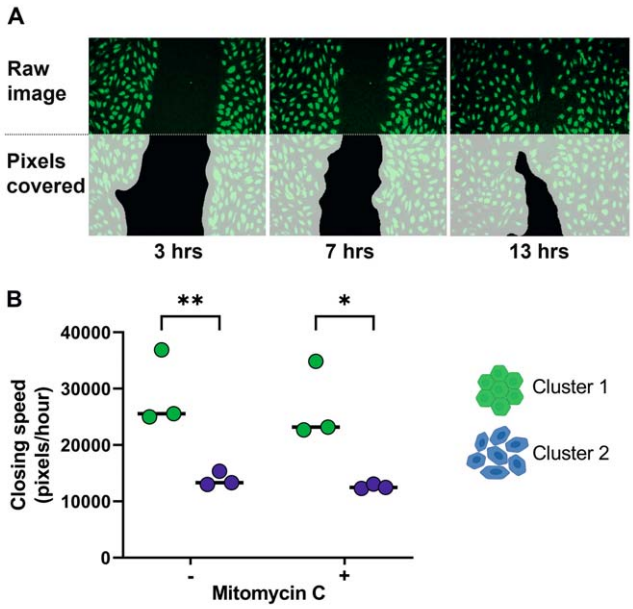

Figure 4. Delayed migration of cluster 2 ECFCs. ECFCs were stained with a live cell marker (Cell tracker), scratched and then imaged every 30 minutes. A) Top, representative image of the scratch at three time points in a cluster 1 ECFC clone. Bottom, a graphic representation of the calculated pixel coverage in white as calculated by a CellProfiler pipeline. Average pixel closing speed per hour was quantified. B) Mean closing speed of three cluster 1 ECFCs and three cluster 2 ECFCs (showing the average of three measurements). On the left without (-) and on the right with (+) inhibition of proliferation by Mitomycin C. Statistical analysis by two-way ANOVA, * $p < 0.05$, ** $p < 0.01$.

Discussion

ECFCs have been used to study the pathogenic mechanisms of various diseases *in vitro* (29, 32, 33, 42). However, considerable phenotypic heterogeneity has been observed in ECFC clones isolated from healthy controls (5, 6), which may preclude unambiguous interpretation of such work. Therefore, we aimed to determine phenotypic and gene expression differences between control ECFCs. In this study, we found that 2 major clusters of ECFCs could be discerned that, in all our subsequent morphological and functional analyses, were phenotypically distinct. Cluster 1 ECFCs are smaller cells that contain large numbers of elongated WPBs and show high migration capacity, whereas cluster 2 ECFCs are large, contain fewer WPBs that are also significantly shorter and display a reduced migratory potential. Elongated morphology of WPBs correlates with their secretion competence as well as the hemostatic potential of their main cargo protein VWF (3), while abnormalities in WPB size and shape can be a direct consequence of the pathogenic mechanisms that underpin

some forms of VWD (32, 33, 43). Moreover, it was reported that ECFCs isolated from VWD patients also have alterations in their migratory and angiogenic potential (29, 31, 44). Our observation that these key parameters already show significant differences between the 2 phenotypic clusters within healthy controls highlights the need for care when interpreting data obtained with ECFCs from healthy as well as diseased subjects. It also offers a potential strategy to minimize the impact of ECFC heterogeneity on experimental results (see below).

Despite unbalanced numbers of replicates between clusters, the high number of detected differentially expressed genes was sufficient to detect biological process changes. Cluster 1 ECFCs showed upregulation of genes associated with proliferation and migration, while cluster 2 ECFCs have upregulated genes associated with inflammation, senescence and apoptosis. This included *Pannexin 1* (data in repository), a senescence marker that was recently found to modulate angiogenic activities and cellular activity in ECFCs (45). RNA expression profiling also showed that *TGFBi, TGFB2, BMP2* and *SMAD1* were upregulated in cluster 2 which are EndoMT/EMT associated genes (39). EndoMT transforms endothelial cells into mesenchymal cells, leading to reduced expression of endothelial markers, increased extracellular matrix proteins, and loss of endothelial functions (46-48), including reduced synthesis of VWF (49). Our transcriptional, morphological and functional data fit with the notion that cluster 2 ECFCs are in the process of EndoMT or are transitioning towards mesenchymal cells. Transcriptional analysis of ECFCs by Kutikhin *et al.* showed that ECFCs overexpress endothelial markers *NRP2, NOTCH4* and *LYVE1* when compared to human coronary artery endothelial cells and human umbilical vein endothelial cells (50). These markers were also strongly expressed in our data. Interestingly, *LYVE1* was expressed in all samples, but was strongly upregulated in cluster 1 ECFCs, suggesting cluster 1 ECFCs have more potential to differentiate into the lymphatic endothelial lineage. Higher levels of *TGFB2* in cluster 2 which has been shown to induce EndoMT and downregulate expression of *LYVE1* may also explain the difference in expression (51).

Why some ECFC isolations result in clones that correspond to cluster 2 clones with EndoMT characteristics, while also yielding cluster 1 clones that have not progressed to that state is currently unclear. It has been shown that EndoMT can be regulated by epigenetic mechanisms (52), which could have led to some of the circulating cells from which ECFC clones originate having been primed upfront towards generating cluster 2 ECFCs. The origin of circulating ECFCs remains unclear. Tura et al. showed that ECFCs are likely not originating from bone marrow but are derived from a CD34(+), CD133(-), CD146(+) cell fraction potentially arising from vessels (53). The transcriptome of ECFCs closely resembles that of cultured microvascular endothelial cells and HUVECs (54). Heterogeneity between clones may arise from different vascular beds, influenced by specific microenvironmental cues (55). Lin et al. identified a fraction of $CD34^{bright}$ and $PROCR^{+}$ umbilical vein cells as a potential ECFC origin.

Interestingly, the genes used by Lin et al to characterize this subset (PROM1, PTPRC, CDH5, PECAM1, MCAM and FLI1) are also expressed similarly by the ECFCs used in our study (56) (see repository). This makes it likely that they are derived from the same pool. Lack of differential expression of these genes between ECFC clusters suggests differentiation occurred after isolation.

Multiple studies have shown that inflammation can cause EndoMT in primary endothelial cells (57-59). This is in line with our findings as the transcriptional profiling and the subsequent GSEA showed a strong upregulation of inflammation and immune response pathways in cluster 2 ECFCs. Collectively, these data suggest that cluster 2 ECFCs create, or are a result of, an inflammatory environment. Additionally, our data shows that expression of the pro-inflammatory cytokine interleukin 8 (*IL-8*) is significantly upregulated in cluster 2 ECFCs. Medina *et al.* showed that endothelial cells after *ex vivo* expansion became enlarged and senescent in an *IL-8* dependent manner (60). We speculate that this represents an autocrine/paracrine inflammatory loop that can initiate or perpetuate the transdifferentiation into cluster 2 ECFCs. Whether this is an ongoing process in which even cluster 1 ECFCs are destined to eventually become cluster 2 is not clear from our data, since the bulk RNA sequencing analysis that we performed is unable to identify single cell differences within clones. Longitudinal studies and single cell RNA sequencing analysis will be necessary to reveal whether ECFC clones are homogenous populations or in various stages of transition.

Lastly, the phenotypic differences in ECFCs could be attributed to isolation and culture conditions, influenced by factors such as prolonged culture times, frequent media changes, and clonal expansion from a single cell. Previous studies have shown the impact of variables on the characteristics of ECFC clones, such as day of first appearance of ECFCs (6), passaging (60), time in culture (61, 62) and as a result, replicative stress that some ECFCs may have experienced during expansion. A number of questions remain regarding the unpredictability of ECFC isolations. Firstly, it has been observed that some isolations from donors or certain disease phenotypes yield no clones, so termed “zero colonies” (63). For example, ECFC isolation from patients with VWD type 3 is possible but with low success rate (29), suggesting a role for VWF in this process. Secondly, donor age also seems to influence outcome as isolations from children (0 to 10 years) yield significantly more ECFCs than adult isolation, but no differences are seen between adults ranging from 20-73 years of age (63). The donors included in the current study were all adults and no age-related differences were observed in this study. Ongoing efforts by the ISTH SSC Vascular Biology aim to standardize ECFC isolation and culturing, proposing recommendations for seeding density, passaging, and clone expansion to reduce variation between laboratories and clone heterogeneity (63, 64). Whether these recommendations will favor the emergence of relatively more cluster 1 or 2 ECFCs remains to be seen.

This study provides crucial insight into the heterogeneity of ECFC clones derived from healthy donors. Whether this heterogeneity between ECFC clones relates to a predisposition within the cell of origin, or if it is introduced as a result of the inherent variations associated with primary cell isolation and culture conditions, remains unclear. In a previous, multicenter study using ECFCs isolated from Dutch and Canadian donors in 2 separate laboratories we showed that, using classification of ECFC clones based on morphology, we could distinguish 3 separate groups that also differed in terms of proliferation, VWF secretion and expression of cell surface receptors (6). We now show that an even further and simpler dimensionality reduction can be achieved using qPCR profiling. While this has only been performed in our laboratory, it broadly aligns with the previous classification of the Dutch and Canadian ECFCs (6). This highlights that these discrete phenotypic clusters are probably not restricted to ECFC isolations from our laboratory, but may also be present within ECFC collections from other investigators. Whether our strategy to dichotomize ECFCs into two distinct clusters can be more generally applied as a solution for phenotypic heterogeneity that is observed by other investigators, will need to be validated in other labs. This should include standardized methods such as proposed by the SSC (65), to rule out the effect of experimental variation during isolation and ex vivo maintenance of ECFCs. Furthermore, it is vital to acknowledge that there are other key aspects of ECFCs not addressed in this study like angiogenic capacity, proliferation, apoptosis or endothelial barrier function. For studies that aim to use ECFCs with such phenotypic readouts it is thus important to confirm that the phenotypic variability that has been observed for those aspects (44) also relates to the 2 ECFC clusters that we identify.

In order to use the ECFCs as a robust model to study pathogenic mechanisms, it is essential that one takes the phenotypic heterogeneity into account in the experimental design. This ensures that findings are not incorrectly attributed to pathogenic mechanisms rather than phenotypic heterogeneity in ECFCs. So far, no objective criteria were available that could be used to stratify ECFCs for this purpose. The benefit of this study is that we present a minimal qPCR panel that can be used as a tool to pre-characterize and dichotomize clones during the isolation workflow into two ECFC subsets, each with distinct morphological and migratory features. The relatively small number of genes that need to be screened, combined with the wide availability of qPCR platforms means that this should be a quick and cost-effective tool that is accessible for all laboratories that study ECFCs. Furthermore, qPCR offers an unbiased approach to pre-select clones, without selection based on outcome parameters. The raw qPCR data of the panel of 34 ECFC clones is made readily available and can be used to aid characterization of small numbers of samples (data in repository). When applying the qPCR panel to match ECFC clones, we recommend to select neighboring clones after hierarchical clustering, or to select clones which, in gene expression, don't differ more than 1 fold change from one another. Classification of ECFC clones provides a rationale to select

matching ECFCs in experimental comparisons. Owing to, among others, their favorable growth characteristics, one would preferentially compare cases with controls using cluster 1 ECFCs. In cases where only cluster 2 ECFCs are available, for instance with rare patients with persistent low yield of ECFCs, this classification can help to minimize the effect of phenotypic variability on experimental outcome by selecting matching cluster 2 control ECFCs. Finally, this knowledge offers an excellent platform for follow-up research to be performed. Our data suggests a strong role of an inflammatory mechanism that could cause, or be the result of, the differences between ECFCs clones. Further understanding of the cause of this inflammatory milieu could lead to improved standardization of the isolation and culturing protocol.

Acknowledgements

The SYMPHONY consortium, which aims to orchestrate personalized treatment in patients with bleeding disorders, is a unique collaboration between patients, health care professionals, and translational and fundamental researchers specializing in inherited bleeding disorders, as well as experts from multiple disciplines (22). It aims to identify the best treatment choice for each individual based on bleeding phenotype. To achieve this goal, work packages (WP) have been organized according to 3 themes (e.g. Diagnostics [WPs 3 and 4], Treatment [WPs 5-9], and Fundamental Research [WPs 10-12]). Principal investigator: M.H. Cnossen; project manager: S.H. Reitsma.

Beneficiaries of the SYMPHONY consortium: Erasmus University Medical Center-Sophia Children's Hospital, project leadership and coordination; Sanquin Diagnostics; Sanquin Research; Amsterdam University Medical Centers; University Medical Center Groningen; University Medical Center Utrecht; Leiden University Medical Center; Radboud University Medical Center; Netherlands Society of Hemophilia Patients (NVHP); Netherlands Society for Thrombosis and Hemostasis (NVTH); Bayer B.V., CSL Behring B.V., Swedish Orphan Biovitrum (Belgium) BVBA/SPRL.

Funding by SYMPHONY: NWO-NWA.1160.18.038 (received by SNJL, IvM, RB and JE), Landsteiner Foundation for Blood Transfusion Research, Grant Number:1707. (received by RB) and Landsteiner Foundation for Blood Transfusion Research, Grant/Award Number: 1852 (received by SB)

All data files are available in a Zenodo repository (https://zenodo.org/records/10422769).

Reference list

1. Valentijn KM, Sadler JE, Valentijn JA, Voorberg J, Eikenboom J. Functional architecture of Weibel-Palade bodies. Blood. 2011;117(19):5033-43.
2. Hordijk S, Carter T, Bierings R. A new look at an old body: molecular determinants of Weibel-Palade body composition and VWF exocytosis. J Thromb Haemost. 2024.
3. Murray EW, Lillicrap D. von Willebrand disease: pathogenesis, classification, and management. Transfus Med Rev. 1996;10(2):93-110.
4. Leebeek FWG, Eikenboom JCJ. Von Willebrand's Disease. New England Journal of Medicine. 2016;375(21):2067-80.
5. Lin Y, Weisdorf DJ, Solovey A, Hebbel RP. Origins of circulating endothelial cells and endothelial outgrowth from blood. J Clin Invest. 2000;105(1):71-7.
6. van den Biggelaar M, Bouwens EA, Kootstra NA, Hebbel RP, Voorberg J, Mertens K. Storage and regulated secretion of factor VIII in blood outgrowth endothelial cells. Haematologica. 2009;94(5):670-8.
7. Berber E, James PD, Hough C, Lillicrap D. An assessment of the pathogenic significance of the R924Q von Willebrand factor substitution. J Thromb Haemost. 2009;7(10):1672-9.
8. Groeneveld DJ, van Bekkum T, Dirven RJ, Wang JW, Voorberg J, Reitsma PH, et al. Angiogenic characteristics of blood outgrowth endothelial cells from patients with von Willebrand disease. J Thromb Haemost. 2015;13(10):1854-66.
9. Randi AM, Laffan MA. Von Willebrand factor and angiogenesis: basic and applied issues. J Thromb Haemost. 2017;15(1):13-20.
10. Starke RD, Ferraro F, Paschalaki KE, Dryden NH, McKinnon TA, Sutton RE, et al. Endothelial von Willebrand factor regulates angiogenesis. Blood. 2011;117(3):1071-80.
11. Starke RD, Paschalaki KE, Dyer CE, Harrison-Lavoie KJ, Cutler JA, McKinnon TA, et al. Cellular and molecular basis of von Willebrand disease: studies on blood outgrowth endothelial cells. Blood. 2013;121(14):2773-84.
12. Wang JW, Bouwens EA, Pintao MC, Voorberg J, Safdar H, Valentijn KM, et al. Analysis of the storage and secretion of von Willebrand factor in blood outgrowth endothelial cells derived from patients with von Willebrand disease. Blood. 2013;121(14):2762-72.
13. de Jong A, Weijers E, Dirven R, de Boer S, Streur J, Eikenboom J. Variability of von Willebrand factor-related parameters in endothelial colony forming cells. J Thromb Haemost. 2019;17(9):1544-54.
14. de Boer S, Bowman M, Notley C, Mo A, Lima P, de Jong A, et al. Endothelial characteristics in healthy endothelial colony forming cells; generating a robust and valid ex vivo model for vascular disease. J Thromb Haemost. 2020;18(10):2721-31.
15. Galili T, O'Callaghan A, Sidi J, Sievert C. heatmaply: an R package for creating interactive cluster heatmaps for online publishing. Bioinformatics. 2017;34(9):1600-2.
16. Ashburner M, Ball CA, Blake JA, Botstein D, Butler H, Cherry JM, et al. Gene Ontology: tool for the unification of biology. Nature Genetics. 2000;25(1):25-9.
17. Consortium TGO, Aleksander SA, Balhoff J, Carbon S, Cherry JM, Drabkin HJ, et al. The Gene Ontology knowledgebase in 2023. Genetics. 2023;224(1).
18. Schindelin J, Arganda-Carreras I, Frise E, Kaynig V, Longair M, Pietzsch T, et al. Fiji: an open-source platform for biological-image analysis. Nature Methods. 2012;9(7):676-82.
19. Stirling DR, Swain-Bowden MJ, Lucas AM, Carpenter AE, Cimini BA, Goodman A. CellProfiler 4: improvements in speed, utility and usability. BMC Bioinformatics. 2021;22(1):433.

20. Laan SNJ, Dirven RJ, Bürgisser PE, Eikenboom J, Bierings R. Automated segmentation and quantitative analysis of organelle morphology, localization and content using CellProfiler. PLoS One. 2023;18(6):e0278009.
21. Goncharov NV, Popova PI, Avdonin PP, Kudryavtsev IV, Serebryakova MK, Korf EA, et al. Markers of Endothelial Cells in Normal and Pathological Conditions. Biochem (Mosc) Suppl Ser A Membr Cell Biol. 2020;14(3):167-83.
22. Dejana E, Hirschi KK, Simons M. The molecular basis of endothelial cell plasticity. Nature Communications. 2017;8(1):14361.
23. Yang J, Antin P, Berx G, Blanpain C, Brabletz T, Bronner M, et al. Guidelines and definitions for research on epithelial–mesenchymal transition. Nature Reviews Molecular Cell Biology. 2020;21(6):341-52.
24. Reimand J, Isserlin R, Voisin V, Kucera M, Tannus-Lopes C, Rostamianfar A, et al. Pathway enrichment analysis and visualization of omics data using g:Profiler, GSEA, Cytoscape and EnrichmentMap. Nature Protocols. 2019;14(2):482-517.
25. Ferraro F, Kriston-Vizi J, Metcalf DJ, Martin-Martin B, Freeman J, Burden JJ, et al. A two-tier Golgi-based control of organelle size underpins the functional plasticity of endothelial cells. Dev Cell. 2014;29(3):292-304.
26. Medina RJ, O'Neill CL, O'Doherty TM, Wilson SE, Stitt AW. Endothelial progenitors as tools to study vascular disease. Stem Cells Int. 2012;2012:346735.
27. Kat M, Margadant C, Voorberg J, Bierings R. Dispatch and delivery at the ER-Golgi interface: how endothelial cells tune their hemostatic response. FEBS J. 2022;289(22):6863-70.
28. Bowman M, Casey L, Selvam SN, Lima PDA, Rawley O, Hinds M, et al. von Willebrand factor propeptide variants lead to impaired storage and ER retention in patient-derived endothelial colony-forming cells. J Thromb Haemost. 2022;20(7):1599-609.
29. Selvam SN, Casey LJ, Bowman ML, Hawke LG, Longmore AJ, Mewburn J, et al. Abnormal angiogenesis in blood outgrowth endothelial cells derived from von Willebrand disease patients. Blood Coagul Fibrinolysis. 2017;28(7):521-33.
30. Tien TY, Wu YJ, Su CH, Hsieh CL, Wang BJ, Lee YN, et al. Pannexin 1 Modulates Angiogenic Activities of Human Endothelial Colony-Forming Cells Through IGF-1 Mechanism and Is a Marker of Senescence. Arterioscler Thromb Vasc Biol. 2023;43(10):1935-51.
31. Sanchez-Duffhues G, Orlova V, ten Dijke P. In Brief: Endothelial-to-mesenchymal transition. The Journal of Pathology. 2016;238(3):378-80.
32. Kalluri R, Weinberg RA. The basics of epithelial-mesenchymal transition. J Clin Invest. 2009;119(6):1420-8.
33. Maleszewska M, Moonen JR, Huijkman N, van de Sluis B, Krenning G, Harmsen MC. IL-1β and TGFβ2 synergistically induce endothelial to mesenchymal transition in an NFκB-dependent manner. Immunobiology. 2013;218(4):443-54.
34. Romero LI, Zhang DN, Herron GS, Karasek MA. Interleukin-1 induces major phenotypic changes in human skin microvascular endothelial cells. J Cell Physiol. 1997;173(1):84-92.
35. Kutikhin AG, Tupikin AE, Matveeva VG, Shishkova DK, Antonova LV, Kabilov MR, et al. Human Peripheral Blood-Derived Endothelial Colony-Forming Cells Are Highly Similar to Mature Vascular Endothelial Cells yet Demonstrate a Transitional Transcriptomic Signature. Cells. 2020;9(4).
36. Yoshimatsu Y, Kimuro S, Pauty J, Takagaki K, Nomiyama S, Inagawa A, et al. TGF-beta and TNF-alpha cooperatively induce mesenchymal transition of lymphatic endothelial cells via activation of Activin signals. PLOS ONE. 2020;15(5):e0232356.

37. Hulshoff MS, Xu X, Krenning G, Zeisberg EM. Epigenetic Regulation of Endothelial-to-Mesenchymal Transition in Chronic Heart Disease. Arteriosclerosis, Thrombosis, and Vascular Biology. 2018;38(9):1986-96.
38. Tura O, Skinner EM, Barclay GR, Samuel K, Gallagher RC, Brittan M, et al. Late outgrowth endothelial cells resemble mature endothelial cells and are not derived from bone marrow. Stem Cells. 2013;31(2):338-48.
39. Toshner M, Dunmore BJ, McKinney EF, Southwood M, Caruso P, Upton PD, et al. Transcript analysis reveals a specific HOX signature associated with positional identity of human endothelial cells. PLoS One. 2014;9(3):e91334.
40. Potente M, Mäkinen T. Vascular heterogeneity and specialization in development and disease. Nature Reviews Molecular Cell Biology. 2017;18(8):477-94.
41. Lin Y, Banno K, Gil CH, Myslinski J, Hato T, Shelley WC, et al. Origin, prospective identification, and function of circulating endothelial colony-forming cells in mice and humans. JCI Insight. 2023;8(5).
42. Sánchez-Duffhues G, García de Vinuesa A, van de Pol V, Geerts ME, de Vries MR, Janson SG, et al. Inflammation induces endothelial-to-mesenchymal transition and promotes vascular calcification through downregulation of BMPR2. J Pathol. 2019;247(3):333-46.
43. Rieder F, Kessler SP, West GA, Bhilocha S, de la Motte C, Sadler TM, et al. Inflammation-induced endothelial-to-mesenchymal transition: a novel mechanism of intestinal fibrosis. Am J Pathol. 2011;179(5):2660-73.
44. Derada Troletti C, Fontijn RD, Gowing E, Charabati M, van Het Hof B, Didouh I, et al. Inflammation-induced endothelial to mesenchymal transition promotes brain endothelial cell dysfunction and occurs during multiple sclerosis pathophysiology. Cell Death & Disease. 2019;10(2):45.
45. Medina RJ, O'Neill CL, O'Doherty TM, Chambers SE, Guduric-Fuchs J, Neisen J, et al. Ex vivo expansion of human outgrowth endothelial cells leads to IL-8-mediated replicative senescence and impaired vasoreparative function. Stem Cells. 2013;31(8):1657-68.
46. Smadja DM, Bièche I, Uzan G, Bompais H, Muller L, Boisson-Vidal C, et al. PAR-1 activation on human late endothelial progenitor cells enhances angiogenesis in vitro with upregulation of the SDF-1/CXCR4 system. Arterioscler Thromb Vasc Biol. 2005;25(11):2321-7.
47. Bompais H, Chagraoui J, Canron X, Crisan M, Liu XH, Anjo A, et al. Human endothelial cells derived from circulating progenitors display specific functional properties compared with mature vessel wall endothelial cells. Blood. 2004;103(7):2577-84.
48. Smadja DM, Melero-Martin JM, Eikenboom J, Bowman M, Sabatier F, Randi AM. Standardization of methods to quantify and culture endothelial colony-forming cells derived from peripheral blood. Journal of Thrombosis and Haemostasis. 2019;17(7):1190-4.
49. Blandinières A, Randi AM, Paschalaki KE, Guerin CL, Melero-Martin JM, Smadja DM. Results of an international survey about methods used to isolate human endothelial colony-forming cells: guidance from the SSC on Vascular Biology of the ISTH. J Thromb Haemost. 2023;21(9):2611-9.
50. Smadja DM, Melero-Martin JM, Eikenboom J, Bowman M, Sabatier F, Randi AM. Standardization of methods to quantify and culture endothelial colony-forming cells derived from peripheral blood: Position paper from the International Society on Thrombosis and Haemostasis SSC. J Thromb Haemost. 2019;17(7):1190-4.
51. Cnossen MH, van Moort I, Reitsma SH, de Maat MPM, Schutgens REG, Urbanus RT, et al. SYMPHONY consortium: Orchestrating personalized treatment for patients with bleeding disorders. J Thromb Haemost. 2022;20(9):2001-11.

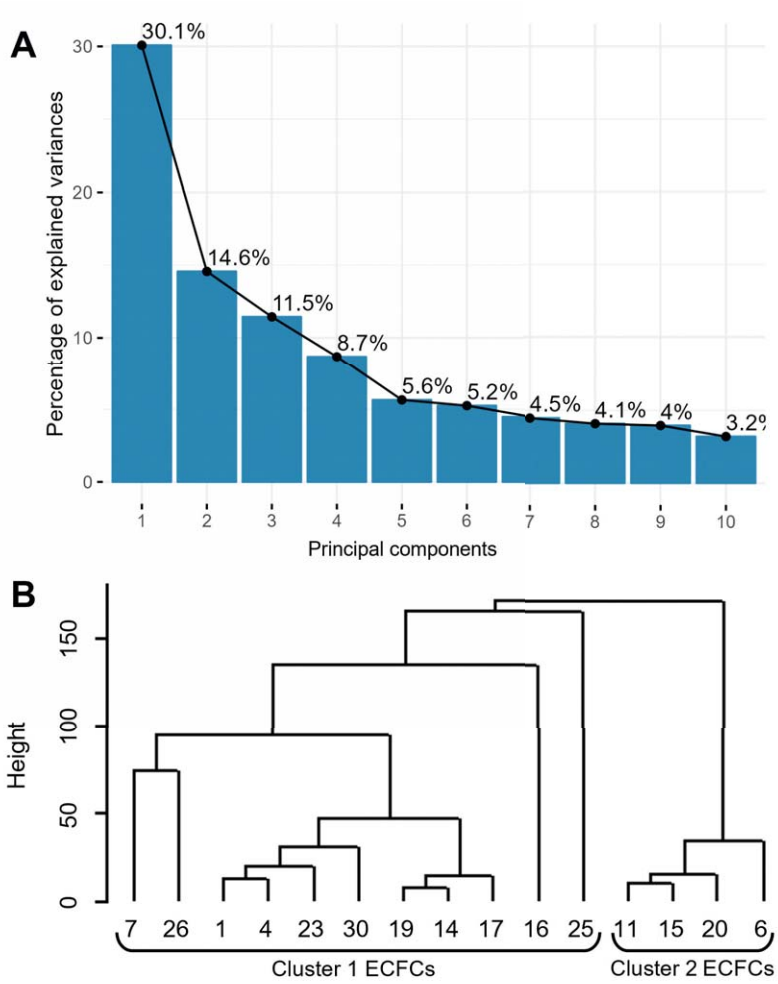

Supplemental Figure 1. Principal Component analysis (PCA) of bulk RNA transcriptomes. A) Percentage of explained variance is shown in a scree plot. The first 10 principal components are shown. B) Dendrogram of the hierarchical clustering of samples based on PCA 1-4 shows 2 distinct clusters.

Supplemental Table 1. Characteristics of ECFC clones.

Sample number	Donor number	Sex	Age	Day of detection*	Time in culture**	Morph. group	Bulk RNA sequencing	Clustering		Morph. analysis	Migration assay
								RNA seq.	qPCR		
1	1	M	64	13	16	2	Yes	1	1	Yes	No
2	1	M	64	13	18	2	No	-	1	Yes	No
3	1	M	64	13	24	1	No	-	1	Yes	No
4	1	M	64	13	18	1	Yes	1	1	No	No
5	2	M	28	14	26	3	No	-	2	Yes	No
6	3	F	23	15	27	3	Yes	2	2	Yes	No
7	3	F	23	13	23	3	Yes	1	1	Yes	No
8	3	F	23	19	25	2	No	-	2	Yes	No
9	4	F	28	19	30	2	No	-	1	Yes	No
10	5	M	49	15	26	3	No	-	2***	Yes	No
11	6	F	23	28	33	3	Yes	2	2	Yes	No
12	6	F	23	15	19	1	No	-	1	No	No
13	6	F	23	15	14	1	No	-	1	No	No
14	6	F	23	15	19	1	Yes	1	1	Yes	No
15	7	M	29	21	54	2	Yes	2	2	Yes	Yes
16	8	F	26	19	24	2	Yes	1	1	Yes	No
17	9	F	26	14	19	2	Yes	1	1	No	No
18	9	F	26	14	19	2	No	-	1	No	No

Supplemental Table 1. *Continued*

Sample number	Donor number	Sex	Age	Day of detection*	Time in culture**	Morph. group	Bulk RNA sequencing	Clustering		Morph. analysis	Migration assay
								RNA seq.	qPCR		
19	9	F	26	12	18	1	Yes	1	1	Yes	No
20	10	F	24	16	24	3	Yes	2	2	Yes	No
21	10	F	24	19	46	3	No	-	2	Yes	Yes
22	11	M	26	15	15	1	No	-	1	Yes	No
23	11	M	26	15	17	1	Yes	1	1	Yes	Yes
24	12	M	23	16	53	3	No	-	2	Yes	Yes
25	13	M	27	14	23	3	Yes	1	1	Yes	No
26	13	M	27	17	22	2	Yes	1	1	Yes	No
27	13	M	27	14	23	2	No	-	1	Yes	No
28	14	F	20	12	23	1	No	-	1	Yes	No
29	14	F	20	12	21	1	No	-	1	No	No
30	14	F	20	12	15	1	Yes	1	1	Yes	Yes
31	15	F	23	16	40	3	No	-	2	Yes	No
32	16	F	27	13	23	2	No	-	1	Yes	Yes
33	16	F	27	13	21	3	No	-	1	Yes	No
34	10	F	24	15	29	3	No	-	2	Yes	No

*Number of days after inclusion. **From day of detection to freezing (in days). ***Could not be successfully clustered based on available measurements. Cluster 2 was assigned. Abbreviations: Morphological (Morph), Sequencing (seq.)

Supplemental Table 2. Primer sequences used for the qPCR panel

Gene	Category	Sense	Anti-sense
GAPDH	Housekeeping	ACCATCTTCCAGGAGCGAGA	GACTCCACGACGTACTCAGC
RAB27A	WPB content protein	GAAGCCATAGCACTCGCAGAGA	CAGGACTTGTCCACACACCGTT
SELP	WPB content protein	TCCGCTGCATTGACTCTGGACA	CTGAAACGCTCTCAAGGATGGAG
VWF	WPB content protein	TTGACGGGGAGGTGAATGTG	ATGTCTGCTTCAGGACCACG
PLAT	WPB content protein	TGGTGCTACGTCTTTAAGGCGG	GCTGACCCATTCCCAAAGTAGC
CD63	WPB content protein	CAACCACACTGCTTCGATCCTG	GACTCGGTTCTTCGACATGGAAG
ALDH1A1	Proliferation	CGGGAAAAGCAATCTGAAGAGGG	GATGCGGCTATACAACACTGGC
SOX18	Proliferation	GTGTGGGCAAAGGACGAG	GTTCAGCTCCTTCCACGCT
BMP2	Inhibitor of EndMT/EMT	TGTATCGCAGGCACTCAGGTCA	CCACTCGTTTCTGGTAGTTCTTC
COL1A1	EndMT/EMT	CAGCCGCTTCACCTACAGC	TTTTGTATTCAATCACTGTCTTGCC
TGFBi	EndMT/EMT	GGACATGCTCACTATCAACGGG	CTGTGGACACATCAGACTCTGC
IFI27	Apoptosis	CGTCCTCCATAGCAGCCAAGAT	ACCCAATGGAGCCCAGGATGAA
BST2	Apoptosis	TCTCCTGCAACAAGAGCTGACC	TCTCTGCATCCAGGGAAGCCAT
ABI3BP	Senescence	CCTTCTACACCTAAACGACGCC	GGTGTTGTCCATGTAGGTTCAGG
SERPINE1	Inflammation	CTCATCAGCCACTGGAAAGGCA	GACTCGTGAAGTCAGCCTGAAAC
CXCL8	Inflammation	GAGAGTGATTGAGAGTGGACCAC	CACAACCCTCTGCACCCAGTTT

Abbreviations: Weibel-Palade Body (WPB), Endothelial to Mesenchymal transition (EndoMT), Epithelial to Mesenchymal transition (EMT).

Supplemental Table 3. Antibodies used in immunofluorescence

Antibody	Manufacturer	Category number	Concentration	Dilution
IF Primary				
VWF (rabbit)	DAKO	A0082	4.1 mg/mL	1:1,000
VE-cadherin (mouse)	BD Pharming	555661	0.5 mg/mL	1:250
Hoechst	Thermo Fisher Scientific	H3569	10 mg/mL	1:10,000
IF Secondary				
Donkey-anti-Rabbit AF647	Invitrogen Molecular Probes	A31573	2 mg/mL	1:750
Donkey-anti-Mouse AF488	Invitrogen Molecular Probes	A21202	2 mg/mL	1:750

Abbreviations: Von Willebrand factor (VWF), Immunofluorescence (IF)

Supplemental Table 4. Bulk RNA sequencing genes of interest with >7.5 CPM and >2 log2FC

Gene	geneID	Average Log2CPM	Average Log2FC	P-values (FDR corrected)	Category
BST2	ENSG00000130303	7,77	-6,98	9,04E-06	Apoptosis
IFI27	ENSG00000165949	8,45	-4,04	1,48E-02	Apoptosis
IFI6	ENSG00000126709	7,94	-5,07	5,80E-05	Apoptosis
CLU	ENSG00000120885	9,91	4,69	5,80E-05	Apoptosis*
GIMAP4	ENSG00000133574	7,84	2,82	1,22E-04	Apoptosis*
GIMAP6	ENSG00000133561	7,68	2,40	2,70E-04	Apoptosis*
GIMAP8	ENSG00000171115	7,86	2,67	3,00E-04	Apoptosis*
SCARA3	ENSG00000168077	7,55	4,09	3,37E-04	Apoptosis*
ANGPTL4	ENSG00000167772	7,71	-3,42	2,73E-03	EndoMT/ EMT
TGFBI	ENSG00000120708	8,63	-4,45	1,21E-03	EndoMT/ EMT
ALCAM	ENSG00000170017	8,51	-2,43	2,53E-04	EndoMT/ EMT
CADM3	ENSG00000162706	8,10	-6,60	4,71E-04	EndoMT/ EMT
CD44	ENSG00000026508	7,59	-2,93	4,71E-04	EndoMT/ EMT
COL1A2	ENSG00000164692	9,24	-5,22	1,59E-03	EndoMT/ EMT

Supplemental Table 4. *Continued*

Gene	geneID	Average Log2CPM	Average Log2FC	P-values (FDR corrected)	Category
COL5A1	ENSG00000130635	10,00	-2,72	1,13E-03	EndoMT/ EMT
COL5A2	ENSG00000204262	9,77	-2,09	1,27E-03	EndoMT/ EMT
COL8A1	ENSG00000144810	9,86	-2,14	4,88E-03	EndoMT/ EMT
FN1	ENSG00000115414	12,95	-2,07	2,13E-03	EndoMT/ EMT
ITGAV	ENSG00000138448	9,73	-2,87	7,20E-04	EndoMT/ EMT
LTBP1	ENSG00000049323	8,64	-2,58	1,13E-03	EndoMT/ EMT
NRCAM	ENSG00000091129	7,55	-2,67	2,35E-03	EndoMT/ EMT
PLOD2	ENSG00000152952	8,63	-2,18	5,76E-04	EndoMT/ EMT
PVR	ENSG00000073008	8,44	-2,65	1,22E-03	EndoMT/ EMT
TPM1	ENSG00000140416	9,93	-2,48	3,30E-04	EndoMT/ EMT
TPM2	ENSG00000198467	7,76	-2,41	9,64E-03	EndoMT/ EMT
MMRN1	ENSG00000138722	11,20	5,18	9,45E-05	Endothelial marker
TFPI	ENSG00000003436	8,46	2,18	1,19E-03	Endothelial marker
TSPAN18	ENSG00000157570	7,57	2,78	1,82E-04	Endothelial marker
VWF	ENSG00000110799	12,67	2,63	5,04E-04	Endothelial marker
CXCL1	ENSG00000163739	8,65	-3,72	6,97E-03	Inflammation
CXCL6	ENSG00000124875	9,28	-6,10	5,18E-03	Inflammation
CXCL8	ENSG00000169429	8,81	-3,67	1,15E-02	Inflammation
IL1RL1	ENSG00000115602	7,64	-2,86	2,29E-03	Inflammation
IL32	ENSG00000008517	7,58	-2,09	9,14E-03	Inflammation
PTX3	ENSG00000163661	10,89	-2,72	3,98E-03	Inflammation
SERPINE1	ENSG00000106366	12,90	-2,62	7,28E-03	Inflammation
SLC7A2	ENSG00000003989	7,89	-3,86	2,56E-04	Inflammation
MYH10	ENSG00000133026	8,87	2,24	2,72E-04	Migration
EMCN	ENSG00000164035	8,12	2,11	1,32E-02	Proliferation
ADGRG6	ENSG00000112414	7,54	2,10	2,08E-02	Proliferation
ALDH1A1	ENSG00000165092	9,54	7,20	5,64E-04	Proliferation

Supplemental Table 4. *Continued*

Gene	geneID	Average Log2CPM	Average Log2FC	P-values (FDR corrected)	Category
ELK3	ENSG00000111145	8,32	2,55	5,76E-04	Proliferation
NDRG4	ENSG00000103034	7,57	2,63	2,40E-03	Proliferation
PPP1R16B	ENSG00000101445	8,13	2,29	1,66E-04	Proliferation
CAVIN2	ENSG00000168497	9,28	2,85	3,45E-05	Proliferation/ migration
DCBLD2	ENSG00000057019	7,87	-2,23	4,69E-03	Proliferation/ migration*
PDE2A	ENSG00000186642	7,89	3,40	9,48E-04	Proliferation/ migration
SOX18	ENSG00000203883	7,99	3,35	2,49E-04	Proliferation/ migration
TAGLN	ENSG00000149591	7,95	-3,02	3,73E-02	Senescence
ABI3BP	ENSG00000154175	9,24	-4,49	3,30E-03	Senescence
SOD2	ENSG00000112096	9,66	-2,96	7,67E-03	†
ABLIM1	ENSG00000099204	7,93	2,44	2,15E-03	†
ESM1	ENSG00000164283	8,31	-2,13	2,32E-02	†
HLA,B	ENSG00000234745	9,61	-2,29	4,35E-04	†
DIPK2B	ENSG00000147113	7,71	2,10	4,34E-03	†

Abbreviations: Count Per Million (CPM), Fold Change (FC), False Discovery Rate (FDR), Endothelial/ epithelial to Mesenchymal Transition (EndoMT/EMT) Symbols: *negatively regulates or inhibits this process, †could not be placed in a category

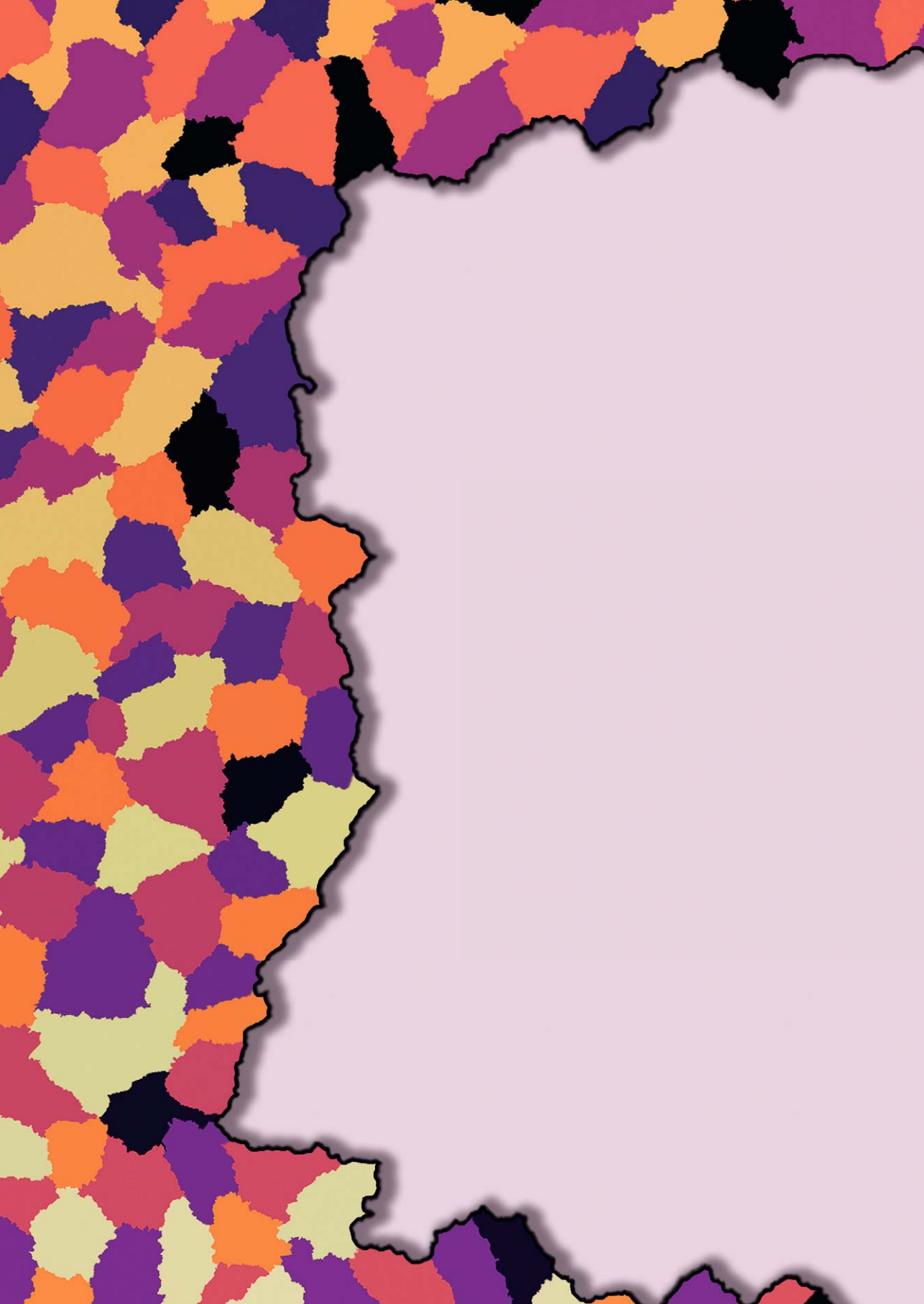

Approaches to induce the maturation process of human induced pluripotent stem cell derived-endothelial cells to generate a robust model

de Boer S, **Laan SNJ**, Dirven RJ, Eikenboom J

PLoS One. 2024 Feb 23;19(2):e0297465.
doi: 10.1371/journal.pone.0297465

Abstract

Background

Endothelial cells generated from induced pluripotent stem cells (hiPSC-ECs) show the majority of endothelial cell characteristics and markers, such as cobblestone morphology and the expression of VEGF and VE-cadherin. However, these cells are failing to show a mature endothelial cell phenotype, which is represented by the low expression and production of von Willebrand factor (VWF) leading to the round morphology of the Weibel Palade Bodies (WPBs). The aim of this study was to improve the maturation process of hiPSC-ECs and to increase the levels of VWF.

Methods

hiPSC-ECs were differentiated by a standard differentiation protocol from hiPSCs generated from healthy control donors. To induce maturation, the main focus was to increase the expression and/or production of VWF by the adjustment of potential parameters influencing differentiation and maturation. We also compared alternative differentiation protocols. Cells were analyzed for the expression of endothelial cell markers, WPB structure, and the production and secretion of VWF by flow cytometry, confocal microscopy and ELISA.

Results

The generated hiPSC-ECs have typical endothelial cell surface expression profiles, with low expression levels of non-endothelial markers as expected. Co-culture with pericytes, varying concentrations and timing of differentiation factors, applying some level of flow, and the addition of HDAC inhibitors did not substantially improve maturation of hiPSC-ECs. Transfection with the transcription factor ETV2 to induce a faster hiPSC-EC differentiation process resulted in a limited increase in VWF production, secretion, and elongation of WPB structure. Alternative differentiation protocols had limited effect.

Conclusion

hiPSCs-ECs have the potential to show a more mature endothelial phenotype with elongated WPBs after >30 days in culture. However, this comes with limitations as there are very few cells detected, and cells are deteriorating after being in culture for extended periods of time.

Introduction

Human endothelial cells are an essential source and tool to study a wide variety of diseases, especially vascular and bleeding disorders. However, obtaining primary endothelial cells or the use of endothelial colony forming cells (ECFCs) (1, 2) remains a challenge with limitations such as the phenotype of interest and *in vitro* culture. The success rates of ECFC isolations is rather low (reported ranging from 46-70%), with some donors never yielding any colonies (3-5). Furthermore, if successful, there is a high probability heterogeneity is observed between ECFC clones (2). Nowadays, human induced pluripotent stem cells (hiPSCs), that can be generated from almost any somatic cell type, are an attractive and versatile cell model that has been used in a wide variety of studies (6, 7). Generated hiPSCs are capable of self-renewal and have the potential to differentiate into almost any cell type of interest, thereby overcoming the lack of disease-specific cells and tissues in several disorders.

We have an interest in cell models for the study of von Willebrand disease (VWD). This bleeding disorder is characterized by reduced circulating levels of functional von Willebrand factor (VWF), which is a multimeric protein that is produced mainly by endothelial cells (8). Even though there are several methods to differentiate hiPSCs into endothelial cells (hiPSC-ECs), the most common and straightforward approach is through 2D protocols (9, 10). These protocols can be divided into a mesoderm and endothelial differentiation phase, with minor alterations in the differentiation factors and/or concentrations used. On average, this two-step differentiation process will take 8-10 days, with a CD31 purification step to follow. CD31 is platelet endothelial cell adhesion molecule (PECAM-1), which is a mature vascular marker and involved in cell adhesion, activation and migration. The $CD31^+$ population can be further differentiated into hiPSC-ECs, whereas the $CD31^-$ group can be differentiated into pericytes (hiPSC-PCs) for co-culture purposes. Approaches like this will generate substantial numbers of both cell types, derived in just 2-3 weeks.

Generated hiPSC-ECs show the typical endothelial cell-like morphology and express endothelial markers at levels comparable to primary endothelial cells such as vascular endothelial (VE-)cadherin (CD144) and melanoma cell adhesion molecule (MCAM; CD146), and have been used in functional studies (11, 12). However, there are some concerns about the efficiency and maturity of hiPSC-ECs using these protocols (9, 10, 13). Most endothelial differentiation protocols that have been developed to date have relatively low endothelial cell yields to use for assays to generate proper power. Like primary endothelial cells in vitro, hiPSC-ECs have restricted proliferative potential and either undergo senescence or endothelium-to-mesenchymal transition after multiple

passages (11, 12). Even though hiPSC-ECs mimic endothelial cells very accurately in their overall endothelial marker and characteristic profiles, the maturity of these cells is lacking behind. While it has been shown that hiPSC-ECs do produce and secrete VWF, levels are significantly lower than in primary endothelial cell sources, such as human umbilical vein endothelial cells (HUVECs) and ECFCs. This is mainly reflected in the shape of the Weibel-Palade bodies (WPBs), which are tubular shaped in mature endothelial cells, but visible as round structures in hiPSC-ECs, indicating immaturity (9, 14).

To produce more mature, differentiated hiPSC-ECs we tried several different modifications following published protocols. This study showed that these adjustments lead to partial improvements in the phenotype. However, more optimization is needed to generate a robust and reproducible endothelial cell model.

Materials and Methods

Study design

The study protocol for peripheral blood mononuclear cell (PBMC) isolation and iPSC generation was approved by the ethics review board of the Leiden University Medical Center (LUMC), the Netherlands (medical research ethics committee (MREC) Leiden Den Haag Delft). Written informed consent was obtained from all participants in accordance with the Declaration of Helsinki. Participants were 18 years or older and healthy donors had not been diagnosed with or known to have VWD or any other bleeding disorder. Participants for this study where recruited between March and April 2019. J. Eikenboom, as the responsible physician of the study, was the only investigator with access to information that could identify individual participants during and after the data collection.

iPSC generation

Blood samples were obtained from three healthy donors (Supplemental Figure 1A) via venipuncture and drawn in sodium heparin Vacutainers (BD Biosciences, Franklin Lakes, NJ, Unites States of America (USA)) for PBMC collection with a Ficoll Paque gradient (LUMC Pharmacy, Leiden, the Netherlands). The PBMC fraction was isolated and washed twice with PBS/10% fetal bovine serum (FBS) (Gibco Invitrogen, Carlsbad, CA, USA), and then cryopreserved until reprogramming. Cells were reprogrammed into hiPSCs using episomal vectors to deliver the reprogramming factors (15), and characterized for pluripotency at the LUMC iPSC Hotel (Supplemental Figure 1B).

ECFCs

Endothelial colony forming cells (ECFCs) were isolated from healthy control donors following the protocol described in de Boer et al (2020) (2). In short, peripheral blood was taken from healthy individuals and isolated PBMCs were put in culture in endothelial growth medium (EGM) for up to 4 weeks. When ECFC colonies appeared, these were expanded and frozen down for further experiments.

Endothelial cell differentiation protocols

Orlova protocol

hiPSCs were differentiated into hiPSC-ECs with a protocol by Orlova et al. (9) (Supplemental Figure 2A). In short, hiPSCs were dissociated with TrypLE (Gibco) and seeded as single cells at $2x10^4$ cells/cm^2 on day -1 on vitronectin (Stem Cell Technologies, Vancouver, Canada) coated plates in E8 medium (Stem Cell Technologies) supplemented with ROCK inhibitor (ROCKi, Y-27632) (Stem Cell Technologies) (10uM). On day 0 cells were replated and cultured in BPEL medium (Supplemental Table 1) supplemented with VEGF (50ng/ml) (R&D Systems, Minneapolis, MN, United States), Activin A (25ng/ml) (Miltenyi, Bergisch Gladbach, Germany), BMP4 (30ng/ml) (R&D Systems) and CHIR99021 (1.5μM) (Tocris Bioscience, Bristol, United Kingdom). On day 3 medium was changed to BPEL supplemented with VEGF (25ng/ml) and SB431542 (10μM) (Tocris Bioscience), followed by a CD31 bead (Invitrogen) isolation step on day 10. Cells were then plated on 0.2% gelatin (Sigma-Aldrich, St. Louis, MO, United States) and cultured in expansion EC-SFM medium (Gibco) supplemented with VEGF (30ng/ml), FGF (20ng/ml) (Miltenyi), and PPP (1%) (Bio-Connect, Huissen, The Netherlands).

Aoki protocol

hiPSCs were differentiated into hiPSC-ECs with an adjusted protocol by Aoki et al. (16) (Supplemental Figure 2B). hiPSCs were dissociated with TrypLE and seeded as single cells at $2x10^4$ cells/cm^2 on day -1 on vitronectin coated plates in E8 medium supplemented with ROCKi (10μM). On day 0 medium was changed to modified DMEM/F12 (Gibco) (Supplemental Table 1) supplemented on day 0 with 5μM CHIR99021, day 1 with 50 ng/ml FGF, day 2-4 with 50 ng/ml VEGF and on day 5 with 30 ng/ml BMP4, cells are incubated for 1 hour with ROCK inhibitor (10uM) before being dissociated with TrypLE. Cells are then plated at $3.5x10^4$ cells/cm^2 on 0.2% gelatin coated vessels in endothelial progenitor cells (EPC) medium (supplemented with 50 ng/ml VEGF and 50 ng/ml FGF). On day 8, cells are incubated for 1 hour with ROCK inhibitor (10μM) before being dissociated with TrypLE for 45-60 seconds at 37°C until some cells are floating. Then, extra cells were stripped completely by tapping the vessel several times. After washing with PBS three times (and aspirating the edge of the dish), purified hiPSC-ECs were treated with TrypLE Select for 6–12 min at 37°C, collected, and centrifuged at

100g for 5 min. Then, purified hiPSC-ECs were resuspended in fresh EPC medium, supplemented with VEGF (10ng/ml), FGF2 (20 ng/ml), ROCKi (10μM), SB431542 (0.5μM) and CHIR99021 (3μM), and seeded onto 0.2% gelatin (1 μg/cm^2)-coated dishes (1.5x10^4 cells/cm^2). Medium was refreshed 3 times a week and cells were passaged 1:3.

Transfection with transcription factor E26 transformation-specific variant 2 (ETV2)

hiPSCs were differentiated into hiPSC-ECs with an adjusted protocol by Wang et al. (14) (Supplemental Figure 2C). In short, iPSCs were dissociated with TrypLE and seeded as single cells at 5x10^4 cells/cm^2 on day -1 on vitronectin coated plates in E8 medium supplemented with ROCKi (10μM). After 24hrs (day 0), the medium was changed to S1 medium to induce the mesoderm stage (basal medium with CHIR 6μM), repeated after another 24hrs (day 1) (total of 48hrs). Basal medium is DMEM/F12, 1x GlutaMax (Gibco) and L-Ascorbic acid (60 μg/ml; Sigma-Aldrich). After 48hrs of S1 medium, cells were harvested seeded on gelatin at 70,000/cm^2 in modETV2 medium and transfection mix (ETV2 mRNA and Lipofectamine MessengerMAX (ThermoFisher)) was added at a final concentration of 26.4μM. The next day (72h), medium was changed with modETV2 medium supplemented with VEGF (50ng/ml).After 96h (day 4) cells were replated onto gelatin in EGM2 medium to expand the iPSC-ECs.

Chemically modRNA encoding ETV2 was generated by TriLink BioTechnologies/Tebu-bio as an unmodified mRNA transcript using wild type bases and capped using CleanCap (Poly-A tail). All the steps were performed by the manufacturer and after the transcript was cloned into the mRNA expression vector pmRNA, we received the purified modRNA-ETV2 product. Besides the modRNA-ETV2 we also ordered an identical construct with modRNA-EGFP as an uptake control. Both constructs are CleanCap and we used Lipofectamine MessengerMAX as transfection reagent (lipofection to deliver the exogenous ETV2).

Confocal microscopy

Cells were plated on glass coverslips coated with collagen I in 24 well plates and grown to 3-5 days post confluency. Cells were fixed and permeabilized with methanol without washing. Cells were then rinsed with PBS and blocked for 20 minutes in blocking buffer (phosphate buffered saline (PBS) (LUMC Pharmacy, Leiden, the Netherlands), 1% bovine serum albumin (BSA) (Sigma-Aldrich) and fetal bovine serum (FBS) (Bodinco, Alkmaar, the Netherlands)).

After fixation, permeabilization and blocking, cells were stained with primary antibodies for VWF and VE-cadherin diluted in blocking buffer. Nuclear staining was performed

with Hoechst (Thermo Fisher Scientific, Waltham, MA, USA) diluted in PBS. Coverslips were mounted by Mounting Media (DAKO, Glostrup, Denmark) or ProLong Diamond Antifade Mountant (Thermo Fisher Scientific) and cells were imaged using the Leica TCS SP8 inverted confocal microscope (Leica Microsystems, Concord, ON, Canada) with the white light laser (WLL), Hybrid detectors (HyD) and the HC PL APO CS2 63x/1.40 oil immersion objective. Images were acquired and analyzed using the LAS-X Software (Leica Microsystems).

Flow cytometry analysis

Cell surface marker expression was analyzed using flow cytometry (FACS). Either cells (100,000 cells/antibody mix) or CompBeads (Thermo Fisher Scientific) were resuspended in FACS buffer (PBS; 1% BSA; 0.01% sodium azide (Sigma-Aldrich)) and incubated on ice for 30 minutes with labelled primary antibodies or isotype controls. Cells and beads were fixed with 2% Paraformaldehyde (PFA, Alfa Aesar, Ward Hill, MA, USA) diluted in PBS. After washing, samples were resuspended in FACS buffer before being analyzed on the BD™ LSR II (BD Bioscience, San Jose CA, USA). Data was analyzed with FlowJo software (FlowJo LLC v10.6.1, BD Bioscience).

VWF production and secretion

Basal VWF secretion of the cells was determined by the release of VWF:Ag over 24 hours in EGM20 medium. For regulated VWF secretion, cells were incubated for one hour in release medium (Opti-MEM™ I Reduced serum media GlutaMAX™ supplement (Gibco); 10mM HEPES, pH 7.4, 0.2% BSA) supplemented with 100 µM histamine (Sigma-Aldrich) and immediately after that one hour of stimulation, release medium was collected. To determine intracellular VWF, wells with hiPSC-ECs were lysed overnight at 4°C in Opti-MEM I/0.1% Triton X-100 (Sigma-Aldrich) supplemented with cOmplete Protease Inhibitor cocktail with EDTA (Roche Diagnostics, Basel, Switzerland). Wells were scraped before lysates were collected. VWF production and secretion was measured as VWF:Ag by ELISA as previously described (2, 3).

Results

hiPSC generation

PBMCs from three healthy donors were reprogrammed into hiPSCs followed by characterizations. Flowcytometry showed that all clones expressed the pluripotency markers (OCT3/4, NANOG and SSEA4) at sufficient levels (expression seen in >86% of cells) indicating that the cells are pluripotent which is a characteristic of stem cells (Supplemental Figure 1A). hiPSCs were also differentiated into cells of the three germ

layers, and showed expression for several markers that identify the three layers (Ectoderm: β3-tubulin, PAX6 and SOX1; Endoderm: SOX17 and FOXA2; Mesoderm: NCAM and Brachyury) (Supplemental Figure 2B). This confirms that the generated hiPSCs are embryonic stem cell like. The hiPSCs were grown to passage ≥10 before being differentiated into hiPSC-ECs.

Comparing hiPSC-ECs and ECFCs

We used an endothelial differentiation protocol from Orlova et al (9) which has been developed at the LUMC. Over time, this protocol has had several small adjustments that we also applied (Supplemental Figure 2A). However, the immature phenotype of hiPSC-ECs is a reoccurring issue independently of the frequently used protocols. Even though characterizations, both at cellular and expression levels, have shown these cells are indeed of the endothelial lineage, the expression and production of VWF is lacking behind.

Even though the hiPSC-ECs generated by us show endothelial morphology and endothelial markers by immunofluorescence (IF) and flowcytometry (FACS) analysis (Figure 1A-B), the difference is particularly evident when looking at the WPBs, the storage organelles containing VWF in endothelial cells. These organelles are formed at the Golgi network as round structures and elongate during maturation when VWF multimers are stored as tubular structures. Therefore, round WPBs indicate an immature endothelial phenotype. Because VWF and the WPBs are important key players in VWD research, it is critical to improve the maturation process of hiPSC-ECs. As VWF production remained low when using the standard Orlova protocol, we have tried to increase the levels of VWF with different approaches, to produce an improved endothelial cell model.

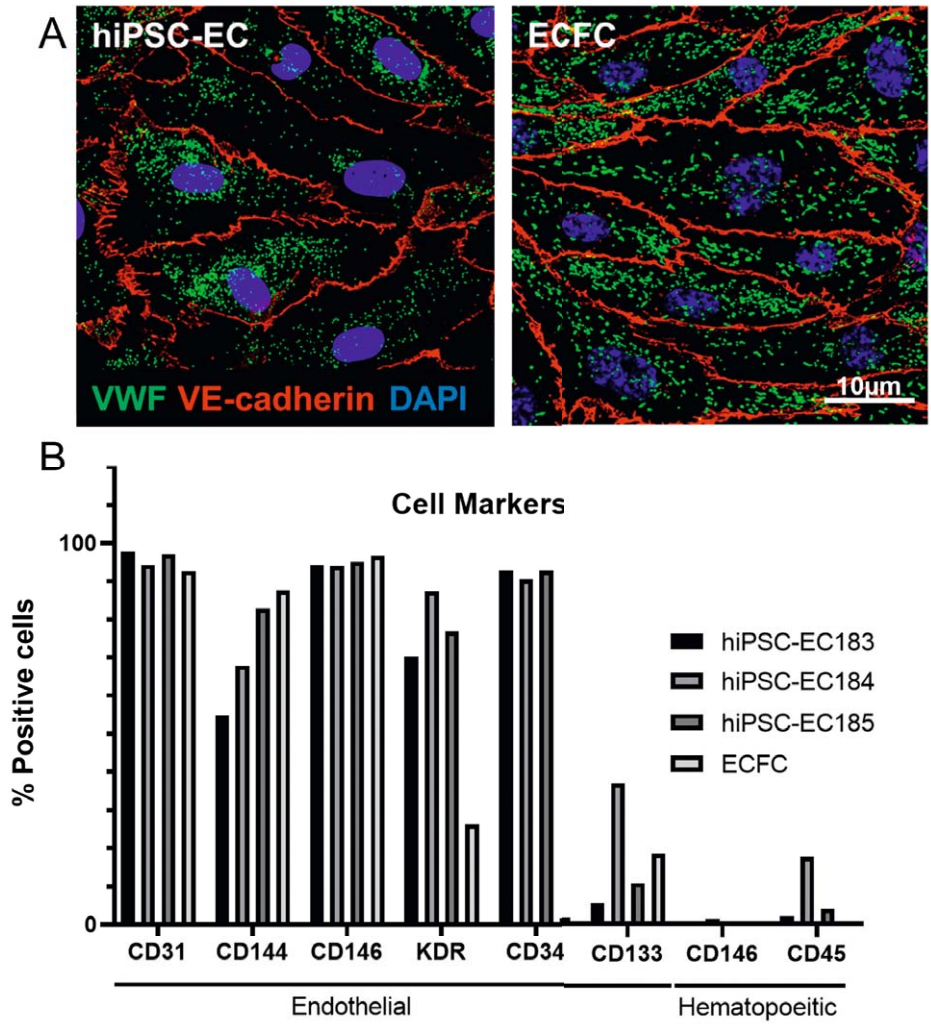

Figure 1. Morphology and endothelial markers of hiPSC-ECs. A) VWF and VE-Cadherin in hiPSC-ECs (left) and ECFCs (right). B) FACS analysis showing endothelial and hematopoietic cell marker expression in the three hiPSC-ECs and ECFCs.

Co-cultures

Our first step was to try coculturing the hiPSC-ECs with hiPSC-PCs (pericytes) which are differentiated in parallel. The Orlova protocol applies a CD31 purification step on day 10 of the differentiation process. The CD31 positive population was differentiated further into hiPSC-ECs, while the negative population give rise to hiPCs, which are also part of the endothelium. By co-culturing these with the hiPSC-ECs, the idea is, that the vasculature is mimicked closer, which might lead to better maturation of the hiPSC-ECs.

We have successfully generated these hiPSC-PCs and performed co-cultures with the hiPSC-ECs. Even though the cells seem to grow for a short period in culture, we did not observe an increase on the VWF levels or improvement of the WPB structures of the hiPSC-ECs (Supplemental Figure 3A).

Endothelial growth factors

Next, we focused on different factors from the endothelial differentiation protocols and started adjusting the VEGF concentrations during the differentiation process. This was driven by a protocol published by Rosa et al. (17), in which they used VEGF to induce different endothelial phenotypes. VEGF is a signaling protein and plays central roles in regulating both vasculogenesis and angiogenesis by inducing endothelial cell proliferation, promoting cell migration, and inhibiting apoptosis. During the vascular induction step, we added either a low or high concentration of VEGF (10 or 50 ng/ml) to generate either venous (low) or arterial (high) like hiPSC-ECs (Figure 2A, C and D). In parallel, we placed the plates on a circular rocker to induce some level of flow to test whether flow would have an influence on the maturation process (Figure 2B); unfortunately we had no methodology available to mimic actual vascular flow. Even though higher VWF production and secretion is seen at 50ng/mL VEGF (Figure 2D), this increase is minimal and the overall levels of VEGF remain far below levels expected at a mature phenotype. Therefore, different VEGF concentrations and/or some flow during and after differentiation does not seem to have an effect on hiPSC-EC maturation, VWF production and secretion, and WPB shape.

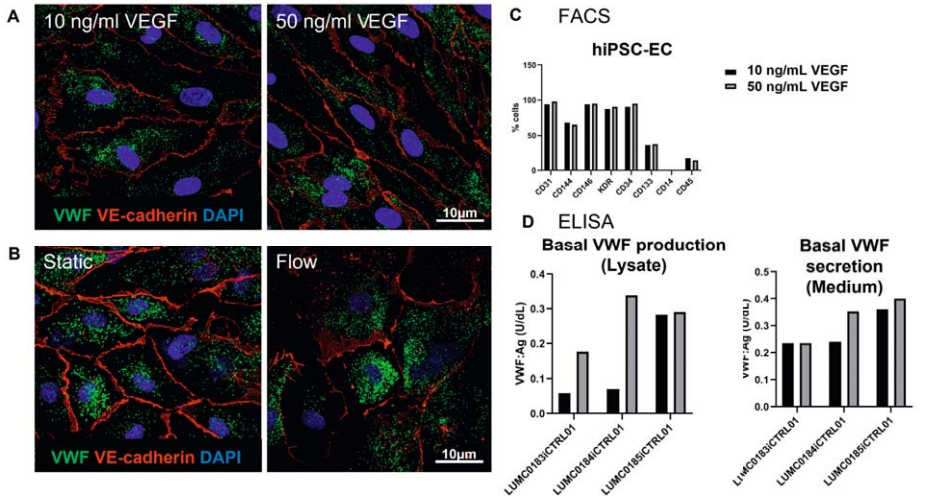

Figure 2. hiPSC-ECs cultured under variable conditions. hiPSC-ECs differentiated with low or high concentrations of VEGF. A) VWF and VE-Cadherin levels by confocal microscopy. B) VWF and VE-Cadherin levels by confocal microscopy when cultured under static (left) or flow (right)

conditions. C) FACS analysis showing endothelial and hematopoietic cell marker levels in hiPSC-ECs. D) ELISA showing VWF production (Lysates) and secretion (medium).

Besides VEGF, we have tried different concentrations of CHIR99021 (1.5-5μM), which is a chemical compound acting as an inhibitor of the enzyme GSK-3 which plays a role in a number of central signaling pathways, but did not observe a difference in differentiation parameters either. Other factors such as SB431542, which is a TGF beta inhibitor (ALK4, 5 and 7) and BMP4, an inducer of mesoderm specification have also been tested at different time points during differentiation and likewise, no improvement in the differentiation process was observed (Supplemental Figure 3B).

pH lowering of culture environment

Parallel to this study, our collaborating group published a paper in which the intracellular pH of hiPSC-ECs was lowered with acetic acid (18). They showed that, in combination with the (adjusted) Orlova protocol, elongated WPBs appeared in the hiPSC-ECs upon lowering the pH, however, the total amount of VWF protein did not show an increase. Following these results, we have tried a similar approach with different substrates to lower pH of the culture environment, to test whether this would lead to increased levels of VWF and elongated WPBs. We tested this on ECFCs, which show a mature endothelial phenotype, to see the effect on the WPBs of the cells. After addition of acetic acid, there was no effect seen on the VWF levels and WBP structures in the cells by IF, but we did notice that the cells started to deteriorated at higher concentrations (Figure 3A). However, when we looked at the lysates, an increase in VWF levels was observed at 5mM acetic acid, but decreased rapidly at higher concentrations (Figure 3B). This increase was not measured in the VWF secretion, and was almost diminished at concentrations over 5mM (Figure 3C).

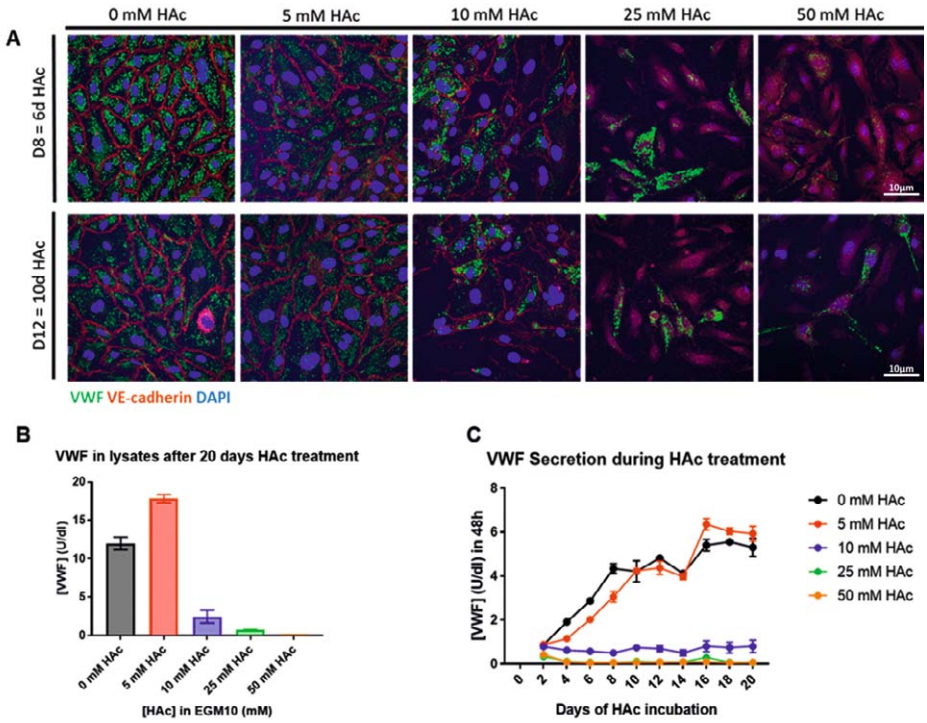

Figure 3. ECFCs cultured with acetic acid. A) Confocal microscopy showing VWF (green) and VE-cadherin (red)after the addition of different concentrations of acetic acid at days 8 (top panel) and 12 (bottom panel). B) ELISA showing VWF production (lysates). C) ELISA showing VWF secretion (medium). HAc, acetic acid.

HDACi

As mentioned before, the formation and elongation of WPBs is driven solely on the production of VWF protein. Therefore, instead of trying to mature the WPBs, we subsequently focused on the production of VWF. We added histone deacetylase inhibitors (HDACi), chemical compounds that inhibit histone deacetylases. This will lead to a state of hypoacetylation which will result in loosening of the chromatin, making it more accessible for transcription factors, leading to active gene expression. The balance of acetylation and deacetylation is important in development and differentiation processes.

We used the HDACi sodium butyrate, which inhibits Class I HDACs, and tested this during multiple steps in the differentiation process and also at different concentrations (0.25-2.5mM). There was a slight increase in VWF:Ag production, measured with ELISA when HDACi was added to the cells, but this did not increase with increasing concentration

of HDACi (Figure 4B). This was confirmed with IF analysis, but unfortunately, the WPBs retained their immature round shape. The cells also started to deteriorate at sodium butyrate concentrations higher than 1mM (Figure 4A). However, at the level of gene expression, we did see an upregulation of the VWF gene in hiPSC-ECs grown with sodium butyrate at low concentrations. Also, several transcription factors involved in VWF transcription showed an increase in expression after the addition of sodium butyrate (Figure 4C). Besides sodium butyrate, we tested Vorinostat (suberanilohydroxamic acid, SAHA) which is a more general HDACi and the substrate sodium acetate which leads to increased acetylation levels. Also with these compounds, there was no significant increase in VWF production and/or the WPB structure (Supplemental Figure 3C).

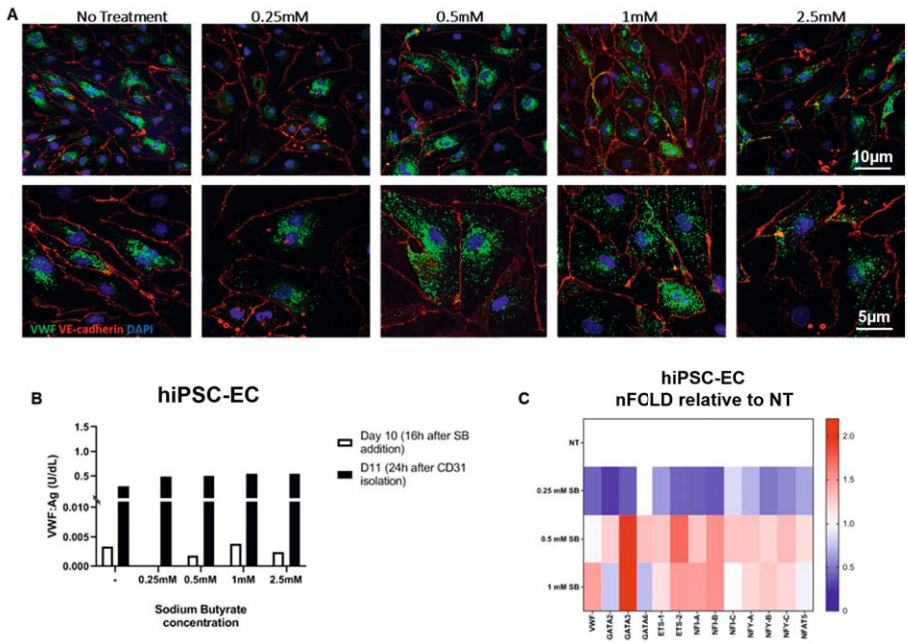

Figure 4. hiPSC-ECs cultured with HDAC inhibitor sodium butyrate. A) Confocal microscopy showing VWF and VE-cadherin after the addition of different concentrations of sodium butyrate. Bottom panel 2x zoomed in. B) ELISA showing VWF secretion (medium). C) Gene expression heatmaps of VWF and VWF related transcription factors. SB, sodium butyrate; NT, no treatment

Aoki protocol

As we did not reach our goal of mature hiPSC-ECs using the in house developed Orlova protocol, we evaluated the efficiency of other published protocols to produce mature hiPSC-ECs. The Aoki protocol (16) uses similar factors as the Orlova protocol, but at slightly different concentrations and time points during the differentiation process

(Supplemental Figure 2B). This paper showed a gradual increase in VWF during and after the differentiation process with comparable mRNA expression in day 35 hiPSC-ECs compared to HUVECs, but did not show any IF stains of VWF. However, this paper only looked at mRNA levels of VWF expression, and did not look at the VWF protein levels and therefore information on the morphology of the WPBs was lacking.

For optimization we also introduced several adjustments to this protocol (Supplemental Figure 2B). When we stained the hiPSC-ECs at the end of the protocol (day 8) for VWF, we detected round and immature WPBs in the early days of expansion (> day 8-20; P1-2). When we continued to passage and expand the cells for more than 23 days (up to day 28; P3), we started to observe elongated WPBs in the cells. However, these were very few and scattered (Figure 5) and the hiPSC-ECs deteriorated substantially over time. Eventually they stopped proliferating with clear changes in their morphology, from the classical endothelial cobble stone into elongated cells. After several rounds, we did not seem to be able to expand this population of 'mature' hiPSC-ECs. However, this shows that it is possible to produce elongated WPBs with VWF in hiPSC-ECs differentiated with the Aoki protocol.

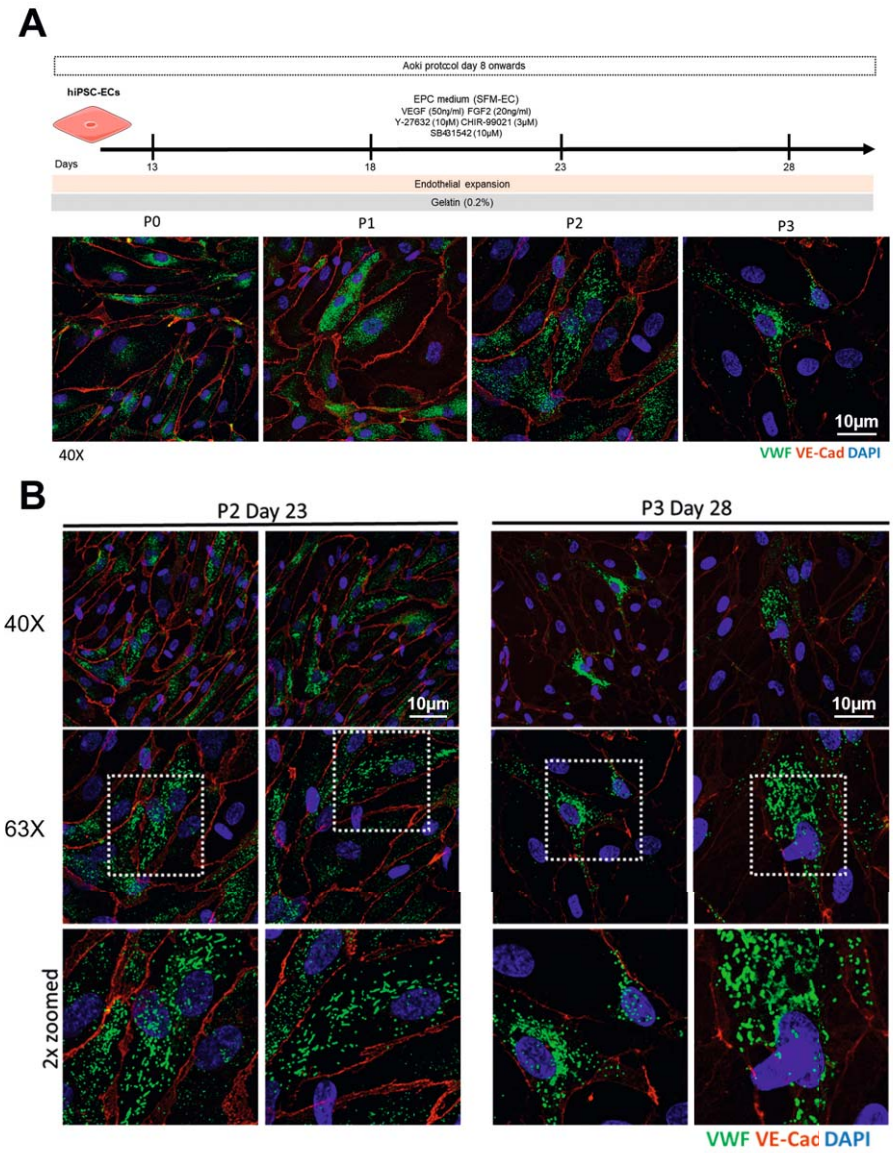

Figure 5. hiPSC-ECs differentiation using the Aoki protocol. A) Timeline and corresponding IF images from day 8 onwards of the expansion of hiPSC-ECs. During this time the hiPSC-ECs were expanded for up to 28 days (passage 3) before they show deterioration in cell morphology. B) IF images showing hiPSC-ECs at day 23 (passage 2) and 28 (passage 3). Some hiPSC-ECs showed elongated WPBs. However, these were very few, surrounded by cells showing the immature rounded WBPs.

This confirmed that the existing protocols are far from optimal in producing hiPSC-ECs with mature phenotypes and emphasizes the complexity associated with these development processes. The majority of endothelial differentiation protocols consist of two stages, where iPSCs transitioning through an intermediate mesodermal phase and an endothelial specification phase. As is described here, and known in literature, current differentiation protocols remain inefficient (about 10% of the differentiated cells may actually be hiPSC-ECs) and lack reliability. Additionally, the differentiation with these protocols take over a week (8 days for Aoki and 10 days for Orlova) before the hiPSC-ECs can be expanded, which can take up additional days to weeks before sufficient cells numbers are reach for further experiments.

ETV2

During our experiments with both Orlova and Aoki protocols, the Wang protocol was published (14). This involves transfection with a vascular transcription factor, which results in hiPSC-ECs within 96h (4 days) (Supplemental Figure 2C). In this approach, cells at the mesodermal phase are transfected with the transcription factor E26 transformation-specific variant 2 (ETV2), differentiating iPSCs into endothelial cells in 96h (4 days). ETV2 plays a crucial role in vascular cell development, however, is only required transiently. It is known that inefficient activation of ETV2 during differentiation, leads to poor outcomes. By using chemically modified mRNA (modRNA) vectors, which are nonviral, nonintegrating, and transient, this paper showed for 13 different iPSC lines, a rapidly and robust differentiation into endothelial cells, with high efficiency (>90%). However, the rationale to go for this approach was to generate hiPSC-ECs in a relative short period of time and proceed from here with optimization steps of the protocol and differentiation factors to produce mature hiPSC-ECs to use for further studies.

With some optimizations and adjustments, we differentiated the cells according to the protocol as outlined in Supplemental Figure 2C. The cells showed the typical endothelial cell morphology, and IF showed cellular VE-Cadherin with low levels of VWF at D8 (P0). When trying to expand and passaging the hiPSC-ECs, up to day 40 (P3), the cells started to deteriorate (Figure 6). Surprisingly, there were few cells with rather high levels of VWF, with several elongated WPBs. Comparable to the Aoki protocol, this approach shows promising results and can have the potential, possibly with some adjustments, to induce the endothelial maturation needed in hiPSC-ECs.

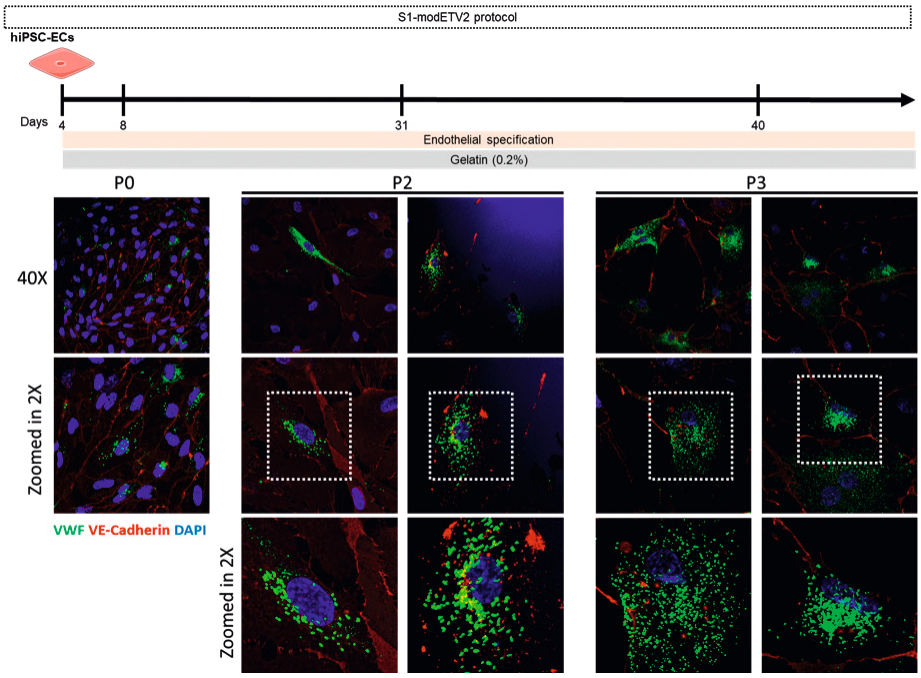

Figure 6. hiPSC-ECs differentiation using the ETV2 protocol. Timeline and corresponding IF images from day 4 onwards of the expansion of hiPSC-ECs. During this time the hiPSC-ECs were expanded for up to 40 days (passage 3) before they show deterioration in cell morphology A limited number of iPSC-ECs showed elongated WPBs, but again, these were very few, surrounded by cells showing the immature rounded WBPs.

Discussion

In recent years, hiPSC-ECs have become an interesting source of experimental endothelial cells, not only for research but also for potential cell therapeutics. Research is developing rapidly to improve the differentiation efficiency of endothelial cells from hiPSCs by new signaling pathways and novel culture conditions. Since our research focuses on VWF and VWD, we are particularly interested in (cell) models mimicking or showing normal levels of functional VWF in cells. After comparing several hiPSC-EC differentiation papers and protocols, we noticed that the reported VWF protein levels are low and the WPBs show round structures instead of their mature tubular shape. Since this protein is important in coagulation and a key endothelial marker, it is of importance to reach normal expression and production levels for hiPSC-ECs to be a proper endothelial cell model.

Here we differentiated hiPSCs from three healthy controls into cells of the endothelial lineage, using different protocols and approaches to attempt to generate more mature hiPSC-ECs. By changing culture conditions, such as altering the timing and concentrations of standard (growth) factors used for endothelial cell differentiation, introducing some level of flow, and/or the addition of different compounds, we made an attempt to induce a more mature endothelial phenotype in these cells than previously reported. The approaches we used were based on information taken from published protocols, but also from the expertise within our institute. The Orlova protocol (2014) (9) was established in-house and has since been adjusted, and additionally, we used two more recently published protocols (2020) (14, 16). The Aoki protocol (16) uses similar differentiation factors, but the timeline is different to the Orlova protocol (9), and finally, we transfected hiPSCs with transcription factor E26 transformation-specific variant 2 (ETV2) (14). This has been shown to lead to hiPSC-ECs in a shorter timeframe (within 4 days) which would give us the opportunity to adjust the differentiation factors and other substances in a more time efficient approach.

WPBs are unique to endothelial cells and the levels of produced VWF induce the formation and maturation of WPBs. The elongated form of the WPBs gives an indication of the matured state of endothelial cells. Therefore our main focus was to increase VWF production to give rise to mature WPBs, like seen in ECFCs. In recent years, we and others have been using ECFCs as an endothelial cell model, to study different diseases. However, heterogeneity is often observed between ECFC clones (2, 3). This inter- and intra-donor variability requires further understanding and standardization in order for ECFCs to be used as a robust cellular model for applications in vascular studies. Therefore, hiPSC-ECs might be a good alternative when a standardized robust differentiation protocol has been established.

We were able to successfully differentiate these iPSCs into endothelial cells (iPSC-ECs) with all three protocols. Generated hiPSC-ECs were analyzed at different timepoints for endothelial cell morphology and characteristics. Literature shows that the expression levels measured with qPCR for VWF in iPSC-ECs vary over time when compared to primary endothelial cells (14, 16). A number of papers do include IF stains, but mostly without using high magnifications to show the structure of WPBs in greater detail (9). This refers to different approaches and protocols for endothelial cell differentiation, such as the monolayer, embryoid body or organoid formation. Nevertheless, there is a paper by Nakhaei-Nejad et al. showing elongated WPBs, using embryoid bodies for differentiation. However, endothelial cells (HUVECs) were the cell source for the generation of iPSCs (13). Therefore it is plausible this could be due to the epigenetic

memory of cells which is not completely erased during the reprogramming process (19-21).

In our modified differentiation and maturation procedures, generally, VWF protein levels remained low compared to primary endothelial cells, but overall, the iPSC-ECs show an endothelial profile looking at morphology, cell surface markers (flow cytometry), proteins (immunofluorescence) and gene expression (qPCR). Even though a slight increase in VWF production was seen at several of the mentioned adjustments before, this was of insignificance when compared to primary endothelial cells. However, most interestingly, we did detect elongated WPBs in hiPSC-ECs when differentiated either with the Aoki or ETV2 protocols. These observations were seen in very few cells that have been in culture for at least 30 days (passage number 3). At this timepoint, the hiPSC-ECs start to deteriorate and are of such low quality, they cannot be used in further experiments. It is known from literature that hiPSC-ECs, have a limited life span before going into senescence in vitro, and are difficult to expand to sufficient numbers to be used in following experiments (11, 12). Nevertheless, this indicates that it is possible with the correct conditions to induce a mature phenotypes in hiPSC-ECs at such a level that VWF production is increased leading to elongated WPBs. As the more mature, elongated WPBs seem to arise after a long culturing period, the challenge will be to improve prolonged culturing times which are currently a limiting factor.

Our attempts to increase VWF levels by using co-cultures with iPSC-PCs or introducing some level of flow into the differentiation process, did not seem to have the desired effect. When looking at factors, VEGF was the evident choice, since this growth factor and signaling protein is an inducer of endothelial cell growth and promotes the formation of new blood vessels. A paper by Rosa et al, showed that with different concentrations of VEGF during the differentiation process, EPCs would either go towards an arterial or venous phenotype (17). However, this and other factors tested did not seem to induce a mature endothelial phenotype in the hiPSC-ECs. In conclusion, some adjustments and/or additions show a slight increase in VWF gene expression and some related transcription factors, however this is still not translated into higher VWF protein levels and morphologically elongated WPB formation. We should, however, consider that there are major differences relating to VWF expression and WPB formation between ECs from different vascular beds. As reviewed by Randi et al. (22) there are differences in VWF expression between ECs from larger vessels and microvessels, and between ECs from veins versus arteries, and there may even be variability within the same vascular bed. Furthermore, not all ECs that express VWF do form WPBs. Based on this existing variability it could be possible that the hiPSC-ECs indeed mimic ECs that may never express high levels of VWF nor form elongated WPBs because of their

potential directionality of differentiation towards a specific EC signature.Research into the maturation of these differentiated endothelial cells into more specific types of endothelium (arterial, venous, lymphatic) through the manipulation of culture media is ongoing. Because these are differentiated in vitro, they are not exposed to impacts from the (tissue) specific environment, such as blood flow and pressure, that play roles in endothelial cell differentiation in vivo. To mimic these in vivo environments more closely, micro-fluidic 3D systems, like organ-on-a-chip, have been developed (23).

We would recommend other groups to, besides reporting there is VWF production in the hiPSC-ECs, also report the maturation status of these differentiated cells. It is highly informative to report the levels of VWF, both as expression and protein levels and to show the WPB structures. This is necessary for the applicability of the hiPSC-ECs and can lead to improved and better standardized differentiation protocols.

The generation and differentiation of iPSCs into endothelial cells, along with the availability of the human genome and genome editing tools has transformed disease research immensely, leading to the development of new strategies to treat or study vascular diseases. This is especially relevant for cells of the internal organs for which biopsies are not routinely available, such as megakaryocytes and endothelial cells. A deeper understanding of the development of the endothelial cell lineage is required for differentiated cells to become a robust model for vascular diseases and the potential to the safe use of these cells as a patient-specific cell therapy in future. Acquiring these cells through patient-specific hiPSC differentiation can enable better insights into VWD and other bleeding disorders, in combination with additional aims such as (high-throughput) drug screening, development and cell therapy.

Acknowledgements

We would like to thank the volunteers that participated in the study and donated their blood. Thanks to the LUMC iPSC Hotel for generating and characterizing the hiPSCs that were used in this study.

References

1. de Boer S, Eikenboom, J. Von Willebrand Disease: From In Vivo to In Vitro Disease Models. HemaSphere. 2019;3(5):e297.
2. de Boer S, Bowman M, Notley C, Mo A, Lima P, de Jong A, et al. Endothelial characteristics in healthy endothelial colony forming cells; generating a robust and valid ex vivo model for vascular disease. J Thromb Haemost. 2020.
3. de Jong A, Weijers E, Dirven R, de Boer S, Streur J, Eikenboom J. Variability of von Willebrand factor-related parameters in endothelial colony forming cells. J Thromb Haemost. 2019;17(9):1544-54.
4. Sadler JE. von Willebrand factor in its native environment. Blood. 2013;121(14):2583-4.
5. Smadja DM, Melero-Martin JM, Eikenboom J, Bowman M, Sabatier F, Randi AM. Standardization of methods to quantify and culture endothelial colony-forming cells derived from peripheral blood: Position paper from the International Society on Thrombosis and Haemostasis SSC. J Thromb Haemost. 2019;17(7):1190-4.
6. Lin Y, Gil CH, Yoder MC. Differentiation, Evaluation, and Application of Human Induced Pluripotent Stem Cell-Derived Endothelial Cells. Arterioscler Thromb Vasc Biol. 2017;37(11):2014-25.
7. Zakrzewski W, Dobrzynski M, Szymonowicz M, Rybak Z. Stem cells: past, present, and future. Stem Cell Res Ther. 2019;10(1):68.
8. Leebeek FW, Eikenboom JC. Von Willebrand's Disease. N Engl J Med. 2016;375(21):2067-80.
9. Orlova VV, van den Hil FE, Petrus-Reurer S, Drabsch Y, Ten Dijke P, Mummery CL. Generation, expansion and functional analysis of endothelial cells and pericytes derived from human pluripotent stem cells. Nat Protoc. 2014;9(6):1514-31.
10. Wimmer RA, Leopoldi A, Aichinger M, Kerjaschki D, Penninger JM. Generation of blood vessel organoids from human pluripotent stem cells. Nat Protoc. 2019;14(11):3082-100.
11. Prasain N, Lee MR, Vemula S, Meador JL, Yoshimoto M, Ferkowicz MJ, et al. Differentiation of human pluripotent stem cells to cells similar to cord-blood endothelial colony-forming cells. Nat Biotechnol. 2014;32(11):1151-7.
12. Samuel R, Daheron L, Liao S, Vardam T, Kamoun WS, Batista A, et al. Generation of functionally competent and durable engineered blood vessels from human induced pluripotent stem cells. Proc Natl Acad Sci U S A. 2013;110(31):12774-9.
13. Nakhaei-Nejad M, Farhan M, Mojiri A, Jabbari H, Murray AG, Jahroudi N. Regulation of von Willebrand Factor Gene in Endothelial Cells That Are Programmed to Pluripotency and Differentiated Back to Endothelial Cells. Stem Cells. 2019;37(4):542-54.
14. Wang K, Lin RZ, Hong X, Ng AH, Lee CN, Neumeyer J, et al. Robust differentiation of human pluripotent stem cells into endothelial cells via temporal modulation of ETV2 with modified mRNA. Sci Adv. 2020;6(30):eaba7606.
15. Okita K, Matsumura Y, Sato Y, Okada A, Morizane A, Okamoto S, et al. A more efficient method to generate integration-free human iPS cells. Nat Methods. 2011;8(5):409-12.
16. Aoki H, Yamashita M, Hashita T, Ogami K, Hoshino S, Iwao T, et al. Efficient differentiation and purification of human induced pluripotent stem cell-derived endothelial progenitor cells and expansion with the use of inhibitors of ROCK, TGF-beta, and GSK3beta. Heliyon. 2020;6(3):e03493.

17. Rosa S, Praca C, Pitrez PR, Gouveia PJ, Aranguren XL, Ricotti L, et al. Functional characterization of iPSC-derived arterial- and venous-like endothelial cells. Sci Rep. 2019;9(1):3826.
18. Tiemeier GL, de Koning R, Wang G, Kostidis S, Rietjens RGJ, Sol W, et al. Lowering the increased intracellular pH of human-induced pluripotent stem cell-derived endothelial cells induces formation of mature Weibel-Palade bodies. Stem Cells Transl Med. 2020;9(7):758-72.
19. Chin MH, Mason MJ, Xie W, Volinia S, Singer M, Peterson C, et al. Induced pluripotent stem cells and embryonic stem cells are distinguished by gene expression signatures. Cell Stem Cell. 2009;5(1):111-23.
20. Guenther MG, Frampton GM, Soldner F, Hockemeyer D, Mitalipova M, Jaenisch R, et al. Chromatin structure and gene expression programs of human embryonic and induced pluripotent stem cells. Cell Stem Cell. 2010;7(2):249-57.
21. Kim K, Zhao R, Doi A, Ng K, Unternaehrer J, Cahan P, et al. Donor cell type can influence the epigenome and differentiation potential of human induced pluripotent stem cells. Nat Biotechnol. 2011;29(12):1117-9.
22. Randi AM, Jones D, Peghaire C, Arachchillage DJ. Mechanisms regulating heterogeneity of hemostatic gene expression in endothelial cells. J Thromb Haemost. 2023;21(11):3056-66.
23. van Duinen V, Stam W, Mulder E, Famili F, Reijerkerk A, Vulto P, et al. Robust and Scalable Angiogenesis Assay of Perfused 3D Human iPSC-Derived Endothelium for Anti-Angiogenic Drug Screening. Int J Mol Sci. 2020;21(13).

A Pluripotency markers

				FACS expression (%)		
iPSC cell line	Sample	Gender	Age	OCT3/4	NANOG	SSEA4
LUCM0183iCTRL	C41	F	22	84.8	92.6	90.5
LUCM0184iCTRL	C42	M	45	94.5	97.7	94.5
LUCM0185iCTRL	C43	F	54	79.2	95.0	81.5
Average expression				86.2	95.1	88.8

B Germline differentiation potential

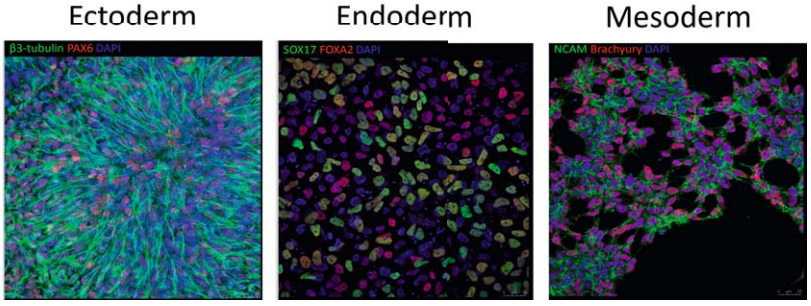

Supplemental Figure 1. Reprogramming characterization of PBMCs into hiPSC. Donor information and FACS data of pluripotency markers. B) IF images of markers showing differentiation potential into the three germlines.

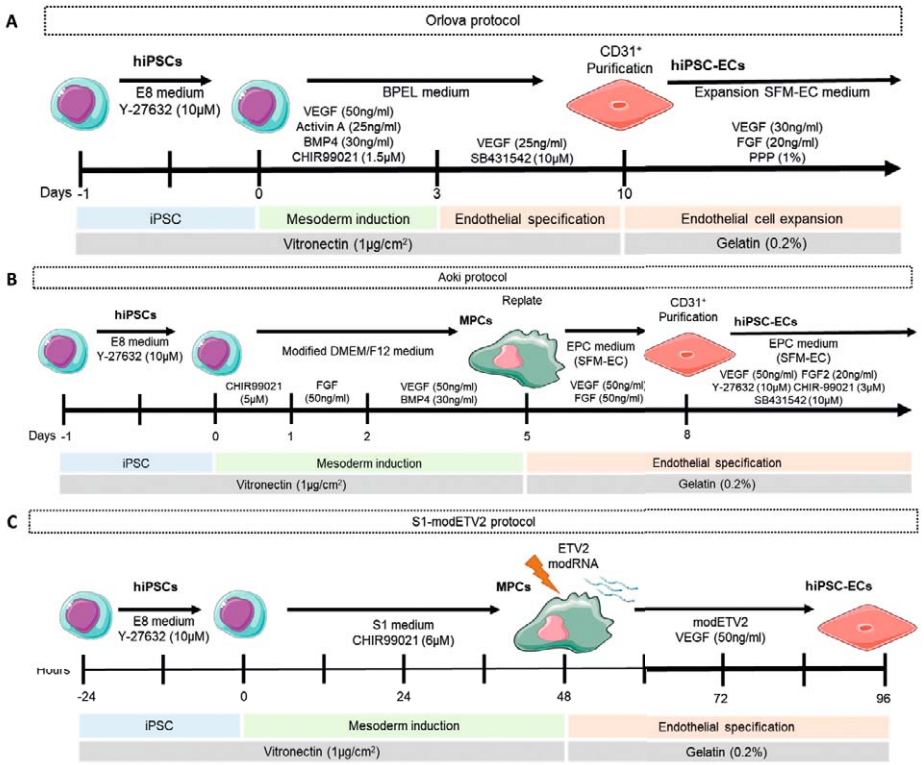

Supplemental Figure 2. Schematic overviews of the (adjusted) three endothelial differentiation protocols used in this study. A) Orlova protocol. B) Aoki protocol. C) ETV2 protocol.

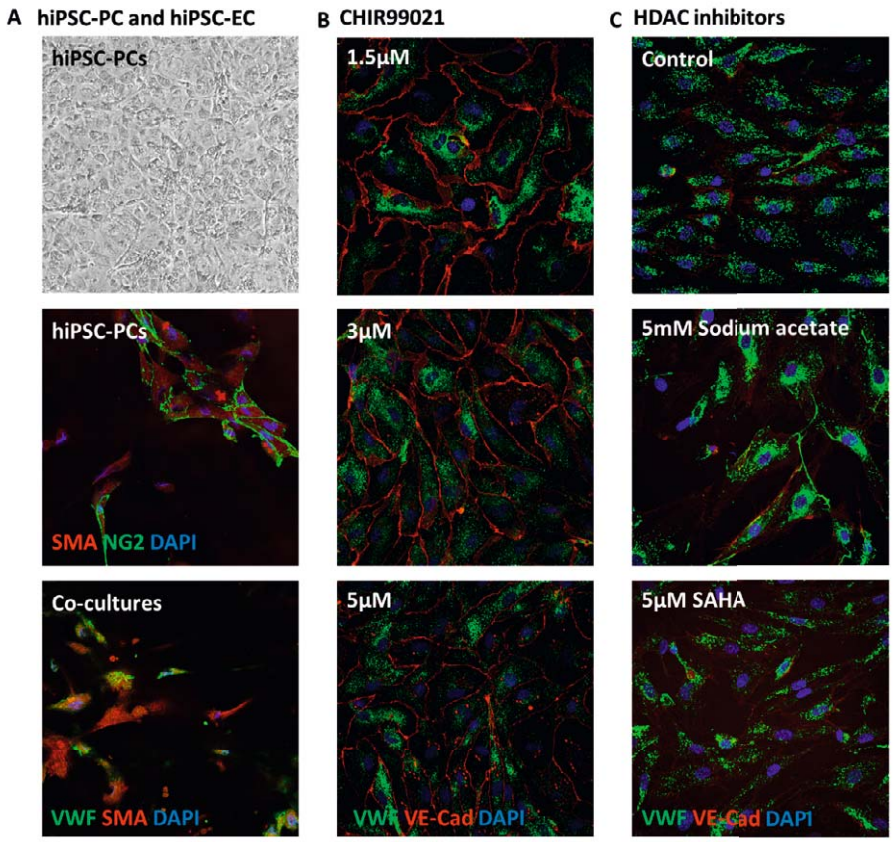

Supplemental Figure 3. Additional optimization strategies. hiPSC-EC cocultures with hiPSC-PCs. B) Varying concentration of endothelial differentiation factor CHIR99021. C) Addition of different HDAC inhibitors.

Supplemental Table 1. Medium and supplements used in this study.

Orlova medium		Aoki medium	
B(P)EL (day 0-9)	**Final concentration**	**Modified DMEM/ F12 (day 0-4)**	**Final Concentration**
IMDM	1x	DMEM/F12	1x
Ham's F12 Nutrient mix	1x	Lipid concentrate	0.1x
PFHM	5%	ITS-X	0.1x
BSA	0,25%	GlutaMax supplement	2mM
Lipid concentrate	0.1x	αMTG	
ITS-X	0.1x	AA2P	0.05mg/mL
1-Thioglycerol (αMTG)	450μM	Pen/Strep	0,50%
L-ascorbic acid phospahte magnesium salt n-hydrate (AA2P)	0.05mg/mL		
GlutaMax supplement	2mM		
Pen/Sterp	0,50%		
EC-SFM full medium (day >10)	**Final concentration**	**EC-SFM full medium (day >5)**	**Final concentration**
EC-SFM		EC-SFM	
Platelet Poor Plasma	1%	Platelet Poor Plasma	1%
		Pen/Strep	0,50%

DDAVP response and its determinants in bleeding disorders: a systematic review and meta-analysis

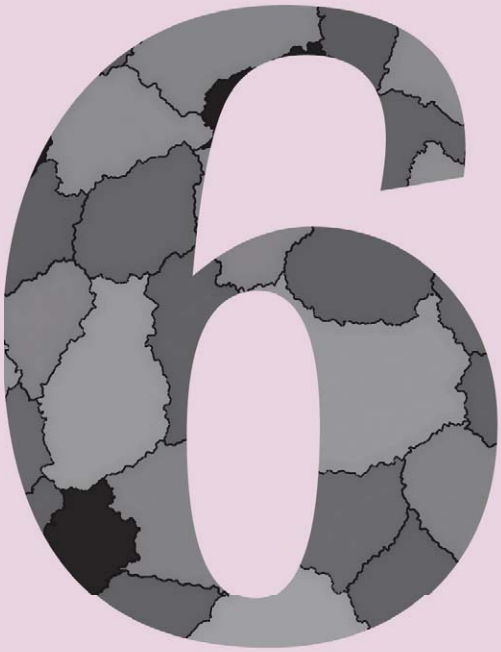

Laan SNJ, Castillo Alferez J, Cannegieter S, Fijnvandraat K, Kruip M, Le Cessie S, Bierings R, Eikenboom J, van Moort I.

Blood 2025; 145 (16): 1814–1825.
doi: https://doi.org/10.1182/blood.2024026804
Accepted after revision

Abstract

Desmopressin (DDAVP) can be used to prevent or stop bleeding. However, large inter-individual variability is observed in DDAVP response and determinants are largely unknown. In this systematic review and meta-analysis we aim to identify the response to DDAVP, and the factors that determine DDAVP response in patients.

We included studies with patients with any bleeding disorder receiving DDAVP. First and second screening round and risk of bias assessment were performed by independent reviewers. The main outcome was proportion of patients with complete (factor level > 50 U/dL), or partial (30-50 U/dL) response to DDAVP. Determinants of response including disease type, age, sex, Von Willebrand factor (*VWF*) and factor VIII *(FVIII)* mutations, and baseline factor levels were investigated.

In total, 594 articles were found and 103 were included. Of these, 81 articles (1982 patients) were suitable for the study's definition of response. Meta-analysis showed a pooled response proportion of 0·74 [0·68;0·79] and a significant difference in response between disease subtypes. For hemophilia A, baseline FVIII:C was a significant determinant of response. In von Willebrand disease (VWD) type 1 patients, VWF:Ag, VWF:Act and FVIII:C were significant determinants. A large variation in response was observed for specific mutations in *VWF and F8*.

Response to DDAVP varied between disease subtypes, and was largely determined by the baseline levels of FVIII:C for hemophilia A and VWF:Ag for VWD. Our findings highlight the significant differences in response and emphasize the need for a standardized response definition and further research into response mechanisms.

Introduction

Patients with bleeding disorders experience frequent bleeding from mucocutaneous tissue of nose, uterus, and bleeding in joints and muscles, causing discomfort and pain. Von Willebrand disease (VWD) and hemophilia A (HA) are two of the most common bleeding disorders worldwide with a prevalence of 1:10000 individuals and 1:5000 males, respectively (1). VWD is characterized by quantitative or qualitative defects of von Willebrand factor (VWF), a large multimeric glycoprotein (2). VWF is produced by endothelial cells and megakaryocytes, can bind to collagen at sites of injury, and mediates the formation of a platelet plug. Furthermore, VWF protects coagulation factor VIII (FVIII) from degradation (3). FVIII is the protein that is (partly) deficient in patients with HA and a cofactor in the FIX mediated activation of FX which is crucial for thrombin generation (4).

The main goal of treatment in patients with bleeding disorders is to prevent or treat bleeding. Treatment options aim to increase plasma FVIII levels in HA or VWF and/or FVIII in VWD (2,5). The most common treatment options are replacement therapy that supplements the (partly) deficient coagulation factor and 1-deamino-8-D-arginine vasopressin (DDAVP), also known as desmopressin (6). DDAVP is a synthetic vasopressin analogue that increases endogenous VWF and FVIII levels by an average of three- to five-fold. The ability to increase plasma FVIII and VWF levels in response to DDAVP depends largely on the availability of stored FVIII/VWF, the efficacy of FVIII/VWF secretion and rate of clearance (7). DDAVP is therefore mostly prescribed in patients in which VWF and FVIII are not completely deficient, such as patients with VWD type 1, moderate and mild HA patients (8), and patients with platelet function disorders (PFD) (9).

DDAVP is one of the cheapest and readily available treatments for patients with bleeding disorders. Furthermore, the intranasal formulation of the drug, which can be administered by patients themselves, greatly improves convenience of use. Large inter-individual differences exist in the response to DDAVP, therefore, each individual patient receives a DDAVP test dose with multiple blood drawings to investigate how well they respond to the drug. When patients do not respond, they are fully dependent on the alternative treatments, which are more costly and may require hospital visits. Several studies have reported that DDAVP response is partly influenced by certain factors such as age, blood group type, disease severity or mutation type (7,10-23). However, most studies were conducted in smaller patient cohorts with a large heterogeneity in patient characteristics. Therefore, it is still largely unknown which factors determine a DDAVP response. For that reason, in this systematic review we aim to identify the response

rate in different diseases and to identify possible determinants that influence DDAVP response in order to gain a better understanding of the reason behind a non-response.

Methods

Search strategy and selection criteria

We performed a systematic review and meta-analysis to explore the factors that determine DDAVP response in patients with a bleeding disorder. Our PROSPERO study protocol is available at https://www.crd.york.ac.uk/prospero/ (CRD42021259033). We performed a comprehensive search in PubMed, Embase, Web of Science, COCHRANE Library, Emcare on October 16, 2020. The search was re-run once before the final analysis on September 1st, 2022 (Supplemental File 1). All studies were entered in Covidence (24), where duplicate records were removed. Title and abstract screening and full text screening was performed by at least two reviewers independently (SL, IvM, JdCA). Published studies were included that were performed in patients with any bleeding disorder treated with DDAVP in any dose or form of administration for the indication to improve hemostasis. Papers written in languages other than English, animal studies, reviews and studies on patients without a bleeding disorder were excluded. Any disagreements were resolved by consensus.

Data extraction

The primary outcome was the DDAVP response classified according to the following definition: complete response is defined as VWF Antigen (VWF:Ag) and/or FVIII activity (FVIII:C) above 50 U/dL, for VWD and hemophilia A respectively after 1 hour. Partial response is VWF:Ag and/or FVIII:C between 30 U/dL - 50 U/dL, and non-response is VWF:Ag and/or FVIII:C levels below 30 U/dL. This definition is a slight adjustment on the ASH ISTH NHF WFH 2021 guidelines (25). In these guidelines, a complete response is defined as VWF or FVIII level increasing at least two-fold over baseline, and levels reach >50 U/dL. We will refer to the adjusted definition as the "study definition". This response definition was used to compare complete responders with partial- and non-responders between studies. DDAVP response was also collected based on the response definitions applied in the respective papers, which usually comprised of the categories; complete-, partial- and non-response, and will be referred to as the "article definition". Data from articles where no definition was given were also collected, referred to as "undefined definition". Data were extracted by three reviewers (SL, IvM, JC) independently, using a template custom made within Microsoft Excel (Supplemental File 2 – Data extraction template). For all articles, summary data were collected and individual patient-level data were obtained if possible. Raw data was requested from

the authors of papers if summary data could not be extracted directly from the article. We collected potential determinants of a DDAVP response in patients with bleeding disorders. Expected determinants were diagnosis, blood group, mutations in *VWF* or *F8,* weight, age, sex, baseline factor levels of VWF or FVIII, multimer pattern of VWF, and dose and administration route of DDAVP. Note that VWF activity was measured with different platelet binding assays, the majority using VWF ristocetin cofactor activity. In this article all VWF activity levels will be indicated as VWF:Act.

Study grouping and data analysis

Analyses were performed separately per disease but also in one of five main disease types. Namely, VWD type 1, VWD type 2, VWD type 3, HA and if not fitting in one of these four disease types, "other". We categorized VWD subtypes as a result of their completely different pathophysiology. Most of the studies reported DDAVP as categorical outcome (e.g. non-, partial-, or complete response), other studies reported continuous variables (VWF:Ag, VWF:Act, FVIII:C). Meta-analysis per disease subtype was performed when data from at least three studies was available. As we were interested in the determinants of the DDAVP response with regard to the actual physiological mechanisms of secretion of factors from endothelial cells we based the "study definition" on the increase in VWF:Ag or FVIII:C. This definition, however, does not necessarily reflect an increase of functional VWF:Act as is usually considered in the context of clinical responsiveness and applicability of DDAVP in VWD. Response in VWF levels in the quantitative sense (on antigen level) or in a qualitative sense (on activity level) both offer different insights into the mechanisms of DDAVP response. Therefore, we also compared VWF:Act as a factor next to VWF:Ag over time in type 1 VWD compared to type 2 VWD patients, which are known to have qualitative defects of VWF. Meta-regression (Supplemental Methods) was performed when the association between a prognostic factor and DDAVP response was evaluated in at least three studies. Finally, the effect of *VWF/F8* mutations on response was analyzed per patient.

Results

Study selection and data extraction

The search strategy identified 570 studies and another 21 original articles were added after the re-run of the search. After 1st and 2nd round of screening, 103 studies (ranging from publication date 1980 to 2022) were included as shown in the PRISMA flow diagram (Figure 1) (7,10-23,26-113). The characteristics of all studies are presented in Supplemental Table 1. The majority of the included studies, are prospective case reports/series.

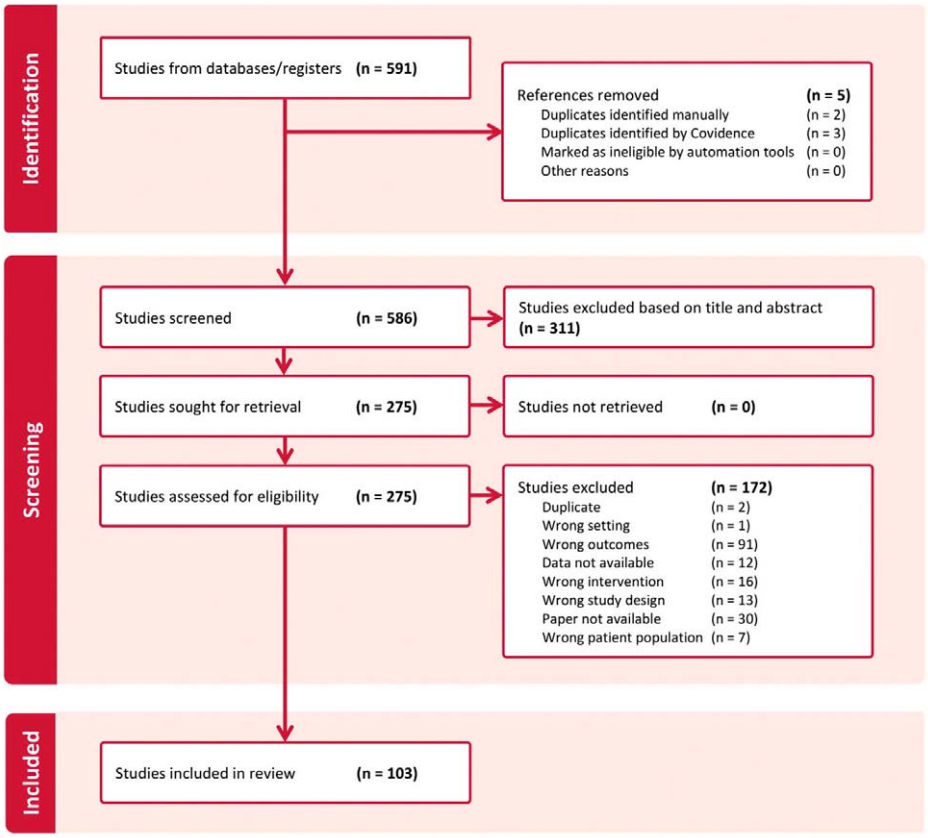

Figure 1. PRISMA flow diagram of inclusion and exclusion of articles.

Data on DDAVP response could be extracted and classified according to the "study definition" in 81 articles and according to the "article definition" in 36 articles (Supplemental Table 1). The definitions that were employed for the "article definitions" are listed in Supplemental Table 2. Data from studies with an "undefined definition" of DDAVP response were also extracted from 52 articles. Unfortunately, due to heterogeneity between article definitions and small patient numbers in the studies only reporting the "article definition" and "undefined definition", these could not be used for further meta-analysis and meta-regression. Risk of bias (RoB) was assessed, with most articles being low (40/103) or moderate RoB (52/103) with some high RoB studies (11/103). Almost all studies reported only intravenous (71/103) or intravenous or subcutaneous administration of DDAVP (13/103). A few reported subcutaneous administration (14/103), intranasal (1/103) or not reported administration (5/103). All

extracted data, e.g. the RoB score, study design, bleeding disorder and administration route, per study can be found in Supplemental File 3.

Meta-analysis on response to DDAVP per disease subtype

For the meta-analysis, 81 articles were used where the "study definition" of response could be applied. In Supplemental Table 1, patient number reflects the patients from which data could be extracted based on the "study definition" (total of 1982 patients). Of these patients, the average age was 34·2 ± 11·6 and 25·6% was female. A large part of the patients were male hemophilia A patients (396 patients). Patient numbers per disease subtype are shown in Figure 2A. Data from three or more articles were obtained for the following subtypes of disease: VWD type 1 (28 studies), VWD type 2A (eight studies), VWD type 2B (nine studies), VWD type 2M (five studies), VWD type 2N (four studies), VWD type 3 (three studies), VWD undefined (four studies), HA carriers (three studies), HA mild (nine studies), HA mild & moderate (11 studies), HA moderate (five studies), PFD (ten studies) and Other (seven studies). As seen in Figure 2A, most patients had either HA (n=923) or VWD type 1 (n=669).

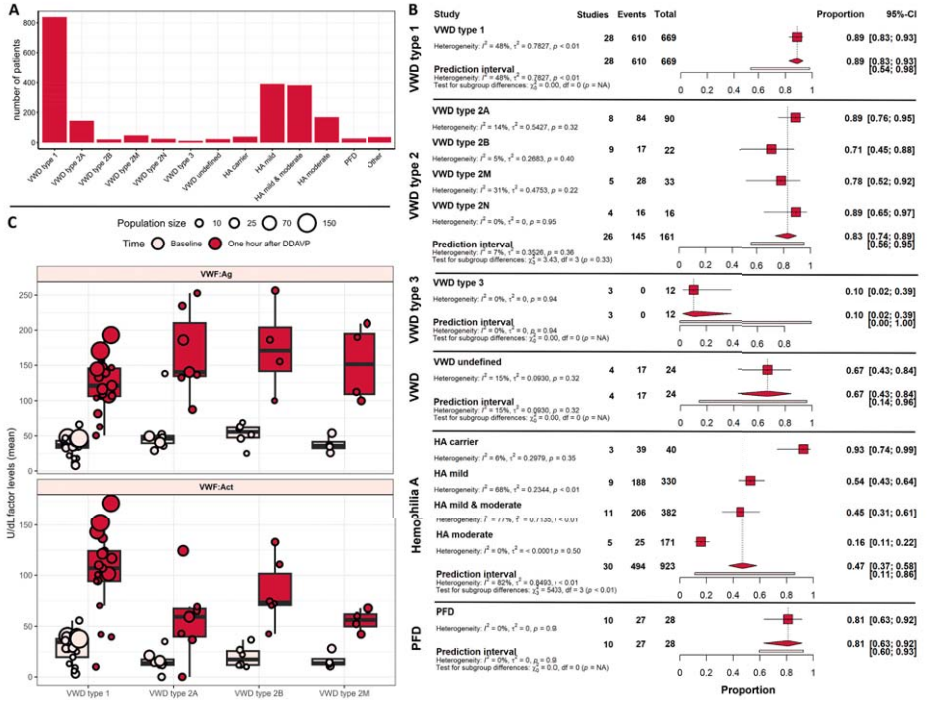

Figure 2. Complete response rate varies per disease subtype according to the study definition. A) Number of patients per disease type. Disease types with <3 articles are excluded from this analysis. "Other" is, everything that is not VWD type 1, 2 or 3, Hemophilia A or PFD. B)

Meta-analysis on response to DDAVP at one hour in patients with various bleeding disorders per subtype according to the study definition. Using a random effect model the proportion of complete response per disease type are shown. The proportion of response is not zero in zero-event studies due to the continuity correction that was performed to prevent mathematical errors. C) Response to DDAVP of patients with VWD type 1 and VWD types 2A, 2B, 2M. In the top panel, VWF:Ag (U/dL) before (light red) and after one hour of DDAVP (dark red) are shown. In the bottom panel, VWF:Act (U/dL) is shown. VWD type 2N is not displayed in this figure as only two studies had data on both VWF:Ag and VWF:Act. Abbreviations: HA = Hemophilia, PFD = Platelet function disorder, VWD = Von Willebrand disease.

The results of the meta-analyses for the complete response rate are given in Figure 2B. Forest plots presenting data points per study instead of subtype summaries are shown in Supplemental Figure 1. Meta-analysis showed a pooled response proportion of 0·74 [0·68;0·80] for all patients and a significant difference in DDAVP response between disease subtypes. The overall proportion of complete response was 0·89 (CI 0·83-0·93) in VWD type 1 patients, 0·83 (CI 0·75-0·89) in type 2 and 0·10 (CI 0·02-0·39) in type 3. The response in HA carriers was 0·93 (CI 0·74-0·99), mild HA 0·54 (CI 0·43-0·64), mild and moderate HA 0·45 (CI 0·31-0·61), and moderate HA only 0·16 (CI 0·11-0·22). We observed significant differences in proportions of complete response between disease subtypes in HA patients with a lower response in moderate patients. VWD type 1 and 2 also showed large differences in proportion of response between subtypes although most subtypes responded quite well to DDAVP according to the "study definition". Finally, the observed proportion of response in PFD patients was 0·81 (CI 0·63-0·92). It should be noted that levels of VWF and FVIII at baseline were above 50 U/dL in almost all PFD patients leading to complete response according to the "study definition".

We analyzed the increase from baseline in VWF:Ag in VWD patients and observed a large increase in VWF:Ag in all type 1 VWD patients as well as in patients affected by types 2A, 2B and 2M VWD (Figure 2C). Median VWF:Ag levels (U/dL) with standard deviation one hour after DDAVP administration is 121·20 ± 35·39 in type 1 VWD, in type 2A, 2B and 2M the levels are 140·28 ± 59·77, 170·79 ± 65·23 and 151·30 ± 54·82 respectively. All subtypes increase above 100 U/dL. However, levels of VWF:Act only increase strongly in VWD type 1 and VWD type 2B (106·93 ± 42·38 and 73·06 ± 32·41). Although limited data was available, the average platelet count in type 2B patients (12 patients in four articles (31,57,76,104)) was reported to be reduced after DDAVP ($90x10^9$/L) compared to before administration ($172x10^9$/L). In VWD type 2A and 2M median levels remain low (59·36 ± 37·84 and 56·20 ± 10·84). Both barely reaching levels above 50 U/dL. In VWD type 2B VWF:Act levels do increase, which makes sense, as type 2B mutations do not cause less activity of VWF, but rather, increased binding affinity to platelets. VWD type 2N was not included in this analysis as only two studies had data on both VWF:Ag and VWF:Act.

Determinants of DDAVP response in patients with bleeding disorders

Based on the meta regression analyses, determinants of DDAVP response, according to the "study definition" differed per disease type (Figure 3). For HA patients higher baseline factor levels of FVIII:C (U/dL) and female sex showed a significant association with higher proportion of complete response (OR=1·054 per U/dL, 95%CI 1·014–1·095 and OR=1·024 per percentage point more women, 95%CI 1·007–1·040). As all females were carriers of HA they logically had higher baseline FVIII levels compared to men which explains the difference is response. Although increased baseline VWF:Ag levels per unit and higher age per year showed a positive association with complete response, these were not significant (OR=1·009 per U/dL, 95%CI 0·973–1·045 and OR=1·055 per year, 95%CI 0·965–1·153 respectively). In VWD type 1 patients, VWF:Ag (OR=1·055 per U/dL, 95%CI 1·016–1·096), VWF:Act (OR=1·048 per U/dL, 95%CI 1·008–1·090) and FVIII:C (OR=1·023 per U/dL, 95%CI 1·002–1·045) were associated with the proportion of complete response, age (OR=1·006 per U/dL, 95%CI 0·935–1·082) and VWF Collagen Binding (CB) did not (OR=1·058 per U/dL, 95%CI 0·896–1·246). No determinants showed a significant association with response in VWD type 2 patients. However, blood group non-O and weight did show some trend (OR=1·037, 95%CI 0·996–1·080 and OR=1·027 per kg, 95%CI 0·986–1·069), respectively. Route of administration is presented in Supplemental Figure 2. However, meta-regression was not performed on the route of administration as not enough data of different routes was available. Other determinants like bleeding time and sex in VWD, showed no positive nor negative effect in our study. All estimated odds ratios with 95% CI of the determinants per disease type are shown in Supplemental Table 3.

Assessing F8 and VWF mutations as determinants of DDAVP response

Genetic variants of *F8* and *VWF* may impact folding, storage, secretion and interaction with other proteins, thereby affecting DDAVP response. We collected patient mutation information from the articles when available (18 studies, eight reported *F8* mutations and ten *VWF* mutations). For HA, data of 389 patients with known *F8* genetic annotations were extracted. Of these patients, 215 were complete-, 113 partial- and 61 non-responders. In total, 165 distinct missense variants were recorded while the rest of the variants represented mutations at noncoding regions, repetitions and possible exon deletions. We plotted peak FVIII:C levels against amino acid positions affected by missense mutations to investigate whether missense mutations at specific protein locations associated with response (Figure 4A). This revealed that mutations were distributed over all *FVIII* domains, but scarcely along the B domain. Importantly, we observed that mutations in the same location were associated with different responses. For instance, in 26 subjects with the variant Arg2169His, nine had a complete response, 13 partial and four were non-responders.

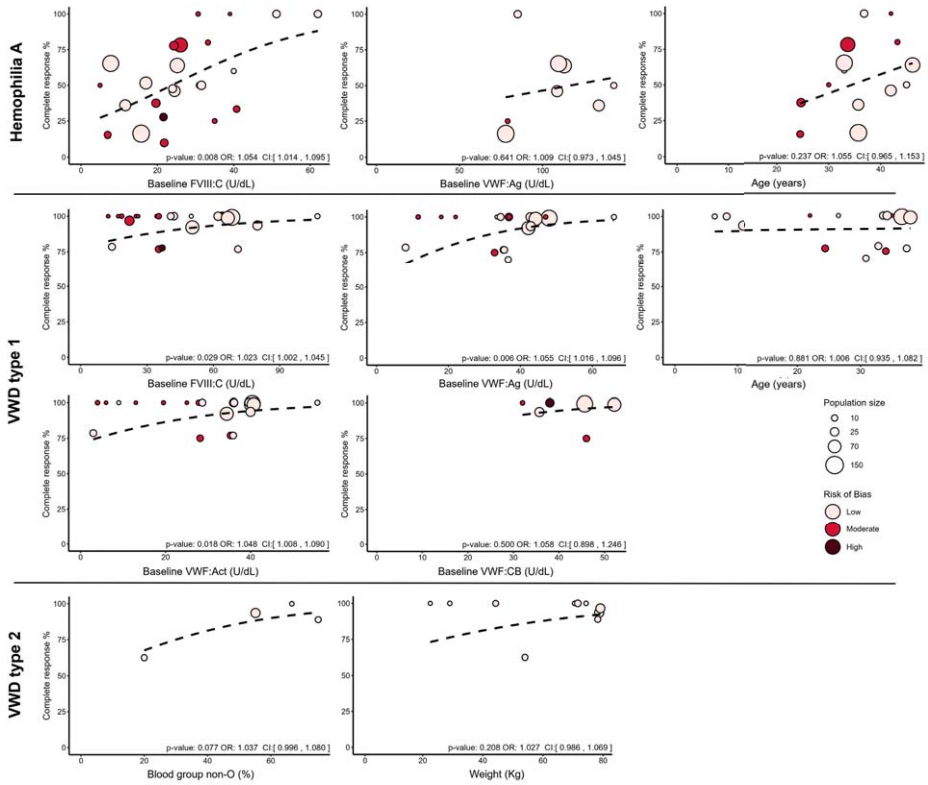

Figure 3. Baseline factor levels and other determinants affect DDAVP response. Complete response rate according to the study definition is plotted against possible determinants for DDAVP response per disease. Bubble size indicates the population size per study. Color indicates risk of bias of the study: low (light red), moderate (red) or high (dark red) risk of bias. The fitted values of the meta regression are indicated by the black dotted line. Odds ratio with Confidence interval and p-value) are shown in the lower right corner. Abbreviations: Odds ratio (OR), Confidence interval (CI).

For VWD data on 209 individuals with genetic information were collected; 136 VWD type 1 patients and 73 VWD type 2 patients. Of these patients, 189 had missense mutations, of which 172 were complete, 13 were partial and only four were non-responders. The majority of the response profiles originated from two studies (10,12). Altogether, 85 different *VWF* missense mutations were reported. To assess possible associations between protein structure and DDAVP response, peak VWF:Ag levels were plotted against amino acid position (Figure 4B).

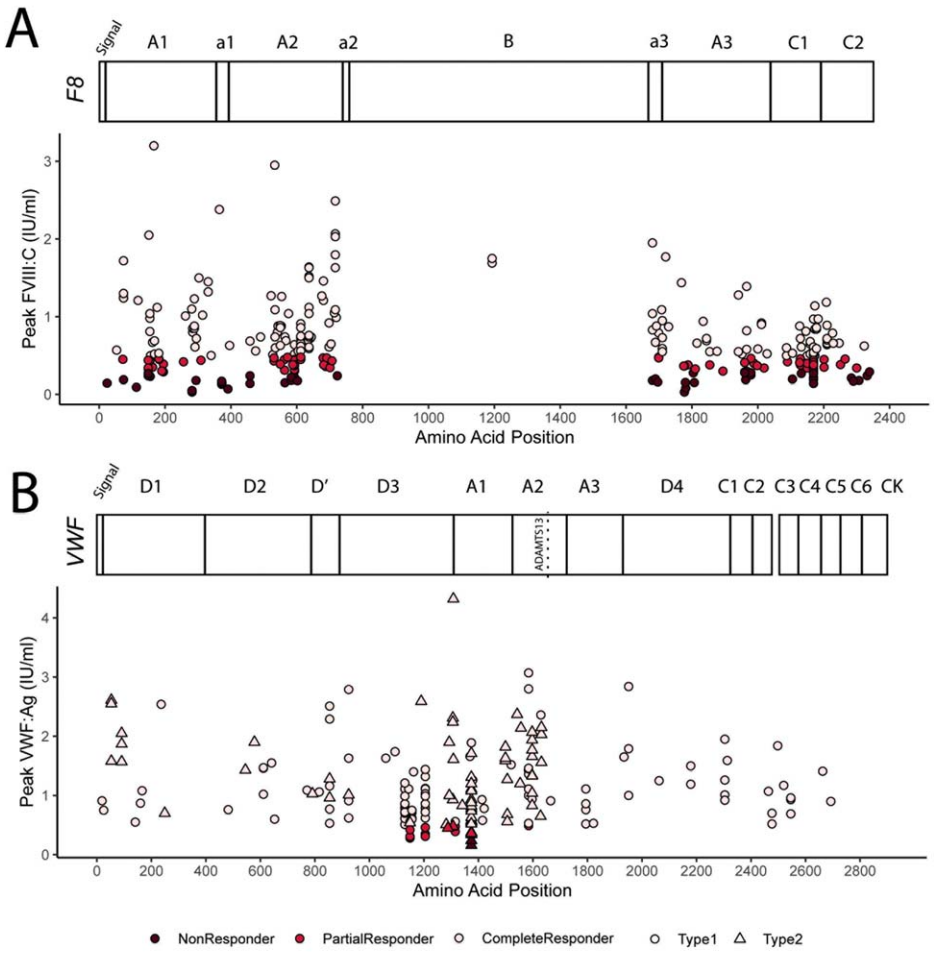

Figure 4: Mutation landscape of individual responses to DDAVP. Each dot represents a patient. Colors represent non (dark red), partial (red) and complete (light red) response. Missense mutation position relative to the protein sequence are plotted on the x-axis against response. A) Variants in HA; y-axis represents peak FVIII:C levels after DDAVP. B) Variants in VWD; y-axis represents peak VWF:Ag levels after DDAVP. Shape depicts VWD type 1 (circle) and type 2 (triangle). Protein domains and relevant annotations are plotted at the top of each graph. Abbreviations: Factor 8 (F8), von Willebrand factor (VWF).

Risk of bias sensitivity analysis

The sensitivity analysis with removal of high RoB studies from the meta-analysis showed that high RoB studies did not substantially influence the results of the meta-analysis on proportion of response. The total proportion of response remained 0·74. The proportion per subtype stayed the same except for a small change in mild & moderate

HA (0·45 to 0·48), PFD (0·81 to 0·79) and VWD type 2B (0·71 to 0·66). The results of the meta regression on the influence of determinants also did not change significantly. An overview of the slightly changed results after removing high RoB articles can be seen in Supplemental Table 4.

Discussion

Patients with bleeding disorders experience frequent bleeding which is often treated by administration of DDAVP. However, despite that DDAVP has long been used, there is still an unexplained large inter-individual heterogeneity in DDAVP response. It is still largely unknown which factors determine a complete DDAVP response. In this systematic review we aimed to identify factors that determine DDAVP response in bleeding disorders from the collective data available in the literature. Our meta-analysis, which was based on 81 out of 103 included articles and contained 1982 patients, found that subtype of disease is a strong determinant of response. Furthermore, we show higher baseline levels of FVIII:C significantly increase response rate in HA and that higher FVIII:C, VWF:Ag and VWF:Act baseline levels increase response rate in VWD type 1. Furthermore, although not significant, a trend is shown that higher age (per year) and weight (per Kg) correlates with better response in HA and VWD. Finally, comparison of mutations with response profiles revealed heterogeneous responses to DDAVP for patients carrying the same mutation. Remarkably, for both *F8* and *VWF* we observed that the same amino acid substitution could be present in complete, partial and non-responders and that in VWD only mutations in the D3 and A1 domain led to non/partial responders.

Our results indicate that disease subtype is an important determinant, which aligns with previous reports (10,22). It is important to note that there is a large discrepancy in VWF:Ag and VWF:Act response for patients with VWD type 2. Especially VWD type 2A and 2M show a strong increase in antigen levels after DDAVP administration, while activity levels only rise slightly, indicating low hemostatic efficacy as the secreted protein is dysfunctional. However, in many patients the activity level did rise above 50 U/dL which may be sufficient for milder bleeding episodes. It is therefore important to test DDAVP effectivity in these patients as well. In addition, we show that patients with VWD type 2B respond quite well to DDAVP. However, due to the risk of thrombocytopenia, DDAVP is contraindicated.

Specific mutations, which are tied to disease type, have also been shown to influence DDAVP response based on activity levels of VWF (10,12) and FVIII:C (7,14,16,21), even

showing that similar mutations lead to similar responses to DDAVP (19). It may be explained by comparable baseline levels of FVIII that is present among patients with the same *F8* mutation (114). Our data showed that missense mutations were present along the whole *VWF* sequence. It also revealed that all partial and non-responders had mutations in the D3, A1 and A2 domain (position 1149-1584). This region is nestled between the intra- and interchain disulfide bridges in D3 and the cleavage site of ADAMTS13 in A2. Interestingly, this section influences VWF multimer stability and includes the binding site for the platelet glycoprotein GP1bα, which is important for platelet plug formation (115). Notably, in both HA and VWD, we observed that mutations on the same location were associated with different responses to treatment. Recently, Guillet *et al.* analyzed a link between desmopressin response and *F8* genotype in hemophilia A patients (116). The authors proposed that mutations could be categorized in four groups of response effectiveness. Our analysis contains 5 similar mutations. Although those classified as group 1 and group 2 mutations seem to respond similarly, group 3 and 4 mutations, labeled as moderately and frequently ineffective (116), also showed complete and partial responders in our dataset. For a complete analysis, adjustments for other determinants should be performed in a multivariate model, but this was not possible in our analysis due to insufficient sample size. Furthermore, as a result of combining diverse groups of patients with the same mutations, we captured a more heterogeneous sample of other determinants that may outweigh the influence of mutations on DDAVP response. Taken together, our analyses suggests that *F8* and *VWF* mutations are not the main determinants of response, which precludes prediction of DDAVP response based on mutations alone.

Other determinants have been described in literature extensively. For instance, higher baseline factor levels have been associated with better response (11,14,17-19) which is confirmed by our meta-regression analysis in the case of FVIII:C in HA and FVIII:C, VWF:Ag and VWF:Act in VWD type 1. This observation may be explained by lower clearance of VWF, higher production rate or storage of VWF. Age was not found to be a significant determinant in our analysis. However, this has been shown previously in children (17-19), and adults (14). This finding was recently confirmed by Atiq *et al.* in low VWF and type 1 VWD patients (117) (not in systematic review). Our study shows no significant effect of blood group on response. Literature has shown a correlation between blood group and response in VWD type 1C Vicenza (13), while no effect was seen in patients with platelet normal VWD (23) and children with VWD type 1 (18). This could be explained by the inherent higher VWF baseline levels of patients with blood group non-O (118). Previously, route of administration has been tested, but no differences in response were observed (15,20). It has also been reported that onset of effect after DDAVP does not differ significantly between administration routes

(199,120). Unfortunately, in our study, administration route could not be analyzed due to insufficient data, although intravenous and subcutaneous administration seem to yield similar responses in HA. For the remaining determinant, weight, no effect was observed in our data and no effect has been described in the literature.

Our meta-analysis has some limitations. First, variation in the setting and route of administration of the DDAVP test might influence the response rate. Most studies reported DDAVP response measurements in steady state, but 21 studies reported measurements perioperatively or in the context of bleeding episodes. Second, none of the included articles excluded patients based on their DDAVP response. However, this does not exclude selection bias as some studies excluded patients with VWD type 3 or type 2B as these patients were expected to have a weak response or where DDAVP is considered contra-indicated. Third, the included studies ranged from 1980 to 2022. As such, the definitions of response as stated by the articles laboratory tests used are exceptionally heterogeneous. Definitions of response varied with respect to time to peak, if fold change was calculated, cut-off for complete response and whether activity or antigen was measured. Due to this heterogeneity, we could not pool the extracted data for our analysis. We therefore strongly recommend standardized definitions of response should be maintained and data should be made available for other definitions of response to be calculated. Fourth, we calculated response based on the rise of VWF:Ag and FVIII above 50 U/dL. Therefore, the "study definition" was not applicable on patients with baseline levels above 50 U/dL. This was the case in PFD, VWD type 2 and HA carriers which could have resulted in an overestimation of response rate. For VWD type 2 we therefore performed an additional analysis on VWF:Act response. Whereas for PFD and HA carriers an alternative definition of response should be used. Fifth, the potential misdiagnosis between severity types in HA and VWD due to variation in assays could influence the response rate calculated in this study. Finally, as we used aggregated data, we can only study the effect of determinants on the response rates between studies, but not assess the effect on individuals within a study. For future research we suggest performing studies using individual patient data.

Our study also has several strengths. First, to the best of our knowledge, this is the first meta-analysis to show the response rate of DDAVP in various bleeding disorders and identify determinants influence this response rate. Second, the high number of studies and disease types included, allowed us to analyze many different aspects of DDAVP response. Furthermore, the large patient numbers with VWD type 1 and HA allowed for accurate analysis in these subtypes. We were able to extract mutation data of 389 patients with HA and 209 patients with VWD. Finally, after sensitivity analysis we

determined that removal of high RoB articles did not significantly change the analysis outcome.

This study offers a comprehensive overview of DDAVP response proportions in various bleeding disorders and which determinants might play a role in DDAVP response. Especially coagulation factor base levels have been found as an important determinant for the response to DDAVP. These factors should be kept in mind when performing DDAVP tests. Our analysis, which indicates that the vast majority of patients with VWD type 1 (baseline VWF:Ag >30 U/dL) have a complete DDAVP response, lends support to the current guidelines regarding DDAVP testing in patients with VWD type 1 (121). Furthermore, the relative low proportion of response in mild and mild/moderate hemophilia A indicates that DDAVP response should be tested in those patients to ensure a sufficient response. This information can be used as a guide by clinicians treating patients with bleeding disorders. However, despite the strong relationship between DDAVP response with baseline factor levels and disease subtype, individual DDAVP tests may still be required in these heterogeneous bleeding disorders. Furthermore, heterogeneity in article definition precluded meta-analysis and therefore we strongly recommend the use of a clear and uniform definition of response in future studies. Finally, our detailed analysis on mutations and DDAVP response can be used in future studies into the biological mechanisms of DDAVP response.

Acknowledgements

The SYMPHONY consortium, which aims to orchestrate personalized treatment in patients with bleeding disorders, is a unique collaboration between patients, health care professionals, and translational and fundamental researchers specializing in inherited bleeding disorders, as well as experts from multiple disciplines (122). It aims to identify the best treatment choice for each individual based on bleeding phenotype. To achieve this goal, work packages (WP) have been organized according to three themes (e.g. Diagnostics [WPs three and four], Treatment [WPs 5-9], and Fundamental Research [WPs 10-12]). Principal investigator: M.H. Cnossen; project manager: S.H. Reitsma.

Beneficiaries of the SYMPHONY consortium: Erasmus University Medical Center-Sophia Children's Hospital, project leadership and coordination; Sanquin Diagnostics; Sanquin Research; Amsterdam University Medical Centers; University Medical Center Groningen; University Medical Center Utrecht; Leiden University Medical Center; Radboud University Medical Center; Netherlands Society of Hemophilia Patients

(NVHP); Netherlands Society for Thrombosis and Hemostasis (NVTH); Bayer B.V., CSL Behring B.V., Swedish Orphan Biovitrum (Belgium) BVBA/SPRL.

We would like to thank J. Schoones from the Walaeus library for his assistance in the set-up of the search strategy.

All collected data is made available as a supplementary file.

Authorship Contributions

SNJL, JdCA and IvM performed article selection, screening and data extraction. SNJL, JdCA and IvM analyzed data; SNJL, JdCA and IvM wrote the manuscript; all authors participated in the design of the research, revised the manuscript and approved the final manuscript.

Conflict of interest disclosures

SNJL, JdCA, IvM, RB and JE, KF received research funding from SYMPHONY: NWO-NWA.1160.18.038. Funding had no role in the writing or decision making of this manuscript.

References

1. Sadler JE, Mannucci PM, Berntorp E, et al. Impact, diagnosis and treatment of von Willebrand disease. *Thromb Haemost*. 2000;84(2):160-174.
2. Leebeek FWG, Eikenboom JCJ. Von Willebrand's Disease. *New England Journal of Medicine*. 2016;375(21):2067-2080.
3. Nogami K, Shima M, Nishiya K, et al. A novel mechanism of factor VIII protection by von Willebrand factor from activated protein C–catalyzed inactivation. *Blood*. 2002;99(11):3993-3998.
4. Lenting PJ, van Mourik JA, Mertens K. The life cycle of coagulation factor VIII in view of its structure and function. *Blood*. 1998;92(11):3983-3996.
5. van Galen KPM, Mauser-Bunschoten EP, Leebeek FWG. Hemophilic arthropathy in patients with von Willebrand disease. *Blood Reviews*. 2012;26(6):261-266.
6. Mannucci. Desmopressin (DDAVP) in the treatment of bleeding disorders: the first twenty years. *Haemophilia*. 2000;6(s1):60-67.
7. Castaman G, Mancuso ME, Giacomelli SH, et al. Molecular and phenotypic determinants of the response to desmopressin in adult patients with mild hemophilia A. *J Thromb Haemost*. 2009;7(11):1824-1831.
8. BOREL-DERLON A, FEDERICI AB, ROUSSEL-ROBERT V, et al. Treatment of severe von Willebrand disease with a high-purity von Willebrand factor concentrate (Wilfactin®): a prospective study of 50 patients. *Journal of Thrombosis and Haemostasis*. 2007;5(6):1115-1124.
9. Leissinger C, Carcao M, Gill JC, Journeycake J, Singleton T, Valentino L. Desmopressin (DDAVP) in the management of patients with congenital bleeding disorders. *Haemophilia*. 2014;20(2):158-167.
10. Atiq F, Heijdra JM, Snijders F, et al. Desmopressin response depends on the presence and type of genetic variants in patients with type 1 and type 2 von Willebrand disease. *Blood Adv*. 2022.
11. Biguzzi E, Siboni SM, Peyvandi F. Acquired Von Willebrand syndrome and response to desmopressin. *Haemophilia*. 2018;24(1):e25-e28.
12. Castaman G, Lethagen S, Federici AB, et al. Response to desmopressin is influenced by the genotype and phenotype in type 1 von Willebrand disease (VWD): results from the European Study MCMDM-1VWD. *Blood*. 2008;111(7):3531-3539.
13. Castaman G, Tosetto A, Eikenboom JC, Rodeghiero F. Blood group significantly influences von Willebrand factor increase and half-life after desmopressin in von Willebrand disease Vicenza. *J Thromb Haemost*. 2010;8(9):2078-2080.
14. Di Perna C, Riccardi F, Franchini M, Rivolta GF, Pattacini C, Tagliaferri A. Clinical efficacy and determinants of response to treatment with desmopressin in mild hemophilia a. *Semin Thromb Hemost*. 2013;39(7):732-739.
15. Lethagen S, Egervall K, Berntorp E, Bengtsson B. The administration of desmopressin by nasal spray: a dose-determination study in patients with mild haemophilia A or von Willebrand's disease. *Haemophilia*. 1995;1(2):97-102.
16. Nance D, Fletcher SN, Bolgiano DC, Thompson AR, Josephson NC, Konkle BA. Factor VIII mutation and desmopressin-responsiveness in 62 patients with mild haemophilia A. *Haemophilia*. 2013;19(5):720-726.

17. Revel-Vilk S, Blanchette VS, Sparling C, Stain AM, Carcao MD. DDAVP challenge tests in boys with mild/moderate haemophilia A. *Br J Haematol*. 2002;117(4):947-951.
18. Revel-Vilk S, Schmugge M, Carcao MD, Blanchette P, Rand ML, Blanchette VS. Desmopressin (DDAVP) responsiveness in children with von Willebrand disease. *J Pediatr Hematol Oncol*. 2003;25(11):874-879.
19. Seary ME, Feldman D, Carcao MD. DDAVP responsiveness in children with mild or moderate haemophilia A correlates with age, endogenous FVIII:C level and with haemophilic genotype. *Haemophilia*. 2012;18(1):50-55.
20. Sharthkumar A, Greist A, Di Paola J, et al. Biologic response to subcutaneous and intranasal therapy with desmopressin in a large Amish kindred with Type 2M von Willebrand disease. *Haemophilia*. 2008;14(3):539-548.
21. Stoof SC, Sanders YV, Petrij F, et al. Response to desmopressin is strongly dependent on F8 gene mutation type in mild and moderate haemophilia A. *Thromb Haemost*. 2013;109(3):440-449.
22. Loomans JI, Kruip M, Carcao M, et al. Desmopressin in moderate hemophilia A patients: a treatment worth considering. *Haematologica*. 2018;103(3):550-557.
23. Castaman G, Rodeghiero F. No influence of blood group on the responsiveness to desmopressin in type I "platelet normal" von Willebrand's disease. *Thromb Haemost*. 1995;73(3):551-552.
24. Covidence. Veritas Health Innovation; 2023.
25. James PD, Connell NT, Ameer B, et al. ASH ISTH NHF WFH 2021 guidelines on the diagnosis of von Willebrand disease. *Blood Adv*. 2021;5(1):280-300.
26. Dewald DL, Briggs B, Smith RE. Intranasal administration of desmopressin acetate (DDAVP) to hemophiliacs. *Thromb Res*. 1980;18(5):617-622.
27. Ockelford PA, Menon NC, Berry EW. Clinical experience with arginine vasopressin (DDAVP) in von Willebrand's disease and mild haemophilia. *N Z Med J*. 1980;92(672):375-378.
28. Korninger C, Niessner H, Lechner K. Impaired fibrinolytic response to DDAVP and venous occlusion in a sub-group of patients with von Willebrand's disease. *Thromb Res*. 1981;23(4-5):365-374.
29. Sweeney JD, Crosby P, McCann SR, Temperley IJ. Clinical experience with deamino-8-D-AGR-Vasopressin (DDAVP) in patients with Factor VIII deficiency. *Ir J Med Sci*. 1981;150(8):236-239.
30. Takahashi H. Studies on the pathophysiology and treatment of von Willebrand's disease. V. Properties of factor VIII after DDAVP infusion in variant von Willebrand's disease. *Thromb Res*. 1981;21(4-5):357-365.
31. Holmberg L, Nilsson IM, Borge L, Gunnarsson M, Sjörin E. Platelet aggregation induced by 1-desamino-8-D-arginine vasopressin (DDAVP) in Type IIB von Willebrand's disease. *N Engl J Med*. 1983;309(14):816-821.
32. Kobrinsky NL, Watson CM, Cheang MS, Bishop AJ. Improved hemophilia A carrier detection by DDAVP stimulation of factor VIII. *J Pediatr*. 1984;104(5):718-724.
33. Mariana G, Ciavarella N, Mazzucconi MG, et al. Evaluation of the effectiveness of DDAVP in surgery and in bleeding episodes in haemophilia and von Willebrand's disease. A study on 43 patients. *Clin Lab Haematol*. 1984;6(3):229-238.
34. Sakariassen KS, Cattaneo M, vd Berg A, Ruggeri ZM, Mannucci PM, Sixma JJ. DDAVP enhances platelet adherence and platelet aggregate growth on human artery subendothelium. *Blood*. 1984;64(1):229-236.

35. de la Fuente B, Kasper CK, Rickles FR, Hoyer LW. Response of patients with mild and moderate hemophilia A and von Willebrand's disease to treatment with desmopressin. *Ann Intern Med*. 1985;103(1):6-14.
36. Vincente V, Alberca I, Gonzalez R, Lopez Borrasca A. DDAVP in a non-haemophiliac patient with an acquired factor VIII inhibitor. *Br J Haematol*. 1985;60(3):585-586.
37. Gralnick HR, Williams SB, McKeown LP, et al. DDAVP in type IIa von Willebrand's disease. *Blood*. 1986;67(2):465-468.
38. Greer IA, McLaren M, Belch JJ, Lowe GD, Forbes CD. Endothelial stimulation by DDAVP in von Willebrand's disease and haemophilia. *Haemostasis*. 1986;16(1):15-19.
39. Marti GE, Rick ME, Sidbury J, Gralnick HR. DDAVP infusion in five patients with type Ia glycogen storage disease and associated correction of prolonged bleeding times. *Blood*. 1986;68(1):180-184.
40. Kentro TB, Lottenberg R, Kitchens CS. Clinical efficacy of desmopressin acetate for hemostatic control in patients with primary platelet disorders undergoing surgery. *Am J Hematol*. 1987;24(2):215-219.
41. Prince S. An alternative to blood product therapy for dental extractions in the mild to moderate haemophiliac patient. *Br Dent J*. 1987;162(7):256-257.
42. Cuthbert RJ, Watson HH, Handa SI, Abbott I, Ludlam CA. DDAVP shortens the bleeding time in Bernard-Soulier syndrome. *Thromb Res*. 1988;49(6):649-650.
43. Ghirardini A, Chistolini A, Tirindelli MC, et al. Clinical evaluation of subcutaneously administered DDAVP. *Thromb Res*. 1988;49(3):363-372.
44. Kim HC, Salva K, Fallot PL, et al. Patients with prolonged bleeding time of undefined etiology, and their response to desmopressin. *Thromb Haemost*. 1988;59(2):221-224.
45. Mannucci PM, Lombardi R, Castaman G, et al. von Willebrand disease "Vicenza" with larger-than-normal (supranormal) von Willebrand factor multimers. *Blood*. 1988;71(1):65-70.
46. Rodeghiero F, Castaman G, Di Bona E, Ruggeri M, Lombardi R, Mannucci PM. Hyper-responsiveness to DDAVP for patients with type I von Willebrand's disease and normal intra-platelet von Willebrand factor. *Eur J Haematol*. 1988;40(2):163-167.
47. Royer JE, Bates WS. Management of von Willebrand's disease with desmopressin. *J Oral Maxillofac Surg*. 1988;46(4):313-314.
48. Williamson R, Eggleston DJ. DDAVP and EACA used for minor oral surgery in von Willebrand disease. *Aust Dent J*. 1988;33(1):32-36.
49. Castaman G, Rodeghiero F, Di Bona E, Ruggeri M. Clinical effectiveness of desmopressin in a case of acquired von Willebrand's syndrome associated with benign monoclonal gammopathy. *Blut*. 1989;58(4):211-213.
50. Fowler WE, Berkowitz LR, Roberts HR. DDAVP for type IIB von Willebrand disease. *Blood*. 1989;74(5):1859-1860.
51. Köhler M, Hellstern P, Tarrach H, Bambauer R, Wenzel E, Jutzler GA. Subcutaneous injection of desmopressin (DDAVP): evaluation of a new, more concentrated preparation. *Haemostasis*. 1989;19(1):38-44.
52. Rodeghiero F, Castaman G, Di Bona E, Ruggeri M. Consistency of responses to repeated DDAVP infusions in patients with von Willebrand's disease and hemophilia A. *Blood*. 1989;74(6):1997-2000.
53. Thomas N, O'Callaghan U, Lowe GD, et al. Response to desmopressin in type IID von Willebrand's disease. *Clin Lab Haematol*. 1989;11(3):189-197.

54. Wijermans PW, van Dorp DB. Hermansky-Pudlak syndrome: correction of bleeding time by 1-desamino-8D-arginine vasopressin. *Am J Hematol.* 1989;30(3):154-157.
55. Baldree LA, Ault BH, Chesney CM, Stapleton FB. Intravenous desmopressin acetate in children with sickle trait and persistent macroscopic hematuria. *Pediatrics*. 1990;86(2):238-243.
56. Casonato A, Fabris F, Girolami A. Platelet aggregation and pseudothrombocytopenia induced by 1-desamino-8-D-arginine vasopressin (DDAVP) in type IIB von Willebrand's disease patient. *Eur J Haematol*. 1990;45(1):36-42.
57. Casonato A, Sartori MT, de Marco L, Girolami A. 1-Desamino-8-D-arginine vasopressin (DDAVP) infusion in type IIB von Willebrand's disease: shortening of bleeding time and induction of a variable pseudothrombocytopenia. *Thromb Haemost*. 1990;64(1):117-120.
58. Quitt M, Froom P, Veisler A, Falber V, Sova J, Aghai E. The effect of desmopressin on massive gastrointestinal bleeding in hereditary telangiectasia unresponsive to treatment with cryoprecipitate. *Arch Intern Med.* 1990;150(8):1744-1746.
59. Van Dorp DB, Wijermans PW, Meire F, Vrensen G. The Hermansky-Pudlak syndrome. Variable reaction to 1-desamino-8D-arginine vasopressin for correction of the bleeding time. *Ophthalmic Paediatr Genet*. 1990;11(3):237-244.
60. Casonato A, Sartori MT, Pontara E, Bertomoro A, Dannhäuser D, Girolami. Discrepant increase in factor VIII: C and von Willebrand factor after DDAVP infusion in a patient with variant von Willebrand's disease. *Blood Coagul Fibrinolysis*. 1991;2(4):567-573.
61. Lopez-Fernandez MF, Gonzalez-Boullosa R, Blanco-Lopez MJ, Perez M, Batlle J. Abnormal proteolytic degradation of von Willebrand factor after desmopressin infusion in a new subtype of von Willebrand disease (ID). *Am J Hematol.* 1991;36(3):163-170.
62. Waldenström E, Holmberg L, Axelsson U, Winqvist I, Nilsson IM. Bernard-Soulier syndrome in two Swedish families: effect of DDAVP on bleeding time. *Eur J Haematol.* 1991;46(3):182-187.
63. Castaman G, Rodeghiero F. Failure of DDAVP to shorten the prolonged bleeding time of two patients with congenital afibrinogenemia. *Thromb Res*. 1992;68(3):309-315.
64. Lethagen S, Nilsson IM. DDAVP-induced enhancement of platelet retention: its dependence on platelet-von Willebrand factor and the platelet receptor GP IIb/IIIa. *Eur J Haematol*. 1992;49(1):7-13.
65. Mannucci PM, Bettega D, Cattaneo M. Patterns of development of tachyphylaxis in patients with haemophilia and von Willebrand disease after repeated doses of desmopressin (DDAVP). *Br J Haematol.* 1992;82(1):87-93.
66. Patrassi GM, Sartori MT, Casonato A, et al. Urokinase-type plasminogen activator release after DDAVP in von Willebrand disease: different behaviour of plasminogen activators according to the synthesis of von Willebrand factor. *Thromb Res*. 1992;66(5):517-526.
67. Sultan Y, Loyer F, Venot A. Impaired fibrinolytic response to DDAVP in patients with von Willebrand's disease. *Nouv Rev Fr Hematol.* 1992;34(1):55-60.
68. Castaman G, Rodeghiero F. Consistency of responses to separate desmopressin infusions in patients with storage pool disease and isolated prolonged bleeding time. *Thromb Res*. 1993;69(4):407-412.
69. Castaman G, Rodeghiero F, Lattuada A, Mannucci PM. Desmopressin-induced thrombocytopenia in type I platelet discordant von Willebrand disease. *Am J Hematol*. 1993;43(1):5-9.

70. Greinacher A, Pötzsch B, Kiefel V, White JG, Müller-Berghaus G, Mueller-Eckhardt C. Evidence that DDAVP transiently improves hemostasis in Bernard-Soulier syndrome independent of von Willebrand-factor. *Ann Hematol.* 1993;67(3):149-150.
71. Kemahli S, Canatan D, Uysal Z, Akar N, Cin S, Arcasoy A. DDAVP shortens bleeding time in Bernard-Soulier syndrome. *Thromb Haemost*. 1994;71(5):675.
72. Mazurier C, Gaucher C, Jorieux S, Goudemand M. Biological effect of desmopressin in eight patients with type 2N ('Normandy') von Willebrand disease. Collaborative Group. *Br J Haematol.* 1994;88(4):849-854.
73. Castaman G, Eikenboom JC, Rodeghiero F, Briët E, Reitsma PH. A novel candidate mutation (Arg611-->His) in type I 'platelet discordant' von Willebrand's disease with desmopressin-induced thrombocytopenia. *Br J Haematol.* 1995;89(3):656-658.
74. Castaman G, Lattuada A, Mannucci PM, Rodeghiero F. Factor VIII:C increases after desmopressin in a subgroup of patients with autosomal recessive severe von Willebrand disease. *Br J Haematol.* 1995;89(1):147-151.
75. Castaman G, Ruggeri M, Rodeghiero F. Clinical usefulness of desmopressin for prevention of surgical bleeding in patients with symptomatic heterozygous factor XI deficiency. *Br J Haematol.* 1996;94(1):168-170.
76. McKeown LP, Connaghan G, Wilson O, Hansmann K, Merryman P, Gralnick HR. 1-Desamino-8-arginine-vasopressin corrects the hemostatic defects in type 2B von Willebrand's disease. *Am J Hematol.* 1996;51(2):158-163.
77. Lozano M, Escolar G, Bellucci S, et al. 1-Deamino (8-D-arginine) vasopressin infusion partially corrects platelet deposition on subendothelium in Bernard-Soulier syndrome: the role of factor VIII. *Platelets*. 1999;10(2-3):141-145.
78. Mauz-Körholz C, Budde U, Körholz D, Göbel U. DDAVP treatment in a child with von Willebrand disease type 2M. *Eur J Pediatr.* 1999;158 Suppl 3:S174-176.
79. Franchini M, de Gironcoli M, Lippi G, Manzato F, Aprili G, Gandini G. Prophylactic use of desmopressin in surgery of six patients with symptomatic heterozygous factor XI deficiency. *Haematologica.* 2000;85(1):106-107.
80. Kavakli K, Aydinok Y, Karapinar D, Balkan C. DDAVP treatment in children with haemophilia B. *Br J Haematol.* 2001;114(3):733-734.
81. Kavakli K, Hüseyinov A, Coker I, Aydinok Y, Nisli G. Intraleucocyte platelet-activating factor levels in desmopressin-treated patients with haemophilia A and von Willebrand disease. *Haemophilia.* 2001;7(5):482-489.
82. Franchini M, Gandini G, Manzato F, Lippi G. Evaluation of the PFA-100 system for monitoring desmopressin therapy in patients with type 1 von Willebrand's disease. *Haematologica*. 2002;87(6):670.
83. Jimenez-Yuste V, Prim MP, De Diego JI, et al. Otolaryngologic surgery in children with von Willebrand disease. *Archives of otolaryngology: head and neck surgery.* 2002;128(12):1365-1368.
84. Michiels JJ, van de Velde A, van Vliet HH, van der Planken M, Schroyens W, Berneman Z. Response of von Willebrand factor parameters to desmopressin in patients with type 1 and type 2 congenital von Willebrand disease: diagnostic and therapeutic implications. *Semin Thromb Hemost*. 2002;28(2):111-132.
85. Brown SA, Eldridge A, Collins PW, Bowen DJ. Increased clearance of von Willebrand factor antigen post-DDAVP in Type 1 von Willebrand disease: is it a potential pathogenic process? *J Thromb Haemost*. 2003;1(8):1714-1717.

86. Fuse I, Higuchi W, Mito M, Aizawa Y. DDAVP normalized the bleeding time in patients with congenital platelet TxA2 receptor abnormality. *Transfusion*. 2003;43(5):563-567.
87. Reiter RA, Knöbl P, Varadi K, Turecek PL. Changes in von Willebrand factor-cleaving protease (ADAMTS13) activity after infusion of desmopressin. *Blood*. 2003;101(3):946-948.
88. Federici AB, Mazurier C, Berntorp E, et al. Biologic response to desmopressin in patients with severe type 1 and type 2 von Willebrand disease: results of a multicenter European study. *Blood*. 2004;103(6):2032-2038.
89. Cordova A, Barrios NJ, Ortiz I, Rivera E, Cadilla C, Santiago-Borrero PJ. Poor response to desmopressin acetate (DDAVP) in children with Hermansky-Pudlak syndrome. *Pediatr Blood Cancer*. 2005;44(1):51-54.
90. Lombardo VT, Sottilotta G. Recombinant activated factor VII combined with desmopressin in preventing bleeding from dental extraction in a patient with Glanzmann's thrombasthenia. *Clin Appl Thromb Hemost*. 2006;12(1):115-116.
91. Giannini S, Mezzasoma AM, Leone M, Gresele P. Laboratory diagnosis and monitoring of desmopressin treatment of von Willebrand's disease by flow cytometry. *Haematologica*. 2007;92(12):1647-1654.
92. Guglielmone H, Minoldo S, Jarchum G. Response to the DDAVP test in a patient with combined deficiency of factor V and factor VIII. *Haemophilia*. 2009;15(3):838-839.
93. Shortt J, Opat SS, Gorniak MB, Aumann HA, Collecutt MF, Street AM. A retrospective study of the utility of desmopressin (1-deamino-8-D-arginine vasopressin) trials in the management of patients with von Willebrand disorder. *Int J Lab Hematol*. 2010;32(1 Pt 1):e181-183.
94. Knöfler R, Koscielny J, Tauer JT, et al. Desmopressin testing in haemophilia A patients and carriers: results of a multi centre survey. *Hamostaseologie*. 2012;32(4):271-275.
95. Santoro C, Hsu F, Dimichele DM. Haemostasis prophylaxis using single dose desmopressin acetate and extended use epsilon aminocaproic acid for adenotonsillectomy in patients with type 1 von Willebrand disease. *Haemophilia*. 2012;18(2):200-204.
96. Akin M. Response to low-dose desmopressin by a subcutaneous route in children with type 1 von Willebrand disease. *Hematology*. 2013;18(2):115-118.
97. Siew DA, Mangel J, Laudenbach L, Schembri S, Minuk L. Desmopressin responsiveness at a capped dose of 15 µg in type 1 von Willebrand disease and mild hemophilia A. *Blood Coagul Fibrinolysis*. 2014;25(8):820-823.
98. Stoof SC, Sanders YV, Cnossen MH, de Maat MP, Leebeek FW, Kruip MJ. Desmopressin response in hemophilia A patients with FVIII:C < 0.10 IU mL(-1.). *J Thromb Haemost*. 2014;12(1):110-112.
99. Archer NM, Samnaliev M, Grace R, Brugnara C. The utility of the DDAVP challenge test in children with low von Willebrand factor. *Br J Haematol*. 2015;170(6):884-886.
100. Arshad F, Stoof SC, Leebeek FW, et al. Infusion of DDAVP does not improve primary hemostasis in patients with cirrhosis. *Liver Int*. 2015;35(7):1809-1815.
101. Mansouritorghabeh H, Shirdel A. Desmopressin acetate as a haemostatic elevator in individuals with combined deficiency of factors V and VIII: a clinical trial. *J Thromb Haemost*. 2016;14(2):336-339.
102. Mason JA, Robertson JD, McCosker J, Williams BA, Brown SA. Assessment and validation of a defined fluid restriction protocol in the use of subcutaneous desmopressin for children with inherited bleeding disorders. *Haemophilia*. 2016;22(5):700-705.

103. Takeyama M, Nogami K, Onaka M, Yada K, Shida Y, Shima M. The utility of VWF multimer analysis in response to the desmopressin administration for the diagnosis of severe type 1 von Willebrand disease. *Haemophilia*. 2016;22(2):e106-e108.
104. Sánchez-Luceros A, Woods AI, Bermejo E, et al. PT-VWD posing diagnostic and therapeutic challenges - small case series. *Platelets*. 2017;28(5):484-490.
105. Stoof SCM, Schütte LM, Leebeek FWG, Cnossen MH, Kruip M. Desmopressin in haemophilia: The need for a standardised clinical response and individualised test regimen. *Haemophilia*. 2017;23(6):861-867.
106. Candy V, Whitworth H, Grabell J, et al. A decreased and less sustained desmopressin response in hemophilia A carriers contributes to bleeding. *Blood Adv*. 2018;2(20):2629-2636.
107. Hews-Girard J, Rydz N, Lee A, Goodyear MD, Poon MC. Desmopressin in non-severe haemophilia A: Test-response and clinical outcomes in a single Canadian centre review. *Haemophilia*. 2018;24(5):720-725.
108. Okoye HC, Nielsen BI, Lee K, Abajas YL, Key NS, Rollins-Raval MA. DDAVP trial in discrepant non-severe haemophilia A patients. *Haemophilia*. 2018;24(3):e152-e154.
109. Polzella P, Coutts K, Bignell P, Curry N. Unexpectedly high response to DDAVP in two patients with moderate haemophilia A. *Haemophilia*. 2018;24(4):e292-e294.
110. Schütte LM, van Hest RM, Stoof SCM, et al. Pharmacokinetic Modelling to Predict FVIII:C Response to Desmopressin and Its Reproducibility in Nonsevere Haemophilia A Patients. *Thromb Haemost*. 2018;118(4):621-629.
111. Atiq F, Schütte LM, Looijen AEM, et al. von Willebrand factor and factor VIII levels after desmopressin are associated with bleeding phenotype in type 1 VWD. *Blood Adv*. 2019;3(24):4147-4154.
112. Guddati AK, Rosovsky RP, Van Cott EM, Kuter DJ. Quantitative analysis of desmopressin (DDAVP) response in adult patients with type 1 von Willebrand disease. *Int J Lab Hematol*. 2019;41(3):325-330.
113. de Jager NCB, Heijdra JM, Kieboom Q, et al. Population Pharmacokinetic Modeling of von Willebrand Factor Activity in von Willebrand Disease Patients after Desmopressin Administration. *Thromb Haemost*. 2020;120(10):1407-1416.
114. Loomans JI, van Velzen AS, Eckhardt CL, et al. Variation in baseline factor VIII concentration in a retrospective cohort of mild/moderate hemophilia A patients carrying identical F8 mutations. *J Thromb Haemost*. 2017;15(2):246-254.
115. Bonazza K, Iacob RE, Hudson NE, et al. Von Willebrand factor A1 domain stability and affinity for GPIbα are differentially regulated by its O-glycosylated N- and C-linker. *Elife*. 2022;11.
116. Guillet B, Pawlowski M, Boisseau P, et al. Genotype-Dependent Response to Desmopressin in Hemophilia A and Proposal of a Predictive Response Score. *Thromb Haemost*. 2024.
117. Atiq F, Blok R, van Kwawegen CB, et al. Type 1 VWD classification revisited: novel insights from combined analysis of the LoVIC and WiN studies. *Blood*. 2024;143(14):1414-1424.
118. Gill JC, Endres-Brooks J, Bauer PJ, Marks WJ, Jr., Montgomery RR. The effect of ABO blood group on the diagnosis of von Willebrand disease. *Blood*. 1987;69(6):1691-1695.
119. De Sio L, Mariani G, Muzzucconi MG, Chistolini A, Tirindelli MC, Mandelli F. Comparison between subcutaneous and intravenous DDAVP in mild and moderate hemophilia A. *Thromb Haemost*. 1985;54(2):387-389.
120. Mannucci PM, Vicente V, Alberca I, et al. Intravenous and subcutaneous administration of desmopressin (DDAVP) to hemophiliacs: pharmacokinetics and factor VIII responses. *Thromb Haemost*. 1987;58(4):1037-1039.

121. Connell NT, Flood VH, Brignardello-Petersen R, et al. ASH ISTH NHF WFH 2021 guidelines on the management of von Willebrand disease. *Blood Advances*. 2021;5(1):301-325.
122. Cnossen MH, van Moort I, Reitsma SH, et al. SYMPHONY consortium: Orchestrating personalized treatment for patients with bleeding disorders. *J Thromb Haemost*. 2022;20(9):2001-2011.

Supplementary Methods

Risk of Bias

Risk of bias was assessed using an adjusted Quality in Prognostic Studies (QUIPS) (1) checklist (see Supplemental File 2 for the edited QUIPS checklist). Each article was evaluated by two reviewers and disagreements were resolved by consensus. In short, questions per domain were weighted based on relevance. A cut-off to decide whether a domain is low, moderate or high risk of bias is reported in the adjusted quips checklist. A DDAVP test is completed a few hours after administration and most studies gathered the data retrospectively. Therefore, the study attrition domain was removed from the checklist as these questions were not applicable for this review. Furthermore, sub question b and c were removed from domain Statistical analysis and reporting. These were removed as data from each study were collected and not values as calculated by statistical analysis. A study was considered as low overall risk of bias when all domain scores were rated as low or if one domain was scored moderate. We scored a study as having high overall risk of bias if two or more of the domains were judged as high. A study was scored as moderate if the criteria for 'low' or 'high' were not met.

Statistical analysis

Logistic random-effects models were applied to pool proportions of complete responders to DDAVP both pooled and separately by disease type according to the "study definition". Heterogeneity between studies was assessed by calculating I^2 and Tau^2 and by calculating a prediction interval for new studies. Forest plots were generated to show the variation between studies. Studies that could not be combined due to lack of sufficient data were assessed qualitatively. Median response in VWF levels over time in the quantitative sense (on antigen level) or in a qualitative sense (on activity level) were reported. The association between the different determinants and the response rate was assessed by performing meta-regressions; bubble plots were generated to visualize the association. As sensitivity analysis, the analyses were repeated using only low or moderate risk of bias studies. All analyses were performed using R (version 4·2·3) (2) with the packages meta (version 7·0-0), to pool the proportions and metareg to perform meta regression. The package forestplot (version 4·2·3) was used to make forest plots and ggplot2 (version 3·4·4) to make bubble plots. P-values < 0·05 were considered statistically significant.

1. Evaluation of the Quality of Prognosis Studies in Systematic Reviews. Annals of Internal Medicine. 2006;144(6):427-437.
2. R development Core Team. R: A language and environment for statistical computing: R foundation for statistical computing; 2024.

Supplemental Table 3: Odds ratio of response per determinant from meta-regression.

	VWD type 1			VWD type 2			Hemophilia A			PFD		
Determinant	**OR**	**95%CI**		**OR**	**95% CI**		**OR**	**95%CI**		**OR**	**95%CI**	
Age (years)	1,006	0,935	1,082	1,006	0,951	1,064	1,055	0,965	1,153	0,953	0,834	1,089
Blood group non-O vs O	0,997	0,941	1,057	1,037	0,996	1,080	0,972	0,920	1,028	x	x	x
Female (%)	1,003	0,976	1,030	x	x	x	1,024	1,007	1,040	0,996	0,963	1,030
Before DDAVP APTT (s)	0,995	0,938	1,056	x	x	x	1,010	0,706	1,446	1,025	0,801	1,312
Bleeding time (min)	0,917	0,759	1,109	0,946	0,822	1,090	x	x	x	0,987	0,785	1,242
FVIII:Ag (U/dL)	x	x	x	x	x	x	x	x	x	x	x	x
FVIII:C (U/dL)	1,023	1,002	1,045	x	x	x	1,054	1,014	1,095	0,996	0,944	1,050
Platelet count	0,998	0,946	1,052	1,001	0,982	1,020	x	x	x	1,000	0,998	1,001
VWF:Ag (U/dL)	1,055	1,016	1,075	x	x	x	1,009	0,973	1,045	0,996	0,956	1,038
VWF:CB (U/dL)	1,058	0,898	1,246	0,999	0,976	1,021	0,986	0,940	1,035	x	x	x
VWF:pp (U/dL)	x	x	x	x	x	x	x	x	x	x	x	x
VWF:Act (U/dL)	1,048	1,008	1,090	x	x	x	0,991	0,951	1,032	1,009	0,973	1,046
Bodyweight (kg)	1,044	0,974	1,119	1,033	0,982	1,086	1,120	0,983	1,276	x	x	x

X indicates determinants for which the meta-regression could not be performed. Abbreviations: VWD, von Willebrand disease; OR, Odds ratio; CI, Confidence interval; DDAVP, 1-deamino-8-D-arginine vasopressin; APTT, Activated partial thromboplastin time; Ag, Antigen; CB, Collagen binding; pp, Propeptide; Act, Activity.

Supplemental Table 4. Sensitivity analysis on Odds ratio of response per determinant

	VWD type 1			VWD type 2			Hemophilia A			PFD		
Determinant	**OR**	**95%CI**		**OR**	**95% CI**		**OR**	**95%CI**		**OR**	**95%CI**	
Age (years)	1,006	0,935	1,082	1,006	0,951	1,064	1,055	0,965	1,153	0,929	0,787	1,096
Blood group non-O vs O	0,997	0,941	1,057	1,037	0,996	1,080	0,972	0,920	1,028	x	x	x
Female (%)	1,003	0,976	1,030	x	x	x	1,024	1,007	1,040	0,996	0,962	1,031
Before DDAVP APTT (s)	0,995	0,938	1,056	x	x	x	1,010	0,706	1,446	1,000	0,774	1,292
Bleeding time (min)	0,917	0,759	1,109	0,927	0,777	1,106	x	x	x	1,125	0,592	2,141
FVIII:Ag (U/dL)	x	x	x	x	x	x	x	x	x	x	x	x
FVIII:C (U/dL)	1,021	1,000	1,043	x	x	x	1,053	1,013	1,095	0,997	0,945	1,051
Platelet count	0,998	0,946	1,052	1,004	0,983	1,024	x	x	x	1,000	0,998	1,001
VWF:Ag (U/dL)	1,054	1,014	1,095	x	x	x	1,009	0,973	1,045	0,992	0,942	1,045
VWF:CB (U/dL)	1,077	0,904	1,283	0,999	0,976	1,021	0,986	0,940	1,035	x	x	x
VWF:pp (U/dL)	x	x	x	x	x	x	x	x	x	x	x	x
VWF:Act (U/dL)	1,047	1,007	1,088	x	x	x	0,991	0,951	1,032	1,009	0,973	1,046
Bodyweight (kg)	1,044	0,974	1,119	1,033	0,982	1,086	1,120	0,983	1,276	x	x	x

X indicates determinants for which the meta-regression could not be performed. Numbers in red have changed when compared to Supplemental Table 3. Abbreviations: VWD, von Willebrand disease; OR, Odds ratio; CI, Confidence interval; DDAVP, 1-deamino-8-D-arginine vasopressin; APTT, Activated partial thromboplastin time; Ag, Antigen; CB, Collagen binding; pp, Propeptide; act, Activity.

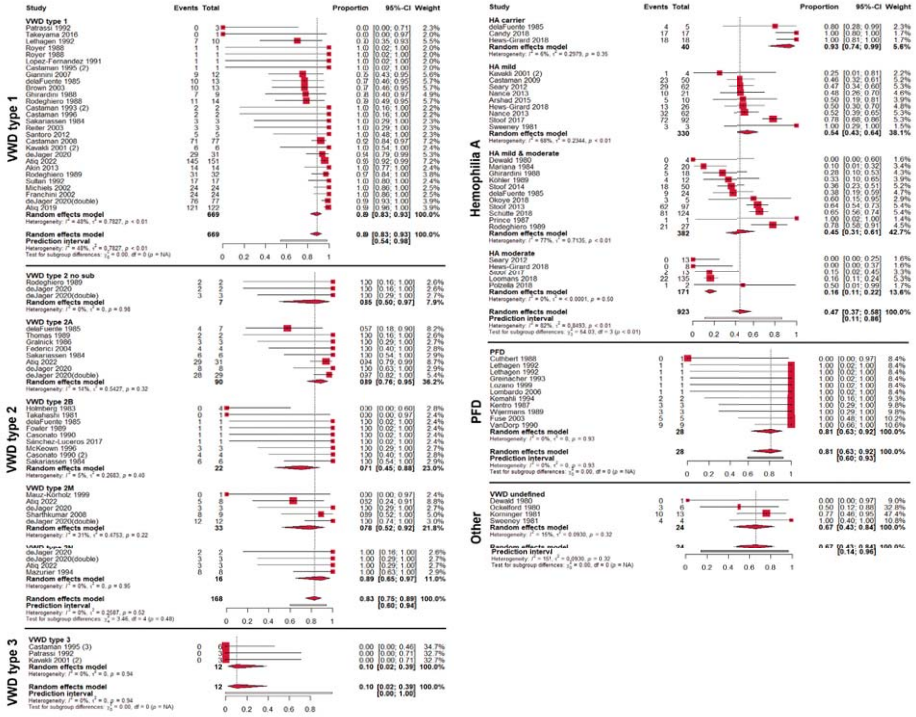

Supplemental Figure 1. Complete response rate varies per disease subtype according to the study definition. Meta-analysis on response to DDAVP at one hour in patients with various bleeding disorders per subtype. Using a random effect model the proportion of complete response per study, divided by subtype, are shown. Random effects are calculated per subtype of disease but also by main type of disease. The proportion of response is not zero in zero-event studies due to the continuity correction that was performed to prevent mathematical errors. Other is, everything that is not VWD type 1, 2 or 3, Hemophilia A or PFD. Abbreviations: HA = Hemophilia, PFD = Platelet function disorder, VWD = Von Willebrand disease.

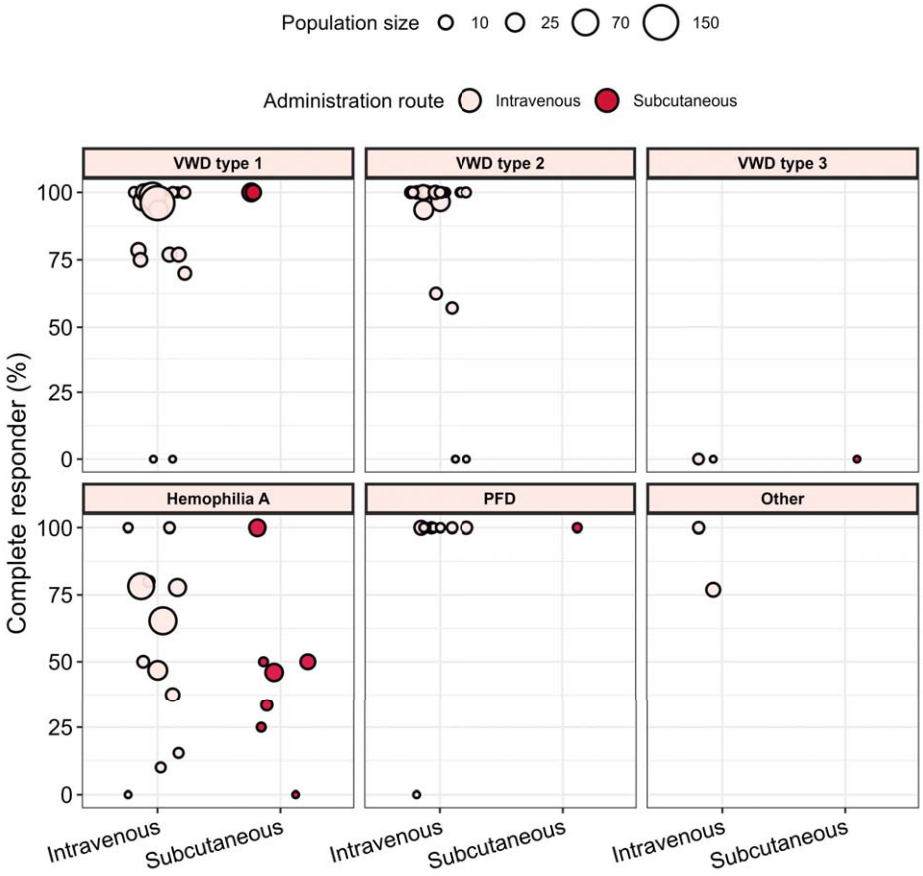

Supplemental Figure 2. Response to DDAVP per disease per administration route. Response to DDAVP of patients with VWD type 1, 2 and 3, Hemophilia A, PFD or Other are shown per administration route of DDAVP. Intravenous is shown in light red and Subcutaneous is shown in dark red. Studies that did not clarify which route was used are excluded from this figure. Intranasal administration is not displayed in this figure as only two studies had this data. Other is everything that is not VWD type 1, 2 or 3, Hemophilia A or PFD. Abbreviations: VWD = Von Willebrand disease, PFD = Platelet function disorder.

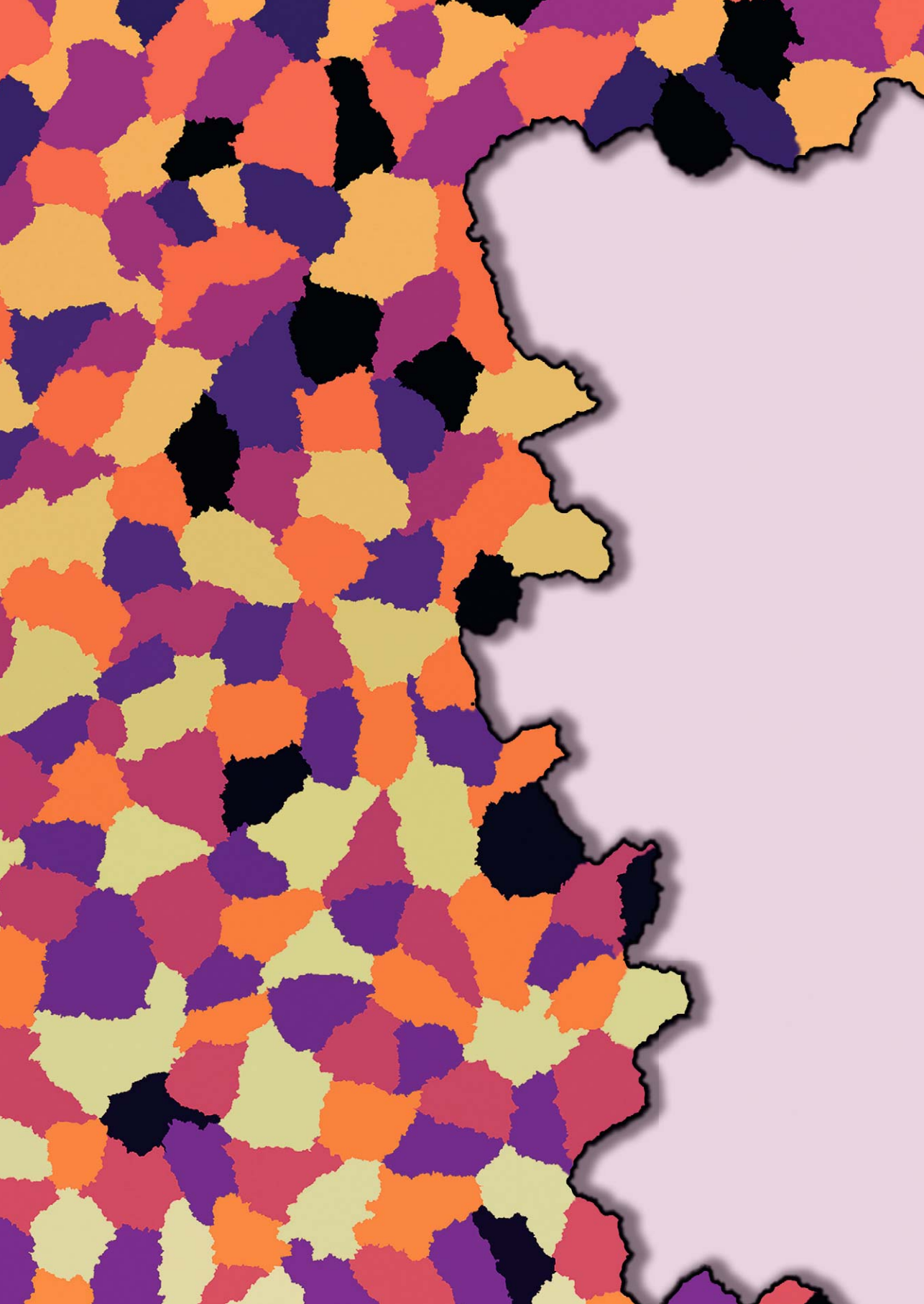

Von Willebrand disease-specific defects and proteomic signatures in endothelial colony forming cells

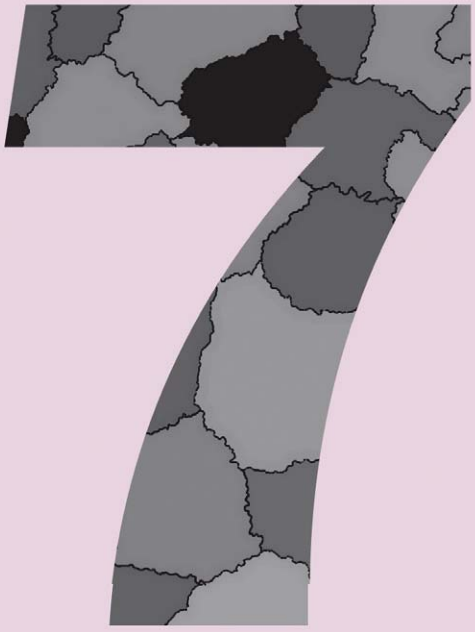

Laan SNJ, Groten S*, Dirven RJ, Bürgisser PE, Leebeek FWG, van Moort I, van Biggelaar M, Bierings R**, Eikenboom J.
*shared first author, ** shared last author

Journal of Thrombosis and Haemostasis. 2025; May 6:S1538-7836(25)00275-2.
doi: 10.1016/j.jtha.2025.04.024.
Accepted after revision

Abstract

Endothelial cells are crucial for hemostasis as they produce Von Willebrand factor (VWF). Von Willebrand disease (VWD) results from a deficiency of, or defects in, VWF. Here, we analyze the endothelial compartment of VWD patients with an unexplained decrease in VWF level or non-response to DDAVP using endothelial colony forming cells (ECFCs).

13 healthy controls and 10 VWD type 1 and 2 patients were included and a total of 29 ECFC clones were derived. Plasma was analyzed and ECFCs were morphologically and functionally characterized by qPCR, ELISA, imaging, migration assay and mass spectrometry.

VWF plasma levels were reduced in all patients. ECFCs were categorized into 2 previously defined transcriptional clusters and matched between patients and controls. Three ECFC clones, all from DDAVP non-responders, retained VWF in the endoplasmic reticulum (ER). Cluster 1 ECFCs from DDAVP non-responders had slower closing speeds in the migration assay and secreted more VWF antigen in rest than control ECFCs. Proteomic data of ECFC lysates showed overlap in clustering with RNA profiles, including ALDHA1, TGFB1 and other EndoMT/ inflammatory markers. However, no patient group specific phenotype was observed. Finally, regulated secretion of VWF and Weibel-Palade body count in ECFCs were correlated with various secretory machinery components.

Lower plasma VWF was linked to reduced production and secretion by patient-derived ECFCs. Furthermore, non-response to DDAVP in some patients was explained by retention of VWF in the ER. The correlation between functional aspects of ECFCs and their qPCR and proteome profile yielded potential targets for further research.

Introduction

Endothelial cells play a key role in hemostasis. Von Willebrand factor (VWF) is one of the main components of primary hemostasis and is produced by endothelial cells and megakaryocytes. VWF is a large multimeric glycoprotein that binds to collagen and platelets, thereby initiating platelet plug formation upon vessel damage. VWF also binds to factor VIII and protects it from degradation. The protein is stored in specialized cigar-shaped secretory organelles called Weibel-Palade bodies (WPBs) (1, 2). These organelles can secrete their content continuously into the vessel which provides a steady level of VWF. However, endothelial cells can also be stimulated by injury or stress to rapidly secrete their content to increase circulating VWF levels (3).

When VWF is deficient or qualitatively defect, bleeding can occur, known as Von Willebrand disease (VWD) (4). This is the most common inherited bleeding disorder in humans found in ~1 in 100 individuals (5). The disease can be divided into 3 subtypes. Type 1 is hallmarked by low levels of functionally normal VWF, whereas in type 3, VWF is not present at all, making it the most severe type. Type 2 VWD is associated with qualitative defects in VWF, like impaired multimerization (type 2A), enhanced or spontaneous binding to platelets (type 2B), decreased binding to platelets or collagen (type 2M) or decreased binding to Factor VIII (FVIII) (type 2N) (4). VWD is usually treated by either administration of 1-deamino-8-D-arginine vasopressin (DDAVP), or by VWF concentrates (6). However, large inter individual differences in response to DDAVP are observed. Several studies have reported differences in response due to disease subtype, mutation, age or blood group (7-20), but the cause of the variation is not fully understood. Although, VWD is the most common bleeding disorder, it is difficult to diagnose due to the large heterogeneity and number of mutations or deletions in the *VWF* gene observed within patients (21). Adding to the complexity, roughly 30-50% of VWD type 1 patients do not have *VWF* gene variants and have been shown to present with a distinctly different bleeding phenotype (22-24). Current assays and genetic testing often do not explain the cause of bleeding in these patients and it is hypothesized that other modifiers cause the low levels and associated bleeding (25).

As endothelial cells are vital in the synthesis, storage and secretion of VWF, we hypothesize that they may play a role in the unexplained VWD phenotype of patients without *VWF* variant and may yield insight into the cause of the poor response to DDAVP. One way to study the molecular and pathophysiological aspects of patient endothelial cells is the endothelial colony forming cell (ECFC) model. One significant benefit of this model is its capability to generate clonally proliferative cells which exhibit endothelial traits, including the production and storage of VWF within WPBs, response to stimuli

and characteristic endothelial cobblestone-like morphology (26). When derived from patients, these cells can be used to study the pathophysiological mechanisms of VWD in the patients (27-31).

In this study, we aimed to investigate the endothelial compartment in the context of VWD as the endothelial cells may play a role in the unexplained low levels of VWF or poor DDAVP response in some patients. We found distinct retention of VWF in the endoplasmic reticulum (ER) in the ECFCs of some patients that did not respond to DDAVP. Furthermore, we highlight the inverse correlation between secreted VWF antigen (VWF:Ag) by ECFCs after stimulation and WPB count with cell area and the correlation between VWF levels and exocytotic machinery.

Materials & Methods

Patient inclusion and ethical approval

Patients were selected from the previous nationwide cross-sectional Willebrand in the Netherlands (WiN) study (32). Informed consent was obtained from 10 patients and 13 healthy donors. Healthy donors had not been diagnosed with VWD or any other bleeding disorder. Inclusion criteria for the patients were as follows: diagnosed with VWD and either 1) no known *VWF* variants or 2) with a *VWF* variant , but non-responsive to DDAVP. Complete response was defined as 2 times increase in VWF platelet binding activity (VWF:Act) from baseline at 1 hour after DDAVP and VWF:Act ≥50 IU/dL until 4 hours after DDAVP (32). At the moment of inclusion, the International Society on Thrombosis and Haemostasis Bleeding Assessment Tool (ISTH-BAT) (33) was obtained and blood samples were drawn (10 mL citrated and 50 mL heparinized blood).

Plasma coagulation factor levels

Citrated plasma samples from patients and controls at the time of inclusion were centrally measured for VWF:Ag, VWF:Act, VWF collagen binding (VWF:CB) and FVIII coagulant activity (FVIII:C). The assays that were used for these central measurements are described in the Supplementary Methods section. Furthermore, from the WiN database, historically lowest plasma levels and levels at the time of inclusion in the WiN study were also used in this study (32). Note that historical VWF activity was measured with different platelet binding assays. In this article all VWF activity levels will be indicated as VWF:Act.

Endothelial Colony Forming Cells acquisition

ECFCs were obtained following study protocols which were approved by the Leiden University Medical Center (LUMC and Erasmus MC (EMC) ethics review boards. Isolation and cell culture of ECFCs was performed as described previously (34). In short, isolation and culture procedures involved venipuncture to collect whole blood, isolation of PBMCs, and subsequent culture in EGM-18 medium (EBM-2 Basal Medium with EGM-2 supplements & growth factors (Lonza, or PromoCell) with 18% heat inactivated FBS (Thermo Fisher). At the EMC, not heat inactivated FBS was used. Clones typically emerged between days 10 and 21, and upon reaching confluency in three T75 flasks (at LUMC) or in four T75 flasks (at EMC) at passage 3, were frozen. A total of 29 clones were isolated in this study, with experiments conducted on clones at passage 5. Detailed information regarding each clone is provided in Table 1.

Brightfield and immunofluorescence image acquisition

For brightfield imaging, ECFCs at passage 5 were imaged three days after confluency was reached with the Leica MC170 HD camera attachment to the DMIL LED (2.5 and 5x lens) (Leica). For immunofluorescence imaging, staining and imaging were performed as described before (35). All samples were stained with antibodies against VWF, V-cadherin and nuclei were stained with Hoechst diluted in blocking buffer. In addition, ER was visualized by staining with antibodies against Protein Disulfide Isomerase (PDI). See Supplemental Table 1 for details on antibodies. Imaging for large tile scans was performed similarly as described before (35) although a 5x5 tile scan was made for a total area of 1059.84 x 1059.84 µm (23261 μm^2). For super resolution imaging, cells were imaged using the Zeiss LSM900 Airyscan2 upright confocal microscope with an 63x oil immersion objective.

Migration assay and image acquisition

For the cell migration assay, all samples were cultured in 48-well plates at passage 5. The protocol was followed as described previously (35). Briefly, each clone was randomly plated in six wells of a 48-well plate. Three days after confluency was reached, cells were labeled with CellTracker Green (Life technologies) diluted 1:10,000 in EGM-18 for 45 minutes. Three wells per clone were treated with 12.5 µg/mL Mitomycin C (Sigma-Aldrich) for 2 hours while the remaining three wells received medium only. The confluent cell layer was damaged by making a scratch using a p100 pipet tip, after which the cells were imaged using the AF6000 (Leica) microscope with a 10x lens at 37^0C and 5% CO2. Each well was imaged every 30 minutes for 24 hours for visualization of cell migration. Time points 1, 2 and 3 had to be removed from analysis due to shifting of the plate during image acquisition.

Automated quantification of ECFC morphology and migration

Automated quantification of ECFC-parameters was done mostly with CellProfiler (version 4.2.1) (36). Confocal imaging tilescans of ECFCs were analyzed using the purpose-made OrganelleProfiler pipeline as described previously (37). The pipeline was optimized as needed for the antibodies used and the measured intensity. For the current study we adjusted the OrganelleProfiler pipeline so that artefacts with high intensity, usually 6 to 7 times higher than the VWF signal, were identified and masked out of the image prior to WPB analysis. For the migration assay analysis, a previously developed CellProfiler pipeline was used to identify, count and track individual cells (35). Analysis parameters and pipeline modifications specific for this study are detailed in the Supplementary Methods section. The CellProfiler pipelines used for morphology and migration analysis are supplied in the Supplemental Files (file 1 and 2) and are made available on GitHub (https://github.com/Clotterdam).

Basal and stimulated release of VWF

Basal and constitutive release of VWF in EGM-18 medium by ECFCs was determined over 24 hours before the cells were stimulated as described previously (34). In addition to histamine, ECFCs were also exposed to 10 µM Epinephrine (Sigma-Aldrich) with 100 µM IBMX (Sigma-Aldrich) to trigger cAMP-mediated secretion of VWF. Cell lysates were collected and media and lysates were measured by VWF:Ag enzyme-linked immunosorbent assay (ELISA) as was described previously (38).

Mass spectrometry sample preparation and acquisition and analysis

For mass spectrometry analysis of EC proteomes, samples were digested with trypsin as described previously (39). Tryptic digests were transferred to an Evotip Pure (Evosep) according to manufacturer's guidelines and analysed with an Evosep One liquid chromatography (LC) system (Evosep) coupled to a TimsTOF HT mass spectrometer (Bruker). Peptides were separated on a 15 cm × 150 µm, 1.5 µm Performance Column (EV1137 from EvoSep) with the 30 samples per day gradient. Buffer A was composed of 0.1 % formic acid, buffer B of 0.1 % formic acid in acetonitrile (Biosolve, NLD). Peptides were ionized and electro sprayed into the mass spectrometer. Data was acquired in DIA-PASEF mode, using an MS1 scan range of 100 - 1700 m/z. Accumulation time was set at 100 ms with a duty cycle of 100%. MS2 acquisition was performed using 32 pyDIAID (40) optimized mass and ion mobility windows, ranging from 400.2 – 1500.8 m/z and 0.70 – 1.50 1/k0 with a cycle time of 1.80 s. A collision energy of 20.00 eV at 0.6 1/k0 and 59 eV at 1.60 1/k0 was used. Raw mass spectrometry data files were processed using the DIANN software (version 1.8) as previously reported (39). Data was analyzed using R 4.2.3 / Rstudio (2022.07.02). Sample S34 could not be included in the analysis due to technical reasons. Detected proteins were filtered for proteotypic and at least

one unique peptide per protein. Proteins should be quantified in at least six different samples. Label free quantification (LFQ) values were transformed in $\log_2$ scale. Missing values were imputed by normal distribution (width = 0.3, shift = 1.5), assuming these proteins were close to the detection limit. All LFQ values are available in Supplemental File 3.

RNA isolation and quantification with quantitative PCR (qPCR)

All ECFC clones were cultured in 24-well plates at passage 4 and were kept in culture for 5-7 days after they reached confluency. Isolation of RNA, synthesis of cDNA and subsequent characterization of ECFCs into clusters by a qPCR gene panel were performed as described previously (35). Primer sequences of all genes tested are available in Supplemental Table 2. Measurements were analyzed using the comparative Ct method where GAPDH was used as the housekeeping gene. Results from the qPCR were analyzed using the prcomp function from stats in Rstudio (version 3.6.2). The script is supplied as Supplemental File 4 (also made available on GitHub (https://github.com/Clotterdam).

Statistical Analysis

Functional aspects of ECFCs between controls and patient groups were compared by Mann-Whitney U test (not normally distributed) and unpaired T test with Welch's correction (normally distributed). Kruskal-Wallis one way ANOVA was used when comparing more than 2 groups. Plasma measurements are presented as boxplot with median or as points per ECFC clone with mean for all others. P value < 0.05 was considered statistically significant. Data were analyzed using GraphPad Prism 9.3.1 (GraphPad Software, San Diego, CA, USA) unless otherwise indicated. For proteome analysis, partition around medoids (PAM)-based clustering was performed using the Cluster package (41), employing a Kmax of 20 with 100 iterations each. To determine differentially abundant proteins, moderated t-tests were performed using LIMMA (42, 43). A BH adjusted $p < 0.05$ and log2 fold change > 1 was considered significant and relevant. Spearman correlations were calculated using Hmisc (44). Gene ontology term enrichment was performed using the clusterProfiler package (45), enrichments with a BH adjusted p-value < 0.05 were considered significant.

Results

VWD study population and ECFC isolation

In this study, we aimed to investigate the endothelial compartment as a potential modifier of VWD phenotype by studying ECFCs derived from 13 healthy controls and

from two groups of VWD patients in which an endothelial contribution to their disease etiology is plausible: (1) patients without pathogenic *VWF* gene variants with a normal response to DDAVP and (2) patients with VWD with a known pathogenic mutation in *VWF* who do not respond to DDAVP (Figure 1A). Patients were classified as type 1 (6 patients) or type 2 (4 patients) VWD based on the current VWD diagnostic guideline (46). Detailed characteristics of the patients and controls are shown in Table 1. Plasma coagulation factor levels (VWF:Act, VWF:Ag, VWF:CB and FVIII:C) were determined again at time of inclusion in this study (Figure 1B-E). All measured coagulation factors were significantly lower in DDAVP non-responders when compared to healthy controls. VWF and FVIII levels were also reduced in VWD patients without pathogenic *VWF* variants, but this was only statistically significant for VWF:CB. When compared to historically lowest levels until WiN inclusion and levels measured during the WiN inclusion (12-16 years ago) (32), current levels have partially corrected (Figure 1B-E) which is likely due to age-dependent increase in plasma VWF levels (23, 47-49).

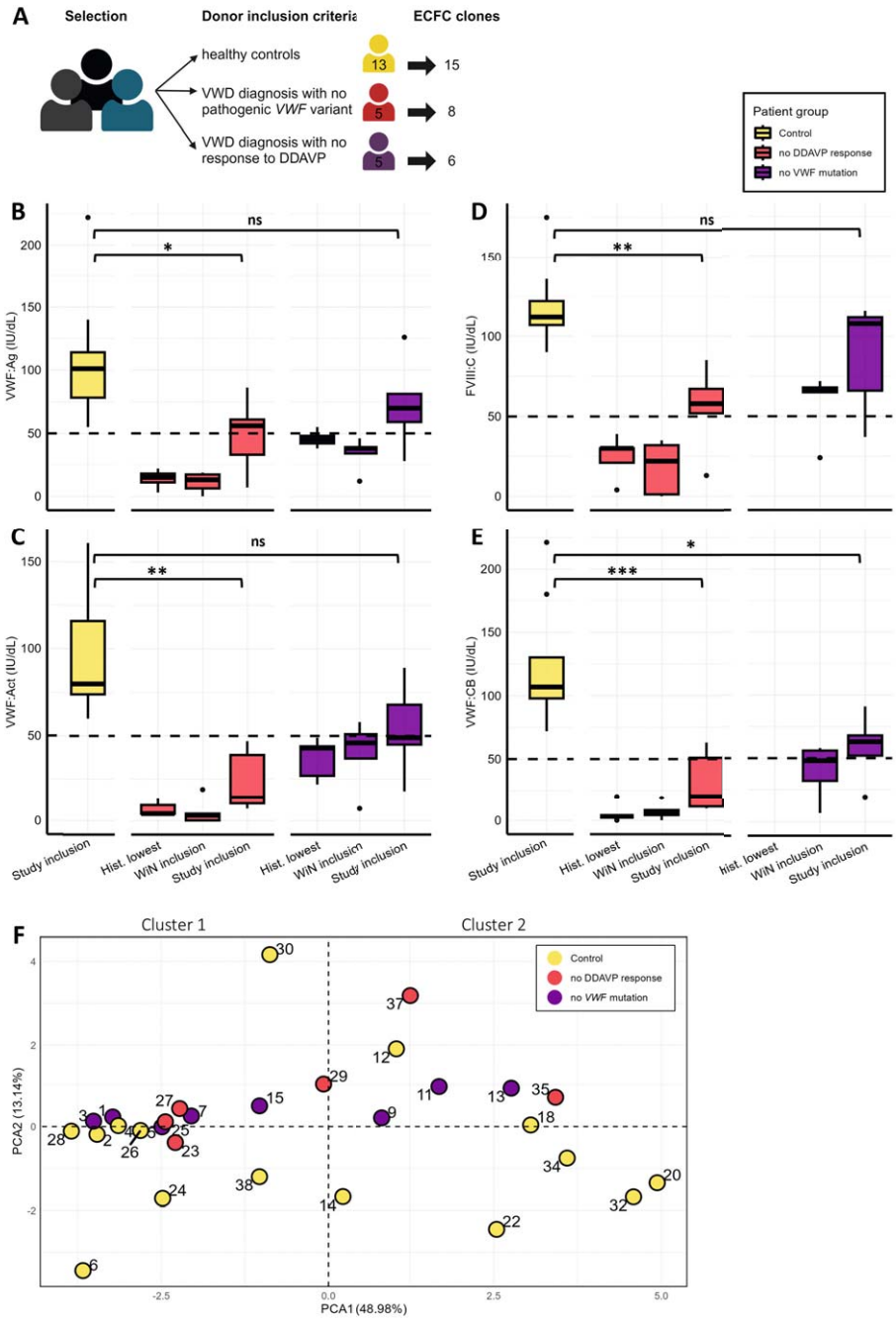

Figure 1. Patient and control plasma levels and ECFC characteristics. A) Schematic overview of donor inclusion. Boxplots of B) VWF:Ag, C) VWF:Act, D) FVIII:C and E) VWF:CB in the plasma of VWD patients and controls at inclusion in the current study. Furthermore, historically lowest factor

levels and levels at time of inclusion in the WiN (32) are shown. Statistical analysis by Kruskal-Wallis one way ANOVA, * $p < 0.05$, ** $p < 0.01$. values 1.5 times outside the interquartile range (IQR) are shown as black dots. Note that previously, VWF activity was measured with different platelet binding assays. In this article all VWF activity levels will be indicated as VWF:Act. F) PCA plot showing heterogeneity between ECFC clones. All clones on the left of the y-axis were categorized as cluster 1, and clones on the right as cluster 2. Numbers correlate with sample numbers and color indicates which group the clone belongs to, controls (yellow), VWD patients without DDAVP response (red) and VWD patients without *VWF* variant (purple). Abbreviations: PCA = Principal Component Analysis; Hist. = Historically; VWF = von Willebrand factor; Ag = Antigen; Act = Activity; WiN = Willebrand in the Netherlands; CB = Collagen binding; DDAVP = 1-deamino-8-D-arginine vasopressin.

ECFC isolation and RNA based characterization

To study VWD-specific signatures of endothelial cells, we isolated at least 1 ECFC clone from all patients and controls. When multiple clones were isolated per donor 2 were taken along in this study, which resulted in 15 clones from controls and 14 from patients (Figure 1A). A complete overview of the ECFC clone and donor characteristics is shown in Table 1. All clones displayed characteristic cobblestone-like endothelial morphology although with large heterogeneity (Supplemental Figure 1) It is widely recognized that substantial phenotypic heterogeneity can exist between ECFC clones isolated from healthy controls and even from the same individuals (34, 38), which can be explained by the existence of at least two discrete transcriptional clusters of ECFCs (35). We carried out a qPCR-based transcriptional analysis of ECFC clones as described previously (35) (Supplemental Table 2) that can distinguish between the aforementioned phenotypic clusters of ECFCs. To visualize the variation between clones we performed principal component analysis (PCA) (Figure 1F), which revealed large intra- and inter-individual heterogeneity and allowed us to categorize ECFC clones in cluster 1 and cluster 2 ECFCs (Table 1). To ensure correct comparison between control and patient ECFCs, we will use this categorization in all following assays to compare ECFC clones with clones within their assigned cluster.

Morphological and migratory characterization of VWD patient-derived ECFCs

Morphology of ECFCs was studied to investigate whether defects in the secretory pathway or abnormal distribution, count and/or shape of WPBs contribute to the VWD phenotype of the patients. All ECFCs were imaged for VWF, VE-cadherin and their nuclei (Figure 2A). Clone S38 is shown as a representative for the control ECFCs and shows typical cigar-shaped WPBs. We observed that 3 out of 5 ECFCs from patients with DDAVP non-response showed signs of retention of VWF in the ER (S29 shown as representative clone of other ECFCs S25, S27 and S35), which was confirmed by PDI staining (Supplemental Figure 2). No uniform morphological phenotype was seen in patients without pathogenic *VWF* variants, but S11 did display very large cells and small

and round WPBs. ECFC characteristics were quantified using an automated image-analysis pipeline developed in CellProfiler (37). Great variation in cell count, WPB count per cell, organelle eccentricity and relative distance to the nucleus between all ECFCs was observed (Figure 2B-E) as was also shown previously in healthy controls (35, 37). Between patient groups and controls, only mean organelle eccentricity was found to be significantly lower in cluster 1 ECFCs of patients without DDAVP response. This effect was primarily attributable to the ECFCs that showed ER retention, which on average had lower organelle eccentricity (0.637±0.015 vs. control 0.721±0.039) and WPB count per cell (35.97±24.20 vs. control 132.30±27.60). Together this data highlights a distinct phenotype in ECFCs of DDAVP non-responders that results in retention of VWF in the ER, thereby reducing its availability for stimulus-induced release of VWF from WPBs.

Table 1. Patient and control ECFC characteristics.

ID	Diagnosis	DNA Change	Protein Change	Age at inclusion	sexe	Blood group	ISTH-BAT bleeding score	Hist. lowest VWF:Ag (U/dL)	Hist. lowest VWF:Act (U/dL)	sample#	Day of detection**	Time in culture***	Cluster
1	Control	n.d.	n.a.	22	Female	O	0	n.d.	n.d.	S2	13	10	1
										S4	13	11	1
2	Control	n.d.	n.a.	28	Female	n.d.	n.d.	n.d.	n.d.	S6	19	30	1
3	Control	n.d.	n.a.	29	Female	O	4	n.d.	n.d.	S12	21	38	2
4	Control	n.d.	n.a.	23	Female	n.d.	n.d.	n.d.	n.d.	S14	13	23	2
										S20	15	27	2
5	Control	n.d.	n.a.	27	Female	O	0	n.d.	n.d.	S18	14	44	2
6	Control	n.d.	n.a.	28	Male	n.d.	n.d.	n.d.	n.d.	S22	14	26	2
7	Control	n.d.	n.a.	30	Female	B	1	n.d.	n.d.	S24	13	29	1
8	Control	n.d.	n.a.	27	Male	n.d.	n.d.	n.d.	n.d.	S26	14	23	1
9	Control	n.d.	n.a.	25	Female	AB	1	n.d.	n.d.	S28	10	14	1
10	Control	n.d.	n.a.	23	Female	B	n.d.	n.d.	n.d.	S30	11	17	1
11	Control	n.d.	n.a.	29	Male	n.d.	n.d.	n.d.	n.d.	S32	21	54	2
12	Control	n.d.	n.a.	23	Male	n.d.	n.d.	n.d.	n.d.	S34	16	53	2
13	Control	n.d.	n.a.	64	Male	n.d.	n.d.	n.d.	n.d.	S38	13	24	1
14	VWD Type 1	no	n.a.	32	Female	A	23	42	49	S1	8	13	1
										S3	11	7	1

Table 1. *Continued.*

ID	Diagnosis	DNA Change	Protein Change	Age at inclusion	sexe	Blood group	ISTH-BAT bleeding score	Hist. lowest VWF:Ag (U/dL)	Hist. lowest VWF:Act (U/dL)	sample#	Day of detection**	Time in culture***	Cluster
15	VWD Type 1	no	n.a.	66	Female	O	14	38	27	S5	13	19	1
										S7	15	20	1
16	VWD Type 1	no	n.a.	39	Female	O	9	48	44	S9	16	35	2
17	VWD Type 1	no	n.a.	50	Male	O	24	55	43	S13	17	45	2
18	VWD Type 2A	no	n.a.	66	Female	O	14	45	22	S11	9	28	2
										S15	16	26	1
19*	VWD Type 2B	4022G>C	Arg1341Pro	73	Male	O	12	11	4	S23	17	20	1
20*	VWD Type 2A	2771G>A	Arg924Gln	88	Male	O	14	15	4	S25	19	25	1
21*	VWD Type 2A	4120C>T	Arg1374Cys	21	Male	n.d.	10	18	9	S29	14	32	1
22*	VWD Type 1	421G>A + 6937C>T	Asp141Asn + Arg2313Cys	39	Female	O	12	22	14	S27	13	20	1
										S35	15	21	2
23*	VWD Type 1	3614G>A	Arg1205His	74	Female	B	12	3	4	S37	12	39	2

*Did not respond to DDAVP. **Number of days after inclusion. ***From day of detection to freezing (in days). Abbreviations: n.d. = not determined; n.a. = not applicable; ISTH-BAT = international society of thrombosis and hemostasis bleeding assesment tool; VWD = von Willebrand Disease; hist = historically; Ag = Antigen.

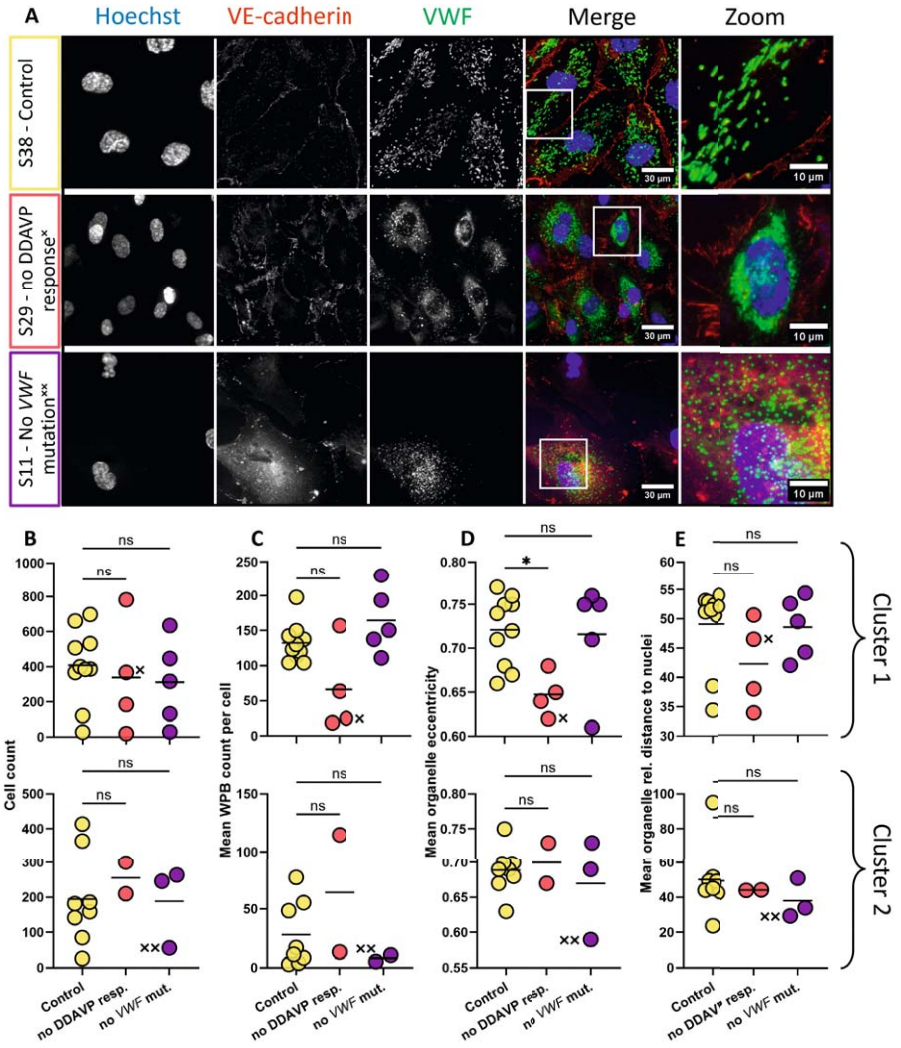

Figure 2. Morphological differences of VWD derived ECFCs. Phenotypic profiling of all ECFCs was done using tile scans (1123261 µm^2). ECFC clones were analyzed per cluster and stained with Hoechst (blue) and antibodies against VE-cadherin (red) and VWF (green). A) Representative confocal images of a control ECFC clone (top - S38), a patient with retention of VWF in the ER (middle - S29) and a patient ECFC with round WPBs (bottom - S11). Scale bar represents 30 µm. The white box indicates the area that is enlarged by 3x of the merge (scale bar represents 10 µm). Images were taken with a 63x objective. B) Cell count per surface area of the tile scan. C) Mean WPB count per cell per ECFC clone. D) Mean eccentricity of WPBs per ECFC clone. E) Distance of the WPB to the nucleus relative to their position in the cell in percentage. S29 and S11 values are indicated by x and xx respectively in B-E. Values per ECFC clone are shown and the line shows the mean. Kruskal-Wallis one way ANOVA was performed; * p <0.05. Abbreviations: VWF = von Willebrand factor; DDAVP = 1-deamino-8-D-arginine vasopressin; ns = not significant; resp = responder; mut = mutation.

It has been shown that VWF plays a role in migration, proliferation and angiogenesis of endothelial cells (50) and that some type 1 and 2 VWD patient-derived ECFCs had lower directionality in wound healing assays (51). Therefore, we also analyzed the migration behavior of all ECFCs using a scratch wound migration assay (Supplemental Figure 3A). We observed that cluster 1 DDAVP non-responder ECFCs have a slower closing speed when compared to control ECFCs, while cluster 2 ECFCs from DDAVP non-responders close the scratch faster than controls (Supplemental Figure 3B). No significant differences were observed for speed of movement, X trajectory and linearity (Supplemental Figure 3C). However, samples 25, 27 and 29 in cluster 1 did show markedly decreased X trajectory. This suggests that ECs with observed ER retention and decreased VWF levels also have implicated migratory processes.

Impaired synthesis and secretion upon stimulation of patient ECFCs

We investigated whether production of VWF and secretory capabilities of the ECFCs may clarify the low VWF levels or lack of response to DDAVP. We measured basal VWF secretion over 24 hours (Figure 3A), intracellular VWF content in the lysate (Figure 3B) and regulated secretion of VWF following Ca^{2+}- (histamine) and cAMP-mediated (epinephrine) stimulation (Figure 3C-D). Cluster 1 control ECFCs secrete more VWF:Ag in rest than ECFCs from patients that did not respond to DDAVP. There is no difference between the ECFCs from controls and patients without *VWF* variant. Histamine and epinephrine stimulated release from ECFCs derived from patients without DDAVP response show a trend to lower response than controls. ECFCs derived from patients with no *VWF* mutation responded similarly to histamine and epinephrine stimulation as the control ECFCs. ECFC VWF synthesis and secretion was correlated to plasma VWF levels (Figure 3E-H). ECFCs in cluster 1 showed positive correlations between plasma VWF:Ag levels and all ELISA measurements while there was no correlation in cluster 2 ECFCs. This suggests that cluster 1 ECFCs are a good representative of VWF synthesis and secretion in the vessels of the patients.

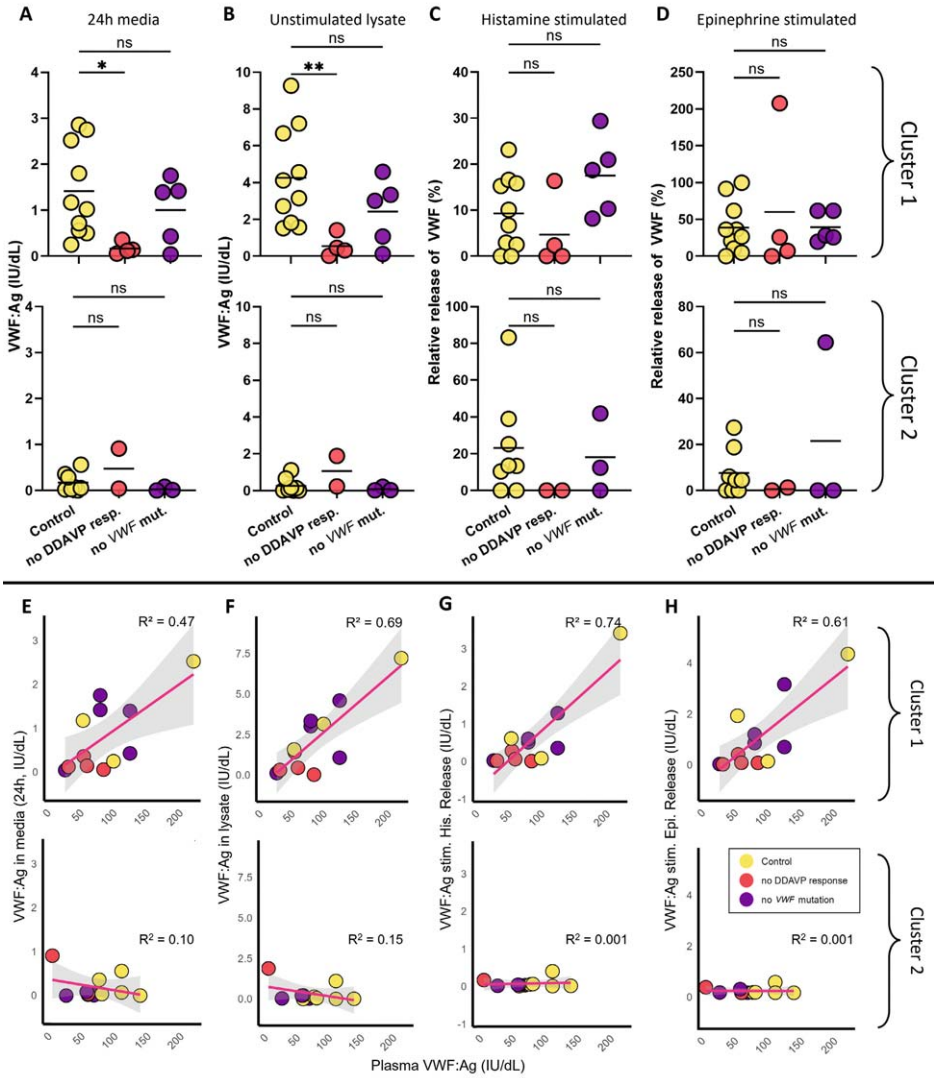

Figure 3. VWF production and secretion lower in patient ECFCs. ECFCs were grown in culture until confluent and then stimulated by histamine and epinephrine + IBMX to secrete VWF. VWF:Ag (IU/dL) levels as measured by ELISA are shown per ECFC clone. A) VWF levels secreted in media during 24 hours of culture of ECFCs preceding the stimulation. B) VWF levels in the lysates of unstimulated cells (DMSO exposure only) C) Secretion of VWF after 1 hour of stimulation as a percentage of the total amount of VWF in the cell. Calculated as the released VWF:Ag in media minus VWF:Ag released without stimulant (DMSO) divided by the total amount of VWF in the cell (the lysate of the unstimulated cells). If stimulated release was not higher than the negative control a value of 0 was noted. Plasma VWF:Ag measurements were correlated to the levels of VWF:Ag secreted by the ECFCs in rest (E), in the lysate (F), secreted after histamine stimulation (G) and secreted after epinephrine + IBMX stimulation (H). Statistical analysis by Kruskal-Wallis one way ANOVA, *$p < 0.05$, **$p < 0.01$. R^2 was calculated by linear regression. Abbreviations:

DDAVP = 1-deamino-8-D-arginine vasopressin; VWF = von Willebrand factor; DMSO = Dimethyl sulfoxide; ns = not significant; his = histamine; epi = epinephrine.

VWD does not drive disease-specific proteomic differences

Next, we investigated whether we could find differences in protein abundance in ECFCs derived from VWD patients. Therefore, we performed unbiased proteomics on 28 ECFC clones using a bottom-up, label-free quantification mass spectrometry workflow (Figure 4A). On average, 8,349 proteins were quantified per sample (Supplemental Figure 4A) with an overall high correlation (Supplemental Figure 4B). Based on principal component analysis, we did not observe a clear distinction between controls and the 2 VWD patient categories (Figure 4B). PAM clustering of the proteomes, identified three ECFCs clusters (A,B,C) (Figure 4C) of which clusters A and B partially overlapped with the annotation based on the qPCR panel (Figure 4D). Statistical analysis comparing ECFCs derived from healthy controls with ECFCs derived from VWD patient groups showed no group-specific differences (LFC > 1, $p < 0.05$), irrespective of proteomics clustering (A,B,C) or subdivision in the qPCR panel (1,2) (Figure 4D-F). Comparison of individual patient ECFC clones versus controls within the proteomics clusters did reveal clone-specific alterations (Supplemental Figure 4C). However, the observed heterogeneity in ECFC clones derived from the same donor (Supplemental Figure 4D) combined with marginal overlap in regulated proteins between ECFCs clones from the same VWD donor (Supplemental Figure 4E), hampers interpretation of donor-specific differences. Taken together, this highlights the challenge to dissect VWD-specific defects in the individual patient.

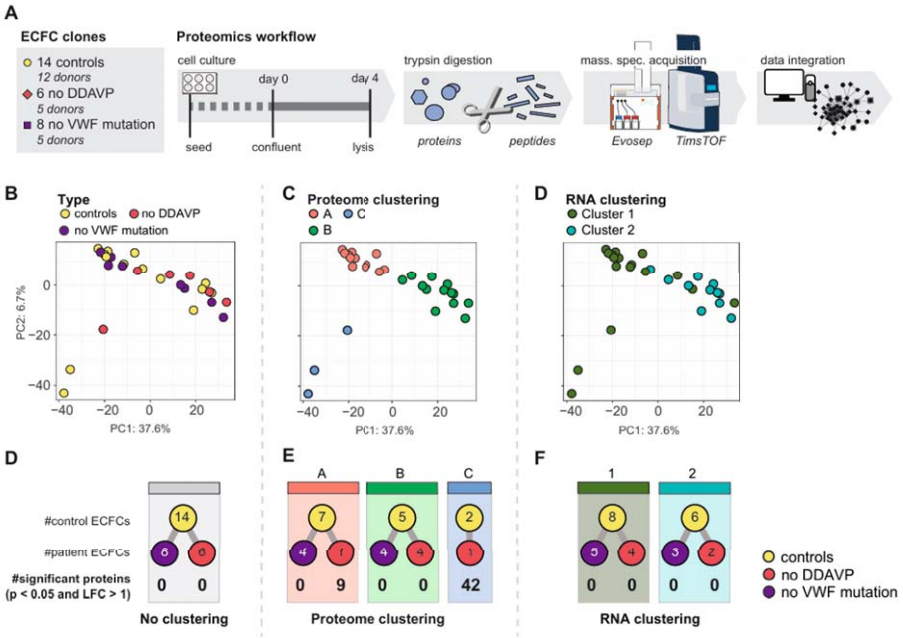

Figure 4. VWD does not drive disease-specific proteomic differences A) Schematic overview of proteomics workflow. Principal component analysis (PCA) of proteomes across PC1 and PC2, colored based on B) disease type, C) proteomics based clustering and D) qPCR based division. Overview of samples and significantly regulated proteins (t-test, $p < 0.05$ and LFC > 1) between D) disease type versus controls, E) disease type versus control per proteome cluster and F) disease type versus controls per qPCR based distinction. Abbreviations: DDAVP = 1-deamino-8-D-arginine vasopressin; VWF = von Willebrand factor; PC = principal component, LFC = Log fold change.

Proteomic signatures of heterogenous ECFC phenotypes

To further investigate endothelial heterogeneity in the context of VWD, we explored the differences that drive separation into clusters A,B,C (Figure 4C). On a morphological level, cluster A contained ECFCs with hallmark cobblestone morphology, while cluster B contained cells with a more inflamed and mesenchymal-like phenotype (Figure 5A), in agreement with qPCR segregation. Among the proteins driving the most variation between proteomic clusters A and B, were ALDH1A1, CLU, and VWF (increased abundance in cluster A) and TGFBI, CD44 and TAGLN (increased abundance in cluster B) which were previously described separating cobblestone-mesenchymal phenotypes by RNA-seq (34) (Figure 5B-C). In total, 316 of the 451 significantly different proteins between group A and B were identified in that study on transcript level as well (Supplemental Figure 5A-B). Interestingly, cells in cluster C showed a unique phenotype of spindle-like ECs that diverged from both other clusters. The variation across PC2, that mostly separated cluster C, was driven by RELN, TIMP3 and CEACAM1 among others

(Supplemental Figure 5C-D). In total 345 proteins were differentially abundant in cluster C compared to both other clusters (LFC > 1, p < 0.05) (Figure 5D). Cell-type-specific enrichment analysis of the upregulated proteins using WebCSEA (52) enriched highest for lymphatic ECs (Figure 5E). Moreover, lymphatic markers PROX1, VEGFR3 (FLT4) and, to a lesser extent, LYVE1 (53-55) were all more abundant in cluster C ECFCs (Figure 5F), suggesting these clones are of lymphatic endothelial lineage.

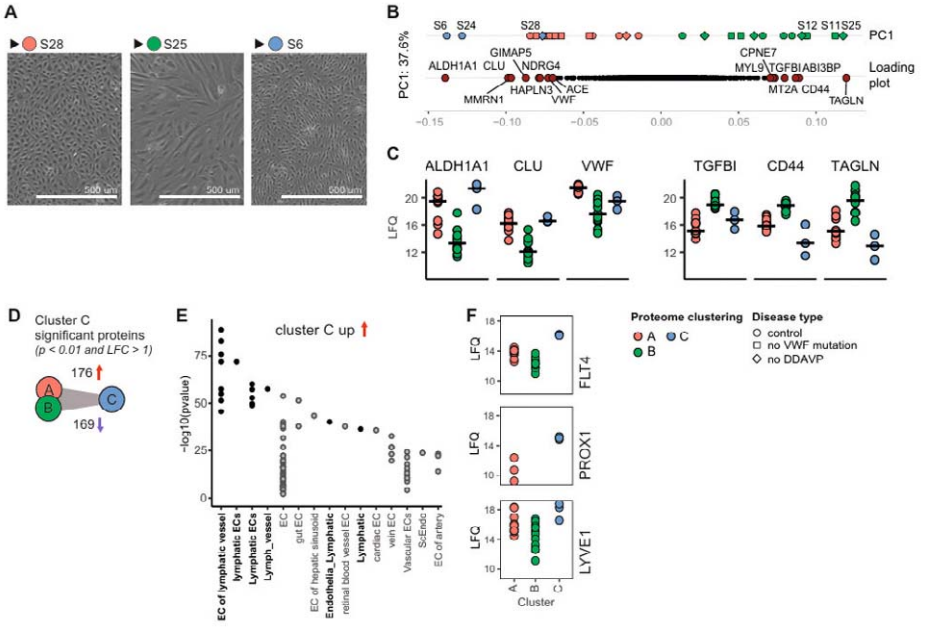

Figure 5. Proteomic signatures of heterogenous ECFC phenotypes A) Brightfield images of hallmark ECFC clones per proteomic cluster, scale bar indicates 500 µm. B) Distribution of samples and loading plot across PC1, shape indicates disease type (control – circle, no DDAVP – diamond, no VWF mutation – square). Highest positive and negative separating proteins in the loading plot are highlighted in red and labeled. C) Dot plots of protein LFQ values with high positive and negative separation across PC1. D) Number of up- and downregulated proteins (t-test, p-value < 0.05, LFC > 1) in Cluster C versus both other clusters. E) Top 15 WebCSEA enriched endothelial cell subtype terms of upregulated proteins in group C. Colors indicate lymphatic EC terms (black) and other EC terms (grey). F) Dot plots of lymphatic proteins LFQ values. PC = principal component, LFC = Log fold change, LFQ = label-free quantification.

Combined data integration to decipher proteomics profiles in the context of VWF

To investigate proteomic profiles in the context of VWF across a heterogeneous ECFC population, we integrated VWF secretion, qPCR cluster profiles, morphological and functional data with protein expression profiles. Correlation analysis revealed

that abundance of an extensive network of proteins (n = 2173) was associated with a functional or cell biological outcome (spearman correlation coefficient > 0.7) (Supplemental Figure 6A). As expected, VWF:Ag levels in lysates and secreted VWF measured by ELISA correlated highly with the proteome VWF LFQ measurements (spearman correlation > 0.85) (Supplemental Figure 6B). VWF LFQ, VWF:Ag and secreted VWF levels also correlated positively with cell - and WPB count, and inversely with cell area (Supplemental Figure 6A). Proteins positively correlating with histamine-induced VWF secretion (n=791), enriched predominantly for the gene ontology biological process term "RNA processing" and proteins inversely correlated (n=550) enriched for "Endomembrane system" (Figure 6A). To specifically look for proteins associated with the VWF exocytosis machinery and WPB bodies, we highlighted known and putative WPB interactor proteins (2) and found that important adaptors in VWF release were positively correlated with increased VWF release, such as RAB27A, RAB3D, and SYTL4(56-58), while others such as GBF1 which is important in ER-Golgi trafficking of VWF was negatively correlating (Figure 6B). Of these proteins only RAB3D also positively correlated with WPB count per cell (Figure 6C). This suggests, while both RAB3D and RAB27A are important in WPB release, RAB3D also functions in managing WPBs in steady state. Surprisingly, IGFBP7, a protein known to be present in WPBs (59), is lower in abundance when more WPBs are present per cell (Figure 6D). Moreover, 18 mitochondrial proteins correlated positively with WPBs count of which mitochondrial membrane protein AGK had the highest correlation. Finally, correlating proteins to organelle eccentricity, which is a proxy for ER retention, were limited. However, several members of the vacuolar-ATPase (ATP6V-B1,-E1,-G1,-H1) negatively correlated with organelle eccentricity (Figure 6E). Counterintuitively, although the v-ATPase proton pump is required for the maturation of WPB bodies (59-61), our analysis shows that higher levels of this protein correlated with round WPB bodies (Figure 6F).

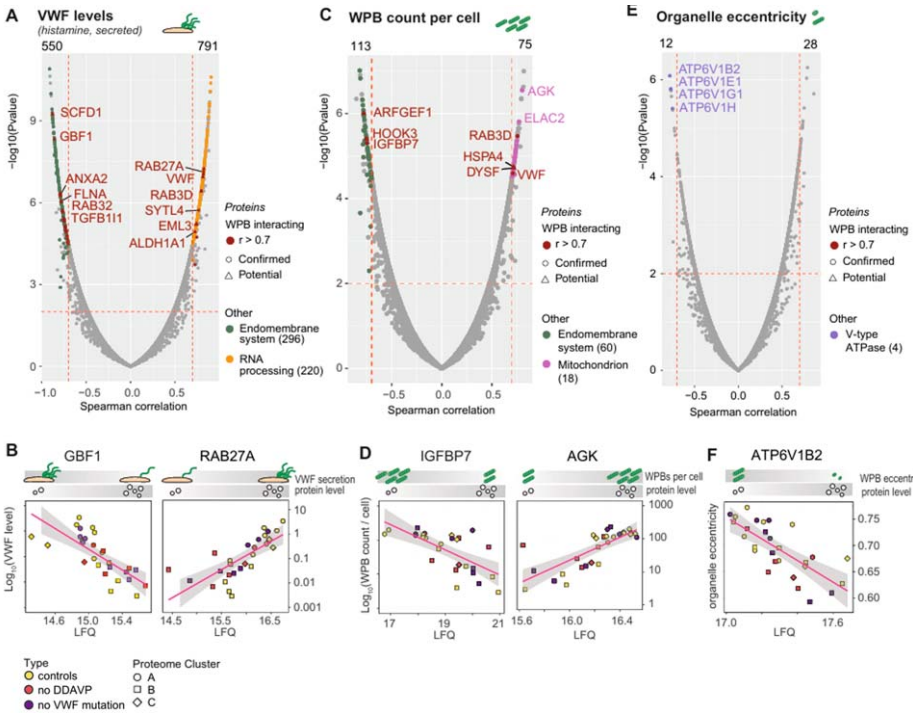

Figure 6. Proteomic and functional data integration A) Spearman correlation plot of histamine-induced secreted VWF levels with protein LFQ levels and B) protein correlations of interest. C) Spearman correlation plot of WPB count per cell with protein LFQ levels and D) protein correlations of interest. E) Spearman correlation plot of organelle eccentricity with protein LFQ levels and F) protein correlation of interest. For all Spearman correlation plots, correlation > 0.7 and p value < 0.01 are indicated by dotted red lines. Total number of proteins above cutoffs are indicated at the top of graph. WPB interacting proteins are indicated in red. Major enriched GO-terms per functional output and number of proteins per term are shown. Abbreviations: WPB = Weibel-Palade body; DDAVP = 1-deamino-8-D-arginine vasopressin; VWF = von Willebrand factor; DMSO = Dimethyl sulfoxide; his = histamine; epi = epinephrine, WPB = Weibel-Palade body, LFQ = label free quantification.

Discussion

ECFCs have been used to study biological processes in endothelial cells and to elucidate the pathogenic mechanisms of various diseases (29, 30, 51). There is a lot of variability in bleeding phenotype in patients with VWD (4) and it is hypothesized that other modifiers cause the low levels of VWF and associated bleeding (25) or perhaps non-response to DDAVP treatment. Therefore, in this study, we used ECFCs to attempt to unravel those mechanisms. Patients were previously diagnosed with VWD based on reduced

levels of plasma VWF:Ag and VWF:Act which correlated with low levels of produced and secreted VWF by ECFCs. Furthermore, we observed retention of VWF in the ER which was connected with very low levels of secreted VWF. Proteomic characterization of the ECFC clones yielded distinct clusters of ECFC clones that were not dependent on patient groups. Proteomic clustering overlapped with RNA based clustering and yielded a third cluster in this study, which seems to be of lymphatic endothelial lineage. Finally, comparing functional outcomes to proteomics, we observed that VWF levels and WPB count per cell correlated inversely with cell area and regulated secretion of VWF and Weibel-Palade body count in ECFCs were correlated with various secretory machinery components. Protein regulation showed strong enrichment of DNA and mRNA processing in cells with high VWF levels and a smaller cell area.

Despite the advantages of ECFCs, considerable phenotypic heterogeneity has been observed (34, 35, 38) which are influenced by day of initial appearance of ECFCs (34), passaging (62), and duration in culture (63, 64). Interestingly, the proteomic heterogeneity between clones was remarkably similar to the transcriptomic differences observed previously (35), even though different ECFCs, cultured in separate labs, were used. 316 from the 451 significantly different proteins between group A and B were measured by RNA-seq previously (35). This large overlap indicates that ECFCs maintain similar patterns on both protein and RNA expression level. Furthermore, endothelial to mesenchymal (EndoMT) associated proteins TGFBI, TGFB2 and BMP2 (65) were also found to be significantly different at the proteome level.

While the origin of circulating ECFCs is uncertain, the heterogeneity that we observed between clones resembles the differences in expression profiles between endothelial cells from distinct vascular beds (39, 66). The proteomic signature showed a distinct cluster enriched for ECs of lymphatic endothelial lineage. These cells were visually smaller and more spindle-like compared to other ECFC clones and they had higher protein levels of transcription factors PROX1 (67) and CEACAM1, which are important in the formation of new lymphatic vessels (68). Whether the observed ECFCs respond differently to external stimuli remains to be elucidated, but provides an interesting avenue to investigate vascular bed- related differences using ECFCs.

We hypothesized that unexplained non-response to DDAVP could be caused by modifiers outside of *VWF*. ECFCs that showed retention of VWF in the ER were all derived from DDAVP non-responsive patients that carried *VWF* mutations. The p.Arg924Gln mutation (S25) is associated with reduced VWF and FVIII levels (69), but ER retention in previous studies has not been confirmed through any staining. S27 and S35 (from the same patient) carry p.Asp141Asn and p.Arg2313Cys. The variant p.Asp141Asn has been

shown to cause ER retention in transfected HEK cells (70), which we now confirmed in ECFCs carrying this mutation. Finally, p.Arg1374Cys (S29) is still disputed as causing either VWD type 2A or 2M (71), but we show here that this variant is accompanied with significant retention within the ER. Collectively, the retention of VWF in the ER, which would prevent it from progressing to WPBs from where it can be released via basal and stimulus-induced secretion, appears to be a common mechanism in VWD that could explain the lower circulating levels of VWF and the subsequent non-response to DDAVP.

In this study we show that circulating VWF plasma levels correlate with the amount of VWF contained in ECFCs and with the amount of VWF that is released from ECFCs upon stimulated secretion, which confirms the relevance of the ECFCs as *ex vivo* cell models for VWF secretion *in vivo*. Moreover, we show that protein levels of various secretion machinery proteins such as RAB27A, RAB3D, VWF and SYTL4 were significantly correlated to stimulated release of VWF and WPB count. Taken together this suggests that the exocytotic machinery that is recruited to WPBs is a determinant of circulating VWF, which is in line with previous findings from genome wide association studies that identified components of the secretory pathway such as *STX2* and *STXBP5* as determinants of VWF plasma levels (72-74). Interestingly, the correlation between plasma VWF:Ag and ECFC VWF levels (intracellular and released after stimulus) was only observed in cluster 1 cobblestone ECFCs, and not in cluster 2 mesenchymal/inflamed-like ECFCs. This raises the question whether cluster 2 ECFCs are representative of the endothelial compartment that is responsible for production of VWF that circulates in plasma and underscores the intricate connection between VWF and inflammation (75).

A limitation of this study was that patient characteristics were very diverse and despite ECFC matching, no common cause for the VWD phenotype was found. ECFC variation between groups was not representative of individual patient heterogeneity. Therefore, we focused on patient-specific qualitative findings rather than quantitative results. Our findings remain to be validated in a different setting or larger cohort to confirm whether these are patient-specific differences that contribute to the bleeding phenotype or arise from ECFC variation. Furthermore, other functional aspects like angiogenesis, proliferation and apoptosis were not included in this study. Analysis on ECFCs from patients with a bleeding disorder of unknown cause (BDUC), especially those with gastrointestinal bleeding might benefit from those assays. Moreover, as bleeding is mediated through the interplay of different cells, incorporation of multiple cell types such as platelets and leukocytes or the addition of shear stress in a flow model might boost future studies in unraveling VWD bleeding phenotypes.

Finally, to our knowledge this study is the first to examine a large panel of ECFCs of both healthy and VWD donors through extensive characterization by both functional assays and proteomics. As such, it highlights the current opportunities and challenges in using ECFCs as a model to study WPB-specific mechanisms and provides a broad EC-wide picture of the molecular regulation of WPB machinery and its outcomes.

Acknowledgements

The SYMPHONY consortium, which aims to orchestrate personalized treatment in patients with bleeding disorders, is a unique collaboration between patients, health care professionals, and translational and fundamental researchers specializing in inherited bleeding disorders, as well as experts from multiple disciplines (76). It aims to identify the best treatment choice for each individual based on bleeding phenotype. To achieve this goal, work packages (WP) have been organized according to 3 themes (e.g. Diagnostics [WPs 3 and 4], Treatment [WPs 5-9], and Fundamental Research [WPs 10-12]). Principal investigator: M.H. Cnossen; project manager: S.H. Reitsma.

Beneficiaries of the SYMPHONY consortium: Erasmus University Medical Center-Sophia Children's Hospital, project leadership and coordination; Sanquin Diagnostics; Sanquin Research; Amsterdam University Medical Centers; University Medical Center Groningen; University Medical Center Utrecht; Leiden University Medical Center; Radboud University Medical Center; Netherlands Society of Hemophilia Patients (NVHP); Netherlands Society for Thrombosis and Hemostasis (NVTH); Bayer B.V., CSL Behring B.V., Swedish Orphan Biovitrum (Belgium) BVBA/SPRL.

Funding by SYMPHONY: NWO-NWA.1160.18.038 (received by SNJL, IvM, RB and JE), Landsteiner Foundation for Blood Transfusion Research, Grant Number:1707 (received by RB).

We would like to acknowledge Suzan de Boer, Yvonne Jongejan, Noa Linthorst, Isabel Bär, Sophie Hordijk, Calvin van Kwawegen and Ferdows Atiq for their collaboration and assistance with patient selection, inclusion and ECFC isolation and culture.

Authorship Contributions

SNJL, RJD, SG, PB performed research; SNJL, RJD, SG analyzed data; SNJL, RJD, IvM, SG, MvB, FL, PB, RB and JE designed the research and wrote the paper and provided feedback on the manuscript.

Conflicts of interest

The WiN study was supported by the Dutch Haemophilia Foundation, the Erasmus MC, CSL Behring and Takeda (funding obtained by FL). FL is a consultant for CSL Behring, Biomarin, and Takeda of which the fees go to the university. JE received research funding from CSL Behring which funds go to the university.

All other authors declare no conflicts of interest.

Data availability

All data files are available in a repository; https://figshare.com/projects/Data_repository_-_Von_Willebrand_disease-specific_defects_and_proteomic_signatures_in_endothelial_colony_forming_cells/229449

Proteome raw- and search-files have been deposited in the ProteomeXchange Consortium (http://proteomecentral.proteomexchange.org/cgi/GetDataset) via the PRIDE partner repository with the dataset identifier *PXD055124*.

References

1. Valentijn KM, Sadler JE, Valentijn JA, Voorberg J, Eikenboom J. Functional architecture of Weibel-Palade bodies. Blood. 2011;117(19):5033-43.
2. Hordijk S, Carter T, Bierings R. A new look at an old body: molecular determinants of Weibel-Palade body composition and von Willebrand factor exocytosis. J Thromb Haemost. 2024;22(5):1290-303.
3. Schillemans M, Karampini E, Kat M, Bierings R. Exocytosis of Weibel-Palade bodies: how to unpack a vascular emergency kit. J Thromb Haemost. 2019;17(1):6-18.
4. Leebeek FWG, Eikenboom JCJ. Von Willebrand's Disease. New England Journal of Medicine. 2016;375(21):2067-80.
5. Murray EW, Lillicrap D. von Willebrand disease: pathogenesis, classification, and management. Transfus Med Rev. 1996;10(2):93-110.
6. Castaman G. How I treat von Willebrand disease. Thromb Res. 2020;196:618-25.
7. Atiq F, Heijdra J, Snijders F, Boender J, Kempers E, van Heerde WL, et al. Desmopressin response depends on the presence and type of genetic variants in patients with type 1 and type 2 von Willebrand disease. Blood Adv. 2022;6(18):5317-26.
8. Biguzzi E, Siboni SM, Peyvandi F. Acquired Von Willebrand syndrome and response to desmopressin. Haemophilia. 2018;24(1):e25-e8.
9. Castaman G, Lethagen S, Federici AB, Tosetto A, Goodeve A, Budde U, et al. Response to desmopressin is influenced by the genotype and phenotype in type 1 von Willebrand disease (VWD): results from the European Study MCMDM-1VWD. Blood. 2008;111(7):3531-9.
10. Castaman G, Mancuso ME, Giacomelli SH, Tosetto A, Santagostino E, Mannucci PM, et al. Molecular and phenotypic determinants of the response to desmopressin in adult patients with mild hemophilia A. J Thromb Haemost. 2009;7(11):1824-31.
11. Castaman G, Tosetto A, Eikenboom JC, Rodeghiero F. Blood group significantly influences von Willebrand factor increase and half-life after desmopressin in von Willebrand disease Vicenza. J Thromb Haemost. 2010;8(9):2078-80.
12. Castaman G, Rodeghiero F. No influence of blood group on the responsiveness to desmopressin in type I "platelet normal" von Willebrand's disease. Thromb Haemost. 1995;73(3):551-2.
13. Di Perna C, Riccardi F, Franchini M, Rivolta GF, Pattacini C, Tagliaferri A. Clinical efficacy and determinants of response to treatment with desmopressin in mild hemophilia a. Semin Thromb Hemost. 2013;39(7):732-9.
14. Lethagen S, Egervall K, Berntorp E, Bengtsson B. The administration of desmopressin by nasal spray: a dose-determination study in patients with mild haemophilia A or von Willebrand's disease. Haemophilia. 1995;1(2):97-102.
15. Nance D, Fletcher SN, Bolgiano DC, Thompson AR, Josephson NC, Konkle BA. Factor VIII mutation and desmopressin-responsiveness in 62 patients with mild haemophilia A. Haemophilia. 2013;19(5):720-6.
16. Revel-Vilk S, Schmugge M, Carcao MD, Blanchette P, Rand ML, Blanchette VS. Desmopressin (DDAVP) responsiveness in children with von Willebrand disease. J Pediatr Hematol Oncol. 2003;25(11):874-9.
17. Revel-Vilk S, Blanchette VS, Sparling C, Stain AM, Carcao MD. DDAVP challenge tests in boys with mild/moderate haemophilia A. Br J Haematol. 2002;117(4):947-51.

18. Seary ME, Feldman D, Carcao MD. DDAVP responsiveness in children with mild or moderate haemophilia A correlates with age, endogenous FVIII:C level and with haemophilic genotype. Haemophilia. 2012;18(1):50-5.
19. Sharthkumar A, Greist A, Di Paola J, Winay J, Roberson C, Heiman M, et al. Biologic response to subcutaneous and intranasal therapy with desmopressin in a large Amish kindred with Type 2M von Willebrand disease. Haemophilia. 2008;14(3):539-48.
20. Stoof SC, Sanders YV, Petrij F, Cnossen MH, de Maat MP, Leebeek FW, et al. Response to desmopressin is strongly dependent on F8 gene mutation type in mild and moderate haemophilia A. Thromb Haemost. 2013;109(3):440-9.
21. de Jong A, Eikenboom J. Von Willebrand disease mutation spectrum and associated mutation mechanisms. Thromb Res. 2017;159:65-75.
22. James PD, Notley C, Hegadorn C, Leggo J, Tuttle A, Tinlin S, et al. The mutational spectrum of type 1 von Willebrand disease: Results from a Canadian cohort study. Blood. 2007;109(1):145-54.
23. Lavin M, Aguila S, Schneppenheim S, Dalton N, Jones KL, O'Sullivan JM, et al. Novel insights into the clinical phenotype and pathophysiology underlying low VWF levels. Blood. 2017;130(21):2344-53.
24. Atiq F, Boender J, van Heerde WL, Tellez Garcia JM, Schoormans SC, Krouwel S, et al. Importance of Genotyping in von Willebrand Disease to Elucidate Pathogenic Mechanisms and Variability in Phenotype. Hemasphere. 2022;6(6):e718.
25. Swystun LL, Lillicrap D. Genetic regulation of plasma von Willebrand factor levels in health and disease. J Thromb Haemost. 2018;16(12):2375-90.
26. de Boer S, Eikenboom J. Von Willebrand Disease: From In Vivo to In Vitro Disease Models. Hemasphere. 2019;3(5):e297.
27. Wang JW, Bouwens EA, Pintao MC, Voorberg J, Safdar H, Valentijn KM, et al. Analysis of the storage and secretion of von Willebrand factor in blood outgrowth endothelial cells derived from patients with von Willebrand disease. Blood. 2013;121(14):2762-72.
28. Selvam SN, Casey LJ, Bowman ML, Hawke LG, Longmore AJ, Mewburn J, et al. Abnormal angiogenesis in blood outgrowth endothelial cells derived from von Willebrand disease patients. Blood Coagul Fibrinolysis. 2017;28(7):521-33.
29. Starke RD, Paschalaki KE, Dyer CE, Harrison-Lavoie KJ, Cutler JA, McKinnon TA, et al. Cellular and molecular basis of von Willebrand disease: studies on blood outgrowth endothelial cells. Blood. 2013;121(14):2773-84.
30. Laan SNJ, Lenderink BG, Eikenboom JCJ, Bierings R. Endothelial colony-forming cells in the spotlight: insights into the pathophysiology of von Willebrand disease and rare bleeding disorders. Journal of Thrombosis and Haemostasis. 2024;22(12):3355-65.
31. Bar I, Barraclough A, Burgisser PE, van Kwawegen C, Fijnvandraat K, Eikenboom JCJ, et al. The severe von Willebrand disease variant p.M771V leads to impaired anterograde trafficking of von Willebrand factor in patient-derived and base-edited endothelial colony-forming cells. J Thromb Haemost. 2024.
32. de Wee EM, Sanders YV, Mauser-Bunschoten EP, van der Bom JG, Degenaar-Dujardin ME, Eikenboom J, et al. Determinants of bleeding phenotype in adult patients with moderate or severe von Willebrand disease. Thromb Haemost. 2012;108(4):683-92.
33. Rodeghiero F, Tosetto A, Abshire T, Arnold DM, Coller B, James P, et al. ISTH/SSC bleeding assessment tool: a standardized questionnaire and a proposal for a new bleeding score for inherited bleeding disorders. J Thromb Haemost. 2010;8(9):2063-5.

34. de Boer S, Bowman M, Notley C, Mo A, Lima P, de Jong A, et al. Endothelial characteristics in healthy endothelial colony forming cells; generating a robust and valid ex vivo model for vascular disease. J Thromb Haemost. 2020;18(10):2721-31.
35. Laan SNJ, de Boer S, Dirven RJ, van Moort I, Kuipers TB, Mei H, et al. Transcriptional and functional profiling identifies inflammation and endothelial-to-mesenchymal transition as potential drivers for phenotypic heterogeneity within a cohort of endothelial colony forming cells. J Thromb Haemost. 2024;22(7):2027-38.
36. Stirling DR, Swain-Bowden MJ, Lucas AM, Carpenter AE, Cimini BA, Goodman A. CellProfiler 4: improvements in speed, utility and usability. BMC Bioinformatics. 2021;22(1):433.
37. Laan SNJ, Dirven RJ, Bürgisser PE, Eikenboom J, Bierings R. Automated segmentation and quantitative analysis of organelle morphology, localization and content using CellProfiler. PLoS One. 2023;18(6):e0278009.
38. de Jong A, Weijers E, Dirven R, de Boer S, Streur J, Eikenboom J. Variability of von Willebrand factor-related parameters in endothelial colony forming cells. J Thromb Haemost. 2019;17(9):1544-54.
39. Groten SA, Smit ER, van den Biggelaar M, Hoogendijk AJ. The proteomic landscape of in vitro cultured endothelial cells across vascular beds. Commun Biol. 2024;7(1):989.
40. Skowronek P, Thielert M, Voytik E, Tanzer MC, Hansen FM, Willems S, et al. Rapid and In-Depth Coverage of the (Phospho-)Proteome With Deep Libraries and Optimal Window Design for dia-PASEF. Molecular & Cellular Proteomics. 2022;21(9):100279.
41. Martin Maechler PR, Anja Struyf, Mia Hubert, Kurt Hornik. cluster: Cluster Analysis Basics and Extensions 2023 [Available from: https://CRAN.R-project.org/package=cluster.
42. Ritchie ME, Phipson B, Wu D, Hu Y, Law CW, Shi W, et al. limma powers differential expression analyses for RNA-sequencing and microarray studies. Nucleic Acids Res. 2015;43(7):e47.
43. Phipson B, Lee S, Majewski IJ, Alexander WS, Smyth GK. Robust Hyperparameter Estimation Protects against Hypervariable Genes and Improves Power to Detect Differential Expression. Ann Appl Stat. 2016;10(2):946-63.
44. F HJ. Hmisc: Harrell Miscellaneous. R package version 5.1-4. 2024.
45. Yu G, Wang LG, Han Y, He QY. clusterProfiler: an R package for comparing biological themes among gene clusters. Omics. 2012;16(5):284-7.
46. James PD, Connell NT, Ameer B, Di Paola J, Eikenboom J, Giraud N, et al. ASH ISTH NHF WFH 2021 guidelines on the diagnosis of von Willebrand disease. Blood Adv. 2021;5(1):280-300.
47. Sanders YV, Giezenaar MA, Laros-van Gorkom BA, Meijer K, van der Bom JG, Cnossen MH, et al. von Willebrand disease and aging: an evolving phenotype. J Thromb Haemost. 2014;12(7):1066-75.
48. Rydz N, Grabell J, Lillicrap D, James PD. Changes in von Willebrand factor level and von Willebrand activity with age in type 1 von Willebrand disease. Haemophilia. 2015;21(5):636-41.
49. Atiq F, Blok R, van Kwawegen CB, Doherty D, Lavin M, van der Bom JG, et al. Type 1 VWD classification revisited: novel insights from combined analysis of the LoVIC and WiN studies. Blood. 2024;143(14):1414-24.
50. Starke RD, Ferraro F, Paschalaki KE, Dryden NH, McKinnon TA, Sutton RE, et al. Endothelial von Willebrand factor regulates angiogenesis. Blood. 2011;117(3):1071-80.
51. Groeneveld DJ, van Bekkum T, Dirven RJ, Wang JW, Voorberg J, Reitsma PH, et al. Angiogenic characteristics of blood outgrowth endothelial cells from patients with von Willebrand disease. J Thromb Haemost. 2015;13(10):1854-66.

52. Dai Y, Hu R, Liu A, Cho KS, Manuel AM, Li X, et al. WebCSEA: web-based cell-type-specific enrichment analysis of genes. Nucleic Acids Research. 2022;50(W1):W782-W90.
53. Harvey NL, Srinivasan RS, Dillard ME, Johnson NC, Witte MH, Boyd K, et al. Lymphatic vascular defects promoted by Prox1 haploinsufficiency cause adult-onset obesity. Nature Genetics. 2005;37(10):1072-81.
54. Wigle JT, Oliver G. Prox1 function is required for the development of the murine lymphatic system. Cell. 1999;98(6):769-78.
55. Chen JM, Luo B, Ma R, Luo XX, Chen YS, Li Y. Lymphatic Endothelial Markers and Tumor Lymphangiogenesis Assessment in Human Breast Cancer. Diagnostics (Basel). 2021;12(1).
56. Zografou S, Basagiannis D, Papafotika A, Shirakawa R, Horiuchi H, Auerbach D, et al. A complete Rab screening reveals novel insights in Weibel-Palade body exocytosis. J Cell Sci. 2012;125(Pt 20):4780-90.
57. Bierings R, Hellen N, Kiskin N, Knipe L, Fonseca AV, Patel B, et al. The interplay between the Rab27A effectors Slp4-a and MyRIP controls hormone-evoked Weibel-Palade body exocytosis. Blood. 2012;120(13):2757-67.
58. Knop M, Aareskjold E, Bode G, Gerke V. Rab3D and annexin A2 play a role in regulated secretion of vWF, but not tPA, from endothelial cells. Embo j. 2004;23(15):2982-92.
59. van Breevoort D, van Agtmaal EL, Dragt BS, Gebbinck JK, Dienava-Verdoold I, Kragt A, et al. Proteomic Screen Identifies IGFBP7 as a Novel Component of Endothelial Cell-Specific Weibel-Palade Bodies. Journal of Proteome Research. 2012;11(5):2925-36.
60. Yamazaki Y, Eura Y, Kokame K. V-ATPase V0a1 promotes Weibel-Palade body biogenesis through the regulation of membrane fission. Elife. 2021;10.
61. Terglane J, Menche D, Gerke V. Acidification of endothelial Weibel-Palade bodies is mediated by the vacuolar-type H+-ATPase. PLoS One. 2022;17(6):e0270299.
62. Medina RJ, O'Neill CL, O'Doherty TM, Chambers SE, Guduric-Fuchs J, Neisen J, et al. Ex vivo expansion of human outgrowth endothelial cells leads to IL-8-mediated replicative senescence and impaired vasoreparative function. Stem Cells. 2013;31(8):1657-68.
63. Smadja DM, Bièche I, Uzan G, Bompais H, Muller L, Boisson-Vidal C, et al. PAR-1 activation on human late endothelial progenitor cells enhances angiogenesis in vitro with upregulation of the SDF-1/CXCR4 system. Arterioscler Thromb Vasc Biol. 2005;25(11):2321-7.
64. Bompais H, Chagraoui J, Canron X, Crisan M, Liu XH, Anjo A, et al. Human endothelial cells derived from circulating progenitors display specific functional properties compared with mature vessel wall endothelial cells. Blood. 2004;103(7):2577-84.
65. Dejana E, Hirschi KK, Simons M. The molecular basis of endothelial cell plasticity. Nature Communications. 2017;8(1):14361.
66. Potente M, Mäkinen T. Vascular heterogeneity and specialization in development and disease. Nature Reviews Molecular Cell Biology. 2017;18(8):477-94.
67. Wigle JT, Harvey N, Detmar M, Lagutina I, Grosveld G, Gunn MD, et al. An essential role for Prox1 in the induction of the lymphatic endothelial cell phenotype. Embo j. 2002;21(7):1505-13.
68. Kilic N, Oliveira-Ferrer L, Neshat-Vahid S, Irmak S, Obst-Pernberg K, Wurmbach J-H, et al. Lymphatic reprogramming of microvascular endothelial cells by CEA-related cell adhesion molecule-1 via interaction with VEGFR-3 and Prox1. Blood. 2007;110(13):4223-33.

69. HICKSON N, HAMPSHIRE D, WINSHIP P, GOUDEMAND J, SCHNEPPENHEIM R, BUDDE U, et al. von Willebrand factor variant p.Arg924Gln marks an allele associated with reduced von Willebrand factor and factor VIII levels. Journal of Thrombosis and Haemostasis. 2010;8(9):1986-93.
70. Yin J, Ma Z, Su J, Wang J-W, Zhao X, Ling J, et al. Mutations in the D1 domain of von Willebrand factor impair their propeptide-dependent multimerization, intracellular trafficking and secretion. Journal of Hematology & Oncology. 2015;8(1):73.
71. Penas N, Pérez-Rodríguez A, Torea JH, Lourés E, Noya MS, López-Fernández MF, et al. von Willebrand disease R1374C: type 2A or 2M? A challenge to the revised classification. High frequency in the northwest of Spain (Galicia). Am J Hematol. 2005;80(3):188-96.
72. Smith NL, Chen MH, Dehghan A, Strachan DP, Basu S, Soranzo N, et al. Novel associations of multiple genetic loci with plasma levels of factor VII, factor VIII, and von Willebrand factor: The CHARGE (Cohorts for Heart and Aging Research in Genome Epidemiology) Consortium. Circulation. 2010;121(12):1382-92.
73. Sanders YV, van der Bom JG, Isaacs A, Cnossen MH, de Maat MP, Laros-van Gorkom BA, et al. CLEC4M and STXBP5 gene variations contribute to von Willebrand factor level variation in von Willebrand disease. J Thromb Haemost. 2015;13(6):956-66.
74. van Loon JE, Leebeek FW, Deckers JW, Dippel DW, Poldermans D, Strachan DP, et al. Effect of genetic variations in syntaxin-binding protein-5 and syntaxin-2 on von Willebrand factor concentration and cardiovascular risk. Circ Cardiovasc Genet. 2010;3(6):507-12.
75. Drakeford C, Aguila S, Roche F, Hokamp K, Fazavana J, Cervantes MP, et al. von Willebrand factor links primary hemostasis to innate immunity. Nature Communications. 2022;13(1):6320.
76. Cnossen MH, van Moort I, Reitsma SH, de Maat MPM, Schutgens REG, Urbanus RT, et al. SYMPHONY consortium: Orchestrating personalized treatment for patients with bleeding disorders. J Thromb Haemost. 2022;20(9):2001-11.

Supplemental table 1. Antibodies used in immunofluorescence

Antibody	Manufacturer	Category number	Concentration	Dilution
IF Primary antibodies				
VWF (Rabbit)	DAKO	A0082	4.1 mg/mL	1:1,000
VE-cadherin (Mouse)	BD Pharming	555661	0.5 mg/mL	1:250
VWF (Sheep)	Abcam	AB11743	1 mg/mL	1:1,000
PDI (Rabbit)	Enzo life sciences	SPA-890	1 mg/mL	1:250
Hoechst	Thermo Fisher Scientific	H3569	10 mg/mL	1:10,000
IF Secondary antibodies				
Donkey-anti-Sheep AF488	Invitrogen Molecular Probes	A11015	2 mg/mL	1:750
Donkey-anti-Mouse AF488	Invitrogen Molecular Probes	A21202	2 mg/mL	1:750
Donkey-anti-Mouse AF568	Invitrogen Molecular Probes	A10037	2 mg/mL	1:750
Donkey-anti-Rabbit AF647	Invitrogen Molecular Probes	A31573	2 mg/mL	1:750

Abbreviations: Von Willebrand Factor (VWF), Immunofluorescence (IF)

Supplemental table 2. Primer sequences used for the qPCR panel

Gene	Sense	Anti-sense
GAPDH	ACCATCTTCCAGGAGCGAGA	GACTCCACGACGTACTCAGC
RAB27A	GAAGCCATAGCACTCGCAGAGA	CAGGACTTGTCCACACACCGTT
SELP	TCCGCTGCATTGACTCTGGACA	CTGAAACGCTCTCAAGGATGGAG
VWF	TTGACGGGGAGGTGAATGTG	ATGTCTGCTTCAGGACCACG
PLAT	TGGTGCTACGTCTTTAAGGCGG	GCTGACCCATTCCCAAAGTAGC
CD63	CAACCACACTGCTTCGATCCTG	GACTCGGTTCTTCGACATGGAAG
ALDH1A1	CGGGAAAAGCAATCTGAAGAGGG	GATGCGGCTATACAACACTGGC
SOX18	GTGTGGGCAAAGGACGAG	GTTCAGCTCCTTCCACGCT
BMP2	TGTATCGCAGGCACTCAGGTCA	CCACTCGTTTCTGGTAGTTCTTC
COL1A1	CAGCCGCTTCACCTACAGC	TTTTGTATTCAATCACTGTCTTGCC
TGFBi	GGACATGCTCACTATCAACGGG	CTGTGGACACATCAGACTCTGC
IFI27	CGTCCTCCATAGCAGCCAAGAT	ACCCAATGGAGCCCAGGATGAA
BST2	TCTCCTGCAACAAGAGCTGACC	TCTCTGCATCCAGGGAAGCCAT
ABI3BP	CCTTCTACACCTAAACGACGCC	GGTGTTGTCCATGTAGGTTCAGG
SERPINE1	CTCATCAGCCACTGGAAAGGCA	GACTCGTGAAGTCAGCCTGAAAC
CXCL8	GAGAGTGATTGAGAGTGGACCAC	CACAACCCTCTGCACCCAGTTT

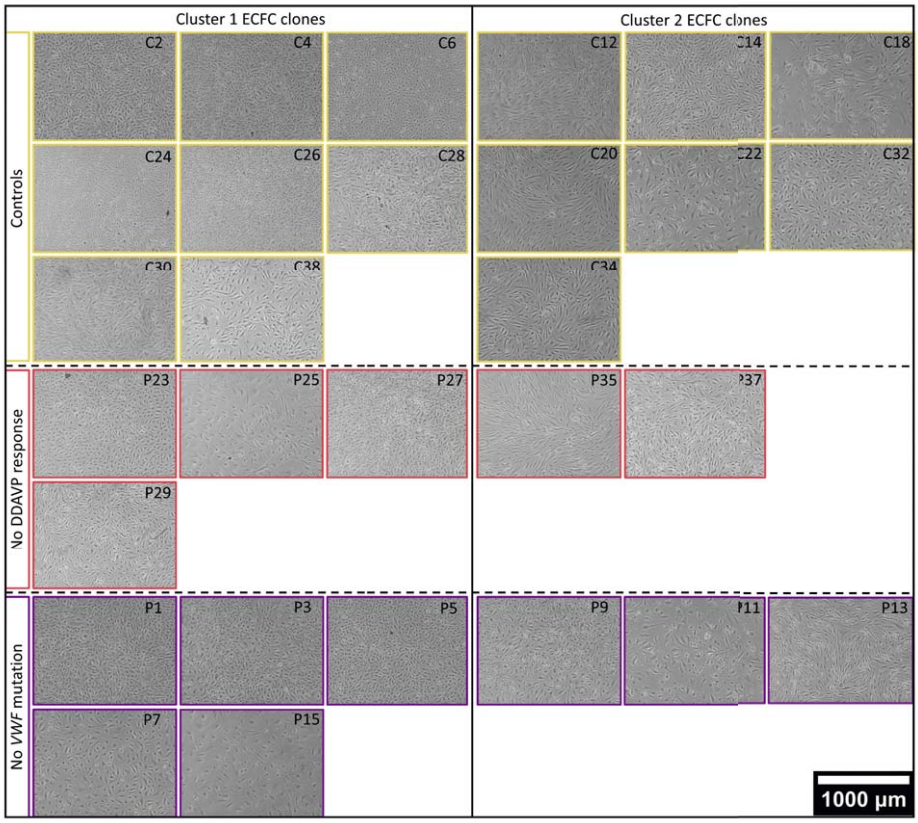

Supplemental Figure 1. Brightfield images of all isolated ECFC clones. Images taken by brightfield microscopy with a 5x magnification. Scale is 1,000 µm. Image border indicates to which group the clone belongs, control (yellow), VWD patients without DDAVP response (red) and VWD patients without VWF variant (purple). Abbreviations: VWF = von Willebrand factor; ECFC = Endothelial colony forming cell; DDAVP = 1-deamino-8-D-arginine vasopressin.

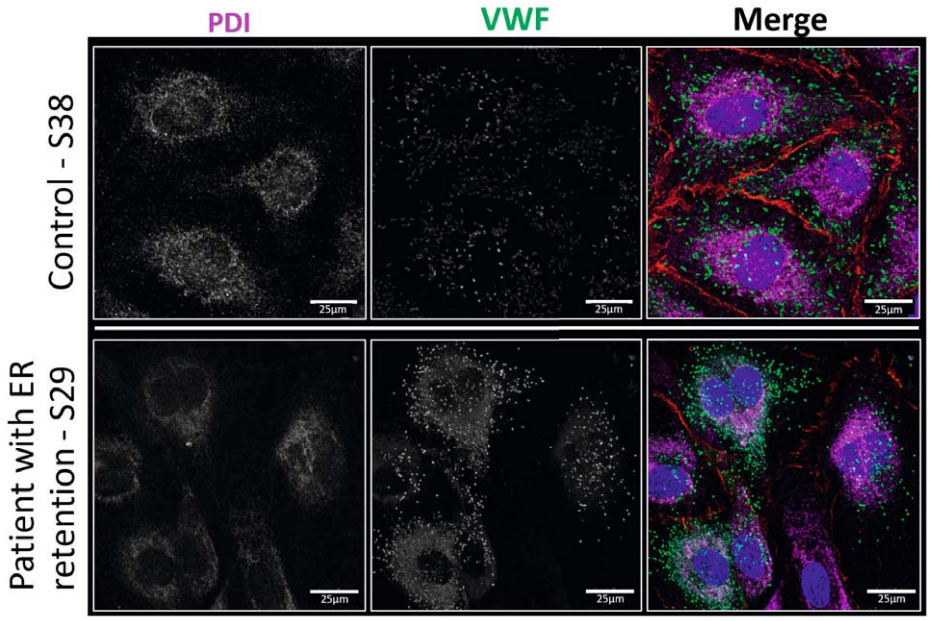

Supplemental Figure 2. Retention of VWF in the ER in representative image. Detailed imaging of ECFCs was done using airyscan super resolution confocal microscopy with a 63x objective. ECFC clones were imaged during the isolation process just before freezing. Representative confocal images of a control ECFC clone (top - S38) and patient ECFCs with retention of VWF in the ER (bottom - S29) stained with Hoechst (blue) and antibodies against VE-cadherin (red), PDI to stain the ER (Magenta) and VWF (green). Scale bar represents 25 µm. In white, the overlap between the VWF and PDI signal is shown. Abbreviations: VWF = von Willebrand factor; PDI = protein disulfide isomerase; ER = endoplasmic reticulum.

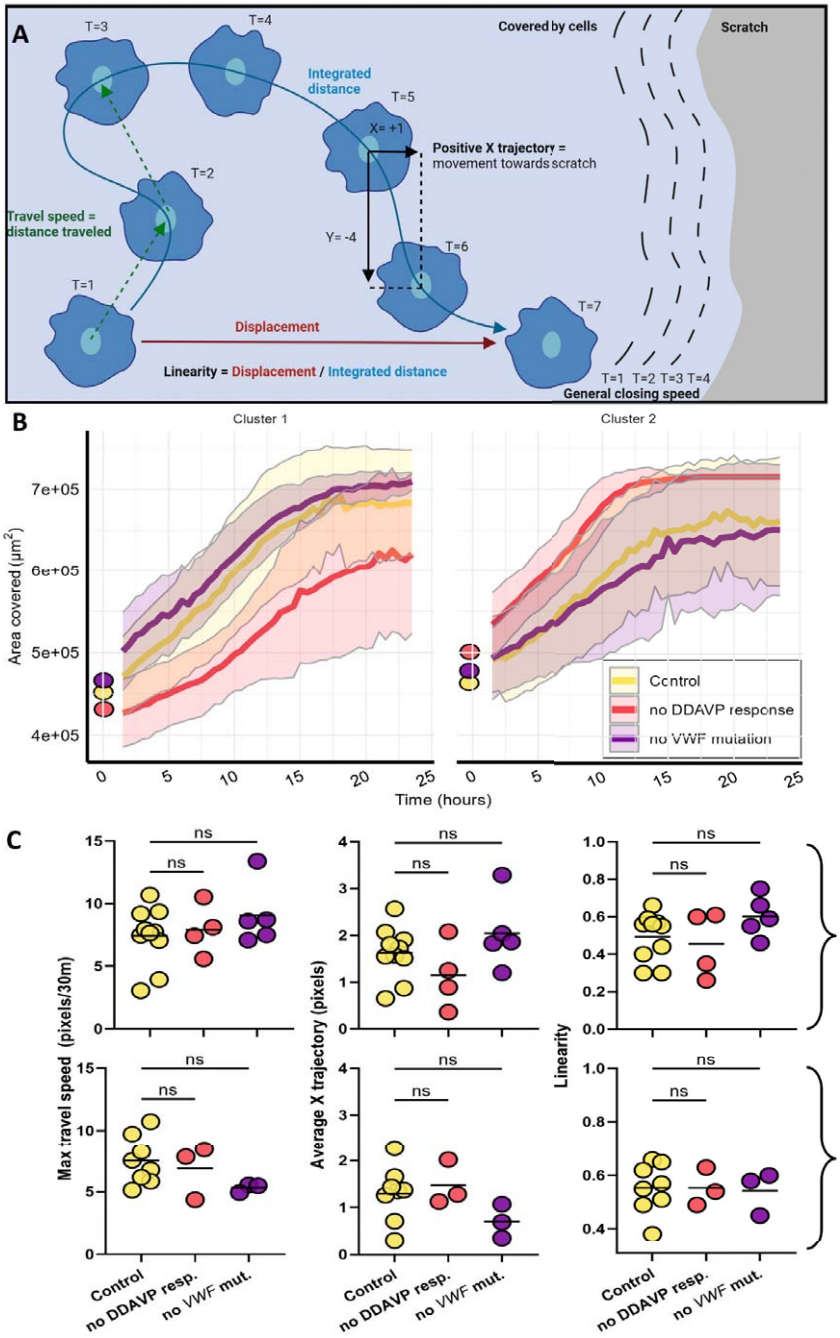

Supplemental Figure 3. ECFC migration analysis shows large variety in speed, direction and linearity. A) Schematic representation of the various parameters measured by the automated quantification pipeline. B) Closing speed of the covered area over 24 hours. Area covered at

t=0 was added as a single data point. Time points 1, 2 and 3 had to be removed due to shifting of the plate during image acquisition. C) Average maximum speed per clone (left), X trajectory (middle) and linearity calculated as displacement / integrated distance (right) for cluster 1 and cluster 2 ECFCs. Statistical analysis by Kruskal-Wallis one way ANOVA, * $p < 0.05$. Abbreviations: DDAVP = 1-deamino-8-D-arginine vasopressin; VWF = von Willebrand factor; ns = not significant.

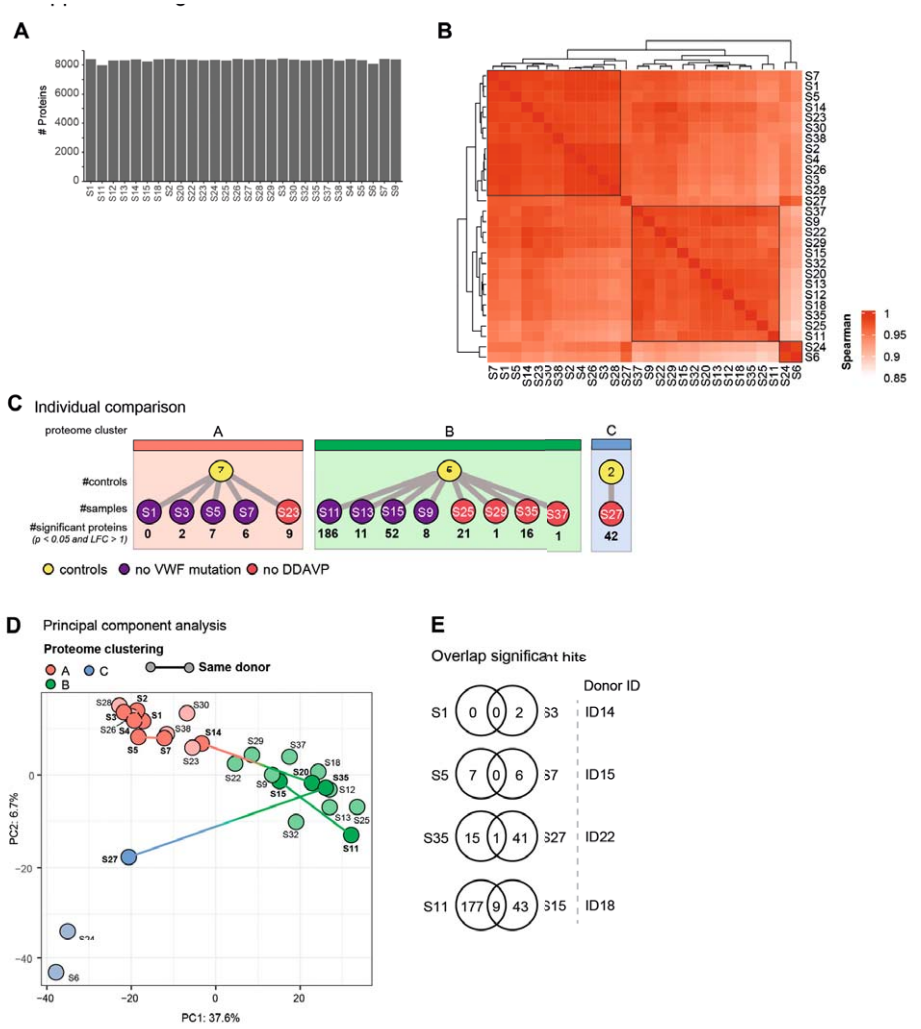

Supplemental Figure 4 A) Bar graph showing number of quantified proteins per sample. B) Heatmap of spearman correlation between samples, three groups are indicated by black squares. Overview of samples and significantly regulated proteins (t-test, $p < 0.05$ and LFC > 1) between C) individual patient ECFC clones versus controls per proteome cluster. D) Principal component analysis (PCA) of proteomes across PC1 and PC2, samples are labeled, clones from the same donor are connected, colors indicate proteome cluster (Cluster A - green, Cluster B – red, Cluster C - blue). E) Overlap in significant hits of ECFCs clones derived from the same donor.

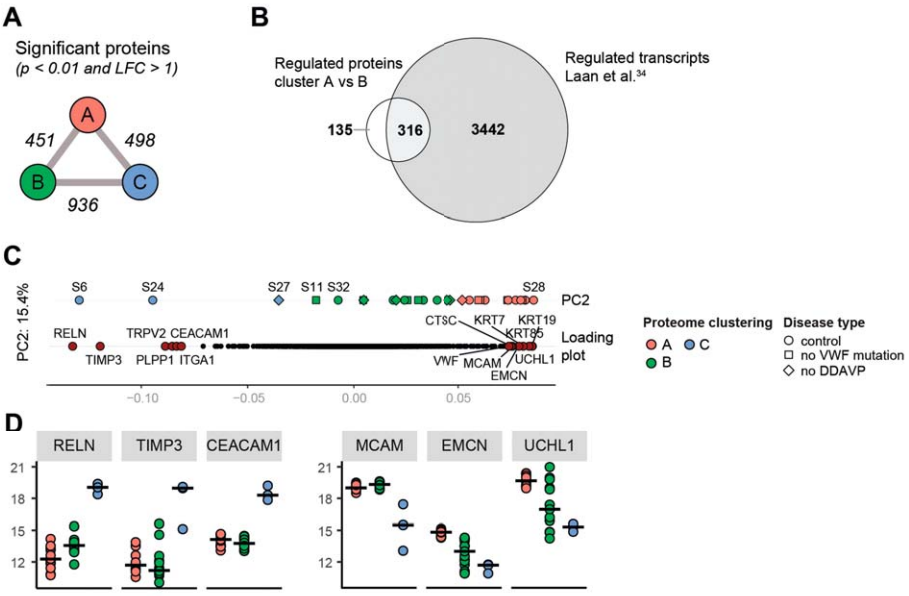

Supplemental Figure 5 A) Number of significant hits (t-test, p value < 0.05, LFC > 1) between proteome clusters as indicated. B) Overlap of significantly regulated proteins between cluster A and B versus regulated transcripts in Laan *et al.* (35) C) Distribution of samples and loading plot across PC2, shape indicates disease type (control – circle, no DDAVP – diamond, no VWF mutation – square). Highest positive and negative separating proteins in the loading plot are highlighted in red and labeled. D) Dot plots of protein LFQ values with high positive and negative separation across PC2.

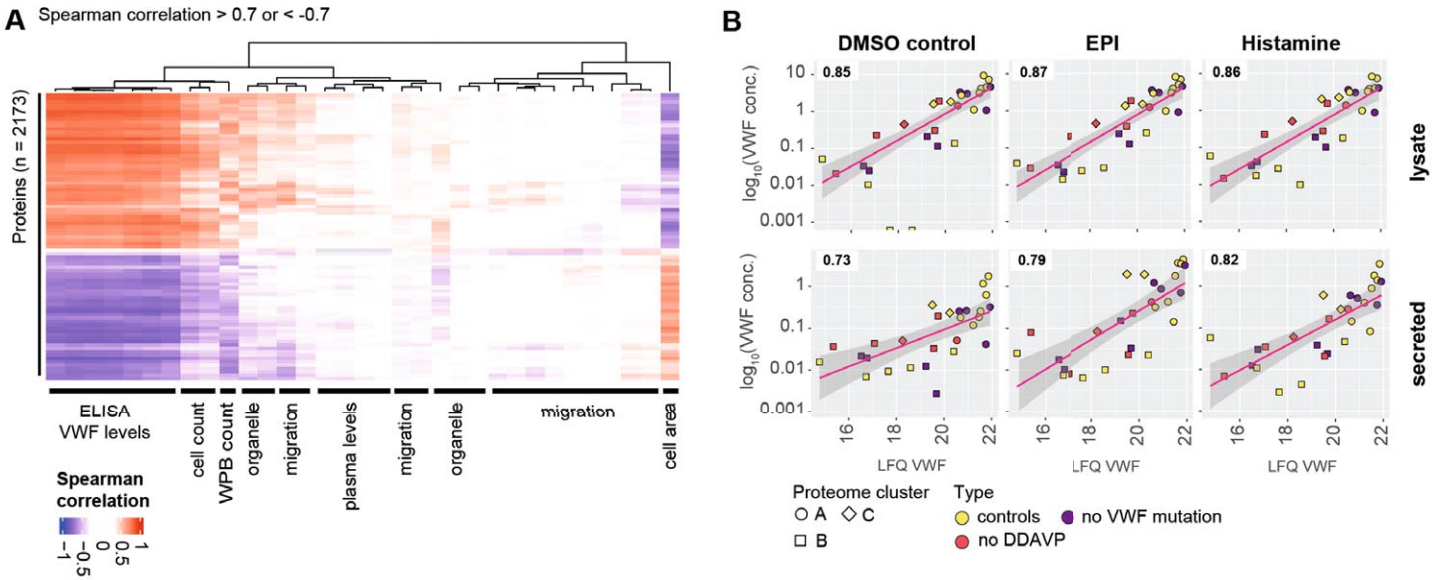

Supplemental Figure 6 A) Heatmap showing protein Spearman correlation > 0.7 between LFQ-levels and functional assay output. Gradient indicates correlation. Functional output terms have been summarized. B) Correlation plots of LFQ levels and ELISA VWF levels in lysates and secreted. Color indicates disease type: controls (yellow), no DDAVP (red) and no VWF mutation (purple), shapes indicate protein cluster: A (circle), B (square) and C (diamond).

Supplementary Methods

Plasma coagulation factor level measurements

VWF:Ag was measured using Polyclonal Rabbit Anti-Human Von Willebrand factor (Agilent Technologies) as coating antibody. Polyclonal Rabbit Anti-Human Von Willebrand factor Horseradish Peroxidase conjugated (Zebra Bioscience (Dako), was used as detection antibody. 2,2′-azino-di-(3-ethylbenzthiazoline sulfonic acid) (ABTS) with 0.1% H_2O_2 was used as substrate buffer and the reaction was stopped by adding 5% acetic acid. Measurement was performed using the Synergy HT gen5TM microplate reader (Biotek). VWF:CB was measured using the HemosIL^{tm} AcuStar system (kit 009802044) as per the manufacturer's protocol. VWF:Act was analyzed with a direct GPIb binding assay (VWF:GPIbM) using the INNOVANCE® VWF Ac (Siemens) as per manufacturer's protocol and measured using the sysmex CN3000 (Siemens). Finally, FVIII coagulation activity was measured by the automated one stage assay on the Sysmex CN3000 with FVIII deficient plasma (Siemens). Commercial pooled plasma (VisuA en VisuN (Stago)) was used as reference.

Automated quantification of ECFC migration

CellTracker Green signal was used to identify and count individual cells per time point in the migration assay. The area that was covered by cells was identified as the total area with cells, while the remaining area was identified as scratch. These parameters were used to calculate the cell density and the closing speed of the scratch. The timepoint where the scratch was closed was defined as the time of closure (ToC). In this study, the pipeline was expanded to include single cell measurements. The TrackObjects module was applied to recognize cell objects over time with a 50 pixel overlap. Objects were filtered out if they were measured in less than 20 frames. Of the tracked objects the displacement, integrated distance, linearity (calculated as displacement / integrated distance), distance traveled (speed), and X and Y trajectory were measured. For displacement, integrated distance and linearity the value at ToC was exported. For distance traveled, the max speed until ToC was exported. Finally, for X and Y trajectory, the average was taken until ToC.

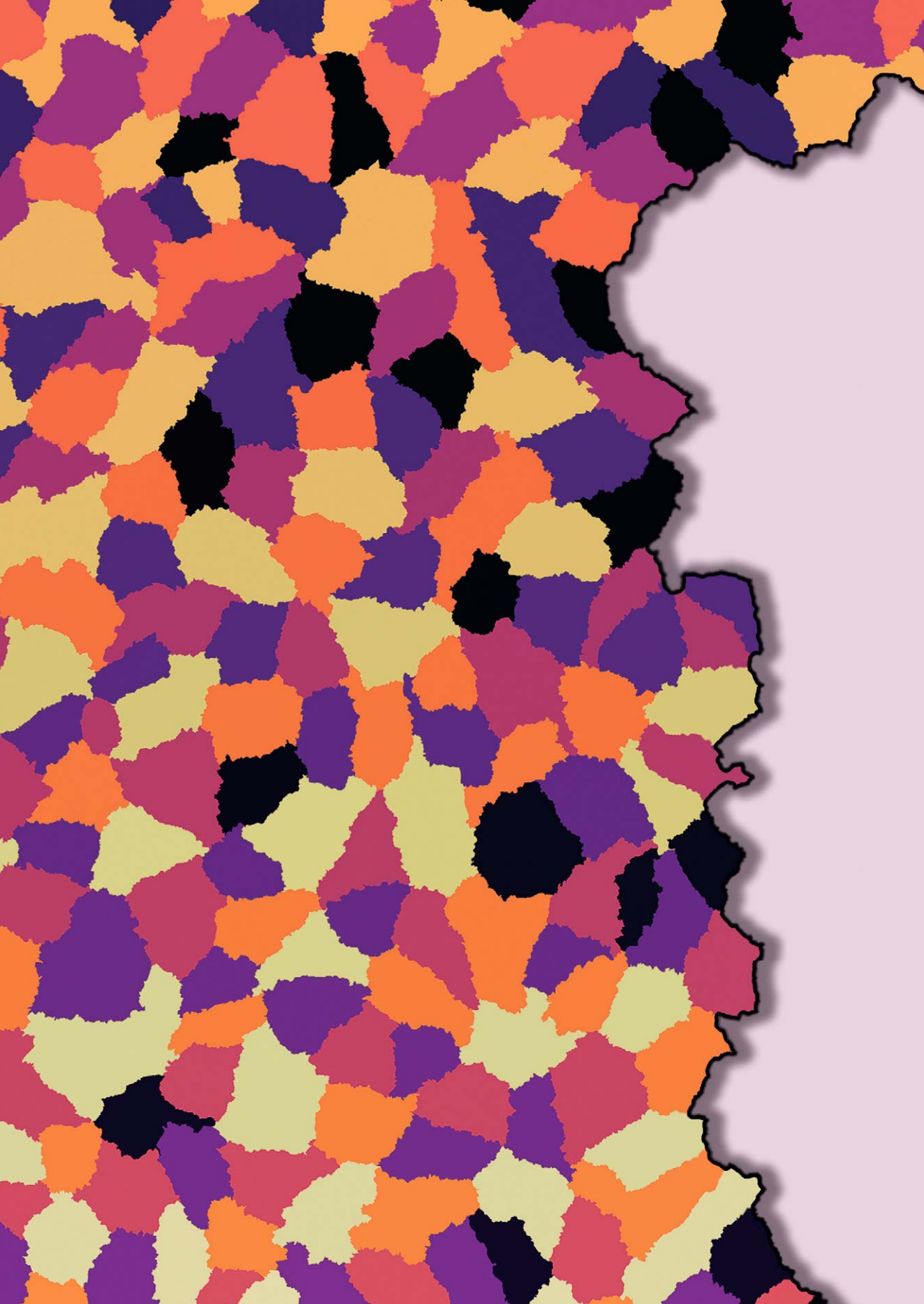

General discussion and perspectives

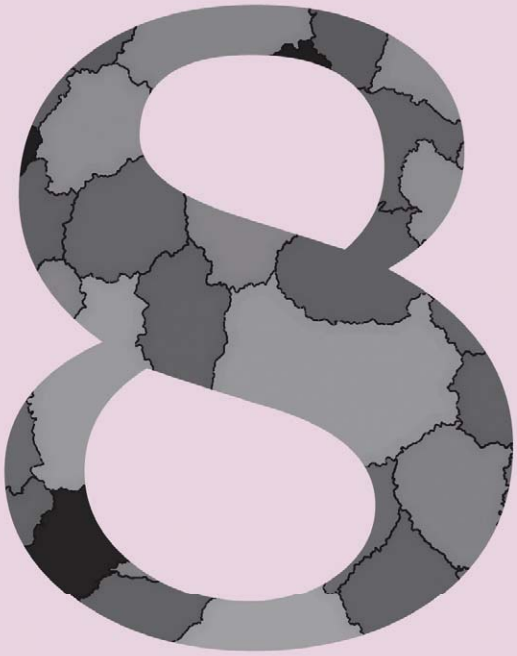

Study objectives

In this thesis, several aspects related to treatment in bleeding disorders, endothelial cell function and endothelial model systems in the context of studying bleeding disorders have been studied. The main aim of this thesis was to find defects in the endothelial secretory pathway that could potentially lead to bleeding which could not be explained through standard clinical testing. Specifically, we investigated patients with von Willebrand disease (VWD) with low von Willebrand factor (VWF) levels without a known pathogenic *VWF* variant or patients with VWD that did not respond to 1-deamino-8-D-arginine vasopressin (DDAVP). We also studied and optimized the method of using the endothelial colony forming cell (ECFC) model for research and how to automatically quantify morphological parameters of those cells. Each of the factors studied in this thesis contribute to our understanding of endothelial cell function in health and disease, but they also raise important questions about the methodologies used, the models chosen, and the future direction of this research which we will discuss here.

Where to look, methods for studying bleeding disorders

Bleeding disorders are complex due to the variety of underlying causes, ranging from genetic mutations to acquired conditions affecting clotting factors, platelets, or the vascular endothelium. For example, VWD is the most common bleeding disorder in humans (1), but it is difficult to diagnose due to multiple assays being needed and variation within those assays. The large heterogeneity and number of mutations or deletions in the *VWF* gene observed within patients further complicate the diagnosis (2). First level diagnostic tests (FVIII:C, VWF:Antigen and VWF:Activity plasma measurements) are performed on patients that present with bleeding symptoms or elevated ISTH-BAT to confirm or reject a VWD diagnosis (3). Second level tests are then performed to determine the subtype of disease. This includes; VWF multimer analysis, VWF:Collagen binding, VWF propeptide and VWF:FVIII binding assays, ristocetin-induced platelet aggregation and genetic testing. These second level tests can give insight into the quantitative or qualitative defects in VWF which allows for more efficient and effective treatment of most patients.

Interestingly, approximately 30-50% of patients with type 1 VWD do not have pathogenic *VWF* gene variants that could explain the lowered levels of VWF (4-6). Although these patients can be treated with factor concentrates or DDAVP (7), current assays and genetic testing often do not fully explain the cause of bleeding in these patients. Furthermore, a substantial portion of patients do not or only partially respond to DDAVP. Several potential determinants for DDAVP response, like disease subtype, mutation, age or blood group (8-17) have been reported, but the cause of the variation is not fully understood. We undertook a systematic review and meta-analysis to elucidate the

rate of response and possible determinants of DDAVP response (**Chapter 6**). We found large differences in response to DDAVP between disease subtypes, which was largely determined by the baseline levels of FVIII:C for Hemophilia A and VWF:Antigen for VWD. The importance of baseline levels of VWF has also been described in other studies. For example, Heijdra *et al.* studied DDAVP response in type 1 VWD patients and concluded that a baseline of 34 IU/dL VWF:Activity or higher will lead to complete response in all patients (18). Clear determinants of response and associated cut-offs can allow clinicians to predict likelihood of response and choose the appropriate medication. A cut-off value based on baseline levels was not determined in our systematic review due to limited individually reported patient data and varying definitions of response. This further emphasizes the need for a standardized definition of response to DDAVP to aid not only clinicians but also fundamental research on DDAVP response. Furthermore, our systematic review highlights that it is still not fully known what determines DDAVP response. It is hypothesized that other modifiers of VWF can cause the low levels and associated bleeding in patients without a *VWF* defect (19). Potentially, modifiers of VWF could also play a role in the response to DDAVP and cause non-response in patients. Further testing on these cohorts that could identify these modifiers is thus needed.

Broad, unbiased methods and studies are effective in finding potential candidates, but not for functional validation of those candidates. Luckily, various *in vivo* and *in vitro* models exist that are used to study VWF and VWD (20). Naturally occurring VWD has been described in mammals such as dogs and pigs (21-23), which offered valuable insight by studying the disease in a complete system. Although, cost of housing limited the use of these models. Mouse VWD models offer a cheaper, easier to handle model but have the challenge of small blood volumes and vessel which make experimentation more difficult (24). Alternatively, a rat VWD model can be used which offers relatively simple housing and larger blood volume than mice (25). VWF can also be expressed in non-endothelial cell types to study pathogenic *VWF* variants and their effect on VWF biosynthesis, storage and secretion (26). However, those models lack endothelial cell specific gene expression and thus lack a true endothelial environment. Unfortunately, none of the models mentioned above could be used in this thesis as they all require knowledge of the pathogenic variant of VWF or other factor that causes the unexplained low levels of VWF or non-response to DDAVP in our patient cohort. It is therefore almost inevitable to analyze the endothelial cells from the patients themselves.

Looking inside, endothelial cell models with intrinsic patient characteristics

Patient endothelial cells can be isolated via invasive surgery or they can be derived directly from whole blood. This can be done by differentiating late appearing endothelial progenitor cells into ECFCs (27) or by reprogramming peripheral blood mononuclear

cells (PBMCs) into induced pluripotent stem cells (iPSCs) and then differentiating those into iPSC endothelial cells (iPSC-ECs) (28). These are excellent model systems to investigate vascular defects as they carry the mutation(s) of the patient (27) and have been used to study pathogenic disease mechanisms (**Chapter 2**). In this thesis we extensively tested ECFCs derived from patients with VWD with either no *VWF* mutation or no response to DDAVP (**Chapter 7**). In three of those patients, clear retention of VWF in the endoplasmic reticulum was found. These three patients all have known *VWF* mutations. In patients carrying the p.Arg924Gln or p.Arg1374Cys mutation, ER retention of VWF had not been described before (29, 30) and was thus a novel finding. For the other patient, carrying both p.Asp141Asn and p.Arg2313Cys mutations, ER retention had been previously shown in HEK293 cells transfected with the p.Asp141Asn mutation (31). Although the retention of VWF can explain the non-response to DDAVP in these patients, it is still unclear what causes the retention. Proteomic analysis on these cells did not reveal other candidates that hint towards other defects in the early secretory pathway or defects in the synthesis of VWF. To continue this research, the known *VWF* mutation in the ECFCs could be corrected through genetic modification or blocked through the use of allele-specific small-interfering RNA (32). Alternatively, through a recently published novel approach, the mutation can be introduced into healthy ECFCs by base editing to confirm the patient phenotype (33). These methods could confirm whether the ER retention is caused by the *VWF* mutation or additional factor in these patients.

There were also ECFC clones from which no clear defect was observed that could explain the bleeding phenotype, especially in ECFC derived from patients without *VWF* mutation. In those patients the defect could be present in an aspect of the endothelial compartment that we did not test like the angiogenic capacity, proliferation, apoptosis or endothelial barrier function. However, as the patients reported with lowered VWF levels we did test the aspects most likely to directly or indirectly affect VWF such as; cell and organelle morphology, VWF synthesis, storage and secretion, cell migration and the proteomic signature. Alternatively, lower VWF levels could be caused by something outside of the endothelial cells. For example, in the clearance of VWF which has been shown in VWD patients with gene variations in CLEC4M (34), or in the later functioning in the primary hemostasis. Defects in these cases cannot be detected by solely analyzing the ECFCs of these patients. In future research we could use models that allow for a more complete analysis of the endothelial function like the vessel-on-a-chip model (35) or the even more intricate hemostasis-on-a-chip model (36). These models allow the simulation of endothelial injury and hemostatic plug formation. A specific example of the hemostasis-on-a-chip, developed by Lam *et al.* (37) is currently being tested with healthy control- and patient-derived ECFCs (data not published). These models can

give crucial insight into the interplay between plasma, endothelial cells, platelets and hemodynamic forces which conventional 2D cell cultures lack.

Alternatively, modifiers of VWF can be found through genome wide association studies (GWAS). Previous GWAS have studied genetic determinants of VWF levels and found a correlation between VWF levels and variants in *VWF*, ABO and genes encoding for WPB secretory machinery components like *STXBP5* and *STX2* (38, 39). The latter have been shown to play an important role in the secretion of WPBs (34, 40). In line with these findings, we found a positive correlation between the quantity of WPBs and secreted VWF in ECFCs and several secretory pathway components such as VWF, Rab27A, Rab3D (41), and SYTL4 (42) (**Chapter 6**). This suggests that the exocytosis machinery of WPB is important in the regulation of VWF levels and should be further studied as it could contain other modifiers of VWF levels. Alternatively, the plasma proteome can be analyzed (43). The plasma proteome contains coagulation factors and secreted proteins by cells. Plasma proteomics has previously been used to identify proteoforms of VWF to aid in VWD diagnostics (44). In patients with unexplained bleeding, the cause could lie in the clearance of coagulation factor levels, or the lack of certain secreted factors. Plasma proteomics could give insight into those aspects. Furthermore, the role of platelets can be analyzed by performing platelet proteomics (45). A next step forward could be to perform plasma proteomics in the patients cohorts also included in this thesis.

Weighing the odds, the challenges of the ECFC model

In previous research, and in this thesis, ECFCs have been shown to be a powerful tool to investigate patient specific defects (**Chapter 2**). However, some challenges regarding their intra- and interindividual phenotypic heterogeneity must be addressed. Firstly, the availability and expansion capacity of ECFCs can be problematic. About 45-70% of all attempts to obtain ECFCs from whole blood are successful (46), which is in line with the success rate of our lab. Secondly, this success rate is further exasperated by situations where repeated isolations are not possible due to patients age or health, or by limited blood volume being available for collection in children. Thirdly is the observed heterogeneity in morphology, proliferation and endothelial markers (47, 48). Using the specifically developed automated quantification pipeline (**Chapter 3**) we showed significant differences in cell size, WPB quantity and shape, and migratory cell speed between ECFC clones. Furthermore, between healthy control-derived ECFCs we found distinct differences between clones based on their transcriptome (**Chapter 4**). The difference between these clusters yielded new insights into the potential cause of heterogeneity as we showed that inflammation and endothelial to mesenchymal transition (EndoMT) may act as potential drivers. Specifically, we showed that *CXCL8*

(IL-8*), TGFBi, TGFB2, BMP2* and *SMAD1* were differentially regulated between ECFC clones, which are pro-inflammatory (49) or EndoMT associated genes (50). Collectively, our transcriptional, morphological and functional data was used to categorize ECFCs as either cluster 1 with a standard endothelial morphology, and cluster 2, which presented with large, more mesenchymal like cells. We also measured this difference in the proteome of a different cohort of control and patient ECFCs further supporting this observation. To deal with this heterogeneity, we developed a qPCR panel based on the transcriptomic signature of the ECFCs that can aid other researchers.

This panel does however, not fix or prevent the heterogeneity from occurring. One of the potential drivers of heterogeneity is EndoMT which is the transformation of endothelial to mesenchymal cells. This results in loss of endothelial markers, reduced VWF synthesis and increase in extracellular matrix proteins (51-54). It has also been shown that inflammation can cause EndoMT in endothelial cells (55-57). We speculated that the expression of inflammatory and EndoMT associated genes is part of an autocrine/paracrine loop that could initiate or maintain the change from cluster 1 to cluster 2 ECFCs. We performed a pilot experiment on the secretome of a small subset of healthy ECFC clones in cluster 1 and cluster 2 (data not shown). We observed that cluster 1 ECFCs secreted more VWF while cluster 2 ECFCs secreted higher levels of EndoMT and inflammation markers ABI3BP, SERPINE1 and IL-8. However, this has to be confirmed with further testing before conclusions can be drawn. The insight that inflammation and EndoMT could drive the phenotypic differences between ECFC clones offers an interesting new direction of research. Members of the transforming growth factor (TGF)-β cytokine superfamily and bone morphogenetic proteins (BMPs) play a crucial role in EndoMT (58). TGF-β has been shown to be a potent inducer of EndoMT (59). Furthermore, it has been shown that inhibition of TGF-β by inhibitors significantly increased endothelial cell function, delayed cellular senescence and increased proliferation in human iPSC-ECs (60). Therefore, we attempted to induce and inhibit EndoMT in ECFC derived from healthy controls (data not published, performed by Britte Lenderink). We exposed a small panel of cluster 1 ECFCs clones (C10 and C22) and cluster 2 ECFC clones (C05 and C07) to EndoMT inducers (TGF-β2) or inhibitors (TGF-βi). We observed that TGF-βi caused slightly higher production of VWF in cluster 1 ECFCs as measured by ELISA in the lysates of the cells compared to the control (Figure 1). Cluster 2 ECFCs did not show any clear changes. Furthermore, ECFCs expressed a more cluster 1-like RNA expression pattern after TGF-βi exposure (data not shown). This suggests that ECFCs might be affected and even improved through this method. However, this pilot has to be repeated with a larger panel of ECFCs, optimizing the dose and duration of exposure and testing various functional assays. Control over ECFC morphology or potentially only generating cluster 1 ECFCs would greatly reduce the

heterogeneity between clones, which is especially useful in cases where there is a low yield of clones or only slowly proliferating clones. Another option to improve the use of slowly proliferating clones would be the immortalization of the cells. Telomerase activity can be prolonged through nucleofection using SV40 large T antigen which has been shown to effectively immortalize human umbilical vein endothelial cells (HUVEC) (61, 62) and chicken intestinal epithelial cells (63) while retaining their normal phenotype. This has been shown in a pilot experiment to effectively prolong the normal phenotype in ECFCs until ~passage 11 after transfection. (Isabel Bär, personal communication). Alternatively, cord-blood (CB) ECFCs have been shown to have significantly higher proliferation rate and remain stable for more passages when compared to whole blood derived ECFCs (46). However, these can only be derived from possible new-born patients if the mother has been diagnosed before or during the pregnancy.

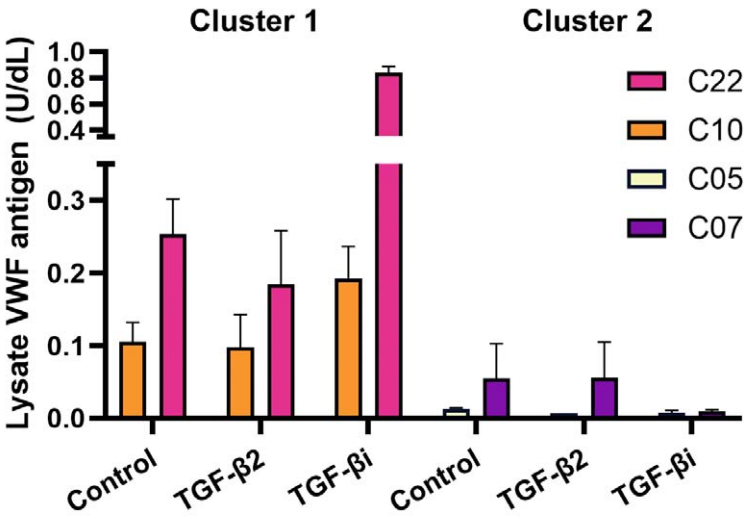

Figure 1. VWF production increased in ECFCs after exposure to EndoMT ligands and inhibitors. VWF antigen levels were determined by ELISA in ECFC lysate after exposure to ligands and inhibitors for 6 days. Abbreviations: von Willebrand factor, VWF; Transforming Growth Factor, TGF. Figure adjusted from data generated by Britte Lenderink.

iPSC-ECs versus ECFCs, which is better?

Other models, such as using iPSCs to generate iPSC-ECs, provide an alternative way to analyze endothelial pathology in cells that carry the patient mutation (64). ECFCs can be difficult to acquire due to a low success rate or limited patient material as previously mentioned. However, iPSCs can be generated from almost any somatic cell type in about 8-10 days and are capable of self-renewal (64). This allows iPSCs

to be acquired despite limited material and can be quickly expanded to very large amounts. IPSCs have the potential to differentiate into many cell types like erythroid, megakaryocytic, myeloid cells (65, 66) or endothelial cells, called iPSC-ECs (67-69). Generated iPSC-ECs have typical endothelial like characteristics and have been shown to produce and secrete VWF (70). However, levels of VWF production in iPSC-ECs are significantly lower than in ECFCs. iPSC-ECs thus lack some of the phenotypic and functional maturity of ECFCs, particularly in producing fully formed WPBs. We showed that small adjustments to existing protocols partially improve the VWF production and elongation of WPBs, although still significantly less than ECFCs (**Chapter 5**). Maturation of WPBs in iPSC-EC is thus a hurdle that must be overcome to use the model in VWF and VWD focused research. Interestingly, it has been shown that the donor cell type influences the epigenome of iPSCs (71) suggesting that the donor material could influence the differentiation of iPSCs. Indeed, one study did show elongated WPBs in iPSC-ECs which were generated from HUVECs (72) although iPSC-EC derived from CB-ECFCs did not seem to produce typical elongated WPBs (73). Thus, starting material could have beneficial results in the maturation of WPB in iPSC-EC, but more research on this is needed. Alternatively, EndoMT has been shown to occur at later passages in iPSC-ECs (74) and inhibition of TGF-β has shown to increase proliferation in human embryonic stem cell endothelial cells (75). Perhaps control over EndoMT as described earlier could yield interesting results in iPSC-EC as well.

The question of which cell model is best suited for endothelial research is complex and largely depends on the research goals. ECFCs, on the one hand, have the advantage of being representative of a mature endothelial state and fully formed WPBs, but present with various challenges in heterogeneity that need be taken into account. On the other hand, iPSC-ECs offer scalability and versatility but do not fully represent normal VWF production and secretion. Ultimately, the research question determines which model is best used and in this thesis, where the production, storage and secretion of VWF is key, the ECFCs take the crown.

How to look, Quantitative imaging and the role of artificial intelligence

One widely used method of analyzing cells and tissues is microscopy. Ranging from relatively simple light microscopy to intricate Cryo-confocal or electron microscopy. These techniques yield insight into the inner workings of cells, protein location and shape and number of organelles. Qualitative observations can be easily made by viewing the output. However, considerable heterogeneity exists between cells and their contents, which can make subsequent analysis difficult and prone to subjective bias (76). Especially the crowded intracellular environment in combination with optical and immunostaining limitations presents an additional, technical challenge. Therefore,

quantification of parameters is usually performed using automated methods to reduce bias and improve the quality of the results.

There are several methods available for the quantification of cellular structures. For instance, Fiji (ImageJ) can make adjustments and measurements to images and allows the use of macros to automate image analysis (77). Other, more specialized software such as CellProfiler offer a more user-friendly module-based approach for high-throughput image analysis (78). Additionally, programs within Python, such as scikit-image are widely used for customized analysis pipelines and allow the user full control and even add functionalities (79). In this thesis we describe a method for automatically quantifying WPBs in ECFCs using CellProfiler (**Chapter 3**). We developed this pipeline with the quantification of WPBs and our own research in mind but it can also be used for other cell types and other organelles. We opted to make this pipeline in CellProfiler, instead of for example ImageJ, so that other groups could easily use and adjust the pipeline method without the need to understand and adjust the underlying code/macro. Despite optimization of software parameters, perfect identification of targets is not always possible. These imperfections may lead to incorrect identification of targets, which could lead to over- or underestimations of numbers and dimensions. Another challenge often encountered in image quantification is that the images are not perfectly suited for analysis due to, for example, inconsistent sample preparation, varying laser settings, or different operators. These variations can lead to small but significant differences between images. It is therefore important that a bioimaging experiment is well thought out before the microscope comes into play (80).

Recent advancements in the use of artificial intelligence (AI) in the field of imaging offer a solution to these problems. AI can "learn" to accurately characterize images through neural network training if supplied with a large, high-quality dataset. There has been considerable progress in the development and application of various AI-based tools that are now available for public use (81). AI is already being used in this field in the diagnosis, prognosis, and distribution of various types of thrombocytopenia (82), diagnostic testing for hematologic Disorders (83) and in analysis of endothelial cells (84, 85). While AI is undoubtedly a hot topic, it's important to recognize its limitations. AI models require large, high-quality datasets for training which are not always available in rare disease research. Another challenge in the use of AI is the "black box" nature of many AI algorithms (86). It is often unclear to the user how AI models analyze features within the images, which makes it difficult for users to trust and/or adjust the models if needed. It is thus needed that the functioning of AI is clearly explained to users. In contrast, traditional image analysis software, such as ImageJ and CellProfiler, offer a more transparent approach from which users can more easily understand the

processing steps being applied to the images. Finally, another aspect of the increasing use of AI that must not be overlooked is the environmental cost (87). Data centers which are needed to run and train AI require vast amounts of energy and water for cooling and are expected to account for over 3% of global carbon emissions in 2025. It is therefore vital that the cost of AI is considered when choosing to use it.

In the context of this thesis, AI could have been used to standardize measurements of endothelial cell function, reducing variability objects and enabling more reliable comparisons across studies. However, considering the complexity, the substantial computing power necessary and the need for a high-quality training data set, the question remains; is it necessary? For many purposes and research questions, an exact answer, or perfectly segmented cells are not necessary. Despite small percentages of false positives or false negatives, strong differences between subsets of data can still be discerned using non-AI tools. To conclude, it is vital for image quantification that the exact question or analysis methods is determined before the microscope is used (80). Furthermore, the use of AI can be a powerful tool to complement traditional methods if needed, but should not be a replacement.

Conclusion

The findings in this thesis contribute to our understanding of endothelial function in bleeding disorders, although there is more to learn. Future research should focus on refining and improving the available endothelial cell models, validating the patient specific defects observed in VWD patients and finally, identify new candidates that could determine VWF levels in VWD patients.

It is important to realize that the isolation, culturing and experimentation on iPSC-ECs and ECFCs is challenging and time consuming, although the lessons learned from these models can be invaluable. Despite the in depth, personalized approach to identify determinants of VWF used in this thesis, many patients remain without a clear cause of either low VWF levels without *VWF* mutation, or cause of non-response to DDAVP. For those patients and others, a wide scale approach like plasma and platelet proteomics might reveal interesting candidates which can then be further studied in ECFC or iPSC-ECs derived from those patients.

To conclude, the endothelial compartment can be studied on a personal scale, or on a larger, population wide scale to reveal novel insights into disease pathology. A good interplay between these methods is needed and by building on the foundations laid here, we can continue to push the boundaries of endothelial research and its clinical applications.

References

1. Murray EW, Lillicrap D. von Willebrand disease: pathogenesis, classification, and management. Transfus Med Rev. 1996;10(2):93-110.
2. de Jong A, Eikenboom J. Von Willebrand disease mutation spectrum and associated mutation mechanisms. Thromb Res. 2017;159:65-75.
3. Seidizadeh O, Eikenboom JCJ, Denis CV, Flood VH, James P, Lenting PJ, et al. von Willebrand disease. Nature Reviews Disease Primers. 2024;10(1):51.
4. Atiq F, Boender J, van Heerde WL, Tellez Garcia JM, Schoormans SC, Krouwel S, et al. Importance of Genotyping in von Willebrand Disease to Elucidate Pathogenic Mechanisms and Variability in Phenotype. Hemasphere. 2022;6(6):e718.
5. James PD, Notley C, Hegadorn C, Leggo J, Tuttle A, Tinlin S, et al. The mutational spectrum of type 1 von Willebrand disease: Results from a Canadian cohort study. Blood. 2007;109(1):145-54.
6. Lavin M, Aguila S, Schneppenheim S, Dalton N, Jones KL, O'Sullivan JM, et al. Novel insights into the clinical phenotype and pathophysiology underlying low VWF levels. Blood. 2017;130(21):2344-53.
7. Castaman G. How I treat von Willebrand disease. Thromb Res. 2020;196:618-25.
8. Atiq F, Heijdra J, Snijders F, Boender J, Kempers E, van Heerde WL, et al. Desmopressin response depends on the presence and type of genetic variants in patients with type 1 and type 2 von Willebrand disease. Blood Adv. 2022;6(18):5317-26.
9. Biguzzi E, Siboni SM, Peyvandi F. Acquired Von Willebrand syndrome and response to desmopressin. Haemophilia. 2018;24(1):e25-e8.
10. Castaman G, Mancuso ME, Giacomelli SH, Tosetto A, Santagostino E, Mannucci PM, et al. Molecular and phenotypic determinants of the response to desmopressin in adult patients with mild hemophilia A. J Thromb Haemost. 2009;7(11):1824-31.
11. Castaman G, Rodeghiero F. No influence of blood group on the responsiveness to desmopressin in type I "platelet normal" von Willebrand's disease. Thromb Haemost. 1995;73(3):551-2.
12. Di Perna C, Riccardi F, Franchini M, Rivolta GF, Pattacini C, Tagliaferri A. Clinical efficacy and determinants of response to treatment with desmopressin in mild hemophilia a. Semin Thromb Hemost. 2013;39(7):732-9.
13. Nance D, Fletcher SN, Bolgiano DC, Thompson AR, Josephson NC, Konkle BA. Factor VIII mutation and desmopressin-responsiveness in 62 patients with mild haemophilia A. Haemophilia. 2013;19(5):720-6.
14. Revel-Vilk S, Schmugge M, Carcao MD, Blanchette P, Rand ML, Blanchette VS. Desmopressin (DDAVP) responsiveness in children with von Willebrand disease. J Pediatr Hematol Oncol. 2003;25(11):874-9.
15. Seary ME, Feldman D, Carcao MD. DDAVP responsiveness in children with mild or moderate haemophilia A correlates with age, endogenous FVIII:C level and with haemophilic genotype. Haemophilia. 2012;18(1):50-5.
16. Sharthkumar A, Greist A, Di Paola J, Winay J, Roberson C, Heiman M, et al. Biologic response to subcutaneous and intranasal therapy with desmopressin in a large Amish kindred with Type 2M von Willebrand disease. Haemophilia. 2008;14(3):539-48.

17. Stoof SC, Sanders YV, Petrij F, Cnossen MH, de Maat MP, Leebeek FW, et al. Response to desmopressin is strongly dependent on F8 gene mutation type in mild and moderate haemophilia A. Thromb Haemost. 2013;109(3):440-9.
18. Heijdra JM, Atiq F, Al Arashi W, Kieboom Q, Wuijster E, Meijer K, et al. Desmopressin testing in von Willebrand disease: Lowering the burden. Res Pract Thromb Haemost. 2022;6(6):e12784.
19. Swystun LL, Lillicrap D. Genetic regulation of plasma von Willebrand factor levels in health and disease. J Thromb Haemost. 2018;16(12):2375-90.
20. de Boer S, Eikenboom J. Von Willebrand Disease: From In Vivo to In Vitro Disease Models. Hemasphere. 2019;3(5):e297.
21. French TW, Fox LE, Randolph JF, Dodds WJ. A bleeding disorder (von Willebrand's disease) in a Himalayan cat. J Am Vet Med Assoc. 1987;190(4):437-9.
22. Olsen EH, McCain AS, Merricks EP, Fischer TH, Dillon IM, Raymer RA, et al. Comparative response of plasma VWF in dogs to up-regulation of VWF mRNA by interleukin-11 versus Weibel-Palade body release by desmopressin (DDAVP). Blood. 2003;102(2):436-41.
23. Hogan AG, Muhrer ME, Bogart R. A Hemophilia-Like Disease in Swine. Proceedings of the Society for Experimental Biology and Medicine. 1941;48(1):217-9.
24. Pendu R, Christophe OD, Denis CV. Mouse models of von Willebrand disease. J Thromb Haemost. 2009;7 Suppl 1:61-4.
25. Garcia J, Flood VH, Haberichter SL, Fahs SA, Mattson JG, Geurts AM, et al. A rat model of severe VWD by elimination of the VWF gene using CRISPR/Cas9. Res Pract Thromb Haemost. 2020;4(1):64-71.
26. Michaux G, Hewlett LJ, Messenger SL, Goodeve AC, Peake IR, Daly ME, et al. Analysis of intracellular storage and regulated secretion of 3 von Willebrand disease-causing variants of von Willebrand factor. Blood. 2003;102(7):2452-8.
27. Zhang Q, Cannavicci A, Kutryk MJB. Exploring Endothelial Colony-Forming Cells to Better Understand the Pathophysiology of Disease: An Updated Review. Stem Cells Int. 2022;2022:4460041.
28. de Boer S, Laan S, Dirven R, Eikenboom J. Approaches to induce the maturation process of human induced pluripotent stem cell derived-endothelial cells to generate a robust model. PLoS One. 2024;19(2):e0297465.
29. HICKSON N, HAMPSHIRE D, WINSHIP P, GOUDEMAND J, SCHNEPPENHEIM R, BUDDE U, et al. von Willebrand factor variant p.Arg924Gln marks an allele associated with reduced von Willebrand factor and factor VIII levels. Journal of Thrombosis and Haemostasis. 2010;8(9):1986-93.
30. Penas N, Pérez-Rodríguez A, Torea JH, Lourés E, Noya MS, López-Fernández MF, et al. von Willebrand disease R1374C: type 2A or 2M? A challenge to the revised classification. High frequency in the northwest of Spain (Galicia). Am J Hematol. 2005;80(3):188-96.
31. Yin J, Ma Z, Su J, Wang J-W, Zhao X, Ling J, et al. Mutations in the D1 domain of von Willebrand factor impair their propeptide-dependent multimerization, intracellular trafficking and secretion. Journal of Hematology & Oncology. 2015;8(1):73.
32. de Jong A, Dirven RJ, Boender J, Atiq F, Anvar SY, Leebeek FWG, et al. Ex vivo Improvement of a von Willebrand Disease Type 2A Phenotype Using an Allele-Specific Small-Interfering RNA. Thromb Haemost. 2020;120(11):1569-79.

33. Bär I, Barraclough A, Bürgisser PE, van Kwawegen C, Fijnvandraat K, Eikenboom JCJ, et al. The severe von Willebrand Disease variant p.M771V leads to impaired anterograde trafficking of Von Willebrand factor in patient-derived and base-edited ECFCs. Journal of Thrombosis and Haemostasis.
34. Sanders YV, van der Bom JG, Isaacs A, Cnossen MH, de Maat MP, Laros-van Gorkom BA, et al. CLEC4M and STXBP5 gene variations contribute to von Willebrand factor level variation in von Willebrand disease. J Thromb Haemost. 2015;13(6):956-66.
35. Moses SR, Adorno JJ, Palmer AF, Song JW. Vessel-on-a-chip models for studying microvascular physiology, transport, and function in vitro. American Journal of Physiology-Cell Physiology. 2021;320(1):C92-C105.
36. Sakurai Y, Hardy ET, Lam WA. Hemostasis-on-a-chip / incorporating the endothelium in microfluidic models of bleeding. Platelets. 2023;34(1):2185453.
37. Sakurai Y, Hardy ET, Ahn B, Tran R, Fay ME, Ciciliano JC, et al. A microengineered vascularized bleeding model that integrates the principal components of hemostasis. Nat Commun. 2018;9(1):509.
38. van Loon J, Dehghan A, Weihong T, Trompet S, McArdle WL, Asselbergs FFW, et al. Genome-wide association studies identify genetic loci for low von Willebrand factor levels. European Journal of Human Genetics. 2016;24(7):1035-40.
39. Sabater-Lleal M, Huffman JE, de Vries PS, Marten J, Mastrangelo MA, Song C, et al. Genome-Wide Association Transethnic Meta-Analyses Identifies Novel Associations Regulating Coagulation Factor VIII and von Willebrand Factor Plasma Levels. Circulation. 2019;139(5):620-35.
40. van Loon JE, Leebeek FW, Deckers JW, Dippel DW, Poldermans D, Strachan DP, et al. Effect of genetic variations in syntaxin-binding protein-5 and syntaxin-2 on von Willebrand factor concentration and cardiovascular risk. Circ Cardiovasc Genet. 2010;3(6):507-12.
41. Hordijk S, Carter T, Bierings R. A new look at an old body: molecular determinants of Weibel-Palade body composition and VWF exocytosis. J Thromb Haemost. 2024.
42. Bierings R, Hellen N, Kiskin N, Knipe L, Fonseca AV, Patel B, et al. The interplay between the Rab27A effectors Slp4-a and MyRIP controls hormone-evoked Weibel-Palade body exocytosis. Blood. 2012;120(13):2757-67.
43. Anderson NL, Anderson NG. The Human Plasma Proteome: History, Character, and Diagnostic Prospects*. Molecular & Cellular Proteomics. 2002;1(11):845-67.
44. Kreft IC, van Duijl TT, van Kwawegen C, Atiq F, Phan W, Schuller MBP, et al. Variant mapping using mass spectrometry-based proteotyping as a diagnostic tool in von Willebrand disease. J Thromb Haemost. 2024;22(7):1894-908.
45. Huang J, Zhang P, Solari FA, Sickmann A, Garcia A, Jurk K, et al. Molecular Proteomics and Signalling of Human Platelets in Health and Disease. Int J Mol Sci. 2021;22(18).
46. Smadja DM, Melero-Martin JM, Eikenboom J, Bowman M, Sabatier F, Randi AM. Standardization of methods to quantify and culture endothelial colony-forming cells derived from peripheral blood. Journal of Thrombosis and Haemostasis. 2019;17(7):1190-4.
47. de Jong A, Weijers E, Dirven R, de Boer S, Streur J, Eikenboom J. Variability of von Willebrand factor-related parameters in endothelial colony forming cells. J Thromb Haemost. 2019;17(9):1544-54.
48. de Boer S, Bowman M, Notley C, Mo A, Lima P, de Jong A, et al. Endothelial characteristics in healthy endothelial colony forming cells; generating a robust and valid ex vivo model for vascular disease. J Thromb Haemost. 2020;18(10):2721-31.

49. Medina RJ, O'Neill CL, O'Doherty TM, Chambers SE, Guduric-Fuchs J, Neisen J, et al. Ex vivo expansion of human outgrowth endothelial cells leads to IL-8-mediated replicative senescence and impaired vasoreparative function. Stem Cells. 2013;31(8):1657-68.
50. Dejana E, Hirschi KK, Simons M. The molecular basis of endothelial cell plasticity. Nature Communications. 2017;8(1):14361.
51. Sanchez-Duffhues G, Orlova V, ten Dijke P. In Brief: Endothelial-to-mesenchymal transition. The Journal of Pathology. 2016;238(3):378-80.
52. Kalluri R, Weinberg RA. The basics of epithelial-mesenchymal transition. J Clin Invest. 2009;119(6):1420-8.
53. Maleszewska M, Moonen JR, Huijkman N, van de Sluis B, Krenning G, Harmsen MC. IL-1β and TGFβ2 synergistically induce endothelial to mesenchymal transition in an NFκB-dependent manner. Immunobiology. 2013;218(4):443-54.
54. Romero LI, Zhang DN, Herron GS, Karasek MA. Interleukin-1 induces major phenotypic changes in human skin microvascular endothelial cells. J Cell Physiol. 1997;173(1):84-92.
55. Sánchez-Duffhues G, García de Vinuesa A, van de Pol V, Geerts ME, de Vries MR, Janson SG, et al. Inflammation induces endothelial-to-mesenchymal transition and promotes vascular calcification through downregulation of BMPR2. J Pathol. 2019;247(3):333-46.
56. Rieder F, Kessler SP, West GA, Bhilocha S, de la Motte C, Sadler TM, et al. Inflammation-induced endothelial-to-mesenchymal transition: a novel mechanism of intestinal fibrosis. Am J Pathol. 2011;179(5):2660-73.
57. Derada Troletti C, Fontijn RD, Gowing E, Charabati M, van Het Hof B, Didouh I, et al. Inflammation-induced endothelial to mesenchymal transition promotes brain endothelial cell dysfunction and occurs during multiple sclerosis pathophysiology. Cell Death & Disease. 2019;10(2):45.
58. Sanchez-Duffhues G, Garcia de Vinuesa A, Ten Dijke P. Endothelial-to-mesenchymal transition in cardiovascular diseases: Developmental signaling pathways gone awry. Dev Dyn. 2018;247(3):492-508.
59. Ma J, Sanchez-Duffhues G, Goumans MJ, Ten Dijke P. TGF-β-Induced Endothelial to Mesenchymal Transition in Disease and Tissue Engineering. Front Cell Dev Biol. 2020;8:260.
60. Bai H, Gao Y, Hoyle DL, Cheng T, Wang ZZ. Suppression of Transforming Growth Factor-β Signaling Delays Cellular Senescence and Preserves the Function of Endothelial Cells Derived from Human Pluripotent Stem Cells. Stem Cells Transl Med. 2017;6(2):589-600.
61. Moldovan F, Benanni H, Fiet J, Cussenot O, Dumas J, Darbord C, et al. Establishment of permanent human endothelial cells achieved by transfection with SV40 large T antigen that retain typical phenotypical and functional characteristics. In Vitro Cell Dev Biol Anim. 1996;32(1):16-23.
62. Hohenwarter O, Zinser E, Schmatz C, Rüker F, Katinger H. Influence of transfected SV40 early region on growth and differentiation of human endothelial cells. J Biotechnol. 1992;25(3):349-56.
63. Ghiselli F, Felici M, Piva A, Grilli E. Establishment and characterization of an SV40 immortalized chicken intestinal epithelial cell line. Poult Sci. 2023;102(10):102864.
64. Zakrzewski W, Dobrzyński M, Szymonowicz M, Rybak Z. Stem cells: past, present, and future. Stem Cell Research & Therapy. 2019;10(1):68.
65. Sugimoto N, Eto K. Ex Vivo Production of Platelets From iPSCs: The iPLAT1 Study and Beyond. Hemasphere. 2023;7(6):e884.

66. Hansen M, Varga E, Aarts C, Wust T, Kuijpers T, von Lindern M, et al. Efficient production of erythroid, megakaryocytic and myeloid cells, using single cell-derived iPSC colony differentiation. Stem Cell Res. 2018;29:232-44.
67. Orlova VV, van den Hil FE, Petrus-Reurer S, Drabsch Y, Ten Dijke P, Mummery CL. Generation, expansion and functional analysis of endothelial cells and pericytes derived from human pluripotent stem cells. Nat Protoc. 2014;9(6):1514-31.
68. Wang K, Lin RZ, Hong X, Ng AH, Lee CN, Neumeyer J, et al. Robust differentiation of human pluripotent stem cells into endothelial cells via temporal modulation of ETV2 with modified mRNA. Sci Adv. 2020;6(30):eaba7606.
69. Aoki H, Yamashita M, Hashita T, Ogami K, Hoshino S, Iwao T, et al. Efficient differentiation and purification of human induced pluripotent stem cell-derived endothelial progenitor cells and expansion with the use of inhibitors of ROCK, TGF-β, and GSK3β. Heliyon. 2020;6(3):e03493.
70. Samuel R, Daheron L, Liao S, Vardam T, Kamoun WS, Batista A, et al. Generation of functionally competent and durable engineered blood vessels from human induced pluripotent stem cells. Proc Natl Acad Sci U S A. 2013;110(31):12774-9.
71. Kim K, Zhao R, Doi A, Ng K, Unternaehrer J, Cahan P, et al. Donor cell type can influence the epigenome and differentiation potential of human induced pluripotent stem cells. Nature Biotechnology. 2011;29(12):1117-9.
72. Nakhaei-Nejad M, Farhan M, Mojiri A, Jabbari H, Murray AG, Jahroudi N. Regulation of von Willebrand Factor Gene in Endothelial Cells That Are Programmed to Pluripotency and Differentiated Back to Endothelial Cells. Stem Cells. 2019;37(4):542-54.
73. Guillevic O, Ferratge S, Pascaud J, Driancourt C, Boyer-Di-Ponio J, Uzan G. A Novel Molecular and Functional Stemness Signature Assessing Human Cord Blood-Derived Endothelial Progenitor Cell Immaturity. PLOS ONE. 2016;11(4):e0152993.
74. Gara E, Zucchelli E, Nemes A, Jakus Z, Ajtay K, Kemecsei É, et al. 3D culturing of human pluripotent stem cells-derived endothelial cells for vascular regeneration. Theranostics. 2022;12(10):4684-702.
75. James D, Nam HS, Seandel M, Nolan D, Janovitz T, Tomishima M, et al. Expansion and maintenance of human embryonic stem cell-derived endothelial cells by TGFbeta inhibition is Id1 dependent. Nat Biotechnol. 2010;28(2):161-6.
76. Lee RM, Eisenman LR, Khuon S, Aaron JS, Chew T-L. Believing is seeing – the deceptive influence of bias in quantitative microscopy. Journal of Cell Science. 2024;137(1).
77. Schindelin J, Arganda-Carreras I, Frise E, Kaynig V, Longair M, Pietzsch T, et al. Fiji: an open-source platform for biological-image analysis. Nature Methods. 2012;9(7):676-82.
78. Stirling DR, Swain-Bowden MJ, Lucas AM, Carpenter AE, Cimini BA, Goodman A. CellProfiler 4: improvements in speed, utility and usability. BMC Bioinformatics. 2021;22(1):433.
79. van der Walt S, Schönberger JL, Nunez-Iglesias J, Boulogne F, Warner JD, Yager N, et al. scikit-image: image processing in Python. PeerJ. 2014;2:e453.
80. Senft RA, Diaz-Rohrer B, Colarusso P, Swift L, Jamali N, Jambor H, et al. A biologist's guide to planning and performing quantitative bioimaging experiments. PLOS Biology. 2023;21(6):e3002167.
81. Moen E, Bannon D, Kudo T, Graf W, Covert M, Van Valen D. Deep learning for cellular image analysis. Nat Methods. 2019;16(12):1233-46.
82. Elshoeibi AM, Ferih K, Elsabagh AA, Elsayed B, Elhadary M, Marashi M, et al. Applications of Artificial Intelligence in Thrombocytopenia. Diagnostics (Basel). 2023;13(6).

83. Gedefaw L, Liu CF, Ip RKL, Tse HF, Yeung MHY, Yip SP, et al. Artificial Intelligence-Assisted Diagnostic Cytology and Genomic Testing for Hematologic Disorders. Cells. 2023;12(13).
84. Hyun Suk P, Sung Young K. Endothelial cell senescence: A machine learning-based meta-analysis of transcriptomic studies. Ageing Research Reviews. 2021;65:101213.
85. Magnusson MMM, Schüpbach-Regula G, Rieger J, Plendl J, Marin I, Drews B, et al. Application of an artificial intelligence for quantitative analysis of endothelial capillary beds in vitro. Clinical hemorheology and microcirculation. 2024;88(1):43-58.
86. Poon AIF, Sung JJY. Opening the black box of AI-Medicine. Journal of Gastroenterology and Hepatology. 2021;36(3):581-4.
87. Katirai A. The Environmental Costs of Artificial Intelligence for Healthcare. Asian Bioeth Rev. 2024;16(3):527-38.

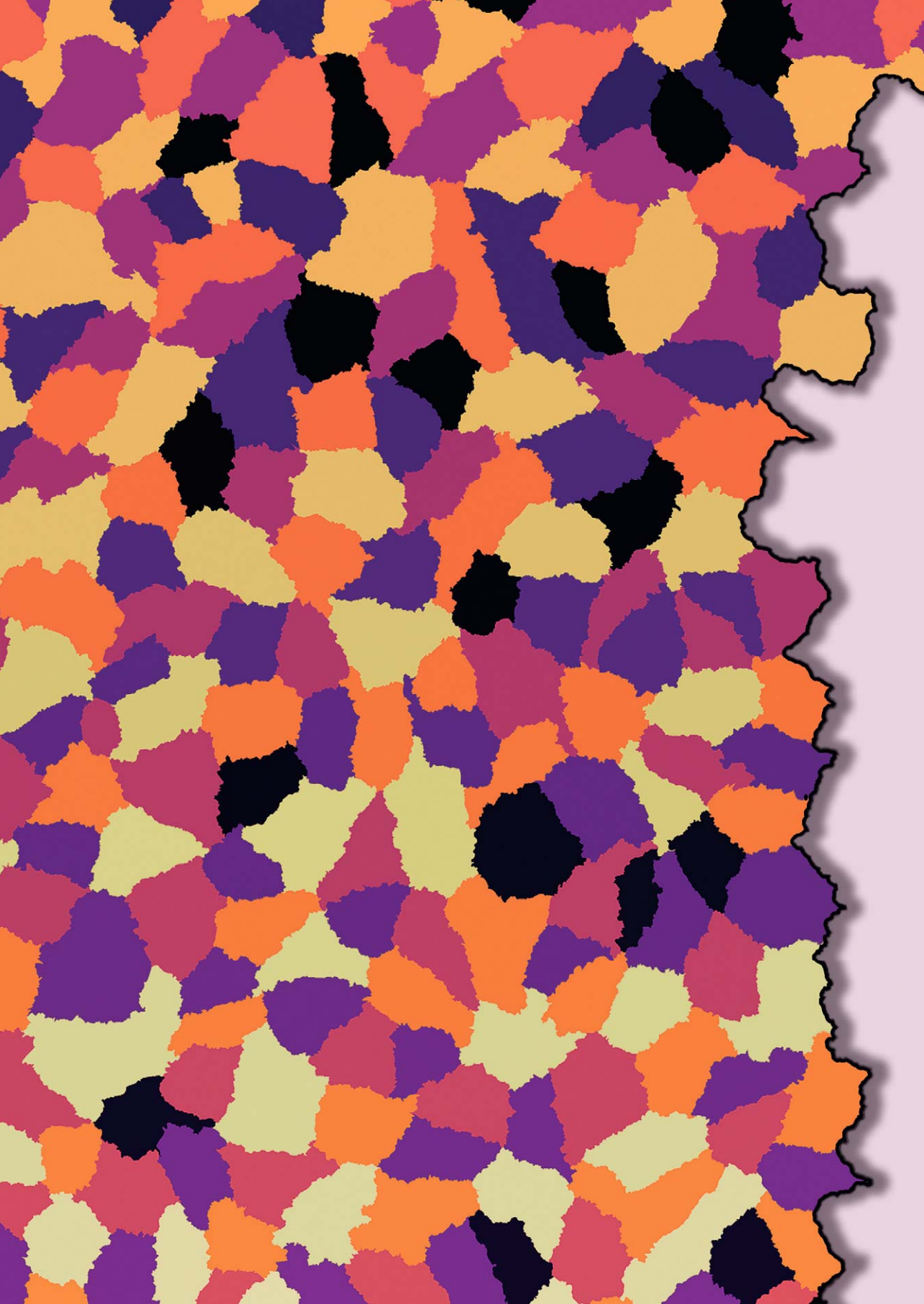

English and Dutch summary

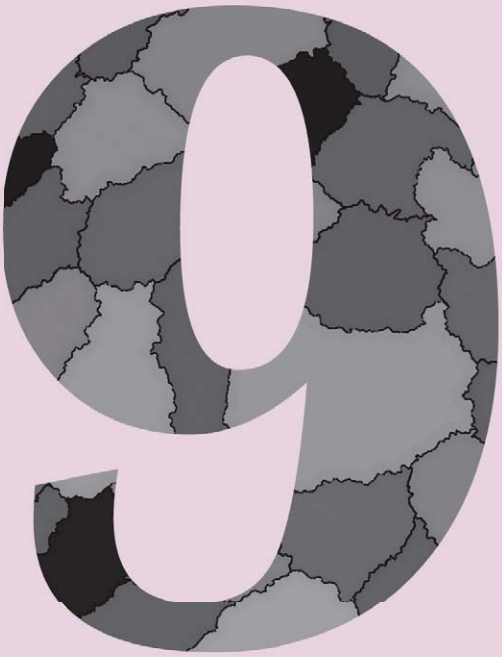

English summary

Endothelial cells form the inner wall of vessels and play a critical role in the primary and secondary hemostasis. One of the main procoagulant roles of endothelial cells is the production of von Willebrand factor (VWF). This is a very large protein that, once activated in the blood, can bind to platelets and start the coagulation process. VWF can also bind to and protect coagulation factor VIII (FVIII). VWF is primarily produced in endothelial cells and stored in specialized secretory organelles called Weibel-Palade bodies (WPBs). These cell specific organelles are filled with dense tubules of VWF which allow for a quick secretion when stimulated. In von Willebrand disease (VWD), VWF is either defect or absent in varying degrees causing mild to severe bleeding abnormalities. This can lead to frequent nosebleeds, menorrhagia, excessive bleeding from injury or surgery, and muscle and joint bleeds. VWD can be treated by administering factor concentrates or by administration of 1-deamino-8-D-arginine vasopressin (DDAVP). This drug can stimulate endothelial cells to secrete their contents and thus quickly increases the levels of VWF and FVIII in the blood. Large variation in bleeding phenotype exist in VWD patients. This variation can be caused by different mutations but interestingly, approximately 30-50% of patients with type 1 VWD do not have pathogenic VWF gene variants. There is also a significant group of VWD patients that do not respond to treatment with DDAVP. We hypothesized that the reduced VWF levels or non-response to DDAVP may be caused by other modifiers of VWF. As primary source of VWF we focused our research on the endothelial cells of these patients. A model that can be used to study endothelial cells is named endothelial colony forming cells (ECFCs). A great advantage of ECFCs is that they carry the genetic background of the donor from which the blood for ECFC isolation was collected. In this thesis we studied various aspects of the endothelial compartment as a disease modifier in bleeding disorders using the ECFC model.

Firstly, a general background for all the studies in this thesis is presented in **Chapter 1**. There, we provide a more detailed description of endothelial cell function, VWD and its treatment options and the available endothelial research models.

In previous studies, ECFCs have already been extensively used as a model to study the pathophysiology in bleeding disorders. We reviewed the published literature in **Chapter 2** to obtain an overview of these findings. The advantages and disadvantages of using ECFCs in patient-specific research are discussed and compared with alternative models like the induced pluripotent stem cells (iPSCs) or transfected models like the human embryonic kidney 293 cells. We also summarized the findings in VWD specific research, secretory organelle exocytosis and insights into role of endothelial cells in angiogenesis.

One widely used method of analyzing cells and tissues is microscopy which yields insight into the inner workings of cells. Qualitative observations can be made by eye, but to statistically analyze the data, quantification is needed. One of the primary analysis tools we used for endothelial cell and WPB morphology was immunofluorescence microscopy. Quantification of parameters was challenging due to the high number and large heterogeneity of WPB shape within the cells. Therefore, we developed an automated quantification method for the analysis of cells and organelles using CellProfiler (**Chapter 3**). The method was specifically designed to measure the size, count and shape of the endothelial cells and to measure the count, shape, length and location of WPB within the cell. Furthermore, to show that this method could also be used by other groups for other purposes, we analyzed endosome morphology in HEK cells.

As mentioned previously, the ECFCs provide a wonderful model to study the pathophysiology in bleeding disorders. Through a relatively simple venipuncture, the ECFCs can be derived from whole blood. Once differentiated, the ECFCs endogenously produce VWF and display all general endothelial markers. Most importantly for our research is that the cells also contain the mutations of the donor which allows for patient specific research. However, there are also challenges in working with ECFCs. It has been shown that within healthy control ECFCs there is large variation in many aspects of the ECFCs like cell size and shape, proliferation speed and VWF production. One can imagine the difficulty of studying VWF production in cells of which the production varies strongly. Therefore, in **Chapter 4** we dive into this variation, the challenge it poses and offer a solution to overcome this problem. First, we explored the transcription signature of a large panel of control-derived ECFCs using RNA sequencing. This revealed that many of the differentially expressed genes were associated with inflammation and with endothelial to mesenchymal transition (EndoMT). These genes may act as potential drivers for the phenotypic heterogeneity. We used this information to create a minimal qPCR panel which can be used to easily characterize and cluster the ECFC clones. Comparing between 2 clusters of ECFCs, we show that WPB count and shape, cell count and migration speed is significantly different. This emphasizes the importance of characterizing ECFCs before using them for patient specific research. An alternative model for endothelial cell research is the iPSC-derived endothelial cell (iPSC-EC). These cells can be derived from any cell type isolated from a donor. For instance, peripheral blood mononuclear cells can be isolated from whole blood, reprogrammed to iPSCs and then differentiated into iPSC-ECs. This means that these cells also carry the genetic background of the donor and can be used for patient-specific research. However, iPSC-ECs do not seem to mature fully, showing low levels of synthesized VWF and small, round WPBs. In **Chapter 5** we performed and adjusted various differentiation

protocols in order to improve the maturation of the WPBs. We show that co-culture with pericytes, changing the concentration or timing of administration of differentiation factors, the addition of flow to the system, and the use of histone deacetylase (HDAC) inhibitors did not significantly improve maturation of iPSC-ECs. Transfection of iPSCs with transcription factor ETV2 resulted in a faster differentiation process with slightly increased VWF production and secretion. Furthermore, the WPBs were more elongated, but only after >30 days in culture.

As mentioned previously, VWD can be treated by administration of DDAVP which quickly raises VWF and FVIII levels in the blood. DDAVP is also used in other bleeding disorders. However, a large portion of patients that receive DDAVP do not or only partially respond. These patients require alternative treatments such as factor concentrates, but the reason for the non-response in most patients is not understood. For this reason, we performed a systematic review and meta-analysis on the response to DDAVP and the possible determinants of DDAVP response in patients with bleeding disorders (**Chapter 6**). In this study we included 103 articles, from which, data of 1982 patients could be extracted. Response rate varied significantly between disease types and subtypes and coagulation factor baseline levels were important determinants of response. Our findings strengthen what is already known and emphasizes the need for a standardized response definition and further research into response mechanisms.

Finally, the lessons learned in this thesis were applied in **Chapter 7**. There, we analyzed ECFCs derived from two groups of patients with VWD. First, patients with VWD without a pathogenic mutation in VWF and second, patients with VWD with a known mutation in VWF but no response to DDAVP. We hypothesized that modifiers of VWF in the endothelial cells are affected in these patients, causing the low levels of VWF or the non-response. ECFCs were analyzed and clustered using the minimal qPCR panel developed in **Chapter 4**. Patient ECFCs were matched to controls and functional aspects of the ECFCs like production of VWF, stimulated secretion, migration and morphology were compared. All morphological aspects were analyzed using the quantification pipeline developed in **Chapter 3**. We found that retention of VWF in the endoplasmic reticulum could be the cause of the DDAVP non-response in some patients. Furthermore, we correlated the extensive range of functional characteristics of endothelial cells to their proteome, uncovering processes and proteins of interest.

To summarize, this thesis adds valuable insight into the use of ECFCs and iPSC-ECs and shows how they could be used to study patient specific defects. It also shows the challenges of using these models and the importance of developing and optimizing them.

Nederlandse samenvatting

Endotheelcellen vormen de binnenwand van bloedvaten en spelen een belangrijke rol in de primaire en secundaire hemostase. Een van de belangrijkste procoagulante functies van endotheelcellen is de productie van de Von Willebrand factor (VWF). Dit is een zeer groot eiwit dat na activatie bloedplaatjes aan de beschadigde vaatwand kan binden en het stollingsproces kan starten. VWF kan ook binden en bescherming bieden aan stollingsfactor VIII (FVIII). VWF wordt voornamelijk geproduceerd in endotheelcellen en opgeslagen in gespecialiseerde secretieorganellen, de zogeheten Weibel-Palade lichaampjes (WPBs). Deze celspecifieke organellen bevatten buisjes van VWF, waardoor snelle secretie mogelijk is na stimulatie. Bij de bloedingsstoornis de ziekte van Von Willebrand (VWD) is VWF in verschillende mate defect of afwezig, wat milde tot ernstige bloedingsafwijkingen veroorzaakt. Dit kan leiden tot bloedingsproblemen, zoals frequente neusbloedingen, menorragie, overmatig bloeden bij verwondingen of operaties, en bloedingen in spieren of gewrichten. VWD kan worden behandeld door het toedienen van stollingsfactoren of door toediening van 1-deamino-8-D-arginine vasopressin (DDAVP). Dit medicijn kan endotheelcellen stimuleren tot het vrijgeven van hun inhoud en leidt tot een snelle, tijdelijke verhoging van de hoeveelheid VWF en FVIII in het bloed. Het is bekend dat er een grote variatie in het bloedingsfenotype bestaat bij VWD patiënten. Deze variatie kan worden veroorzaakt door verschillende *VWF* mutaties, maar opvallend genoeg hebben ongeveer 30-50% van de patiënten met type 1 VWD geen pathogene varianten in het VWF gen. Bovendien is er een aanzienlijke groep VWD patiënten die niet reageren op behandeling met DDAVP zonder dat daar een duidelijk aanwijsbare oorzaak voor is. Onze hypothese was dat de verlaagde VWF niveaus of het niet reageren op DDAVP veroorzaakt zou kunnen worden door andere factoren die VWF kunnen beïnvloeden. Als primaire bron van VWF hebben we ons in dit onderzoek gericht op de endotheelcellen van deze patiënten. Een model dat gebruikt kan worden om endotheelcellen te bestuderen zijn de endotheel kolonievormende cellen (ECFCs). Een groot voordeel van ECFCs is dat ze de genetische achtergrond dragen van de donor uit wiens bloed de ECFCs zijn geïsoleerd. In dit proefschrift hebben we verschillende aspecten van de endotheelcel bestudeerd met behulp van het ECFC-model bij mensen met bloedingsstoornissen.

Ten eerste wordt in **hoofdstuk 1** een algemene achtergrond gegeven voor alle onderzoeken in dit proefschrift. Hierin geven we een meer gedetailleerde beschrijving van de functie van endotheelcellen, VWD, de behandelopties en de beschikbare onderzoeksmodellen voor endotheelcellen.

In eerdere studies zijn ECFCs al gebruikt als model om de pathofysiologie van bloedingsstoornissen te bestuderen. In **hoofdstuk 2** hebben we de gepubliceerde literatuur hierover verzameld om een overzicht van deze bevindingen te verkrijgen. De voor- en nadelen van het gebruik van ECFCs in patiëntspecifiek onderzoek wordt besproken en vergeleken met alternatieve modellen zoals geïnduceerde pluripotente stamcellen (iPSCs) of getransfecteerde modellen zoals de humane embryonale niercellen 293 (HEK293). Daarnaast hebben we de bevindingen samengevat die specifiek betrekking hebben op VWD, de uitscheiding van secretieorganellen en de rol van endotheelcellen in angiogenese.

Een veelgebruikte methode om cellen en weefsels te analyseren is microscopie. Dit geeft inzicht in de interne werking van cellen. Hoewel kwalitatieve observaties met het blote oog kunnen worden gedaan, is kwantificatie nodig om de gegevens statistisch te analyseren. Eén van de belangrijkste apparaten die wij gebruikten voor de analyse van de morfologie van endotheelcellen en WPBs was immunofluorescentie microscopie. Het kwantificeren van eigenschappen was uitdagend vanwege het grote aantal en de grote variatie van WPBs binnen de cellen. Daarom hebben we een geautomatiseerde kwantificatiemethode ontwikkeld voor de analyse van cellen en organellen met behulp van CellProfiler (**hoofdstuk 3**). De methode is specifiek ontworpen om het formaat, het aantal en de vorm van endotheelcellen te meten, evenals het aantal, de vorm, de lengte en de locatie van WPBs binnen de cel. Bovendien hebben we de morfologie van endosomen in HEK-cellen geanalyseerd om aan te tonen dat deze methode ook door andere onderzoeksgroepen voor andere doeleinden kan worden gebruikt.

Zoals eerder vermeld bieden ECFCs een uitstekend model om de pathofysiologie van bloedingsstoornissen te bestuderen. Door middel van een relatief eenvoudige bloedafname kunnen ECFCs worden verkregen uit het bloed. Na differentiatie produceren de ECFCs VWF en hebben ze alle algemene endotheelkenmerken. Het belangrijkste voor ons onderzoek is dat deze cellen ook de mutaties van de donor bevatten, waardoor patiëntspecifiek onderzoek mogelijk is. Er zijn echter ook uitdagingen bij het werken met ECFCs. Uit onderzoek blijkt dat er binnen gezonde controle-ECFCs grote variatie bestaat in aspecten zoals celgrootte en -vorm, proliferatiesnelheid en productie van VWF. Het is duidelijk dat het bestuderen van VWF-productie moeilijk is in een model waarin deze sterk varieert. Daarom bespreken we in **hoofdstuk 4** deze variatie, de uitdagingen die het met zich meebrengt en bieden we een oplossing voor dit probleem. Eerst onderzochten we het transcriptieprofiel van een grote groep controle-ECFCs door middel van RNA-sequencing. Dit toonde aan dat veel van de genen geassocieerd zijn met ontsteking en endotheel-naar-mesenchymaal-transitie (EndoMT). Deze genen kunnen mogelijk de fenotypische variatie aansturen. Op basis van deze

informatie hebben we een klein qPCR panel ontwikkeld dat eenvoudig kan worden gebruikt om ECFC-klonen te karakteriseren en te groeperen. Vergelijkingen tussen twee groepen van ECFCs tonen aan dat het aantal cellen, het aantal WPBs, hun vorm en de migratiesnelheid significant verschillen. Dit benadrukt het belang van karakterisering van ECFCs voordat ze worden gebruikt voor patiëntspecifiek onderzoek.

Een alternatief model voor endotheel onderzoek zijn iPSC-afgeleide endotheelcellen (iPSC-EC). Deze cellen kunnen worden afgeleid van elk celtype dat geïsoleerd is van een donor. Bijvoorbeeld, perifere mononucleaire bloedcellen kunnen uit volbloed worden geïsoleerd, geherprogrammeerd worden tot iPSCs en vervolgens weer gedifferentieerd worden tot iPSC-ECs. Deze cellen dragen ook de genetische achtergrond van de donor en kunnen worden gebruikt voor patiëntspecifiek onderzoek. iPSC-ECs lijken echter niet volledig te matureren. Ze vertonen namelijk lage niveaus van geproduceerd VWF en kleine, ronde WPBs. In **hoofdstuk 5** hebben we verschillende differentiatieprotocollen uitgevoerd en aangepast om de maturatie van WPBs te verbeteren. We laten zien dat verscheidene zaken de maturatie van iPSC-ECs niet significant verbeteren. Transfectie van iPSCs met de transcriptiefactor ETV2 leidde tot een snellere differentiatie met een licht verhoogde VWF-productie en secretie. Bovendien waren de WPBs langwerpiger, maar alleen nadat de iPSC-ECs meer dan 30 dagen in kweek waren.

Zoals eerder vermeld kan VWD worden behandeld met DDAVP, dat snel de niveaus van VWF en FVIII in het bloed verhoogt. DDAVP wordt ook gebruikt bij andere bloedingsstoornissen. Een aanzienlijk deel van de patiënten reageert echter niet of slechts gedeeltelijk op DDAVP. Deze patiënten hebben alternatieve behandelingen nodig, zoals factorconcentraten. Echter is de reden voor de slechte respons bij de meeste patiënten niet bekend. Daarom voerden we een systematische review en meta-analyse uit over de respons op DDAVP en de mogelijke determinanten van DDAVP respons bij patiënten met bloedingsstoornissen (**hoofdstuk 6**). In deze studie includeerden we 103 artikelen, waaruit we de gegevens van 1982 patiënten konden extraheren. Het responspercentage varieerde aanzienlijk tussen ziektes en subtypes, en de basale niveaus van stollingsfactoren waren belangrijke determinanten voor de respons. Onze bevindingen versterken de bestaande kennis en benadrukken de noodzaak van een gestandaardiseerde definitie van respons en verder onderzoek naar responsmechanismen.

Tot slot werden de bevindingen uit dit proefschrift toegepast in **hoofdstuk 7**. Hier analyseerden we ECFCs van twee groepen patiënten met VWD: patiënten zonder pathogene mutatie in VWF en patiënten met een bekende mutatie in VWF maar zonder respons op DDAVP. Onze hypothese was dat de factoren in endotheelcellen die VWF

kunnen beïnvloeden, bij deze patiënten zijn aangetast, wat kan leiden tot lage VWF-niveaus of geen respons. ECFCs werden geanalyseerd en gegroepeerd met behulp van het qPCR panel ontwikkeld in **hoofdstuk 4.** ECFCs van patiënten werden gekoppeld met controles en functionele aspecten van de ECFCs zoals VWF-productie, gestimuleerde secretie, migratie en morfologie, werden geëvalueerd. Alle morfologische aspecten werden geanalyseerd door middel van de kwantificatiepijplijn ontwikkeld in **hoofdstuk 3**. We vonden dat VWF-retentie in het endoplasmatisch reticulum de oorzaak kan zijn voor het niet reageren op DDAVP bij sommige patiënten. Daarnaast correleerden we het uitgebreide scala aan functionele kenmerken van endotheelcellen met hun proteoom. Hierin vonden we processen en eiwitten van belang in de secretie van VWF.

Samenvattend biedt dit proefschrift waardevolle inzichten in het gebruik van ECFCs en iPSC-ECs en laten we zien hoe ze gebruikt kunnen worden om patiëntspecifieke defecten te bestuderen. Het laat ook de uitdagingen zien van het gebruik van deze modellen en benadrukt het belang van hun ontwikkeling en optimalisatie.

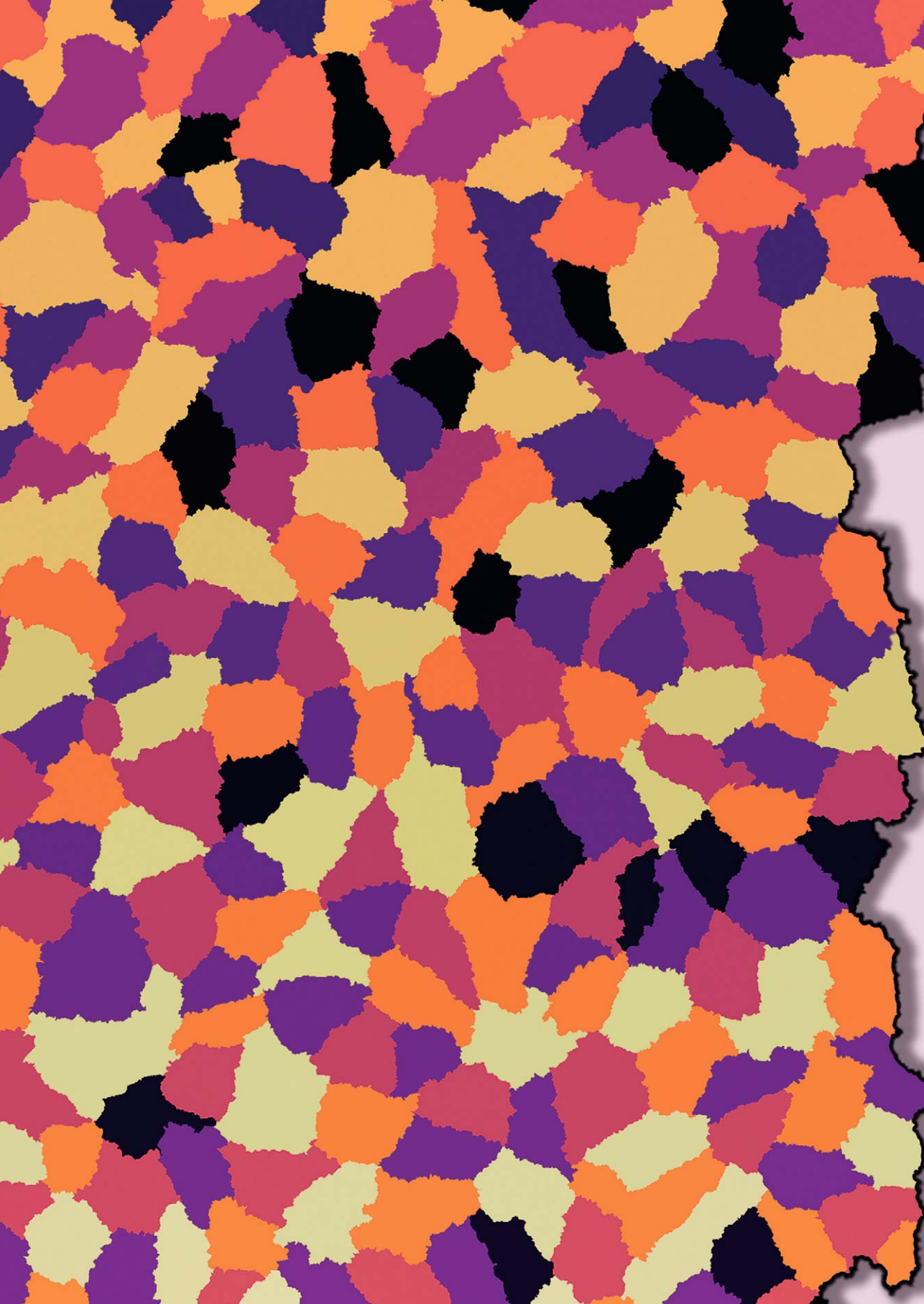

Appendices

Dankwoord

Dit boek is niet het werk van één persoon geweest, maar een langdurige samenwerking tussen heel veel mensen. Het was nooit gelukt om dit af te maken zonder mijn familie, vrienden, collega's en natuurlijk de patiënten en donoren die hebben meegedaan aan dit onderzoek.

Jeroen, bedankt voor de afgelopen 5 jaar aan begeleiding. Ik heb erg veel van je geleerd en waardeer de balans die je gaf tussen de vrijheid in mijn project en de nodige bijsturing. Ondanks de drukte was er altijd wel 5 minuten tijd voor een snelle schakeling. Ruben, jij was de perfecte aanvulling op de klinische expertise van Jeroen. Jouw uitgebreide fundamentele kennis, ervaring met verschillende technieken en creatieve blik op het project zorgden ervoor dat het hele traject soepel verliep. Frank, bedankt voor de adviezen en bemoedigende woorden.

Yv, ik had geen betere persoon naast me kunnen hebben als paranimf. Als senior en "grote zus" heb je mij door de afgelopen 5 jaar geholpen. Al ging het om kleine dingen zoals presentaties verbeteren en gemiste hoofdletters of om belangrijke keuzes en discussies, ik kon altijd bij je terecht voor advies en een knuffel, bedankt!

Richard, als de grote baas van het lab was jij gelukkig ook betrokken bij bijna al mijn projecten. Geen experiment was te groot en geen vraag te moeilijk, bedankt voor alle hulp! Noa, helaas hadden onze projecten weinig overlap en hebben we niet veel samengewerkt, maar het was wel altijd leuk tijdens de vele meetings, feestjes, uitjes en congressen die we hebben gehad! Suzan, Annika, Maria Teresa en mijn studenten Johannes en Britte, bedankt voor de leuke samenwerking in het VWF-team.

Een PhD op twee locaties kan uitdagend zijn, maar dat was voor mij niet het geval door de leuke groep in het EMC. Iris, wat ben ik ongelofelijk blij dat jij achter me stond gedurende mijn hele PhD. Je was een bron van kennis, steun en een altijd geduldig oor voor mijn frustraties. Het beest, en nu een pronkstuk in mijn boekje, was zonder jouw hulp niet gelukt. Petra, Sophie, Isabel, Maurice, Calvin, Ferdows en alle anderen op de 13e verdieping, bedankt voor de gezellige tijd en de leuke uitjes.

Ik wil ook graag alle andere collega's op C7 en D2 bedanken. De Fundamentals Ray, Viola, Kelley, Rob, Maaike, Araci, Dejvid, Caroline, Dongyue, Dagmar en de artsen Emily, Sabine, Dieuwke, Cindy, Fleur, Milou, Gordon, Linde, Sophie en Jurjen. Ook mijn andere collega's van de Epi en nieren, bedankt voor alle gezellige lunches, koffiepauzes en natuurlijk de geweldige feesten in onder andere London, Montreal, Venetië en Koudekerke!

Het SYMPHONY consortium heeft me ook veel unieke kansen gegeven om mijn netwerk uit te breiden, kennis te vergaren, samenwerkingen op te starten en vooral te praten over wetenschap met mede-fanatiekelingen. Alle mede-PhDs, de WP-leaders en vooral Marjon en Simone, erg bedankt.

Voor alle projecten waar ik met anderen heb samengewerkt, Maartje, Stijn, Karin, Marieke, Saskia, Leon en Thom, bedankt voor jullie expertise die de kwaliteit en schaal van het onderzoek significant hebben verbeterd.

De Zweden vriendjes, Auk, Mark, Maumau, Nini, Lien, Thomas en Tommie, mijn wetenschappelijke reis is samen met jullie begonnen en ik ben erg dankbaar dat ik dat nog steeds met jullie kan delen. Onze leuke uitjes en etentjes en natuurlijk het vele sporten zorgde voor de nodige ontspanning tussen alle hectiek.

De Poertiepappels, een groep te groot om allemaal bij naam te noemen, maar wat fijn dat de groep nog steeds zo groot is. Bedankt voor alle leuke activiteiten en uitjes de afgelopen 17 jaar en voor jullie interesse in mijn project.

Mijn team en bestuursgenoten, bedankt voor de vele jaren plezier en de nodige fysieke uitlaatklep op het veld.

De Labratjes, bedankt voor de leuke verhalen en gezellige etentjes.

Peter, Christine, Hanna, Maarten, Geert en Mutia, ik wil jullie ook graag bedanken voor alle steun die jullie me hebben gegeven en de open armen waarmee ik in de Sturm/van Dijk familie ben ontvangen.

De Laantjes, er is hier niet genoeg ruimte om jullie genoeg te bedanken. Muti en Vati, jullie hebben mij de kans gegeven, van jongs af aan, om mijn eigen pad te volgen. Met onvoorwaardelijke steun en toeverlaat kon ik vol vertrouwen de uitdaging aan. Jullie woorden van bemoediging betekenen heel veel voor me. Inge, Merel en Nick, met z'n vieren is het altijd gezellig, de band die we hebben met elkaar is erg speciaal en waardeer ik enorm.

Carlijn, mijn rots in de branding. Geen enkel probleem of uitdaging was te groot of te moeilijk met jou aan mijn zijde. Ik kijk ernaar uit om deze dag en de rest van ons leven samen te vieren.

Curriculum Vitae

Sebastiaan (Bas) Laan was born on November 18, 1995, in Zwaagdijk-Oost, the Netherlands. After completing secondary school at the Oscar Romero in Hoorn, he moved to Leiden to pursue a Bachelor's degree at Leiden University. During his studies, he took part in the Honors College and the BW-Plus program, and spent a semester abroad at the Karolinska Institute in Stockholm. After completing his Bachelor's degree in 2017, Bas continued with a research Master's in Biomedical Sciences at Leiden University, graduating in 2019. As part of his Master's, he conducted research on immune cells in a drosophila model at the Sir William Dunn School of Pathology in Oxford. A second internship was performed at the department of hematology of the Leiden University Medical Center where he studied T-cell immunology in the context of AML.

In 2020, Bas began his PhD project titled "The endothelial compartment as a disease modifier in bleeding disorders" at the department of Internal Medicine, division of Thrombosis and Hemostasis (LUMC) and the department of Hematology (Erasmus MC). In this research, supervised by Prof. Dr. H.C.J. Eikenboom, Dr. Ir. R. Bierings and Prof. Dr. W.G. Leebeek, he focused on functional and transcriptional defects in endothelial cells in patients with bleeding disorders. Throughout his PhD, he has worked with various endothelial cell models, developed automated image analysis pipelines, and contributed to several peer-reviewed publications. His work has been recognized with multiple awards, including the NVTH Award of Excellence and the ECTH Best Poster Prize. He now continues to work in the academic field as a microscopy specialist at the Leiden University – Leiden cell observatory.

List of publications

This thesis

1 **Laan SNJ**, Dirven RJ, Bürgisser PE, Eikenboom J, Bierings R. Automated segmentation and quantitative analysis of organelle morphology, localization and content using CellProfiler. PLoS One. 2023 Jun 14;18(6):e0278009. doi: 10.1371/journal.pone.0278009

2. De Boer S, **Laan SNJ**, Dirven RJ, Eikenboom J. Approaches to induce the maturation process of human induced pluripotent stem cell derived-endothelial cells to generate a robust model. PLoS One. 2024 Feb 23;19(2):e0297465. doi: 10.1371/journal.pone.0297465

3. **Laan SNJ**, de Boer S, Dirven RJ, van Moort I, Kuipers TB, Mei H, Bierings R, Eikenboom J; SYMPHONY consortium. Transcriptional and functional profiling identifies inflammation and endothelial-to-mesenchymal transition as potential drivers for phenotypic heterogeneity within a cohort of endothelial colony forming cells. J Thromb Haemost. 2024 Jul;22(7):2027-2038. doi: 10.1016/j.jtha.2024.03.018.

4. **Laan SNJ**, Lenderink BG, Eikenboom JC, Bierings R. Endothelial Colony Forming Cells in the spotlight, insights into the pathophysiology of von Willebrand disease and rare bleeding disorders. Journal of Thrombosis and Haemostasis. 2024 Sep 5:S1538-7836(24)00497-5. doi: 10.1016/j.jtha.2024.08.011

5. **Laan SNJ**, Castillo Alferez J, Cannegieter S, Fijnvandraat K, Kruip M, Le Cessie S, Bierings R, Eikenboom J, van Moort I. DDAVP response and its determinants in bleeding disorders: a systematic review and meta-analysis. Blood. 2025 Apr 17;145(16):1814-1825. doi: 10.1182/blood.2024026804.

6. **Laan SNJ**, Groten S*, Dirven RJ, Bürgisser PE, Leebeek FWG, van Moort I, van Biggelaar M, Bierings R**, Eikenboom J. Von Willebrand disease-specific defects and proteomic signatures in endothelial colony forming cells. Journal of Thrombosis and Haemostasis. 2025, doi: https://doi.org/10.1016/j.jtha.2025.04.024. online ahead of print. *shared first author, ** shared last author

Other

1. Linthorst NA, Jongejan YK, Dirven RJ, **Laan SNJ**, Bierings R, Casari C, Cordfunke RA, Dahlman JE, Dolezal N, Drijfhout JW, Leebeek FWG, Ruhaak LR, Schrader Echeverri E, Voorberg J, van Vlijmen BJM, Denis CV, Eikenboom JCJ. Amelioration of a von Willebrand disease type 2B phenotype in vivo upon treatment with allele-selective siRNAs. Blood Adv. 2025 Jan 28;9(2):310-320. doi: 10.1182/bloodadvances.2024014601

2. Jongejan YK, Linthorst NA, Schrader Echeverri E, **Laan SNJ**, Dirven RJ, Dahlman JE, van Vlijmen BJM, Denis CV, Eikenboom JCJ. Impact of allele-selective silencing of von Willebrand factor in mice based on a single nucleotide allelic difference in von Willebrand factor. Thromb Res. 2024 Apr;236:201-208. doi: 10.1016/j.thromres.2024.03.002.

3. Hordijk S, Groten SA, Bürgisser PE, **Laan SNJ**, Korenke G, Honzik T, Beysen D, Leebeek FWG, Skehel PA, van den Biggelaar M, Carter T, Bierings R. A Novel Cause of Type 1 VWD: Impaired Exocytosis of Weibel-Palade Bodies Due to Biallelic Variants in MADD. (2025) - **under review**

PhD portfolio

Name PhD candidate:	S.N.J. Laan
LUMC department:	Internal Medicine, Division of Thrombosis and Hemostasis
EMC department:	Department of Hematology
PhD period:	April 2020 – April 2024
Title Thesis:	The endothelial compartment as a disease modifier in bleeding disorders
Promotors:	Prof. Dr. H.C.J. Eikenboom Prof. Dr. F.W.G. Leebeek Dr. Ir. R. Bierings

Mandatory courses	Year
Leiden University Onboarding Program Inform & Connect	2020
Scientific Conduct	2020
BROK (Basic Course Regulations and Organization for Clinical Researchers)	2020
Basic Methods and Reasoning in Biostatistics	2020

Courses/ transferable skills	
Mindfulness	2020
NVTH course	2021
NVTH course	2022
Meta-analyse course	2022
Writing course - EMC - 2022	2022
NVTH course	2023

Conferences	type	
Regeneration day		2021
ISTH conference	Poster	2021
BIC conference		2021
ECTH conference	Poster	2021
RICS conference	Poster	2021
NVTH conference	Poster	2021
ISTH conference	Poster	2022
RICS conference	Plenary Oral	2022

NVTH conference	Poster Oral	2022
SYMPHONY general assembly	Poster 2x	2022
NEM symposium		2023
DHC symposium	Parallel Oral	2023
ISTH conference	Poster 2x Parallel Oral	2023
BIC conference	Poster	2023
RICS conference	Poster blitz	2023
NVTH conference	Poster	2023

Teaching activity	
FOS - the pathophysiology of Coagulation - 2021	2021
Supervision of Bachelor student	2022
FOS - the pathophysiology of Coagulation - 2022	2022
Supervision of Master student	2023
FOS - the pathophysiology of Coagulation - 2023	2023

Awards and prizes	
Poster prize ECTH “best poster award” 2021	2021
Poster prize symphony general assembly 2022	2022
NVTH “award of excellence” based on abstract. 2022	2022
Rembrandt heart of science award 2023	2023

Other	
SYMPHONY PhD committee	2020
SYMPHONY CPA committee	2021
Pi-life sciences seminar series.	2021

A